

**AN ADAPTIVE 3-D PUSHOVER PROCEDURE FOR DETERMINING THE
CAPACITY OF EXISTING IRREGULAR REINFORCED CONCRETE (RC)
BUILDINGS**

**Ph.D. Thesis by
Reşat Atalay OYGUÇ**

Department : Civil Engineering

Programme : Earthquake Engineering

JUNE 2011

**AN ADAPTIVE 3-D PUSHOVER PROCEDURE FOR DETERMINING THE
CAPACITY OF EXISTING IRREGULAR REINFORCED CONCRETE (RC)
BUILDINGS**

**Ph.D. Thesis by
Reşat Atalay OYGUÇ
(501032205)**

**Date of submission : 13 May 2011
Date of defence examination: 23 June 2011**

**Supervisor (Chairman) : Prof. Dr. Hasan BODUROĞLU (ITU)
Members of the Examining Committee : Prof. Dr. Ertaç ERGÜVEN (ITU)
Prof. Dr. Tuncer ÇELİK (BEYKENT)
Prof. Dr. Zekai CELEP (ITU)
Prof. Dr. Nesrin YARDIMCI
(YEDİTEPE)**

JUNE 2011

İSTANBUL TEKNİK ÜNİVERSİTESİ ★ FEN BİLİMLERİ ENSTİTÜSÜ

**MEVCUT DÜZENSİZ BETONARME YAPILARIN KAPASİTELERİNİN
BELİRLENMESİ İÇİN ÜÇ BOYUTLU UYARLAMALI İTME ANALİZİ
YÖNTEMİ**

**DOKTORA TEZİ
Reşat Atalay OYGUÇ
(501032205)**

Tezin Enstitüye Verildiği Tarih : 13 Mayıs 2011

Tezin Savunulduğu Tarih : 23 Haziran 2011

**Tez Danışmanı : Prof. Dr. Hasan BODUROĞLU (İTÜ)
Diğer Jüri Üyeleri : Prof. Dr. Ertuç ERGÜVEN (İTÜ)
Prof. Dr. Tuncer ÇELİK (BEYKENT)
Prof. Dr. Zekai CELEP (İTÜ)
Prof. Dr. Nesrin YARDIMCI
(YEDİTEPE)**

HAZİRAN 2011

*Dedicated to the memory of my dear grandmother;
Nadide OYGUÇ (1920-2004)*

FOREWORD

Determination of the capacity of existing structures under an earthquake excitation is an ongoing dilemma. Researchers proposed many ways of determining the structural capacity of these structures effectively. The main aim of this study is to assess the structural capacity of an irregular building with a short computational time and effort. To achieve this, a 3-D adaptive pushover procedure has been executed. Istanbul Technical University, Institute of Science and Technology, Earthquake Engineering Division supported this work.

I would first like to express my deep appreciation and thanks for my advisor Prof. Dr. Hasan BODUROĞLU. His continuous supports and advices motivate me during my study. It would be really hard if he did not encourage me.

I specifically thank Dr. Seong-Hoon JEONG and Prof. Dr. Amr S. ELNASHAI for their great support during gathering the ELSA Lab test data for the SPEAR building.

I would finally thank my mother, Berna OYGUÇ, and my father, Mehmet Zihni OYGUÇ. This PhD thesis would not have been conducted and completed without their continuous support, love and patience.

June 2011

Reşat Atalay OYGUÇ
Earthquake Engineering

TABLE OF CONTENTS

	<u>Page</u>
FOREWORD	vii
TABLE OF CONTENTS	ix
ABBREVIATIONS	xi
LIST OF TABLES	xiii
LIST OF FIGURES	xv
SUMMARY	xix
ÖZET	xxi
1. INTRODUCTION	1
1.1 Purpose of the Thesis	3
1.2 Background	4
1.3 Overview	13
2. PERFORMANCE BASED DESIGN	15
2.1 Performance Levels	15
2.2 Effects of Hysteretic Behaviour on Seismic Response	20
2.2.1 Elasto-Plastic Behaviour	20
2.2.2 Strength-Hardening Behaviour	21
2.2.3 Stiffness Degrading Behaviour	22
2.2.4 Pinching Behaviour	23
2.2.5 Cyclic Strength Degradation	23
2.2.6 Combined Stiffness Degradation and Cyclic Strength Degradation.....	24
2.2.7 In-Cycle Strength Degradation	25
2.2.8 Cyclic Envelope	26
2.3 Plasticity Concept.....	27
3. ANALYSIS METHODS FOR PERFORMANCE ASSESSMENT	33
3.1 Dynamic Analysis	35
3.1.1 Modal and Spectral Analysis Methods	36
3.1.2 Response History Analysis	39
3.1.3 Incremental Dynamic Analysis	40
3.2 Static Analysis	42
3.2.1 Equivalent Static Analysis Method.....	42
3.2.2 Pushover Analysis	43
3.3 Evaluation of Structural Response Using Conventional Pushover Procedures	44
3.3.1 Determining the Performance Point By Capacity Spectrum Method	48
3.3.2 Determining the Performance Point By Coefficient Method.....	52
3.3.3 Improvements in FEMA 356 and ATC 40 Procedures, FEMA 440.....	55
3.3.4 N2 Procedure.....	56
3.3.5 Modal Pushover Analysis	59
3.3.6 Energy Based Pushover Procedure	61
3.3.7 Direct Displacement Based Pushover Procedure	62
3.3.8 Issue of Torsion in Pushover Analysis.....	64
3.3.9 Deficiencies of Conventional Pushover Analysis	69

3.4 Adaptive Pushover Methods.....	70
3.4.1 Fibre Modelling approach For Determining the Inelastic Response.....	73
3.4.2 Adaptive Spectra Based Pushover Procedure	75
3.4.3 Incremental Response Spectrum Analysis (IRSA)	77
3.4.4 Consecutive Pushover Procedure	78
3.4.5 Displacement Based Adaptive Pushover Procedure	80
3.4.6 Story Shear Based Adaptive Pushover Procedure	82
4. PERFORMANCE EVALUATION OF EXISTING IRREGULAR 3-D	
BUILDINGS	89
4.1 The Theory and Basis of OpenSees.....	89
4.2 Description of the Seismic Performance Assessment and Rehabilitation of Existing Buildings Project (SPEAR).....	91
4.2.1 Material and Mass Representation of the SPEAR structure	94
4.2.2 Determination of Cross Sections.....	97
4.2.3 Determination of the Irregularities Effect for SPEAR	99
4.2.4 Determination of the Earthquake Record.....	100
4.3 A Nonlinear Adaptive Structural Analysis Program (NASAP)	102
4.4 Adaptive Pushover Results and Comparison of SPEAR Building.....	114
5. CONCLUSIONS AND RECOMMENDATIONS	123
5.1 Application of The Work.....	123
5.2 Conclusions	124
5.3 Outlook.....	125
REFERENCES	127
APPENDICES	135
CURRICULUM VITAE	171

ABBREVIATIONS

ADRS	: Spectral acceleration-spectral displacement response spectrum
ATC	: Applied Technology Council
App	: Appendix
BSE	: Basic safety earthquake
CMP	: Consecutive modal pushover procedure
CSM	: Capacity Spectrum Method
CQC	: Complete quadratic combination
CP	: Collapse Prevention
DAP	: Displacement based adaptive procedure
EC8	: Eurocode 8
ELSA	: European Laboratory for Structural Assessment
EPP	: Elastic perfectly plastic
FEMA	: Federal Emergency Management Agency
FFT	: Fast Fourier Transform
GLD	: Gravity load design
IDA	: Incremental Dynamic Analysis
IQ	: Immediate Occupancy
IRSA	: Incremental Response Spectrum Analysis
LS	: Life Safety
MDOF	: Multi degree of freedom system
MMP	: Multi mode pushover procedure
MMPA	: Modified Modal Pushover Analysis Procedure
MPA	: Modal pushover analysis procedure
MSD	: Moderate strength degradation
NASAP	: Nonlinear adaptive structural static analysis program
NE	: Nonlinear elastic
NEHRP	: National Earthquake Hazards Reduction Program
NSP	: Nonlinear Static Analysis Procedure
PF	: Modal participation factor
PRC	: Pushover results combination
RSA	: Response Spectrum Analysis
SD	: Strength degradation
SDOF	: Single degree of freedom system
SPEAR	: Seismic Performance Assessment and Rehabilitation
SRSS	: The square root of the sum of the squares
SSAP	: Story shear based adaptive pushover procedure
SSD	: Severe stiffness system

LIST OF TABLES

	<u>Page</u>
Table 3.1 : Comparisons of requirements for static and dynamic analyses.....	34
Table 3.2 : Analysis Procedures for Earthquake-Resistant Design	41
Table 3.3 : Values for Modification Factor C_0	54
Table 3.4 : Values for Modification Factor C_2	54
Table 4.1 : Center of Mass and Mass properties of SPEAR building.....	96
Table 4.2 : Torsional characteristics of the SPEAR building	100
Table 4.3 : Values for Modification Factor C_0	100
Table 4.4 : Modal participation factors calculated using NASAP.	116
Table 4.5 : Period and Mass ratio values for both directions.....	116
Table 4.6 : Peak story shear profiles	116
Table A.1 : 1.15g scaled artificial Montenegro Earthquake Record.....	136

LIST OF FIGURES

	<u>Page</u>
Figure 1.1 : Flowchart of an inelastic pushover procedure	5
Figure 1.2 : Capacity and demand curves in ADRS format	6
Figure 1.3 : Bi-linearization of the actual capacity curve	7
Figure 1.4 : Determination of inelastic response using inelastic spectra	7
Figure 1.5 : Pushover results of SAC20 building for different loads	9
Figure 1.6 : Comparison of pushover and dynamic analysis	10
Figure 1.7 : Comparison of different pushover analysis for tall frames	10
Figure 1.8 : Comparison of loading force vector determination	11
Figure 1.9 : Adaptive pushover schema	12
Figure 1.10 : Story shear based adaptive pushover (SSAP) procedure	12
Figure 2.1 : Target building performance levels	16
Figure 2.2 : Relative costs of various rehabilitation objectives	17
Figure 2.3 : Correlation Matrix showing performance levels	18
Figure 2.4 : Ductile performance and structural demand	18
Figure 2.5 : Non-Ductile performance and structural demand	19
Figure 2.6 : Basic hysteretic models used in the current procedures	20
Figure 2.7 : Elasto-plastic non-degrading model	21
Figure 2.8 : Strength-hardening non-degrading model	21
Figure 2.9 : Stiffness-degrading models	22
Figure 2.10 : (a) Moderate pinching (b) Severe pinching	23
Figure 2.11 : (a) Increasing displacement (b) Cyclic displacement	24
Figure 2.12 : (a) Moderate stiffness (b) Severe stiffness	24
Figure 2.13 : In-cycle strength degradation	25
Figure 2.14 : (a) Cyclic degradation (b) In-cyclic degradation	25
Figure 2.15 : Representation of a capacity boundary	26
Figure 2.16 : Representation of a cyclic envelope	26
Figure 2.17 : Idealized models of beam-column elements	27
Figure 2.18 : Axial load and strength interaction surface for concrete	28
Figure 2.19 : (a) Hinge element (b) Moment-rotation relationship	29
Figure 2.20 : P-M interaction diagram for reinforced concrete columns	30
Figure 2.21 : Generalized component acceptance criteria	31
Figure 3.1 : Common methods of analysis used in earthquake engineering.	33
Figure 3.2 : Methods of dynamic analysis of structures	36
Figure 3.3 : IDA curve for a five story steel braced frame	40
Figure 3.4 : Pushover curves comparison	45
Figure 3.5 : Yielding sequence of pushover analysis	46
Figure 3.6 : Load pattern model for conventional pushover analysis	47
Figure 3.7 : Response spectra in traditional and ADRS format	49
Figure 3.8 : Conversion of spectral coordinates to ADRS format	50
Figure 3.9 : Bilinear representation of capacity curve	51
Figure 3.10 : Intersection point of capacity and demand spectrums	51

Figure 3.11 : Capacity spectrum procedure B	52
Figure 3.12 : Capacity spectrum procedure C	53
Figure 3.13 : Force-displacement curve with positive post-yield slope	53
Figure 3.14 : Types of inelastic behavior considered in FEMA440	56
Figure 3.15 : Elastic spectrum in ADRS format	57
Figure 3.16 : Demand spectra for constant ductility factors in ADRS format	58
Figure 3.17 : Elastic and inelastic demand spectra versus capacity diagram	59
Figure 3.18 : Sample force distribution of SAC building for MPA procedure	61
Figure 3.19 : Capacity curves of an equivalent SDOF system	62
Figure 3.20 : Fundamentals of displacement based design	63
Figure 3.21 : Design displacement response spectra	64
Figure 3.22 : Difference of interstory drifts	67
Figure 3.23 : Effect of torsion on member displacements	68
Figure 3.24 : Adaptive force distribution for a regular framed building	71
Figure 3.25 : Comparison for regular structures	72
Figure 3.26 : Comparison for irregular structures	72
Figure 3.27 : Flowchart of the adaptive pushover procedure	73
Figure 3.28 : Discretization of a typical reinforced concrete cross-section	74
Figure 3.29 : Fibre model for a reinforced concrete section	75
Figure 3.30 : Lumped plasticity model elements	75
Figure 3.31 : Scaling of modal displacements through response spectrum	78
Figure 3.32 : Comparison of the DAP method with other pushover procedures	81
Figure 3.33 : Comparison of capacity curves for different pushover procedures	82
Figure 3.34 : Lateral load pattern for force based adaptive procedures	83
Figure 3.35 : Variation of the incremental applied load pattern at different steps....	83
Figure 3.36 : Determination of modal story forces and story shear profiles	84
Figure 3.37 : Determination of the combined modal story shear profile	85
Figure 3.38 : Evaluation of the load pattern	85
Figure 3.39 : Flowchart of the proposed procedure	86
Figure 3.40 : Drift comparisons of SAC-20 for different earthquake excitations ...	87
Figure 4.1 : Domain and Analysis objects of OpenSees	90
Figure 4.2 : Test model of SPEAR building in ELSA, Ispra	92
Figure 4.3 : Geometry of the test model	92
Figure 4.4 : Plan view of SPEAR building	93
Figure 4.5 : Reinforcement layout for a typical beam (units are in mm)	93
Figure 4.6 : Cross section properties of SPEAR (units are in mm)	94
Figure 4.7 : Footings plan of SPEAR (units are in mm)	94
Figure 4.8 : XTRACT modeling of the materials (kN-mm).	95
Figure 4.9 : Gravity load distribution	96
Figure 4.10 : Common hysteresis for inelastic springs in lumped models	97
Figure 4.11 : P-M interaction for C6 column in both directions.	98
Figure 4.12 : P-M interaction for other columns in x direction.	98
Figure 4.13 : M- ϕ relation for the beam elements.	99
Figure 4.14 : Center of mass and center of stiffness of the SPEAR building	99
Figure 4.15 : Accelerograms for longitudinal and transverse directions.	101
Figure 4.16 : Response spectrum of Montenegro'79 earthquake.	101
Figure 4.17 : Local Axes of NASAP.	103
Figure 4.18 : Input menus for Story Levels and Material properties.	103
Figure 4.19 : Section input menu.	104
Figure 4.20 : Hinge input screen of NASAP.	105

Figure 4.21 : Analysis case menu of NASAP.....	106
Figure 4.22 : Flowchart of NASAP for non-adaptive pushover procedure.	107
Figure 4.23 : Flowchart of NASAP for an adaptive pushover procedure.....	109
Figure 4.24 : Lateral drifts of multi-story building	111
Figure 4.25 : Geometric Nonlinearities	111
Figure 4.26 : P- Δ and P- δ effects for elastic cantilever column	112
Figure 4.27 : P- δ effect when column yields	113
Figure 4.28 : 3-D SPEAR model of NASAP.....	114
Figure 4.29 : Mode Shapes and periods of the 3-D Spear model.	115
Figure 4.30 : Mode Shapes of the 3-D NASAP-Spear model.	115
Figure 4.31 : Story shear profiles for longitudinal direction.....	117
Figure 4.32 : Story shear profiles for transverse direction.....	117
Figure 4.33 : Story drifts in longitudinal direction.	118
Figure 4.34 : Store drifts in transverse direction.....	118
Figure 4.35 : Comparison of conventional and SSAP curves.....	119
Figure 4.36 : Longitudinal direction load pattern.	119
Figure 4.37 : Transverse direction load pattern.	120
Figure 4.38 : Comparison of ELSA test results with pushover curves for Story-1	120
Figure 4.39 : Comparison of ELSA test results with pushover curves for Story-2	121
Figure 4.40 : Comparison of ELSA test results with pushover curves for Story-3	121

AN ADAPTIVE 3-D PUSHOVER PROCEDURE FOR DETERMINING THE CAPACITY OF EXISTING IRREGULAR REINFORCED CONCRETE (RC) BUILDINGS

SUMMARY

Especially in the last two decades, determining the structural capacity by using the nonlinear conventional static analysis methods has been widely used. Besides the fact that they lack of investigating the sign changes and the reversal effects of the higher modes, the static approaches need less computational time than the dynamic ones. This is the main reason why the majority of the design engineers prefer to use them.

To overcome the mentioned deficiencies, the researchers proposed to determine the capacity by using different techniques. Adaptive pushover procedures, energy based approaches might be some examples to them. The main difference between the proposed adaptive procedures is the determination of the lateral load pattern. When the literature is checked, it can be concluded that majority of the investigated procedures are not able to take in to account the higher mode effects and the sign changes of the modal quantities since they use SRSS or CQC to combine the modal effects. Besides, most of the techniques are only applicable for 2-D models. They neglect the issue of torsion, whilst today it is a known fact that, irregularities should be investigated especially when higher modes are effective.

Story shear adaptive based procedure is where the lateral load pattern is defined basing on the story forces. In the procedure, the lateral load pattern is calculated by investigating the sign changes. In this study, the story shear based adaptive pushover procedure has been improved for including the torsional effects by using a computer code, NASAP, which is capable of 3-D modeling. SPEAR building which was tested in ELSA laboratories, has been chosen as the test model since it is an irregular reinforcement concrete (RC) building assembling the majority of existing structures in Turkey.

The results of the adaptive pushover procedure is compared with the time history analysis that are implemented using Perform 3-D and the drift profiles are determined. The experimental results that are gathered from ELSA, are compared with the theoretical results of the developed nonlinear static program. It has been stated that, the calculated results using the proposed procedure are in good agreement with the experimental ones. It is also shown that, the conventional procedures overestimates the capacity according to the time history domain analysis by 20%.

MEVCUT DÜZENSİZ BETONARME YAPILARIN KAPASİTELERİNİN BELİRLENMESİ İÇİN ÜÇ BOYUTLU UYARLAMALI İTME ANALİZİ YÖNTEMİ

ÖZET

Özellikle son 20 yılda, yapıların kapasiteleri doğrusal olmayan klasik statik metotlar kullanılarak tespit edilmektedir. Statik yaklaşımlar, dinamik metotlara nazaran daha az bilgisayar emeği ve daha az hesaplama zamanına ihtiyaç duydukları için, çoğu tasarım mühendisi tarafından tercih edilirler. Buna rağmen, statik yöntemlerle yüksek modların etkilerini ya da modların işaret değişimlerini incelemek mümkün olamamaktadır.

Bu olumsuzlukların önüne geçebilmek için, araştırmacılar yaygın olarak kullanılan klasik yöntemlerin geliştirilmesi gerektiği konusunda birleşmişlerdir. Uyarlamalı yöntemler ya da enerjiye dayalı yaklaşımlar bu çalışmaların sonuçlarına örnek olarak gösterilebilirler. Önerilen uyarlamalı yöntemlerin esas farklılıkları, yanal yük vektörünün tespiti sırasında ortaya çıkmaktadır. Literatür taraması yapıldığında, önerilen bu yöntemlerin çoğunda dahi, yüksek modların etkileri ve modların tersinir etkilerinin ihmal edildiği gözlemlenmektedir. Söz konusu metotların çoğu, iki boyutlu düzlemde modelleme esasına dayanır ve burulma etkilerini analizlerde dikkate almamaktadırlar. Oysaki günümüzde, burulma etkilerinin özellikle de, yüksek modların etkileri önemli olduğunda dikkate alınması gereken bir etmen olduğu bilinmektedir.

Kat kesme kuvvetlerine dayalı uyarlamalı yöntemin temelinde, yanal yük bileşeninin kat kesme kuvvetleri dikkate alınarak hesaplanması yatmaktadır. Bu yöntemle modların tersinir etkilerini de dikkate almak mümkündür. Bu çalışmada, kat kesme kuvveti esasına dayalı uyarlamalı itme analizi yöntemi, üç boyutlu modelleme ve çözüm yapabilen bir program, NASAP, ile burulma etkilerini de dikkate alacak şekilde geliştirilmiştir. ELSA Laboratuvarında deneyleri gerçekleştirilen ve Türkiye'deki mevcut birçok yapı gibi düzensizlikleri bulunan SPEAR binası, geliştirilen yazılım ile test edilmek üzere örnek model olarak seçilmiştir.

Uyarlamalı statik itme analizi sonuçları, PERFORM 3-D kullanılarak yapılan zaman tanım alanı sonuçları ile mukayese edilmiş ve kat ötelemeleri karşılaştırmaları belirlenmiştir. ELSA Laboratuvarından elde edilen deney verileri, geliştirilen yazılım ile bulunan teorik hesap sonuçları ile karşılaştırılmıştır. Önerilen yöntem ile bulunan sonuçların, deney sonuçları ile tutarlı oldukları gösterilmiş ve klasik yöntemle elde edilen sonuçlar ile zaman tanım alanı sonuçları arasında %20'ye yakın fark olduğu tespit edilmiştir.

1. INTRODUCTION

In recent years, performance-based design methods have been started to use widely among the engineers. Those methods rely on nonlinear static analysis procedures (NSP). Although, nonlinear time history analysis is known as the most accurate way to determine the structural demand, it needs expertise and more effort in computation process. That is the main reason why structural engineers prefer to use nonlinear static procedures for evaluating the seismic capacity of both existing and newly form buildings.

Modern standards and guidelines, such as FEMA 440 [1], FEMA 356 [2] and ATC-40 [3] proposed solution methods for the inelastic analysis procedures. In fact, all the documents present similar approaches. FEMA 356 uses Coefficient Method, whereas ATC-40 uses Capacity Spectrum Method while determining the capacity. Both of the methods represent the inelasticity of the building using pushover techniques with a difference in the calculation of the inelastic displacement demand [1].

Recent studies showed that, conventional procedures should be improved. Their deficiencies make the results unreliable and mislead the structural engineers. The main disadvantages of the method can be summarized as follows;

- a) Conventional static methods are only adequate when the fundamental mode is predominant.
- b) They neglect the progressive changes in the modal properties and the higher mode effects [4].
- c) They imply a separation between structural capacity and earthquake demand, whereas recent researches have shown a correlation between structural capacity and demand of an earthquake.
- d) Conventional procedures neglect the dynamic effects and as a result of this, the kinetic and viscous damping energy changes during a monotonic push cannot be determined [4].

- e) Ongoing studies have also shown that, conventional pushover analyses give inaccurate results for 3-D irregular structures. Torsional effects and irregularities cannot be taken into account during a monotonic push [5]. Majority of the conventional procedures rely on 2-D plane which also leads to an inaccurate modelling of the structure.

Researchers developed different analysis strategies in order to overcome all the above mentioned deficiencies. Elnashai et al. (2005) suggested a combination of pushover analysis with fibre models, where the moment-curvature response is derived from the material characterization [5]. Chopra et al. [6] developed multi-mode pushover analyses.

Cornell et al. suggested incremental dynamic analysis procedures (IDA) where at each analysis step multi modal time history analyses are implemented [7]. In addition, Aydınoğlu [8] has developed an Incremental Response Spectrum Analysis (IRSA) method, where he proposed to perform pushover analysis according to the incremental displacements. The instantaneous inelastic spectral displacements are used to calculate the modal story displacements at each step. Then the capacity curves are transformed in to spectral acceleration-spectral displacement response spectrum (ADRS) format.

Recent studies rely on adaptive pushover procedures, which take into account the higher mode effects, and update the load pattern at instantaneous states of inelasticity with a less computational time and effort. Shakeri et al. (2010) proposed a story shear based adaptive pushover procedure [9], where at each analysis steps the load pattern, which is derived from the modal story shear profiles, is updated. The higher mode effects and the reversal of the modes are also taken into account. While the other adaptive pushover procedures combine the different modal quantities by using SRSS or CQC; Shakeri et al. [9] proposed first to calculate the combined modal story shear forces using SRSS or CQC and then to calculate the story shears for each mode. This gives the opportunity to investigate the sign reversal effects of the modal forces especially in the upper stories. Negative quantities can be taken into account along the height of the structure.

However, adaptive pushover procedures are still need to be developed. Irregularity and torsional effects should be considered in the adaptive analysis. 3-D adaptive pushover analysis is still a phenomenon for the structural engineers and designers. Today it is a well-known fact that, discarding the irregularity effects will make the analysis results doubtful. More studies should be implemented on including the torsional effects in the adaptive pushover analysis.

1.1 Purpose of the Thesis

Main idea of the thesis is to explain briefly the need of a newly adaptive pushover procedure, which can investigate the negative sign changes of the modal quantities. As mentioned before, majority of the adaptive procedures use SRSS or CQC while combining the modal effects, which concludes omitting the reversal effects of the modes. It will be explained in the study that, force based story shear adaptive procedure [9] overcomes this deficiency, though it still needs some improvements.

The original procedure proposed by Shakeri et al. [9] neither uses a 3-D model nor considers the irregularity effects of a 3-D structure. Today it is a well-known fact that, omitting torsional effects misleads the analysis results. That is why in this study, the investigated procedure has been modified for existing irregular reinforced concrete (RC) buildings. Torsional effects are taken into account and the main procedure has been updated for 3-D planar structures.

In order to consider the torsional effects, a 3-D software package is developed in the present work and it is named as “*NASAP*” (Oyguç, Özçitak, 2010). This is a tool for finite element analysis of structural components, meaning “*Nonlinear Adaptive Structural Analysis Program*”. It is feasible for three-dimensional modelling and it prosecutes the adaptive pushover procedure proposed by Shakeri et al. [9]. In its background, *NASAP* uses the developed modules for open code program “*OpenSees*” [10]. *OpenSees* is an open source software which is coded in C++ and uses several Fortran and C numerical libraries.

NASAP uses the concentrated plastic hinge concept while performing nonlinear analysis. The target displacement for the adaptive pushover analysis is calculated by the formulas given in FEMA 356 [2]. P-Delta effects are neglected in the analysis.

A 3-D irregular reinforced concrete building, which was built in 2003 within the European network Seismic Performance Assessment and Rehabilitation (SPEAR) project [11], has been examined with NASAP. SPEAR building was designed for gravity loads with the concrete code applied in Greece between 1954 and 1984 and with construction practice and materials commonly used in Southern Europe in the early 70's. It's also a representative of older constructions that were built in Southern European. Since the majority of the existing concrete buildings in Turkey have the same design properties with SPEAR, it will be an appropriate example to examine.

In this study, the pseudo-dynamic experiment results of the ELSA Laboratory are compared with the adaptive pushover results of the developed computer code. The adaptive pushover curves are found to be in good correlation with the experimental results. Besides, Montenegro'79 [12] time-history analysis of SPEAR building are conducted with PERFORM 3-D (CSI) [13]. The results of the time history analysis are compared with the adaptive and non-adaptive pushover results of NASAP, and the applicability of the proposed method has been discussed.

1.2 Background

Design engineers use inelastic analysis procedures for the seismic evaluation and design of existing buildings as well as the design of new constructions. The main objective of inelastic seismic analysis procedures is to predict the expected behaviour of the structure under an earthquake excitation. During the past decade, significant progress has been made in nonlinear static analysis procedures [1].

Nonlinear static procedures are based on converting the multi degree of freedom system (MDOF) to an equivalent single degree of freedom system (SDOF). They produce estimates of the maximum displacement, story drifts and other structural components. Structural capacity is determined by the pushover or capacity curve that was used to generate the equivalent SDOF model. As a known fact, in pushover analysis, static forces are distributed along the height of the structure and the structure is pushed until a predefined target displacement is reached. If the lateral load pattern is kept constant through the analysis, the method is called as *conventional pushover* and if the load pattern is constantly updated through each analysis step in the inelastic range, then the analysis method is called as *adaptive pushover method*.

Flowchart of a conventional inelastic pushover procedure using elastic spectrum is illustrated in Figure 1.1 [1].

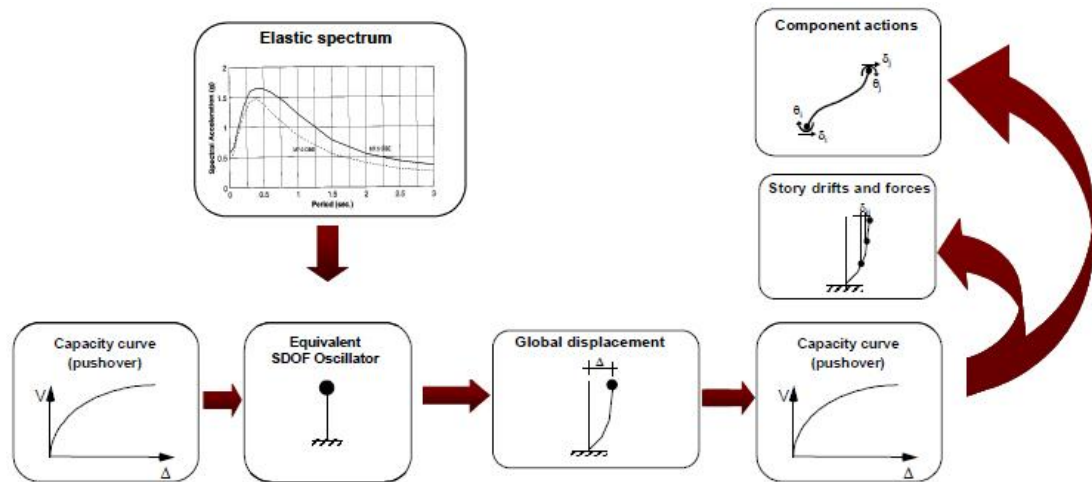


Figure 1.1 : Flowchart of an inelastic pushover procedure [1].

Freeman proposed a graphical procedure to determine the capacity of a structure excited by an earthquake. The proposed procedure is called as the *Capacity Spectrum Method (CSM)* [14]. The method is still widely used among the structural engineers. The main aim of the procedure is to compare the capacity of a structure to the demands of earthquake response with a graphical evaluation. The intersection of the capacity and demand curve represents the force and displacement of the structure for the investigated earthquake. This makes it easy to decide how the structure will perform when subjected to a ground motion.

Paret et al. [15] and Sasaki [16] suggested *Multi-Mode Pushover Procedure (MMP)* which take into account the higher mode effects. They use the capacity spectrum method (CSM), which was proposed by Freeman [14], while determining the capacity of the structure. Figure 1.2 shows the intersection of capacity and demand curves in *Acceleration-Displacement Response Spectrum (ADRS)* format. Capacity curves were generated ignoring the modal combination effects. This modal pushover procedure predicts performing several pushover analyses, using different lateral load pattern based on different elastic mode shapes. The proposed procedure takes into account the higher mode effects but neglects the modal changes during plastification. As stated before, the purpose is determining the capacity curves, which represent the response of the building using Capacity Spectrum Method (CSM) [14].

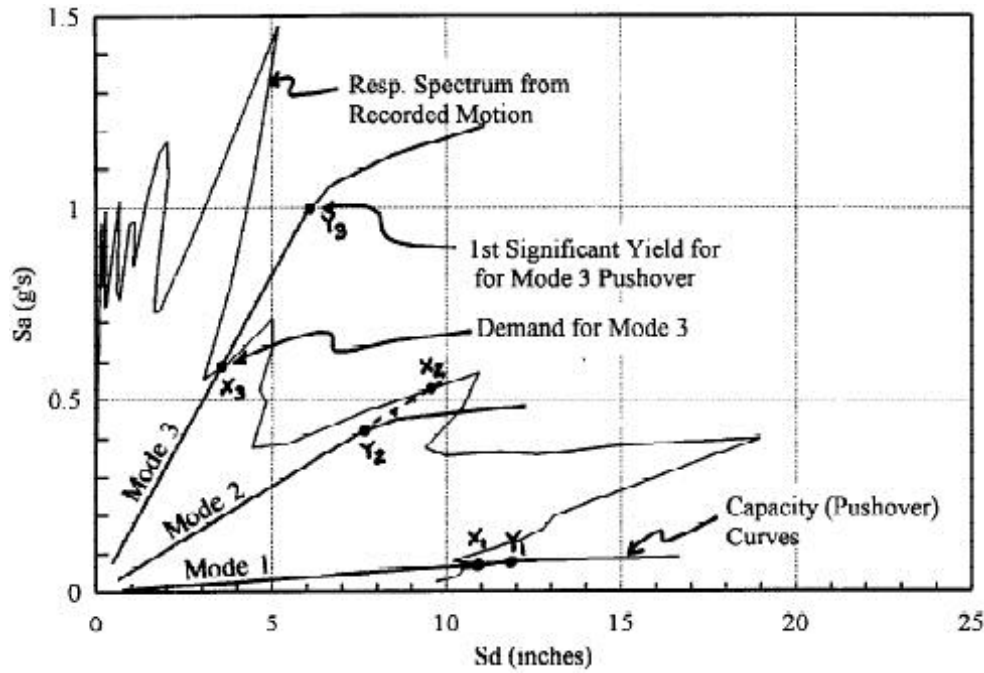


Figure 1.2 : Capacity and demand curves in ADRS format [15].

Moghadam [17] proposed a modal combination procedure, *Pushover Results Combination (PRC)*, for multi-mode pushover analysis. According to this method, several pushover analysis are carried out by using the modal load pattern. The maximum response is then estimated by combining the pushover results of each different mode.

Chopra and Goel [18] developed *Modal Pushover Analysis Procedure (MPA)*. The procedure is nearly same as Paret et al [15], except the modal capacity curves are idealized as bi-linear curves of an equivalent single degree of freedom (SDOF) system. Figure 1.3 shows the bi-linearization of the actual pushover curve. Total demand is calculated by combining the modal responses using the SRSS rule.

Since MPA procedure can not consider the effect of reversal and the modal interaction effectively, *Modified Modal Pushover Analysis Procedure (MMPA)* has been proposed by Chopra, Goel and Chintanapakdee [19]. The main idea of the proposed procedure is that the seismic demands are obtained by combining the inelastic response of fundamental modal pushover analysis with the elastic response of higher modes.

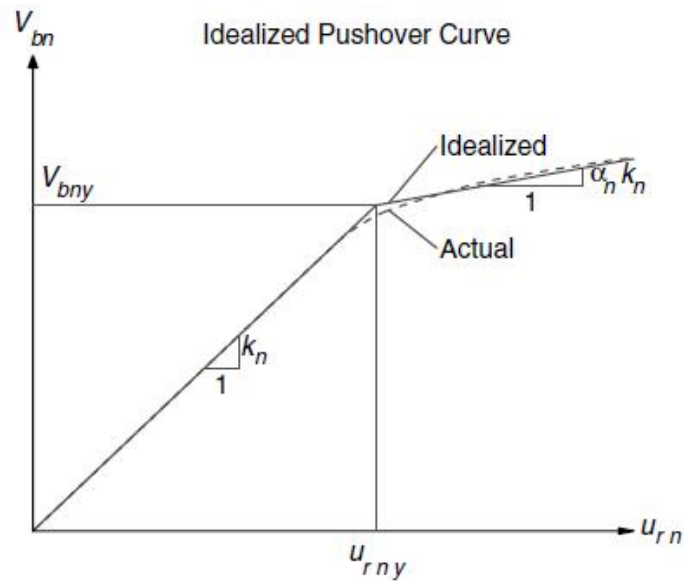


Figure 1.3 : Bi-linearization of the actual capacity curve [18].

Reinhorn [20] suggested techniques for the evaluation of inelastic response and the inelastic deformation for both single degree of freedom systems (SDOF) and multi degree of freedom systems (MDOF) through a spectral approach. Building response is determined by using inelastic spectra, which is evaluated for various strength reduction factors from selected ground motions. The maximum displacement is determined by the capacity envelope of the inelastic response. Figure 1.4 shows how to determine inelastic response by using inelastic spectra and capacity diagram according to the proposed method. The inelastic demand can be obtained using either single mode or multiple modes considerations using the above procedures. From numerical studies of regular structures, it can be concluded that only the first mode characteristics and spectral ratios seem to be important while determining the capacity.

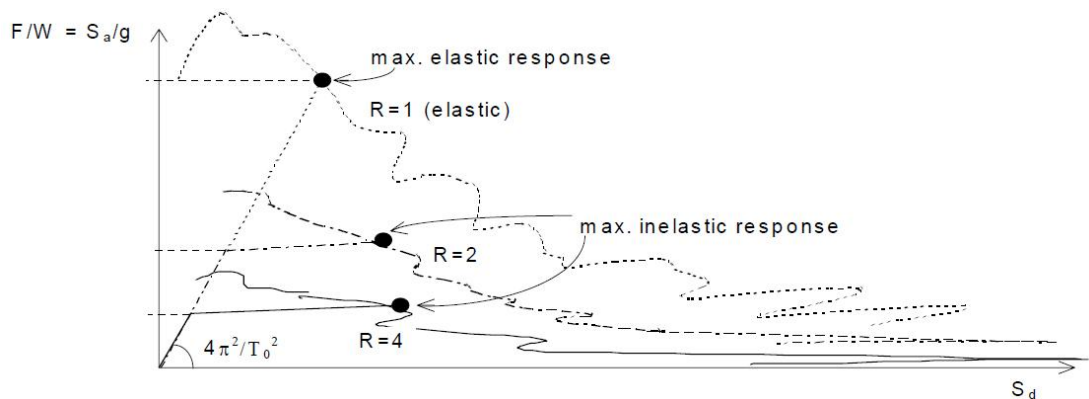


Figure 1.4 : Determination of inelastic response using inelastic spectra [20].

If we consider the adaptive methods; it can be stated that, Bracci et al. [21] were the first using a fully adaptive procedure. They proposed an adaptive procedure, where, the equivalent elastic story shear and drift demand curves are determined using modal superposition rules. They propose to start the analysis by an assumed load pattern, mostly inverted triangular, and then imply the additional loads that are calculated from the previous step. The stiffness matrix is updated during that step, if there is a change in the elements. Load is applied until a predefined target limit is exceeded. Story capacities are then superimposed with the story response demand curves and the performance point is calculated.

Satyarno et al., [22] proposed a procedure, where the modal properties updated constantly due to the simultaneous changes through a modified Rayleigh method.

Requena and Ayala [23] have established a procedure, which takes into account the instantaneous higher mode effects. They proposed either deriving the story loads through SRSS combination or by using an equivalent fundamental mode until the plastic hinges started to form. In fact, the proposed method is a variation of the CSM [14]. The main difference of the proposed method is that, while determining the performance point, the capacity curve is not compared with the response spectrum of the excitation. Multi degree of freedom system (MDOF) is transformed into an equivalent single degree of freedom system (SDOF) system, and the maximum displacement is determined including the higher mode effects.

Gupta and Kunnath [24] proposed a methodology, where the applied load pattern is derived from the Response Spectrum Analysis. Depending on the instantaneous dynamic properties of the structure, load pattern is simultaneously updated. After performing eigenvalue analysis, the modal participation factor for that mode is calculated. Using the modal participation factor, story forces at each level for each mode is determined. Modal base shears are then computed, and they are combined using the SRSS to derive the structural base shear. Before performing a static analysis, the story forces are scaled using a scaling ratio. This means, for modes other than the fundamental mode, the structure will be pushed and pulled simultaneously.

Figure 1.5 shows the pushover results of SAC20 building [25] using different load patterns. In the study of Gupta et al. [24], they showed that uniform load pattern may only be applicable to structures in which higher modes are not significant. As additional modes are considered, the drift profiles approach to the ones obtained from the nonlinear time-history analysis. They concluded that, ignoring the higher mode effects misleads the demand results.

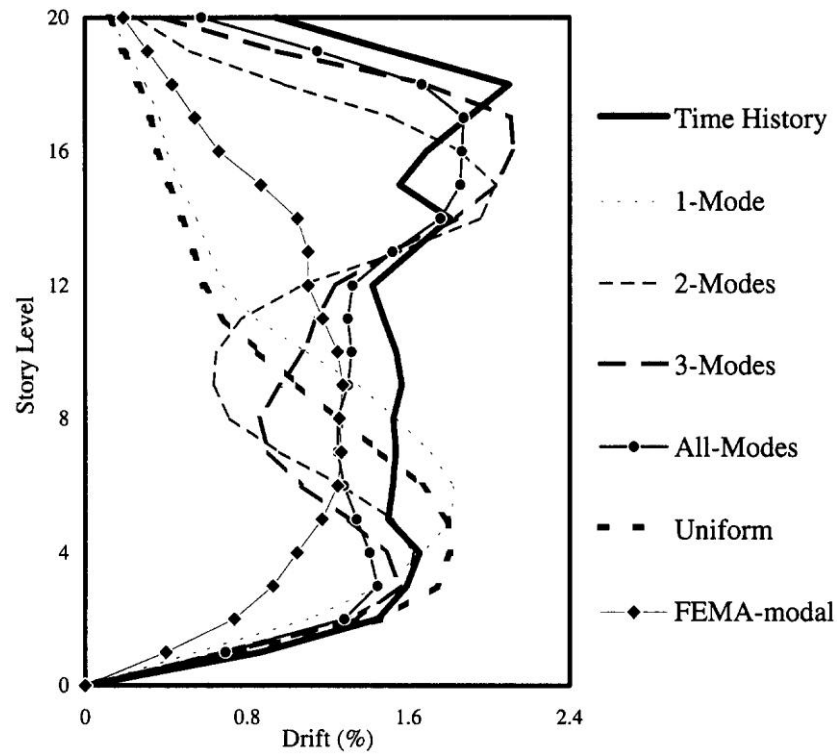


Figure 1.5 : Pushover results of SAC20 building for different loads [24].

Elnashai et al. [26-33] proposed a force-based adaptive procedure, where inelasticity is spread through the element length and across the section depth. In this procedure, the lateral load pattern is not kept constant during the analysis; it is continuously updated based on the instantaneous mode shapes. After defining the lateral load pattern, modal combination rules were used to determine the updated load vector. They also implemented an open source computer code called Zeus-NL, which was compared with time history analysis and determined to be very robust. For more detailed information, Elnashai et al. [28-32] can be examined. Regarding the fault effect, it can be stated that, adaptive pushover approach performs better than the conventional ones, especially at lower drift levels. This is shown for a 6-degree of freedom regular structure in Figure 1.6 [33].

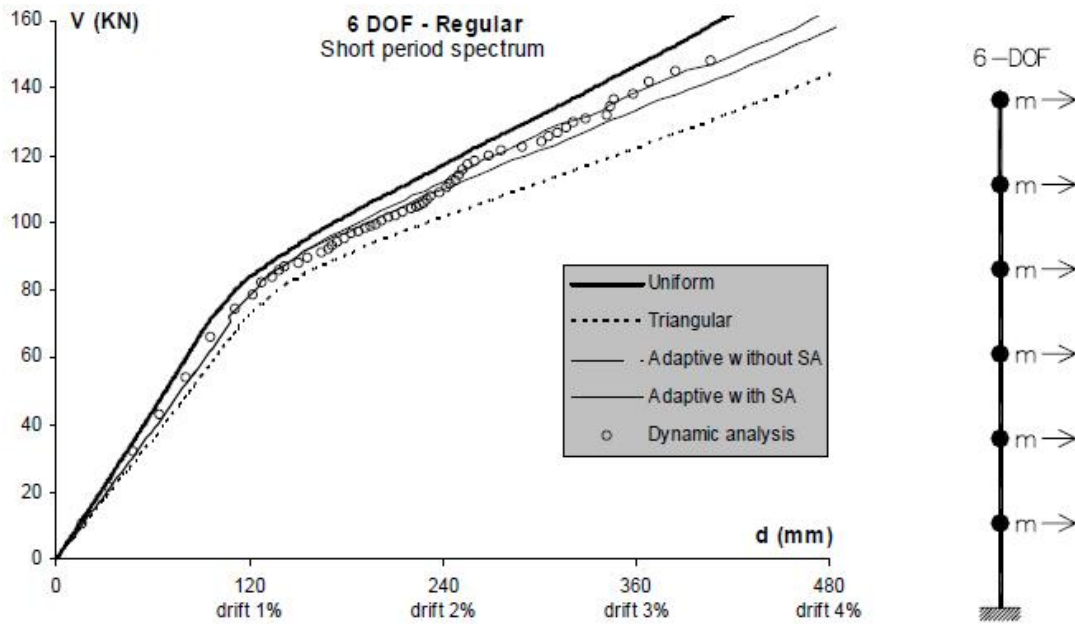


Figure 1.6 : Comparison of pushover and dynamic analysis [33].

Albanesi et al. [34] proposed energy based adaptive pushover procedure, where at each step they consider the kinetic energy properties as well as the inertial properties of the structure. They consider their method as robust in their work. It can be seen from Figure 1.7, energy based procedure is in good agreement with force and displacement based adaptive pushover procedures.

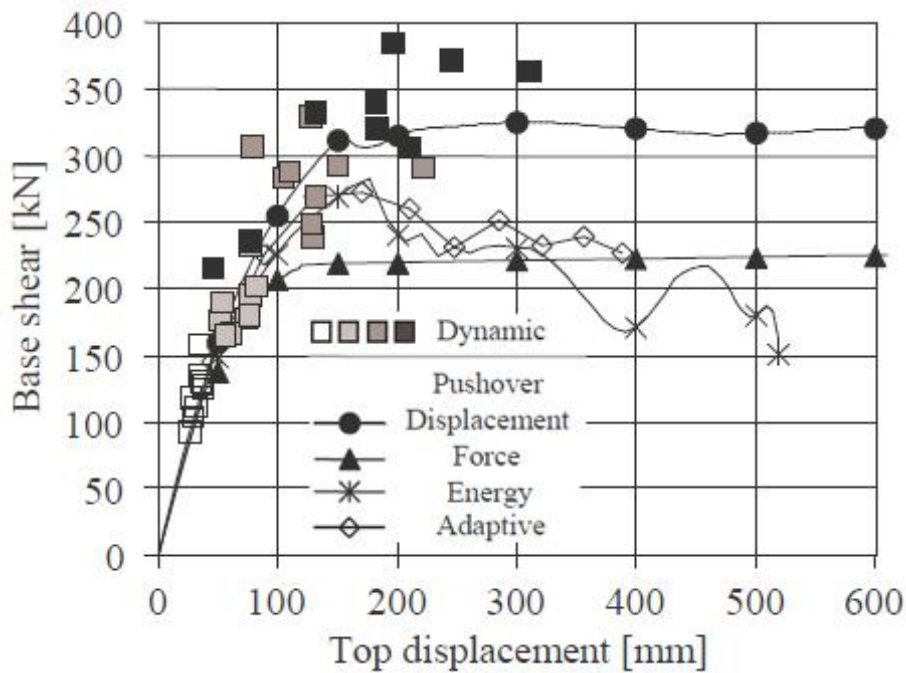


Figure 1.7 : Comparison of different pushover analysis for tall frames [34].

Antoniou [35] proposed a modal adaptive pushover procedure which is indeed similar to Reinhorn's, but differs in the incremental scaling approaches. The graphical representation of incremental updating of the load pattern is shown in Figure 1.8.

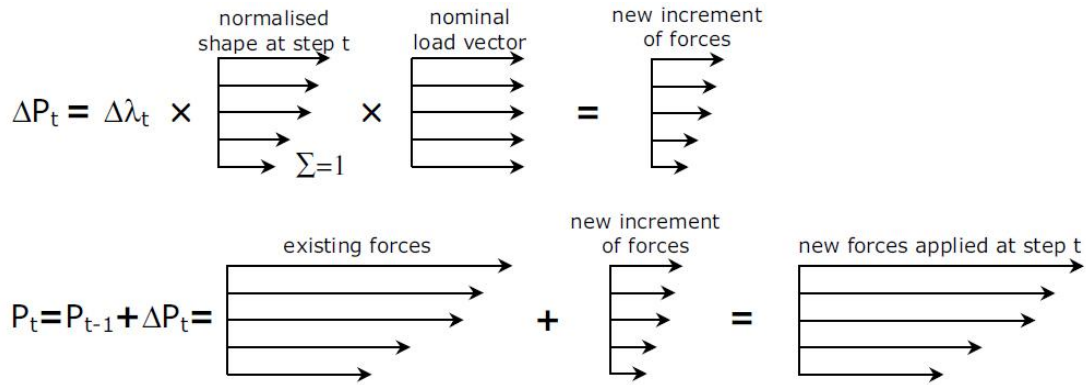


Figure 1.8 : Comparison of loading force vector determination [35].

Aydinoğlu [8] proposed an *Incremental Response Spectrum Analysis*, similar to Gupta and Kunnath's procedure. However, in this procedure, the pushover analysis is performed according to incremental displacements where in each step inelastic spectral displacements are used to determine the modal story displacements. IRSA procedure uses either SRSS or CQC while combining the modal responses, though CQC gives more realistic results when torsional response is important and close modes occur.

Antoniou and Pinho [36-38] developed displacement-based adaptive pushover method (DAP) where at each step; displacement load pattern is applied to the structure. Story forces are calculated as a response of the displacement loads. Figure 1.9 shows the shape of load vector, which is updated at each analysis step for the displacement-based adaptive pushover procedure.

Shakeri et al. [9] proposed a *Story Shear Based Adaptive Procedure (SSAP)* for nonlinear static analysis. It is based on the story shear forces. Reversal of sign changes and higher mode effects are taken into account. At each step, the load pattern is derived from the modal story shears of the instantaneous step. Using the energy concept, multi degree of freedom system (MDF) is converted to an equivalent single degree of freedom system (SDOF), and the target displacement is determined.

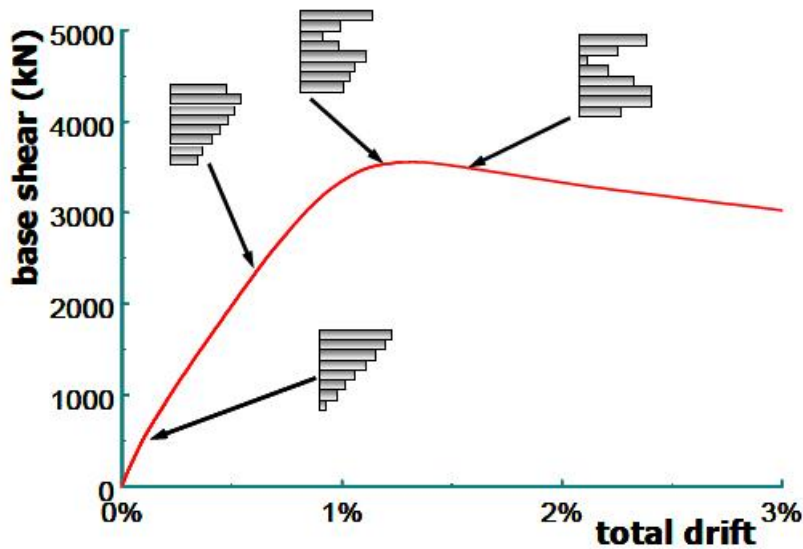


Figure 1.9 : Adaptive pushover schema [37].

Figure 1.10 shows the basic steps of the SSAP procedure. In the conventional force based adaptive procedures, modal story forces (Figure 1.10.a) are combined with SRSS to determine the load pattern (Figure 1.10.d'). In SSAP, modal story shears profiles are calculated (Figure 1.10.b) and then the combined modal story shears are determined (Figure 1.10.c). Load pattern is derived by subtracting the modal story shears (Figure 1.10.d).

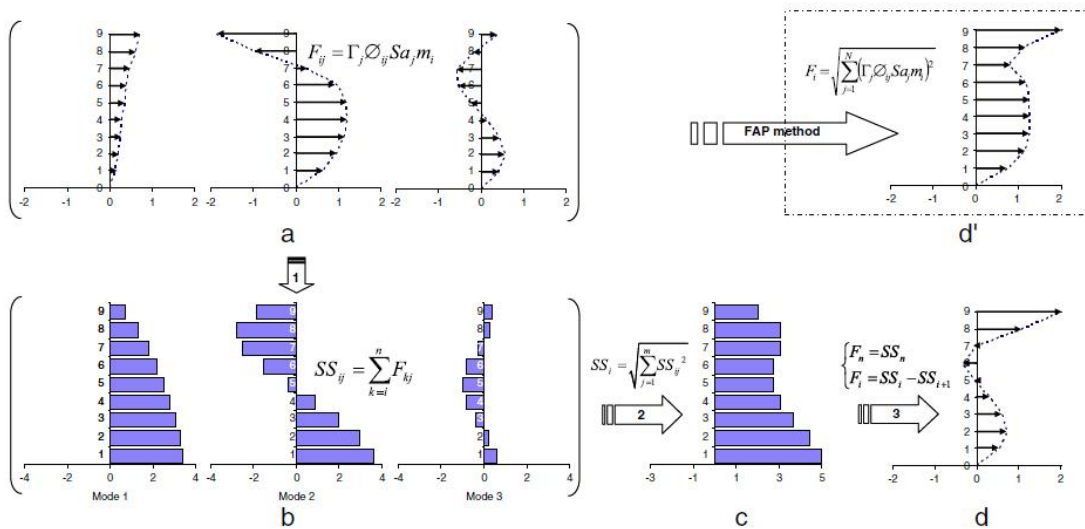


Figure 1.10 : Story shear based adaptive pushover (SSAP) procedure [9].

Even if the SRSS combination rule is used in the proposed procedure, the applied force will be negative when the calculated modal shear in one story is less than the upper story. That is the main advantage of the method on the others. Both sign reversals and higher mode effects can be taken into account in this procedure.

1.3 Overview

Chapter-1 is the introduction section of the implemented study. Previously executed researches to determine the nonlinear seismic capacity of structures are considered by their basic points in this section. The basic assumptions and the main differences between the conventional and the adaptive pushover procedures are investigated throughout a literature review.

Performance based design approach has been discussed in Chapter-2. The given performance levels in FEMA 356 [2] has been considered briefly. Structural and non-structural performance objectives are defined. Correlation matrix has been used to determine the correlation between the structural characteristics and the socio-economic factors. The difference between the ductile and non-ductile structural demand has been checked. Effects of hysteretic behaviour on seismic response are examined in detail. The defined nonlinear parameters in FEMA 440 [1] have also been examined briefly. Elasto-plastic, strength-hardening, stiffness degrading, pinching, cyclic strength degradation and in-cycle strength degrading are briefly studied. Definitions of backbone curve and cyclic envelope concepts are given. At the end of the chapter, plasticity concept is examined. Different types of plasticity are given. Yield surface concept and the methodology of determining the P-M interaction curves are discussed.

Chapter-3 is where the analysis methods for determining the capacity of the structures have been discussed briefly. At the beginning of the chapter, the common methods that are used in earthquake engineering are investigated. The basic differences between the static and dynamic analysis are stated. Types of dynamic and static analysis are figured out. The mainly discussed subject in the chapter is the pushover analysis concept. Evaluations of the structures using conventional pushover procedures are examined. The defined methods to determine the nonlinear structural capacity in FEMA 356 [2] and ATC 40 [3] are considered. Capacity curve and the displacement coefficient concepts are explained. At the end of the chapter, N2 procedure, modal pushover method, energy based approaches and displacement based procedures considered. Issue of torsion and the ways of including the torsional effects to the analysis have been discussed briefly. Deficiencies of the conventional pushover methods and the need to improve them are determined. Adaptive pushover techniques and the flow diagram of them are stated in this chapter.

Fibre modelling and the concentrated plasticity approaches are also studied in chapter-3. The methodology of adaptive spectra based procedures, incremental response spectrum analysis and the consecutive procedures are examined in details. Story shear based adaptive pushover procedure has been discussed briefly through the chapter. Its methodology and flow diagram have been given.

The developed 3-D nonlinear adaptive structural analysis program (NASAP) and its basis are investigated in chapter-4. The developed program is based on the theory of OpenSees [10] scripts. The modules of OpenSees are explained in details. The properties of the “Seismic Performance Assessment and Rehabilitation of Existing Buildings Project, SPEAR” are briefly explained in this chapter. Its geometry, material properties and design parameters are stated briefly. The analysis model is explained in detail. $M-\phi$ relations of column and beam elements are calculated using XTRACT [79]. Determination of the artificial earthquake record is investigated in this Chapter. The 1.15g and 0.2g scaled and EC8 fitted response spectrums are determined in the chapter. At the end of the chapter, properties of NASAP are given in detail. Its flowchart has been reviewed. The important part of the chapter may be classified as the section, where the results of the adaptive pushover analysis and their comparison with the pseudo-dynamic tests are given. In that section, the calculated modal quantities, peak story shear profiles of the chosen analysis steps are figured out. Time-history, which are conducted using Perform 3-D [13], drift results are compared with the adaptive pushover results of NASAP using the response spectra previously defined. The comparison graphs are given. Also the comparison of the adaptive and non-adaptive pushover curves with the conventional pushover analysis has been determined. The adaptive load pattern for the chosen analysis steps are given in this chapter. In addition to this, pseudo-dynamic test results of the SPEAR building have been compared with the adaptive pushover results of the developed computer code.

Conclusions and recommendations are discussed in Chapter-5 briefly. Application of work, the usage of the proposed method and the results are briefly examined in this chapter. At the end of the chapter, outlook of the study has been stated.

2. PERFORMANCE BASED DESIGN

Performance based design criteria are an important structural factor that shows the capacity of the building. Today, besides retrofit strategies newly formed buildings are also designed using the performance criteria's. Some structural definitions should be made before explaining the performance criteria; *Stiffness* can be defined as the ability of a component to resist deformations under earthquake excitation. It is not a constant value; it changes according to the structural capacity. *Strength* is defined as the capacity of a component for a given response. It is also not a constant value. *Ductility* is the ability of a component to deform beyond the elastic limits. *Demand* is the deformation imposed on a component when subjected to ground motion. Demand varies as the structural characteristics vary during inelastic response [39].

2.1 Performance Levels

It has been defined six structural and five non-structural performance levels in FEMA-356 [2]. Building performance is defined as a combination of both structural and non-structural components performance levels. Besides, *Target Building Performance Levels* are designated alphanumerically with a number representing the Structural Performance Level and a letter representing the non-structural performance level (e.g., 1-B, 3-C) in FEMA-356 [2].

After an earthquake, if there is minimal or no damage in the structural and non-structural components then the level is named as *Operational Building Performance Level* and denoted by *1-A*. Although it is not economically practical to design all the buildings for this target level, buildings meeting this target will have a low risk to life safety.

If a minor damage in the non-structural elements and no damage in the structural elements are occurred, then the level is called as *Immediate Occupancy Building Performance Level* and denoted by *1-B*. The risk to life safety is very low at this level.

If an expensive damage is observed on both the structural and nonstructural components then the level is called as *Life Safety Building Performance Level* and is denoted by 3-C. Repairs should be made before reoccupancy. Life safety in this level is low.

Collapse Prevention Performance Level is denoted by 5-E. This level is essential in for seismic rehabilitation. In this level, the structure does not collapse but a failure of nonstructural components is observed. This level poses a significant hazard to life safety.

Building Performance Levels						
Non-structural Performance Levels	Structural Performance Levels					
	SP-1 Immediate Occupancy	SP-2 Damage Control (Range)	SP-3 Life Safety	SP-4 Limited Safety (Range)	SP-5 Structural Stability	SP-6 Not Considered
NP-A Operational	1-A Operational	2-A	NR	NR	NR	NR
NP-B Immediate Occupancy	1-B Immediate Occupancy	2-B	3-B	NR	NR	NR
NP-C Life Safety	1-C	2-C	3-C Life Safety	4-C	5-C	6-C
NP-D Reduced Hazards	NR	2-D	3-D	4-D	5-D	6-D
NP-E Not Considered	NR	NR	3-E	4-E	5-E Structural Stability	Not Applicable

Figure 2.1 : Target building performance levels [40].

This building performance levels are shown in Figure 2.1 [40]. In the figure, SP denotes structural performance, NP nonstructural performance and NR means not recommended. These numbered performance levels are called as *Target Building Performance Levels*. Each performance objective is a statement of the acceptable risk of incurring specific levels of damage. A decision team of building owner, structural design engineer and building officials should decide building performance objective. Once the performance objectives are set, a series of simulations should be performed to estimate the probable performance of the building under various design scenario events [41].

Due to earthquake excitations, FEMA356 [2] defines hazard levels which are either probabilistic or deterministic basis. Probabilistic ones are stated in terms of the probability of exceedance in a 50 years period, while the deterministic ones are in terms of specific magnitude of an active fault.

The Hazard Levels defined in FEMA 356 [2] are called as *Basic Safety Earthquake 1 (BSE-1)* and *Basic Safety Earthquake 2 (BSE-2)*. Rehabilitation Objectives can also be defined depending on this Hazard Levels. *BSE-1* has a probability of exceedance of 50% in 50 years while *BSE-2* has a probability of exceedance of 2% in 50 years. FEMA 274 [41] has investigated the relative cost value as the performance level increases. Figure 2.2 shows the surface of relative costs for various rehabilitation objectives.

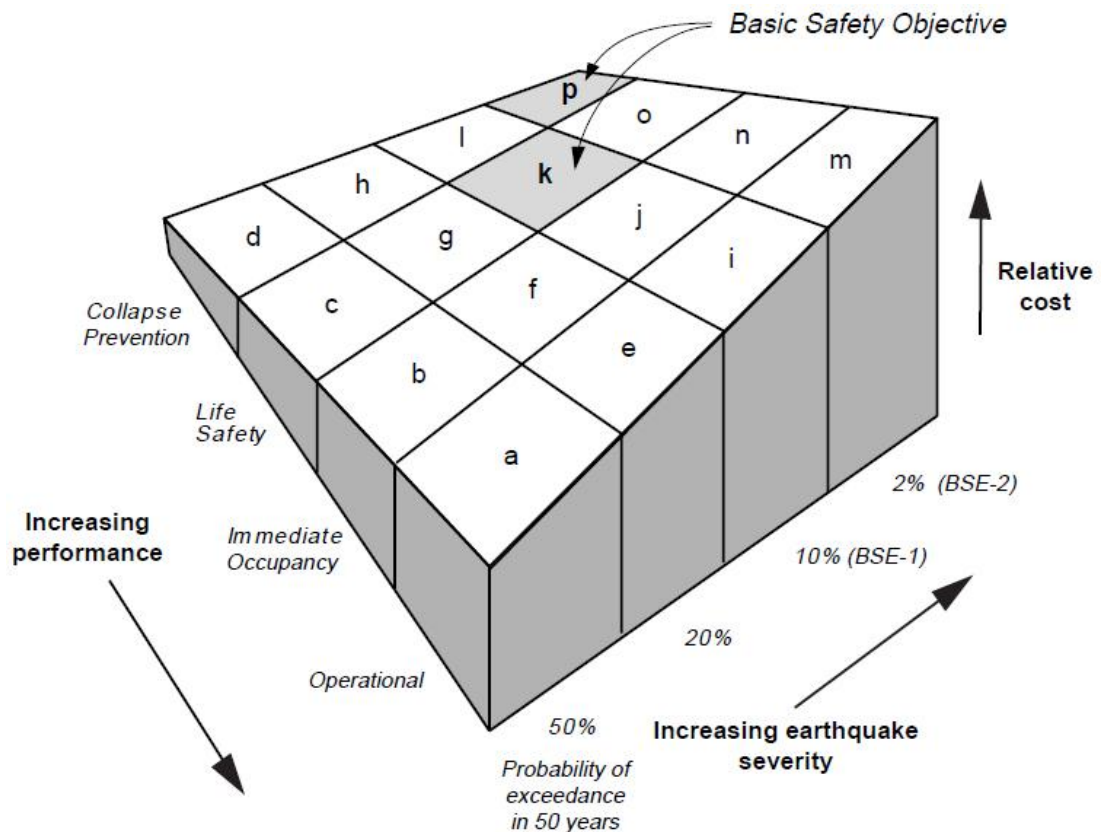


Figure 2.2 : Relative costs of various rehabilitation objectives [41].

Serviceability Limit State is defined as the state that has a return period of 75 years with a probability of exceedance of 50% in 50 years. *Damage Control Limit State* has a return period of 475 years with a probability of exceedance of 10% in 50 years, whereas *Collapse Prevention Limit State* has a return period of 2475 years with a probability of exceedance of 2% in 50 years [39]. Elnashai et al. explained this concept with a correlation matrix showing the performance levels in Figure 2.3 [39]. Performance and structural demand of a ductile and non-ductile structure under increasing lateral deformation are given in Figure 2.4 and Figure 2.5 respectively [41].

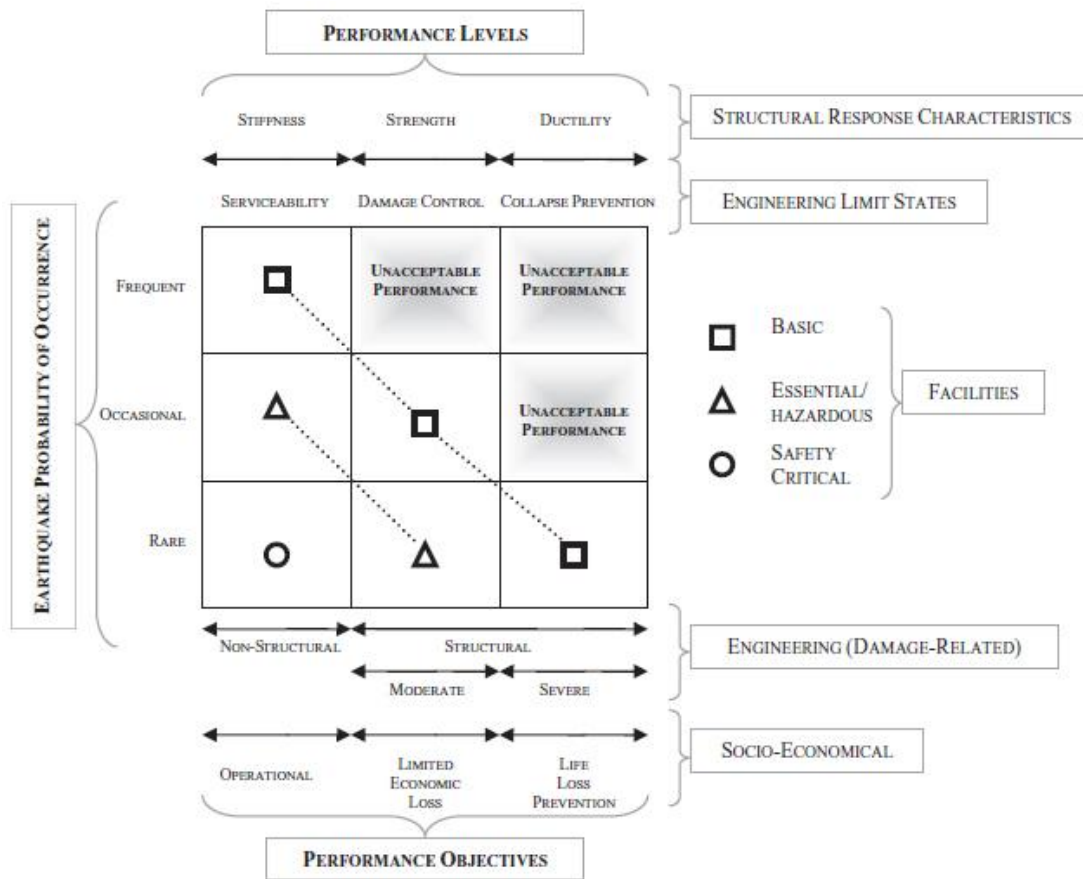


Figure 2.3 : Correlation Matrix showing performance levels [39].

Three discrete Performance Levels; *Immediate Occupancy*, *Life Safety* and *Collapse Prevention* are indicated in Figure 2.4 and Figure 2.5. It can be stated from the figures that the *collapse* occurs if the lateral deformation exceeds the defined collapse prevention performance level.

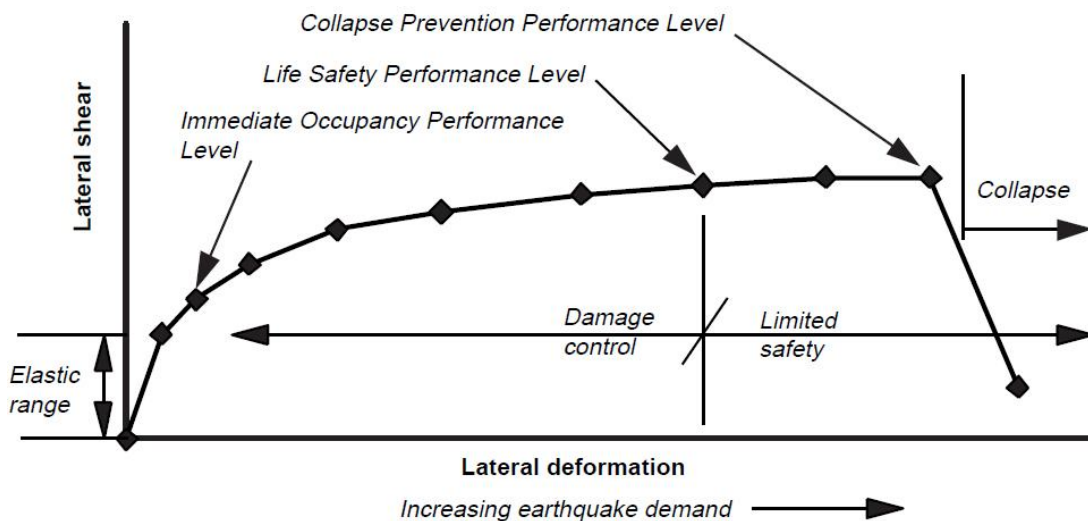


Figure 2.4 : Ductile performance and structural demand [41].

At the *Immediate Occupancy Level*, damage is limited and the structure protects its stiffness and strength, whereas at the *Collapse Prevention Level* structure experiences an extreme damage. Increasing lateral deformations might cause collapse. *Life Safety Level* is the stage where substantial damage is observed on the structure. In addition, significant stiffness loss may be observed in this stage as shown in Figure 2.4 and Figure 2.5. Last researches show that structures reaching the Life Safety Level might still experience at least 33% greater lateral deformation before collapse occurs [41].

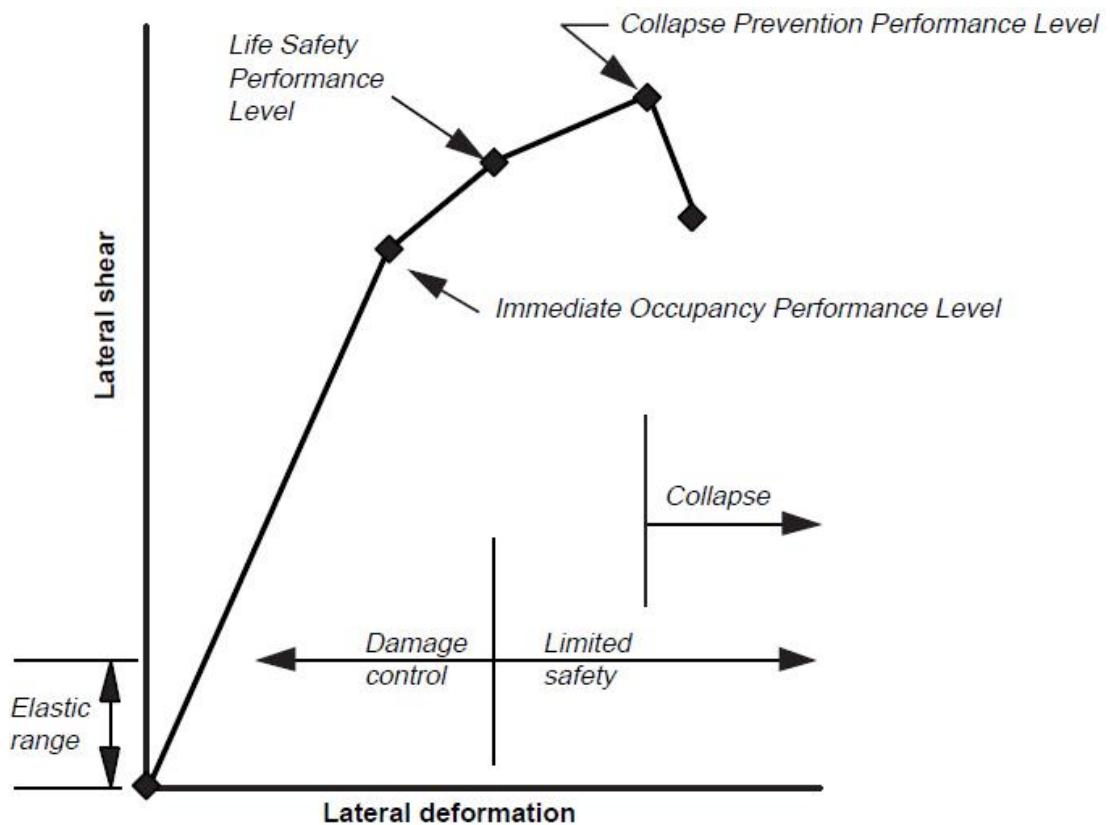


Figure 2.5 : Non-Ductile performance and structural demand [41].

In FEMA445 [42], it has been stated that, an earthquake excitation case can be simulated by using nonlinear analysis procedures. If the simulated performance meets the performance objectives, then the design is complete. If not, the design is revised in an iterative process until the performance objectives are met [41].

2.2 Effects of Hysteretic Behaviour on Seismic Response

FEMA 356 [2] and ATC 40 [3] defined some inelastic methods in order to evaluate the maximum displacement of the structural system, which is called as the *Performance Point* [3]. This spectral displacement is determined as the roof displacement in ATC 40 [3], whereas the *Target Displacement* in FEMA 356 [2].

Some assumptions had to be made in order to determine the target displacement. FEMA 440 [1] defined four basic hysteretic models used in the evaluation of current procedures, which are stated as *elastic perfectly plastic (EPP)*, *stiffness degrading (SD)*, *strength and stiffness degrading (SSD)*, and *nonlinear elastic (NE)* models. Basic hysteretic models are shown in Figure 2.6 [1].

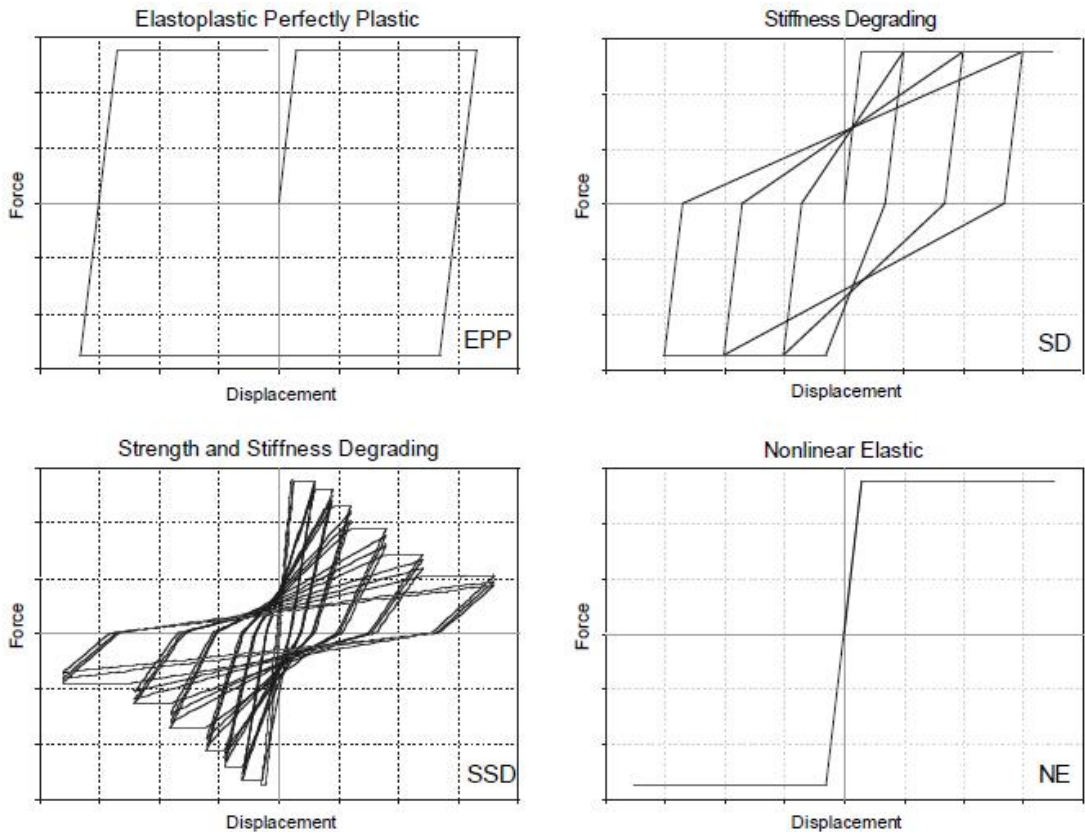


Figure 2.6 : Basic hysteretic models used in the current procedures [1].

2.2.1 Elasto-Plastic Behaviour

In the literature, the researches that are investigating the nonlinear behaviour mostly uses non-degrading hysteretic models. These models do not incorporate stiffness or strength degradation when subjected to repeated cyclic load reversals. The simplest non-degrading model can be stated as an *elasto-plastic model*. Figure 2.7 shows a non-degrading elasto-plastic model.

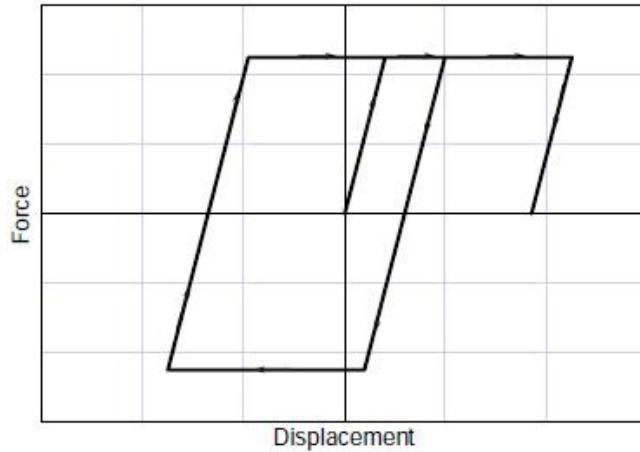


Figure 2.7 : Elasto-plastic non-degrading model [43].

Considering the above figure, it can be stated that,

- a) the stiffness switches from elastic to zero value at yield point
- b) during unloading cycles, the stiffness is equal to the loading (elastic) stiffness.

Veletsos and Newmark (1960) showed that moderate and long period single degree of freedom (SDOF) systems with elasto-plastic behaviour have approximately the same peak lateral displacements with linearly elastic systems. This statement formed the basis of *equal displacement rule*, which they also stated that was not applicable for short period structures [43].

2.2.2 Strength-Hardening Behaviour

Another commonly used non-degrading hysteretic model is a strength-hardening model, given in Figure 2.8. In fact, it is similar to the elasto-plastic model, except that the post-yield stiffness is greater than zero [43].

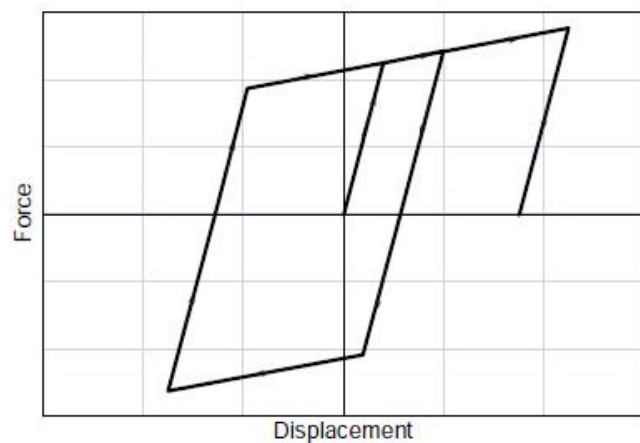


Figure 2.8 : Strength-hardening non-degrading model [43].

FEMA 440A [43] stated that, positive post-yield stiffness may also be referred as “strain hardening” because many materials reach their maximum strength value, when subjected to large strain levels after yield. Recent studies have provided quantitative information on the effects of positive post-yield stiffness on response. It has been shown that, positive post-elastic stiffness leads to a small reduction in peak displacement for structures with moderate and long-periods.

2.2.3 Stiffness Degrading Behaviour

Reinforced concrete structural components exhibit some level of *stiffness degradation (SD)* depending on their characteristics when they are subjected to large cyclic load reversals, which results with cracking.

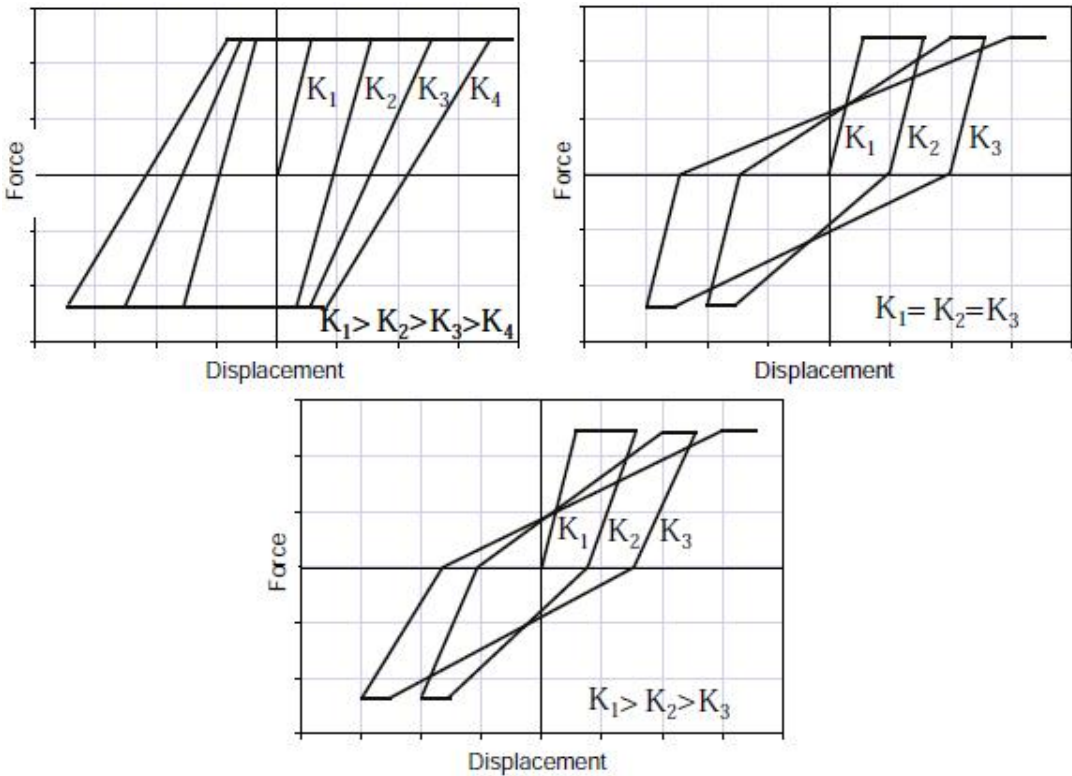


Figure 2.9 : Stiffness-degrading models [43].

Figure 2.9 shows three examples of stiffness degrading models. In the first model, the loading and unloading stiffness is the same. Stiffness degrades as displacement increases. In the second model the loading stiffness decreases as displacement increases. The unloading stiffness is kept constant and equal to the initial stiffness. In the third model, both the loading and unloading stiffness degrade as displacement increases. In addition, the stiffness values are different from each other [43].

Recent studies showed that, simpler hysteretic models, which do not take into account the stiffness degradation, can be used to estimate the demands for moderate and long period structures (systems with fundamental periods longer than 1.0s).

2.2.4 Pinching Behaviour

Reinforced concrete structures may exhibit a *pinching behaviour* when subjected to reverse cyclic loading. It occurs, when large stiffness degradation occurs during loading and unloading. Figure 2.10 shows moderate and severe pinching behaviours respectively.

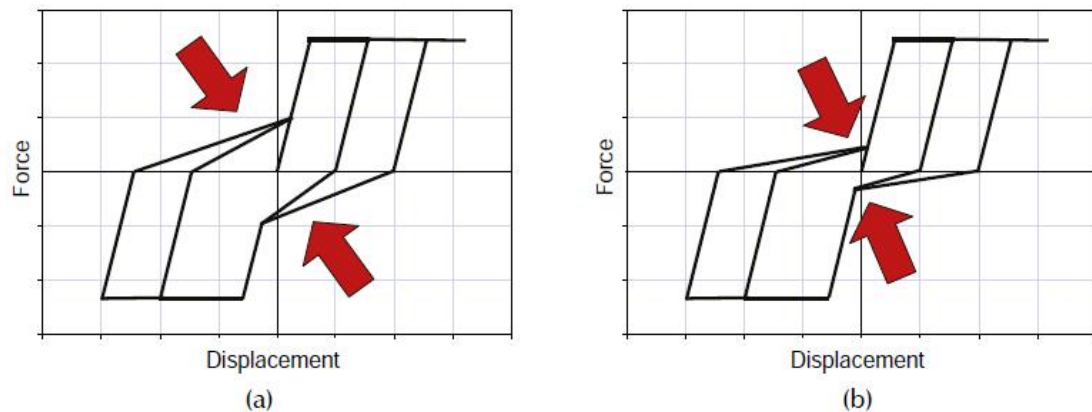


Figure 2.10 : (a) Moderate pinching (b) Severe pinching [43].

In reinforced concrete, pinching behaviour is mostly produced by opening of cracks when displacement is imposed in one direction. It is also a result of opening and closing of flexural cracks in reinforced masonry. The level of pinching depends on the structural properties such as the material properties, geometry, connections of the elements etc. According to the recent studies, pinching has a small effect on displacement demand for moderate and long period systems, as the post yield stiffness remains positive [43].

2.2.5 Cyclic Strength Degradation

Cyclic strength degradation occurs when a structural system experiences a reduction in strength because of cyclic load reversals. In cyclic strength degradation, reductions in strength occur after the loading has been reversed. Due to increasing inelastic displacement and repeated cyclic displacement, cyclic strength degradation is shown in Figure 2.11 respectively.

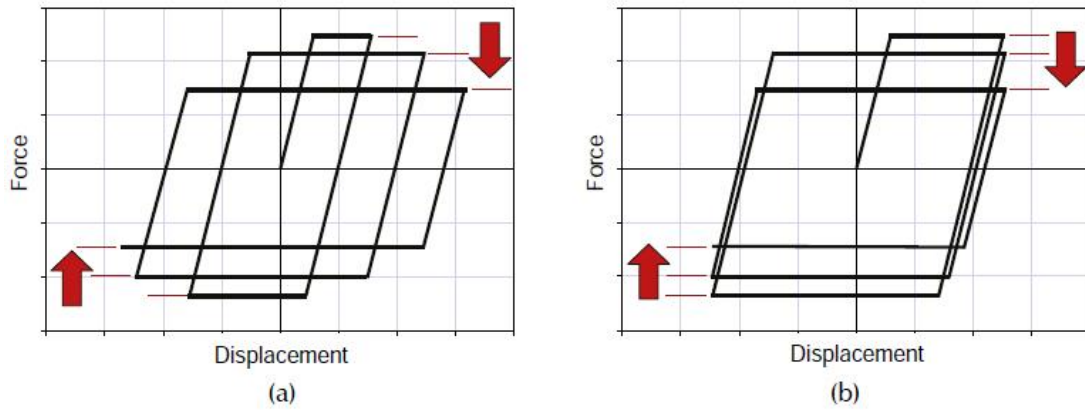


Figure 2.11 : (a) Increasing displacement (b) Cyclic displacement [43].

Most structural systems exhibit a combination of the types of cyclic strength degradation shown in Figure 2.11. Recent studies showed that, for moderate and long periods systems, the effects of cyclic strength degradation can be neglected, whilst for short period structures this effect should be considered.

2.2.6 Combined Stiffness Degradation and Cyclic Strength Degradation

Recent studies examined the effects of stiffness degradation in combination with cyclic strength degradation. Figure 2.12 shows moderate stiffness system with cyclic strength degradation (MSD), and severe stiffness system cyclic strength degradation (SSD) respectively. In these systems, lateral strength is reduced by a function of both the peak displacement demand and the hysteretic energy demand. These effects are only observed to be significant for short-period systems.

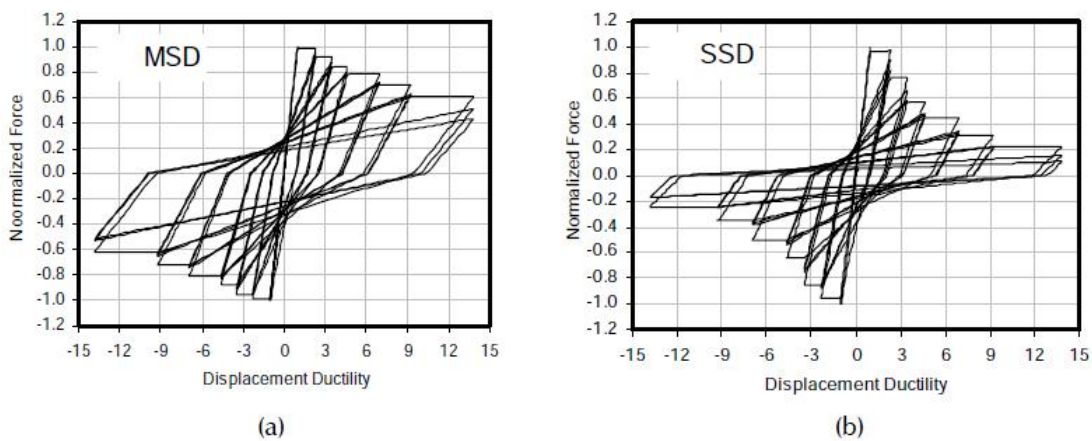


Figure 2.12 : (a) Moderate stiffness (b) Severe stiffness [43].

2.2.7 In-Cycle Strength Degradation

Structural systems may experience in-cycle strength degradation in combination with stiffness degradation. It arises when both strength loss and yielding occurs in the same cycle. In-cycle strength degradation can occur because of geometric nonlinearities (P-Delta effects), material nonlinearities, etc. [43]. Figure 2.13 shows in-cycle strength degradation.

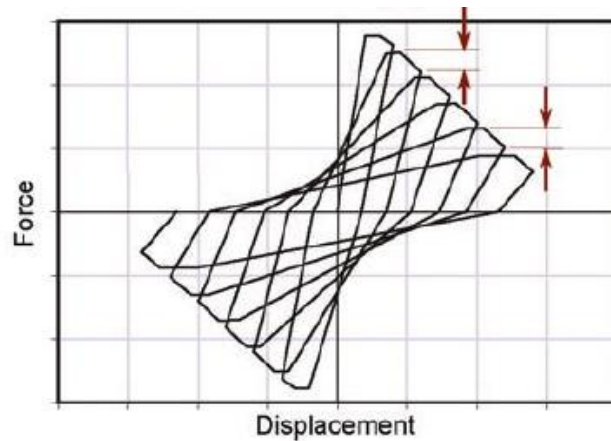


Figure 2.13 : In-cycle strength degradation [43].

FEMA 440 [1] identified the distinction between cyclic and in-cycle degradation to be very important. It is stated that, dynamic response of systems with cyclic strength degradation is generally stable, while in-cycle strength degradation can lead to lateral dynamic instability for a structural system. Figure 2.14 shows comparison for the hysteretic behaviour of cyclic and in-cyclic strength degradation.

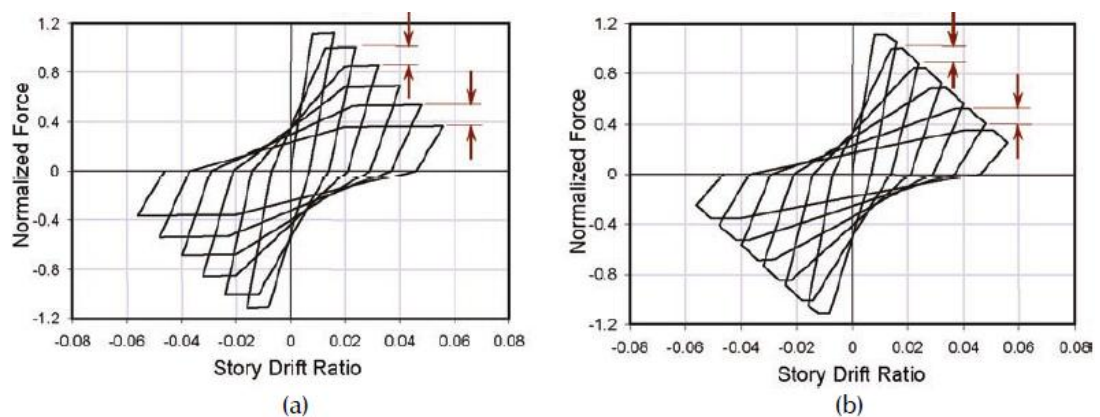


Figure 2.14 : (a) Cyclic degradation (b) In-cyclic degradation [43].

2.2.8 Cyclic Envelope

Other terminologies used in FEMA 440 [1] in order to define nonlinear characteristics are the *backbone curve*, *force displacement capacity boundary*, and the *cyclic envelope*. Backbone curve has been used for to describe limitations on the force deformation behaviour of structural components. Recent studies showed that, all degrading models start by a definition of the maximum strength that a structural member can develop at a given level of deformation. The boundary for the strength of a member in force displacement space is called the force displacement capacity boundary, shown in Figure 2.15 [43].

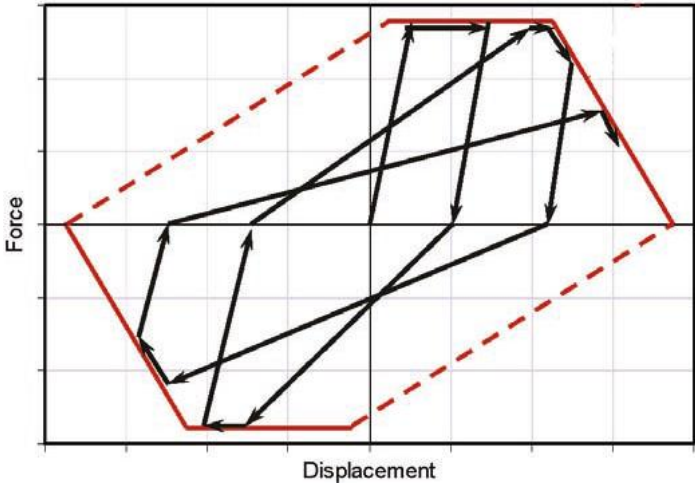


Figure 2.15 : Representation of a capacity boundary [43].

A *cyclic envelope* is a force deformation curve that envelopes the hysteretic behaviour of a component that is subjected to cyclic loading. Figure 2-16 shows a cyclic envelope, which is defined by connecting the peak force responses at each displacement level.

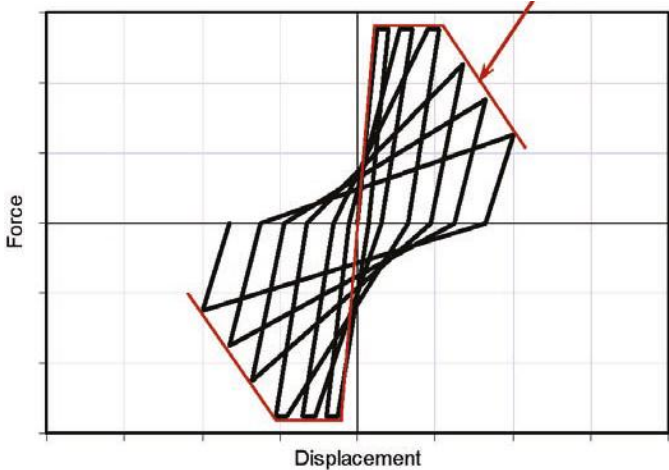


Figure 2.16 : Representation of a cyclic envelope [43].

2.3 Plasticity Concept

Performance levels defined for intensities of ground shaking should be checked using appropriate demand parameters and acceptance criteria. For a given building and set of demand parameters, the structure must be modelled and analysed so that the values of the demand parameters are calculated with sufficient accuracy for design purposes.

The performance is checked by comparing the *demand values* to the acceptance criteria (*capacities*) for the desired performance level. The acceptance criteria may vary depending on whether static or dynamic nonlinear analysis is used in determining the performance. For example, the demand parameters used in nonlinear static procedures need to take account for cyclic degradation effects although they are not modeled in the static analysis [44].

Plasticity is another distinguishing factor for inelastic structural distribution. In Figure 2.17, five beam-column element models are idealized for simulating the inelastic response. It can be categorized as, either *concentrated* at the end of the structural component or *distributed* throughout the element. Inelastic deformations can be concentrated at the end of the element through a rigid plastic hinge (Figure 2.17.a) or with an inelastic hysteretic spring element (Figure 2.17.b).

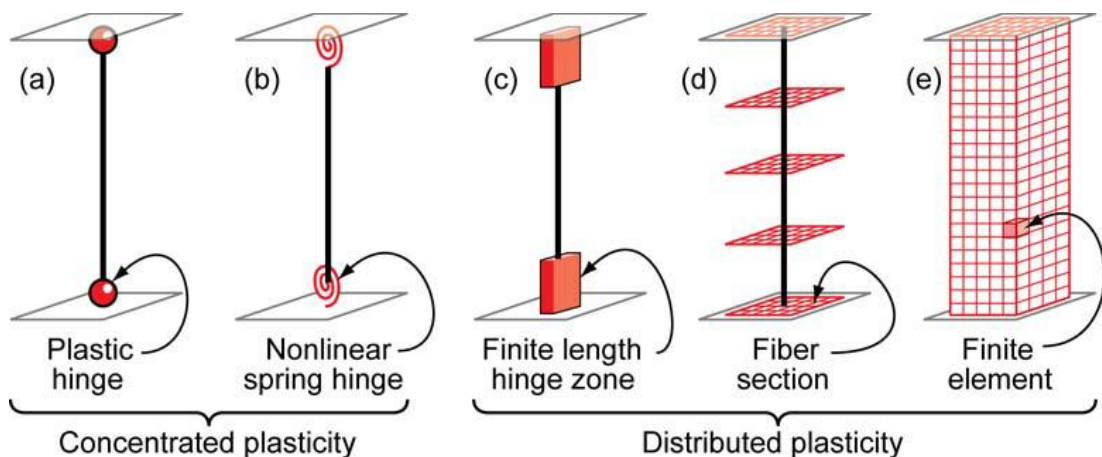


Figure 2.17 : Idealized models of beam-column elements [44].

In the distributed plasticity concept, the finite length hinge model (Figure 2.17.c) is an efficient distributed plasticity formulation with hinge zones at the member ends. The inelastic hinge length may be fixed or variable and can be determined from the moment-curvature characteristics of the section [44].

The fiber formulation (Figure 2.17.d) models distribute plasticity by numerical integrations through the member length. *Fibers* are numerically integrated over the cross section to obtain stress resultants and incremental moment-curvature. The cross section parameters are then integrated numerically along the member length. It is studied that, integration of deformations along the hinge length captures the yield spreading more realistically than the concentrated hinges [44].

The most complex model is shown in Figure 2.17.e. Plasticity is distributed through member length by dividing the cross sections into small (micro) finite elements with nonlinear hysteretic properties.

Concentrated and finite length hinge models (Figure 2.17) may consider the axial force-moment, *P-M interactions*, through yield surfaces. Figure 2.18 shows a representative of an idealized axial force-moment demands and strength interaction surface for a concrete structural element.

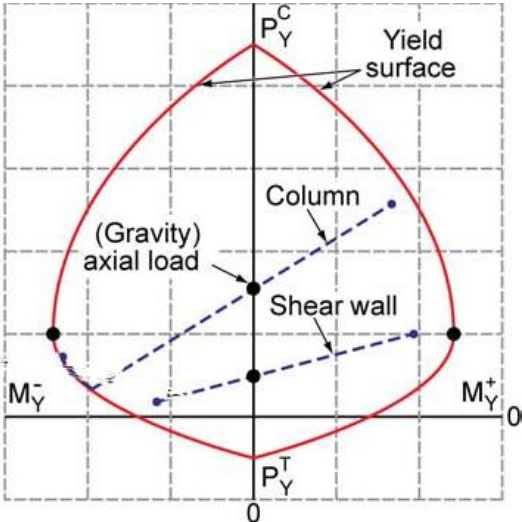


Figure 2.18 : Axial load and strength interaction surface for concrete [44].

These models generally do a good job at tracking the initiation of yielding under axial load and bending, however sometimes they may not capture accurately the post-yield and degrading response. A simple check on the model capabilities is to analyse a concrete column under a low and high value of axial load. To develop a flexural mechanism, the member shear strength must be larger than the flexural strength, which is required in capacity design provisions.

Ongoing researches for developing high order beam elements have been devoted to advanced analysis methods. Intermediate solutions include *plastic-zone*, *quasi-plastic hinge*, *elastic-plastic hinge* methods and various modifications. In the plastic zone, spread of plasticity is traced and a constant residual stress pattern is assumed, whereas in quasi-plastic zone, the spread of plasticity is considered by flexibility coefficients and a simplified residual stress pattern is used. Elasto-plastic hinges can consider second order geometric effects, no residual stress is considered. In refined plastic hinge method, inelasticity is considered by forces rather than strains. Connection flexibility can be modeled using rotational spring elements [45].

The most crucial step of pushover analysis is the determination of hinges. Generally, there are five types of plastic hinges, such as *moment hinge*, *axial hinge*, *torsion hinge*, *shear hinge* and *P-M2-M3 hinge*. Generally, the P-M2-M3 hinge is used for the common frame columns. Combinations of the shear hinge and moment hinge are used for deep beams [46].

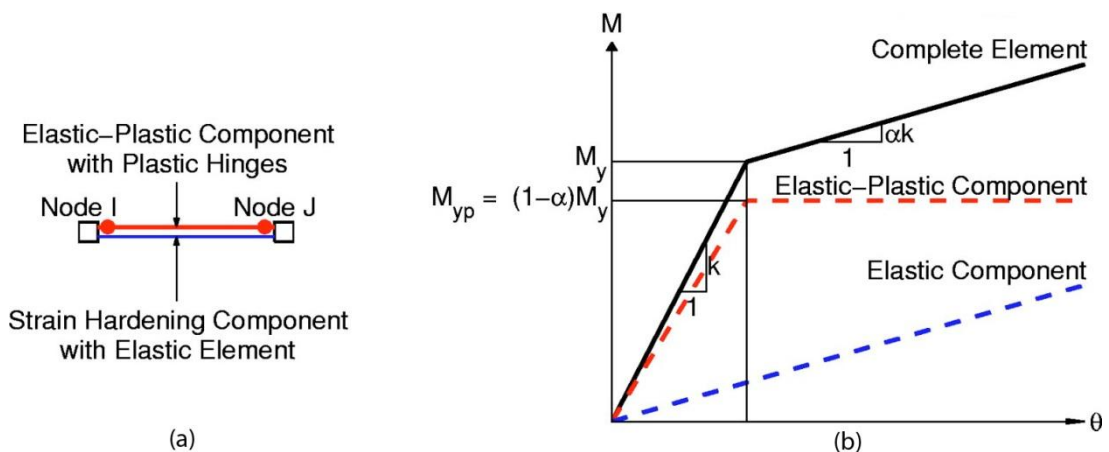


Figure 2.19 : (a) Hinge element (b) Moment-rotation relationship [47].

Hinge element is generally modelled with a bilinear moment-rotation relationship as shown in Figure 2.19.b. Here; M_y represents the yield moment, θ is the rotation, k is the initial stiffness, αk is the stiffness of the strength hardening part. The axial force (P) and the bending moment (M) interactions which are used for determining the elasto-plastic components are shown in Figure 2.20.

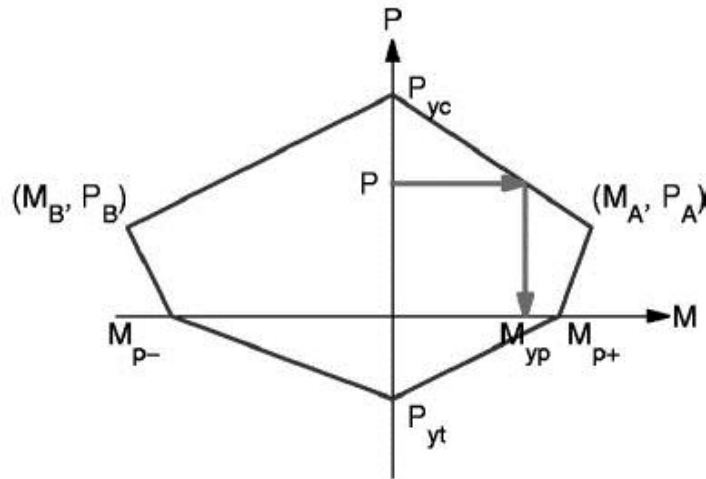


Figure 2.20 : P-M interaction diagram for reinforced concrete columns [47].

The procedure for computing the bending moment can be summarized as follows [47],

1. The axial force, P , is determined.
2. The bending moment at each ends I and J , M_I and M_J , of the nonlinear element is computed.
3. M_{yp} , is the yield moment of the elasto-plastic component corresponding to the axial force, P , computed in Step 1 from the specified P-M interaction diagram shown in Figure 2.20.
4. Total yield moment is calculated by adding the moment of the elastic component.
5. Comparison of the bending moments, M_I and M_J , with the yield moment, M_y should be checked. M_I and M_J should be smaller than M_y to represent the bending moment demands.
6. The rotations θ_I and θ_J are determined.
7. Bending moment of the elastic component is calculated.
8. Total bending moment is the sum of elastic bending with the plastic moment.

A generalized force deformation curve which is defined by FEMA 356 [2] is given in Figure 2.21. Linear response is expected between point A and yield point B . The slope from B to C is called as *strain hardening*. C has an ordinate that represents the strength of the component, and an abscissa value equal to the deformation at which significant strength degradation begins (line CD).

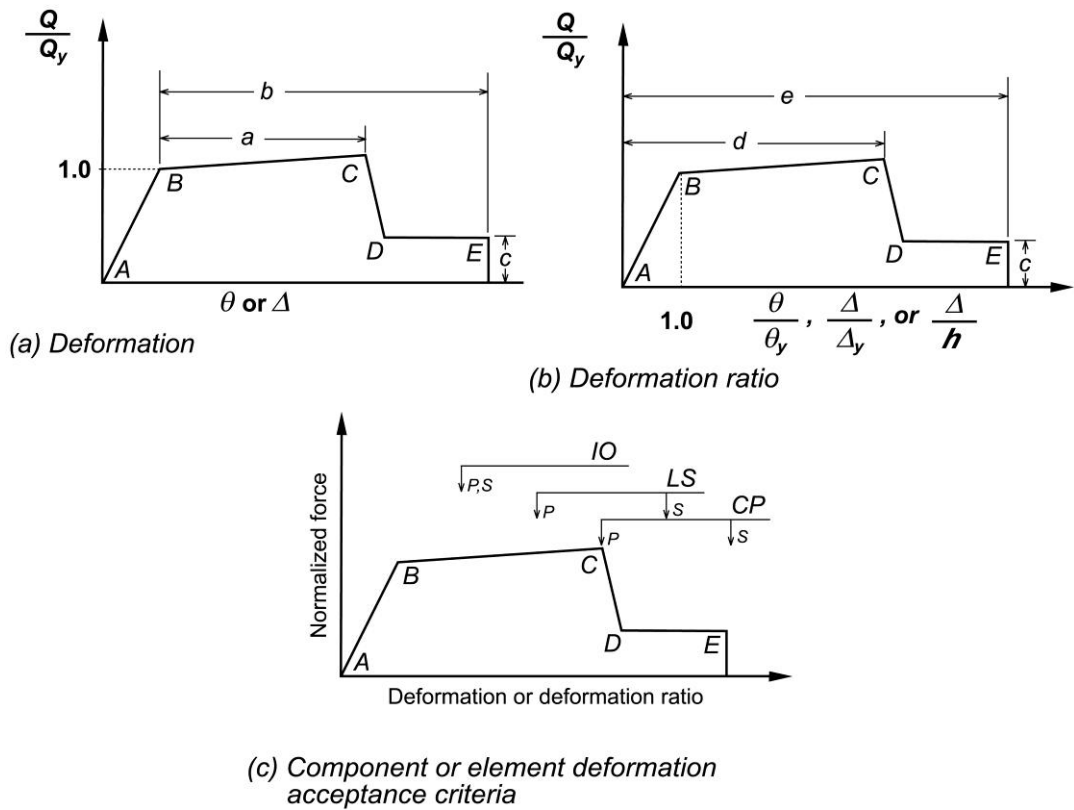


Figure 2.21 : Generalized component acceptance criteria [2].

Beyond point *D*, the component responds with substantially reduced strength to point *E*. At deformations greater than point *E*, the component strength is essentially zero. The sharp transition as shown on idealized curves in Figure 2.21 between points *C* and *D* can result in computational difficulty. Acceptance criteria for deformation or deformation ratios for primary members (*P*) and secondary members (*S*) corresponding to the target Building Performance Levels of Collapse Prevention (*CP*), Life Safety (*LS*), and Immediate Occupancy (*IO*) are shown in Figure 2.21 [2].

3. ANALYSIS METHODS FOR PERFORMANCE ASSESSMENT

The analysis methods can be grouped into two main categories, one is the *Dynamic Analysis* and the other one is *Static Analysis*. Both of the analysis type may be applicable for determining the capacity of elastic and inelastic structures. The categorization of the methods is shown in Figure 3.1 [39]. In the figure, *E* represents elastic zone while *I* represents inelastic zone.

Prediction methods for response depend on the design objective. No attempt is made to express preferences on analysis methods based on different design objectives. Instead, good seismic design includes more than code-based quantitative demand assessment, usually represented by demand/capacity ratios. Simple nonlinear static analysis methods can provide valuable qualitative insight in the evaluation and design process, but care is necessary when they are used alone to establish design quantities [48].

Linear analysis techniques are widely used in practice whereas it is known that nonlinear analysis methods give more accurate results than linear methods.

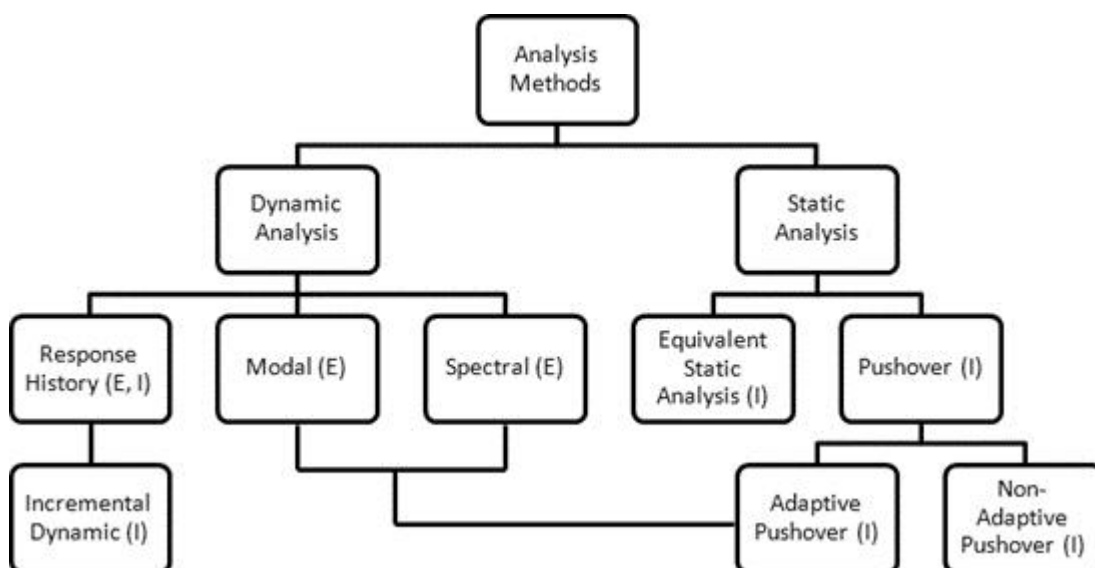


Figure 3.1 : Common methods of analysis used in earthquake engineering.

It is a well-known fact that, dynamic analysis is the most accurate way of determining the structural response, whilst it is more time consuming and needs more computational effort than static analysis.

Table 3.1 shows the comparisons of requirements for static and dynamic analyses. A detailed model and a stiffness representation are needed for both of the methods to start the analysis. While mass, damping representations and input ground motions are necessity for dynamic analysis, static analysis needs a previously determined target displacement value. As stated before, static analysis is much more time saving than the dynamic analysis.

Table 3.1: Comparisons of requirements for static and dynamic analyses [39].

Properties	Static Analysis	Dynamic Analysis
Detailed Models	Required	Required
Stiffness and strength representation	Required	Required
Mass representation	Not Required	Required
Damping representation	Not Required	Required
Additional operators	Not Required	Required
Input motion	Not Required	Required
Target displacement	Required	Not Required
Action distribution fixed	Required	Not Required
Short analysis time	Required	Not Required

It can be said that, the two main methods have very common with some slight differences. Both use the same material relationships, whereas static analysis does not require loading and unloading models. Dynamic analysis uses damping effects while determining the characteristic equation of motion. Both methods use iterative procedures. Dynamic analysis uses time, whereas force or displacement is the variable in static one.

Elnashai and Papanikolaou (2005) [4] stated three main differences between static and dynamic analysis;

- Static analysis requires monotonic models.
- Dynamic analysis requires structural damping and mass distribution.
- Dynamic procedure repeats static analysis as many times as the duration of the earthquake divided by the time step for response history analysis.

It can be concluded that, static analysis needs simpler models. This is the main reason for the increased use of static pushover analysis among practical engineers.

3.1 Dynamic Analysis

The equation of motion for multi degree of freedom (MDOF) systems is given in equation (3.1). Each of the forces represented on the left hand side is a function of displacement x . In accordance with d'Alembert's principle, the inertial force is the product of the mass and acceleration; the damping force is the product of the damping constant c and the velocity; the elastic force is the product of the stiffness and the displacement [49]. Those terms are given in (3.2) equations.

Here F_I is the inertia force vector, F_D is the damping force vector, F_R is the vector of restoring forces and F_Z is the vector of earthquake loads.

$$F_I + F_D + F_R = F_Z \quad (3.1)$$

$$F_I = \underline{M}\ddot{x} \quad (3.2.a)$$

$$F_D = \underline{C}\dot{x} \quad (3.2.b)$$

$$F_D = \underline{K}x \quad (3.2.c)$$

$$F_Z = -\underline{M}I\ddot{x}_g \quad (3.2.d)$$

When equations (3.2) are replaced in equation (3.1) then the equation of motion for multi degree freedom of structures (MDOF) can be expressed as in equation (3.3).

$$\underline{M}\ddot{x} + \underline{C}\dot{x} + \underline{K}x = -\underline{M}I\ddot{x}_g \quad (3.3)$$

In the equation (3.3), I represents the unity matrix, \underline{M} , \underline{C} and \underline{K} are the mass, damping and stiffness matrixes respectively. In addition, x_g resembles the ground motion, \ddot{x} is the acceleration component and \dot{x} is the velocity relative to the ground.

The most commonly used methods for dynamic analysis of structures subjected to earthquake loads are *modal*, *spectral* and *response history*. Recent studies develop *incremental dynamic analysis* [7] and *incremental response spectrum analysis* [8] briefly. Each of the analysis methods will be discussed in this section but for more detailed literature review might be done. Elnashai [39] explained that dynamic analysis can be solved either in the *time-domain* or in the *frequency-domain*. The options to solve the dynamic analysis are given in Figure 3.2 [39].

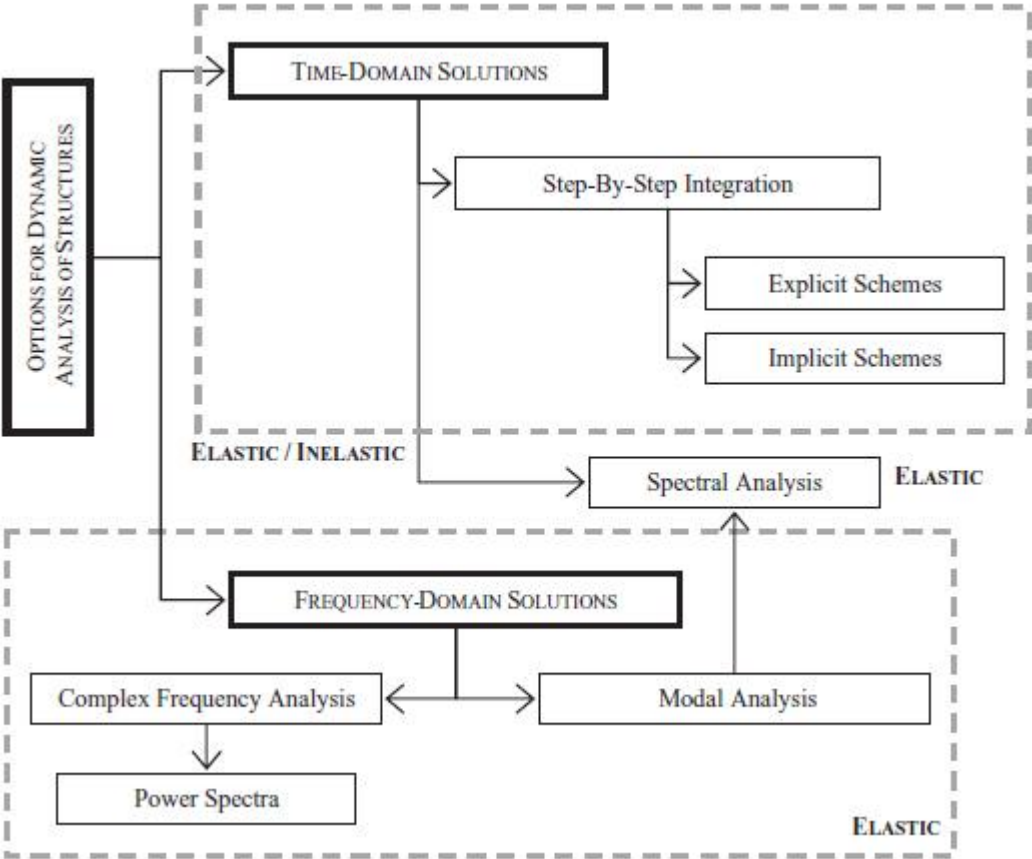


Figure 3.2 : Methods of dynamic analysis of structures [39].

3.1.1 Modal and Spectral Analysis Methods

In modal analysis concept, in order to assess the response, MDOF system is firstly transformed in to an equivalent SDOF system. The response of the each equivalent SDOF systems is calculated in the time domain and then they are combined using SRSS or CQC to determine the response of the MDOF system.

If the aim of the analysis is just to determine the maximum response quantities then a response spectrum is needed to represent the earthquake excitation. This type of analysis is called as *modal spectral analysis* or shortly *spectral analysis* [39].

Under an earthquake excitation, structures might have inelastic tendencies. In order to determine the inelastic response the coupled dynamic equilibrium equation (3.3) should be integrated directly [39].

The procedure can be summarized as follows;

- a) Displacement vector should be defined in terms of modal coordinates as shown in equation (3.4). Here, $\underline{\Phi}$ is the modal matrix and $Y(t)$ is the modal coordinates.

$$x = \underline{\Phi}Y(t) \quad (3.4)$$

- b) Eigenvalue problem for MDOF system should be conducted as given in equation (3.5).

$$\underline{K}\Phi_i = w_i^2 \underline{M}\Phi_i \quad (3.5)$$

- c) Eigenvalues and eigenvectors should be determined using equation (3.5). This is called as a *conventional eigenvalue analysis*. Alternatively, Ritz vectors can also be employed, especially for complex structural systems. Once the frequencies are known, they can be substituted one at a time into the equation (3.6) with an assumption that the mode shapes are orthogonal with respect to the \underline{M} mass and \underline{K} stiffness matrices.

$$(\underline{K} - w^2 \underline{M})x = 0 \quad (3.6)$$

- d) Damping should be assumed. In most codes, the *mass and stiffness proportional damping* is used as an efficient technique of assembling a damping matrix [39]. If only two modes are involved, this is called as *Rayleigh damping* and is calculated using (3.7). α and β values can be derived for different damping ratios by using the equation (3.8) [39].

$$\underline{C} = \alpha \underline{M} + \beta \underline{K} \quad (3.7)$$

$$\xi_i = \frac{\alpha + \beta w_j^2}{2w_j} \quad (3.8)$$

e) Equation of motion (3.3) is formulated in terms of generalized coordinates Y_i to get (3.9). Where w is determined from (3.10). \widehat{M}_i and \widehat{K}_i are the generalized mass and stiffness respectively and are given in equation (3.11) and (3.12). Γ_i is the *modal participation factor* defined in equation (3.13). L_i is defined in equation (3.14).

$$Y_i + 2\xi_i w_i Y_i + w_i^2 Y_i = -\Gamma_i x_g \quad (3.9)$$

$$w_i = \sqrt{\frac{\widehat{K}_i}{\widehat{M}_i}} \quad (3.10)$$

$$\widehat{M}_i = \phi_i^T \underline{M} \phi_i \quad (3.11)$$

$$\widehat{K}_i = \phi_i^T \underline{K} \phi_i \quad (3.12)$$

$$\Gamma_i = \frac{L_i}{\widehat{M}_i} \quad (3.13)$$

$$L_i = \phi_i^T \underline{M} \underline{I} \quad (3.14)$$

f) N coupled equations in normal coordinates (3.9) should be computed. The response of the i^{th} mode of vibration at any time t can be expressed by the use of the convolution (Duhamel) integral in (3.15) [39]. $A_i(t)$ is the solution of SDOF system in the time or frequency domain. These approaches are known as the *direct integration method* and *fast Fourier transform* respectively.

$$Y_i(t) = \frac{L_i}{\widehat{M}_i w_i} A_i(t) \quad (3.15)$$

g) Total elastic restoring force is computed.

h) Total base shear can be computed using (3.16).

$$V_B = \sum_{i=1}^N \frac{L_i^2}{\widehat{M}_i} A_i(t) \quad (3.16)$$

i. Relative displacement is computed in terms of the relative displacement as given in equation (3.17).

$$x_i = \underline{\Phi} Y_i(t) = \frac{L_i}{\bar{M}_i} A_i(t) \Phi_i \quad (3.17)$$

Both the modal analysis and the modal spectral analysis are applicable only to linear elastic systems. In Figure 3.2, it was explained by Elnashai [39] that the nature of modal and spectral analysis is considered as spanning between time and frequency domains.

The most important issue in modal analysis is the combination of modal responses. There are two methods to combine the modal effects. One is *the square root of the sum of the squares (SRSS)* and the other is *the complete quadratic combination (CQC)* method. Researches show that, if the difference between two modal frequencies is less than 10%, SRSS may underestimate the structural response. Especially when higher modes are effective in the structural response, then SRSS should not be used [39]. When the differences between modes are distinct, CQC is the appropriate method to assess the structural response. More details about modal analysis can be found in literature review [39, 49, 50].

3.1.2 Response History Analysis

Response history analysis are time domain based procedures, where the damping effects are included as well as the inertia forces. It is a more time consuming method than the modal analysis approach.

In contrast to the frequency - domain solutions, the response of MDOF systems may be calculated by time - stepping techniques where series of coupled equations of motion are solved as static equilibrium systems. Although response analysis is the most accurate method, it needs more computational effort.

As the principle of superposition is not applicable, the equations of equilibrium (3.1) and (3.3) needs to be integrated directly. Many numerical integration schemes are available in the literature. Last researches in this field come out with time-domain solution methods. All methods have in common procedure that the response history is divided into equal time steps, Δt .

During each Δt time interval, structure is assumed to be linear and elastic, whilst the second order effects are induced in the stiffness matrix. Nonlinear response of the structure is determined by a series of piece-wise linear systems. At each Δt time step, the stiffness matrix is recalculated and updated. This is the main reason that these types of analysis are more time consuming.

Mostly known time stepping methods might be named as the central difference method, Newmark’s method, linear acceleration method, Wilson’s method, Hilber-Hughes-Taylor α -integration scheme and average acceleration method. Brief explanations of these interpolation methods can be found in Chopra [50].

3.1.3 Incremental Dynamic Analysis

Incremental Dynamic analysis method (IDA) is known to be the most reliable among the other dynamic analysis methods. In this method, structure is firstly subjected to plenty of scaled ground motion records. Latter step is to conduct many dynamic analyses and to plot the response versus the record intensity level. This curve is known as the *IDA curve*.

Although IDA is not a new concept, it gained popularity with the researches of Vamvatsikos and Cornell in 2002 [7]. An example of an IDA curve for 30 earthquake records of a five story steel braced frame is given in Figure 3.3. For more detailed information Vamvatsikos and Cornell’s paper [7] may be checked.

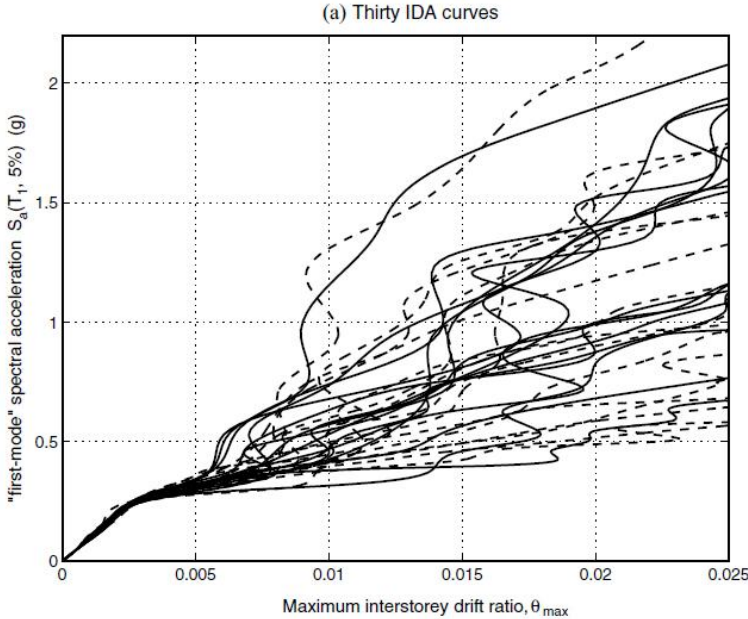


Figure 3.3 : IDA curve for a five story steel braced frame [7].

Vamvatsikos and Cornell [7] stated the beneficence of the method as follows;

- a) IDA curves lead up to a brief understanding of demands versus the range of levels of a ground motion record.
- b) A better structural implication is possible.
- c) Detailed search in the change of the structural response during the intensity increases.
- d) It produces good estimates of the dynamic capacity.
- e) Stability of the different ground parameters can be checked.

As explained in the preceding chapters and to make a short summary, the analysis step of a structural system might be the most important step to design an earthquake resistant structure. All of the analysis methods have in common, that they need a structural model and a representation of the earthquake ground motion. Decision has to be made either the force displacement relation is elastic or inelastic [51].

Earthquake ground motion induces the mass of a structure to accelerate and the response can be computed by dynamic analysis. Traditional design procedures use static linear analysis by modifying the results to represent the effects of nonlinear behaviour. Whereas, recent studies propose nonlinear static (pushover) analysis to be conducted in order to determine the inelastic deformation of structures. Since the equilibrium equations may have a large number of degrees of freedom, a computer based analysis should be conducted.

Table 3.2 summarizes the previously defined structural analysis methods [51]. FEMA 356 [2], ATC 40 [3] and FEMA 273 [55] emphasize the need and use of nonlinear static procedures (pushover procedures) to determine the capacity of structures. The proposed code provisions are also available for newly structures.

Table 3.2 : Analysis Procedures for Earthquake-Resistant Design [51].

Category	Procedure	Earthquake Load	Analysis Methods
Equilibrium	Plastic Analysis	Equivalent Lateral	Equilibrium
	Linear Static	Equivalent Lateral	Linear static
Linear	Linear Dynamic	Response Spectrum	Response Spectrum
	Linear Dynamic	Ground motion	Linear time history
	Nonlinear Static	Equivalent Lateral	Nonlinear static
Nonlinear	Nonlinear Dynamic	Ground motion	Nonlinear time history

As described before, linear static procedures have been widely used for many years but they are lack of determining the nonlinear behaviour of the structure whereas plastic analysis can establish the location of plastic hinges and determine the collapse load level. Nonlinear analysis methods can provide the relationship between a lateral load and the structural displacement. The results are presented as a pushover or capacity curve for the structure. [51].

3.2 Static Analysis

Main aim of the static methods is to assess the capacity of the structure in terms of deformations and determine whether the structure achieves the performance goals defined in Chapter 2. Whilst, recent studies showed that, static methods are only reliable when the structure is regular. Torsional effects make the results inaccurate.

As showed in Figure 3.1, the most commonly used static methods are the *equivalent static analysis method* and the *pushover method*. Both methods have inelastic capability of determining the structural capacity.

3.2.1 Equivalent Static Analysis Method

The equivalent static analysis (equivalent lateral force, ELF method) is the simplest type of analysis that is used to assess the seismic response of structures. It assumes the material as linear elastic, but can take into account the geometrical nonlinearities ($P - \Delta$).

The horizontal loads, which are considered equivalent to the earthquake forces, are applied along the height of the structure and they are combined with vertical gravity loads. In general, the equation of equilibrium for multi degree of freedom system (MDOF) is defined as in equation (3.1). Static analysis is the case when F_I inertia force vector and F_D damping vector is zero. Then equation (3.1) can be expressed as,

$$R = F(t) \tag{3.18}$$

Where, R is the restoring force vector and $F(t)$ is the vector of applied earthquake loads. The restoring forces might be assumed as proportional to the vector of nodal displacements.

The most common load patterns that are used in the codes are the inverted triangular or parabolic ones for the building structures. The magnitude of the load is calculated from the fundamental mode shape. Researches show that; for medium rise buildings, which are predominantly vibrating in the first mode, inverted triangular load pattern provides a good approximation of earthquake excitation [39].

The steps required to assess structures by equivalent static analysis are summarized as follows [39];

- a) Lateral load pattern is assumed.
- b) Gravity and horizontal loads are added to the assumed load pattern.
- c) Displacements are calculated.
- d) Scaling might be proceeded.

This method provides approximate estimates of the deformation, whereas stiffness degradation, hysteretic effects cannot be modelled in this procedure.

3.2.2 Pushover Analysis

In pushover methods, force or displacements are laterally applied to the structural system. Lateral loads are distributed along the height of the structure. The system is pushed until the structural capacity is reached. In this type of analysis, the hinge mechanism can be easily determined, and the structure can be modelled to the desired performance level. Pushover methods are named according to the applied load pattern. If the applied load pattern is constant through the analysis, then the method is referred as *conventional pushover procedure*. If it changes depending to the simultaneous modal effects in the inelastic range, then it is called as *adaptive pushover method*.

As given in the literature review of the methods in Chapter 1, there are numerous pushover methods, such as *modal pushover method*, *multi modal pushover method*, *energy based pushover procedure* etc. Since the main subject of this study is the pushover techniques, the type of pushover procedures, analysis cases etc. are investigated in detailed under new captions through Chapter 3.3-Chapter 3.5.

3.3 Evaluation of Structural Response Using Conventional Pushover Procedures

Inelastic static analyses were first introduced by the research of Güllkan and Sözen, 1974 [52]. In their work, they stated that the increase in energy dissipation capacity and the reduction in stiffness are the main parameters effecting the response of a reinforcement concrete structure. At the end of their study, they concluded that, as the displacement of the structure increases the stiffness decreases, while the capacity of dissipating energy increases.

Nowadays many codes preferred different ways of assessing the nonlinear static performance. The main purpose of pushover analysis is to evaluate the expected performance of existing or newly build structural systems. The evaluation is based on an assessment of inelastic parameters such as drift, inelastic deformations etc. In pushover analysis, the lateral load pattern can be in terms of either horizontal forces or displacements. Lateral loading is terminated when the calculated target displacement is achieved.

In fact, conventional static pushover procedures have no rigorous background. They are based on representing the multi degree of freedom structure (MDOF) as an equivalent single degree of freedom (SDOF) system. This leads up to determination of the dynamic response of MDOF system only by a single mode, which is also assumed as constant throughout the analysis. This assumption makes the results of the conventional pushover procedures suspectable. Menjivar et al [53] give representation of this in Figure 3.4.

Elnashai defined conventional pushover methods as a capacity estimation method under a set of functions that represent inertial effects from the earthquake [39]. He also pointed out that, the method is capable of determining the design weaknesses that elastic analysis cannot detect.

As explained before, pushover analysis is based on the assumption that the response of the structure can be related to the response of an equivalent single degree of freedom (SDOF) system. Whilst, in real neither the response is controlled by a single mode nor the modal shape remains constant through the analysis [54].

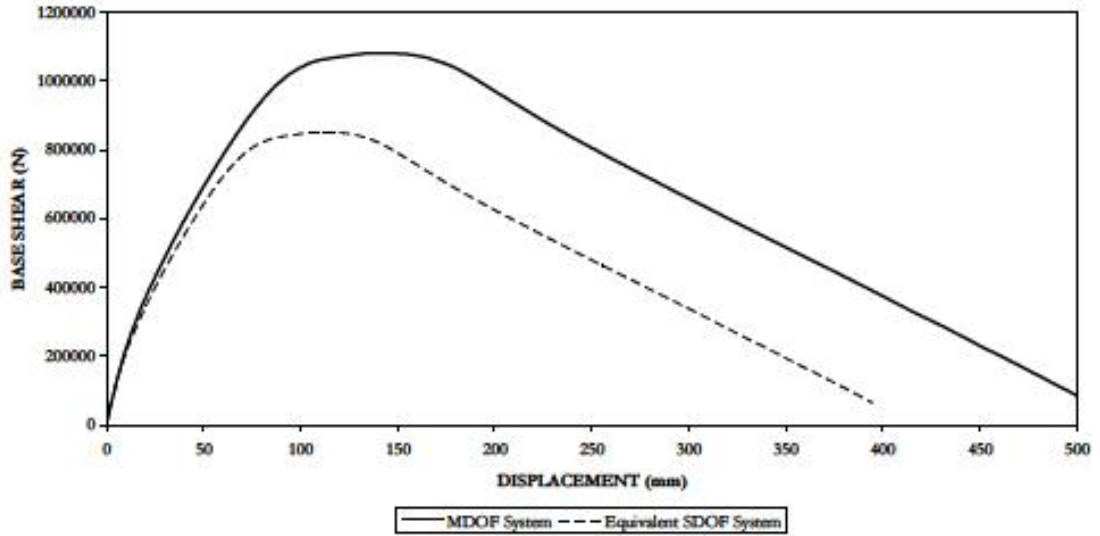


Figure 3.4 : Pushover curves comparison [53].

Accepted that $\{\Phi\}$ deflected shape vector of MDOF system is constant, displacement vector defined in (3.3) can be assumed as given in equation (3.19), where x_1 is the displacement of the roof.

$$X = \{\Phi\}x_1 \quad (3.19)$$

If we evaluate (3.19) in (3.3), the equation of motion for a MDOF system can be obtained as (3.20). Here Q denotes the story force vector of the MDOF system.

$$\underline{M}\{\Phi\}\ddot{x}_1 + \underline{C}\{\Phi\}\dot{x}_1 + Q = -\underline{M}I\ddot{x}_g \quad (3.20)$$

The displacement of the equivalent SDOF system x^* , might be defined by multiplying Γ , transformation factor with x_1 as given in equation (3.21).

$$x^* = \frac{\{\Phi\}^T M \{\Phi\}}{\{\Phi\}^T M \{1\}} x_1 \quad (3.21)$$

If we pre-multiply (3.20) by $\{\Phi\}^T$ and substitute (3.21) then the equation becomes,

$$\{\Phi\}^T M \{1\} \ddot{x}^* + \{\Phi\}^T C \{\Phi\} \frac{\{\Phi\}^T M \{1\}}{\{\Phi\}^T M \{\Phi\}} \dot{x}^* + \{\Phi\}^T Q = -M^* \ddot{x}_g \quad (3.22.a)$$

$$M^* = \{\Phi\}^T M \{1\} \quad (3.22.b)$$

$$C^* = \{\Phi\}^T C \{\Phi\} \frac{\{\Phi\}^T M \{1\}}{\{\Phi\}^T M \{\Phi\}} \quad (3.22.c)$$

$$Q^* = \{\Phi\}^T Q \quad (3.22.d)$$

$$M^* \ddot{x}^* + C^* \dot{x}^* + Q^* = -M^* \ddot{x}_g \quad (3.22.e)$$

Here; M^* , C^* and Q^* denote the properties of the equivalent SDOF system.

Conventional pushover analysis is the nonlinear incremental-iterative solution of the given equilibrium equations. Force-deformation characteristics of the equivalent SDOF system can be derived from the results of a nonlinear incremental static analysis of the MDOF system.

Calculated demand is compared with the structural capacity. The result curve is known as *pushover curve* or the *capacity curve*, and is expressed in terms of V base shear versus δ top lateral displacement. Since the direction of earthquake excitation that will cause collapse is not known, pushover curves are computed for both push and pull.

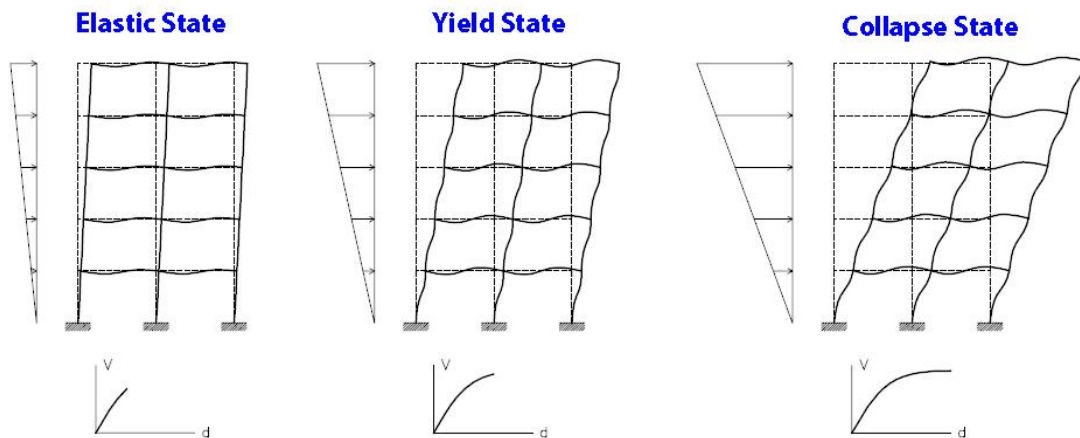


Figure 3.5 : Yielding sequence of pushover analysis [4].

Figure 3.5 shows the yielding sequence of pushover procedures under lateral force distribution [4]. The basic steps of conventional pushover can be summarized as below [39];

- a) Gravity loads are applied in a single step.
- b) Load pattern is defined either in terms of V force vector or δ displacement vector as shown in Figure 3.6.

- c) Control node is selected, generally roof is the control node.
- d) Lateral load distribution is determined.
- e) The iteration is repeated until a predefined target displacement is reached or collapse occurs.
- f) If torsional effects are effective then structure should be loaded both in positive and negative directions.
- g) Base shear-top displacement curve, capacity curve, is plotted.

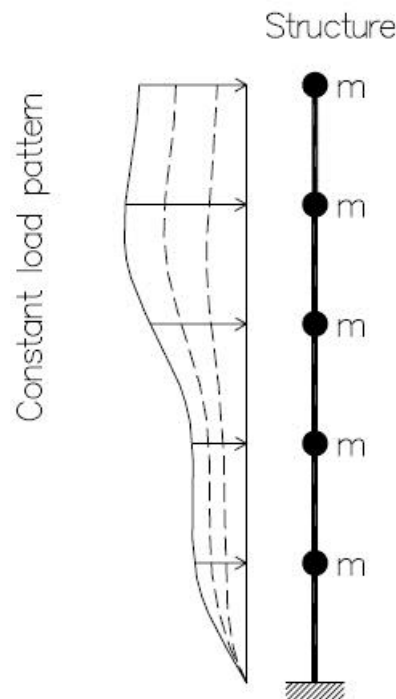


Figure 3.6 : Load pattern model for conventional pushover analysis [4].

Seismic codes commend using at least two vertical distributions of lateral forces. The uniform load pattern should be used with the modal pattern. The latter can be the inverted triangular distribution, which is applicable when more than 85% of the total mass participates in the fundamental mode. There are currently two alternatives to estimate the nonlinear demand. One is the FEMA 356 procedure, *the Displacement Coefficient Method (DCM)*, and the other one is the ATC 40, *the Capacity Spectrum Method (CSM)*.

FEMA uses the results of time histories of SDOF to generate inelastic spectra, then states some coefficient factors to modify the response of a linear system, whereas in ATC 40 inelastic system is utilized by using equivalent linearization concept. Both of the methods have been improved in the last decade. FEMA 440 [1] is the modified and improved version of these codes.

3.3.1 Determining the Performance Point By Capacity Spectrum Method

Capacity spectrum method (CSM) uses the intersection of the capacity (pushover) curve and a reduced response spectrum to estimate maximum displacement. It was firstly proposed by Freeman [14]. Determination of three key point is the aim of this simplified procedure; *capacity*, *demand* and *performance*.

Freeman categorized the procedure into five steps [14], which are given below;

- a) Determination of the capacity curve in terms of base shear and roof displacement from the pushover analysis of structures.
- b) Modal properties such as period, mode shapes or modal participation factors are calculated.
- c) Capacity curve is transformed into *Spectral acceleration-spectral displacement curve* (S_a-S_d) format by using the modal quantities calculated in the second step.
- d) Response spectra are calculated for several levels of damping including 5% damped spectrum.
- e) Capacity spectrum is plotted in *acceleration displacement response spectrum* (ADRS) format and intersected with the appropriate response spectrum.

It is mentioned in ATC 40 [3] that, the constructed capacity curve would represent the first mode response, basing on the theory that the fundamental mode is the predominant response of the structure. This may be valid for structures that have fundamental period up to one second. If the fundamental period is greater than one second then the higher mode effects should be taken in to account.

The demand and capacity intersects at a point on the capacity spectrum called the *performance point*. This performance point represents the condition for which the seismic capacity of the structure is equal to the seismic demand [3].

It is stated in ATC 40 that the location of the performance point had to satisfy two statements. One is the point must be on the capacity spectrum curve and second is the point must be on a spectral demand curve which is reduced from the elastic 5% damped spectrum. For this iterative calculation first a trial performance point is needed.

ATC 40 proposed three different procedures in order to determine the performance point using iterative process; *procedure A*, *procedure B* and *procedure C*. All three methods depend on the same concepts but differ on analytical graphical techniques. Procedure A is a formula based step by step procedure and the most appropriate one for engineers due to its easiness. Procedure B is based on bi linearization of the capacity curve and procedure C is a graphical method used to determine performance point. The main steps of the procedures will be investigated in this work. For more details of the procedures, ATC documents may be searched.

a) Procedure A

This is a formula based procedure where the spectral acceleration-period graph is converted to spectral acceleration-spectral displacement form. Also, capacity curve has to be converted to ADRS format to develop the capacity spectrum by using the equations (3.23-3.26). Figure 3.7 shows the conversion of spectral acceleration-period graph to spectral acceleration-spectral displacement format.

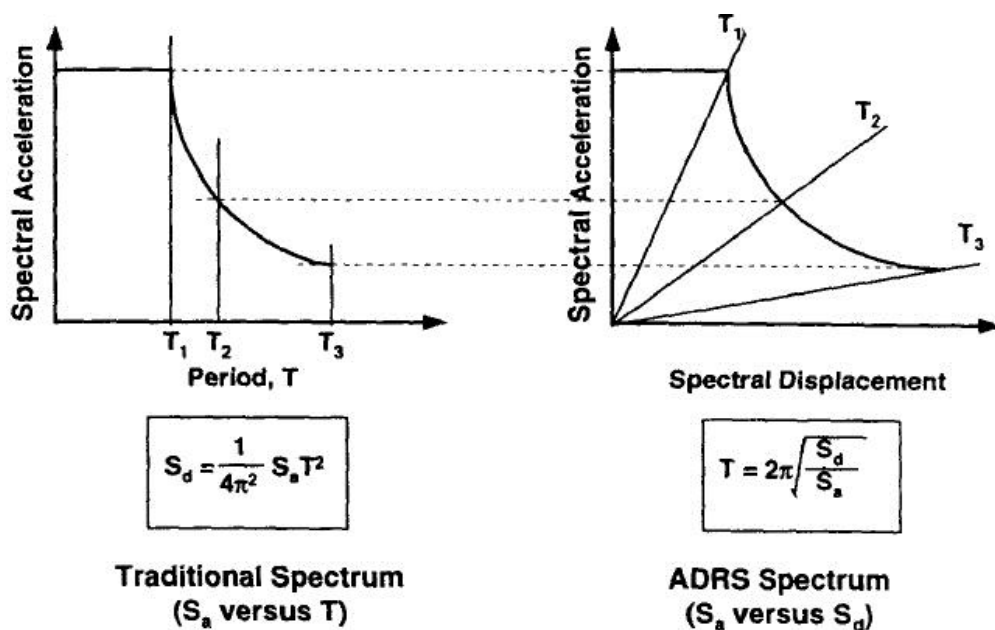


Figure 3.7 : Response spectra in traditional and ADRS format [3].

$$PF_1 = \left[\frac{\sum_{i=1}^N (w_i \phi_{i1}) / g}{\sum_{i=1}^N (w_i \phi_{i1}^2) / g} \right] \quad (3.23)$$

$$\alpha_1 = \frac{[\sum_{i=1}^N (w_i \phi_{i1}) / g]^2}{[\sum_{i=1}^N w_i / g][\sum_{i=1}^N (w_i \phi_{i1}^2) / g]} \quad (3.24)$$

$$S_a = \frac{V/W}{\alpha_1} \quad (3.25)$$

$$S_d = \frac{\Delta_{roof}}{PF_1 \phi_{roof,1}} \quad (3.26)$$

$$S_d = \frac{1}{4\pi^2} S_a T^2 \quad (3.27)$$

In the above equations PF_1 is the modal participation factor for the first mode, α_1 is the modal mass coefficient of the first mode, N is the level, V base shear, W structure weight, Δ_{roof} is the roof displacement, S_a is the spectral acceleration and S_d is the spectral displacement. Conversion of the capacity curve to ADRS format is given in Figure 3.8.

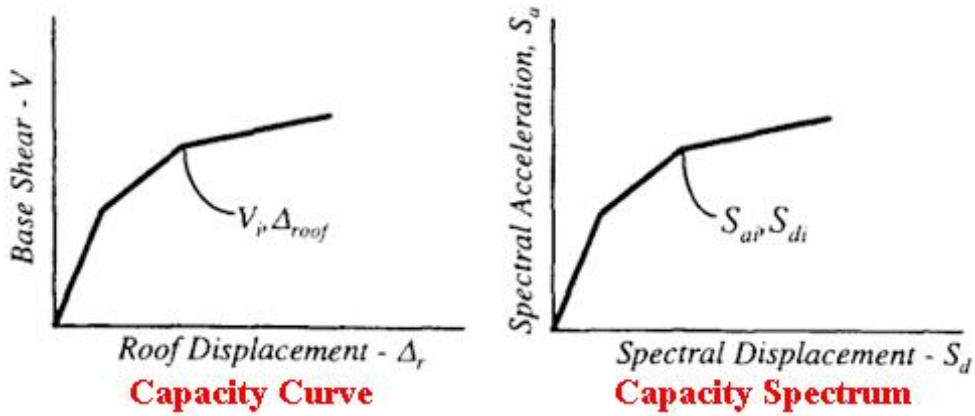


Figure 3.8 : Conversion of spectral coordinates to ADRS format [3].

A bilinear representation of the capacity spectrum is given in Figure 3.9. A trial point is needed in order to construct the bilinear representation of the capacity curve. This point is called as performance trial point. If the reduced response spectrum is found to intersect the capacity spectrum at the estimated (a_{pi}, d_{pi}) point, then that point is the performance point.

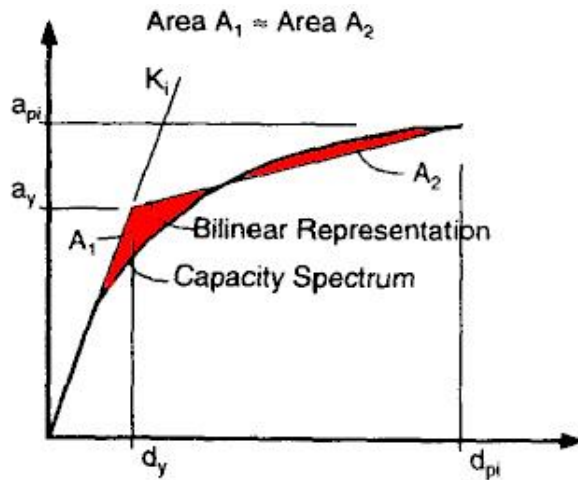


Figure 3.9 : Bilinear representation of capacity curve [3].

The next step should be reducing the response spectrum using the response reducing factors given ATC 40 [3]. This redacted response spectrum is then intersected with the capacity spectrum to determine the performance point.

Figure 3.10 shows the intersection of the reduced spectrum and the bilinear capacity spectrum in spectral acceleration-spectral displacement format. In addition, the trial performance point is plotted on the graph. If the demand spectrum intersects the capacity spectrum within acceptable tolerance, then the trial performance is called the performance point.

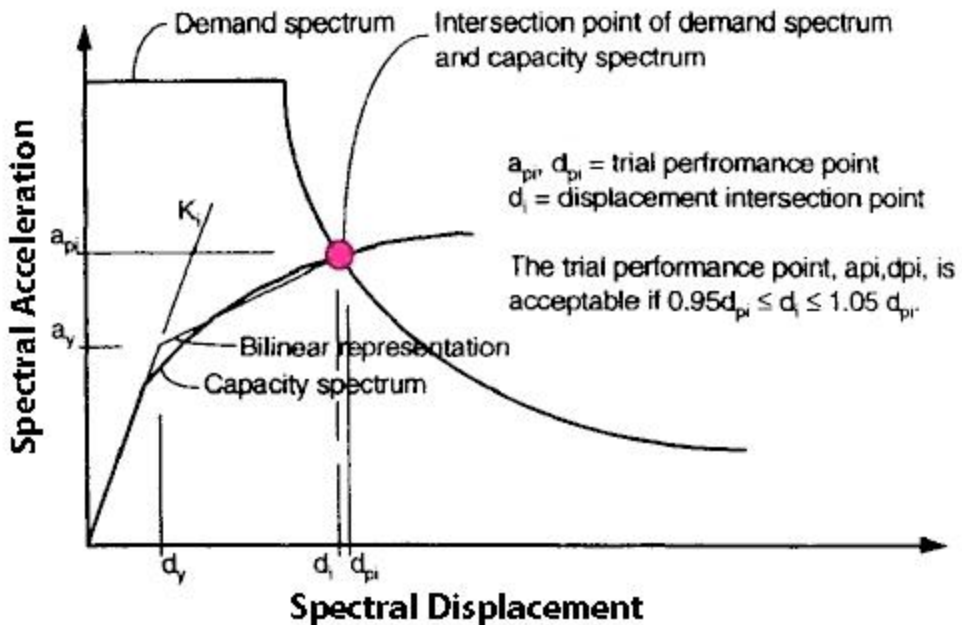


Figure 3.10 : Intersection point of capacity and demand spectrums [3].

b) Procedure B

This procedure assumes that the initial slope of the bi-linear representation of the capacity curve and the post-yield slope remain constant. The curve transformations and bi-linearization of the capacity curve is still valid. The initial stiffness is taken as the slope of the bilinear line [3]. Figure 3.11 shows the representation of performance point assessment using procedure B. For more information, ATC 40 [3] should be checked.

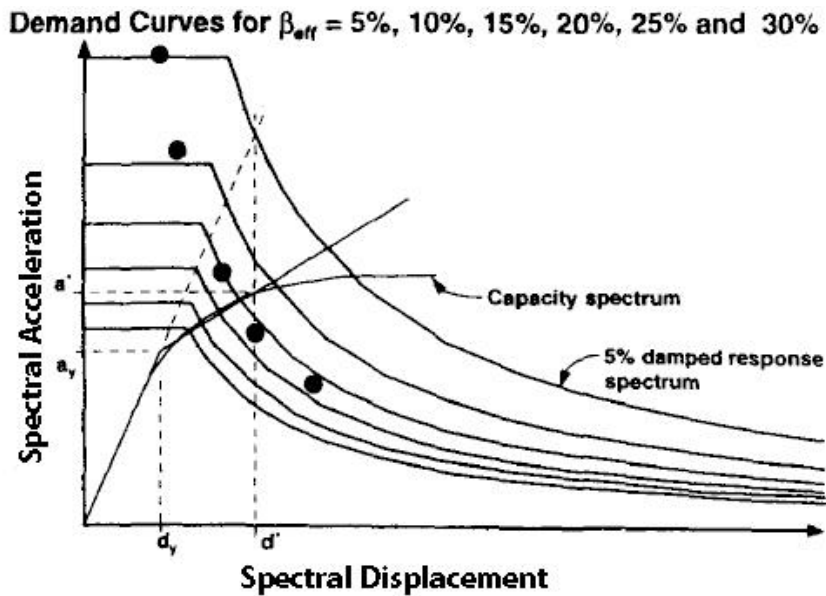


Figure 3.11 : Capacity spectrum procedure B [3].

c) Procedure C

This is a graphic based procedure to assess the performance point of the structure. It has been stated in ATC 40 [3] that, generally the first try gives the performance point of the structure. Figure 3.12 shows the last step of the procedure. For more information, ATC 40 [3] might be referred.

3.3.2 Determining the Performance Point By Coefficient Method

The displacement coefficient method is a direct numerical process for determining the demand [2]. There is no need to convert the capacity curve to ADRS coordinates. The performance point concept in ATC 40 [3] is named as the *target displacement* in FEMA 356 [2].

The base shear-displacement curve should be idealized to calculate the effective lateral stiffness as shown in Figure 3.13. K_e is the effective stiffness; K_i is the initial stiffness of the structure and α is the post yield slope.

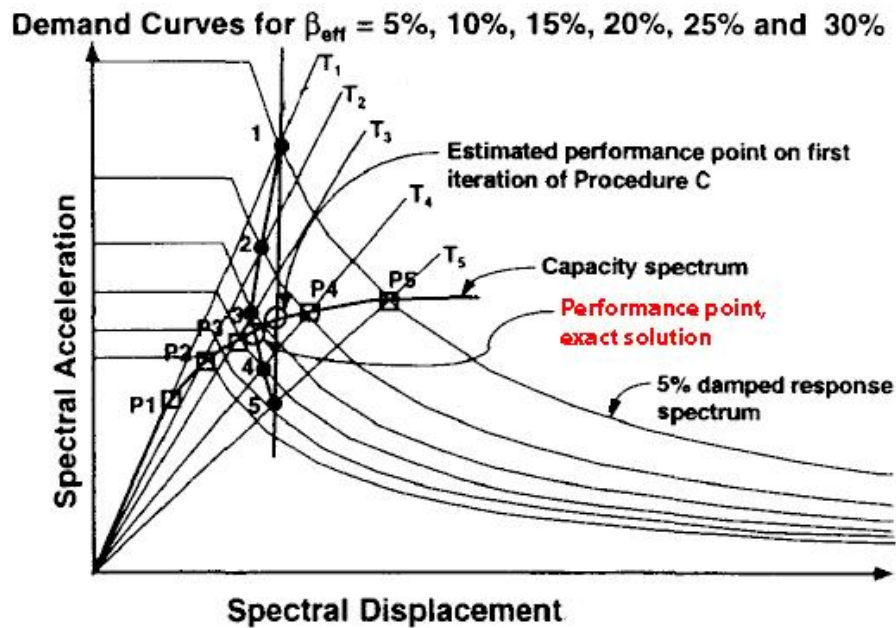


Figure 3.12 : Capacity spectrum procedure C [3].

Force-displacement curve is idealized by using an iterative graphical procedure assuming that the area above and under the curve is equal. FEMA 356 stated that, K_e effective stiffness is equal to secant stiffness at a base shear of 60% of the effective yield strength.

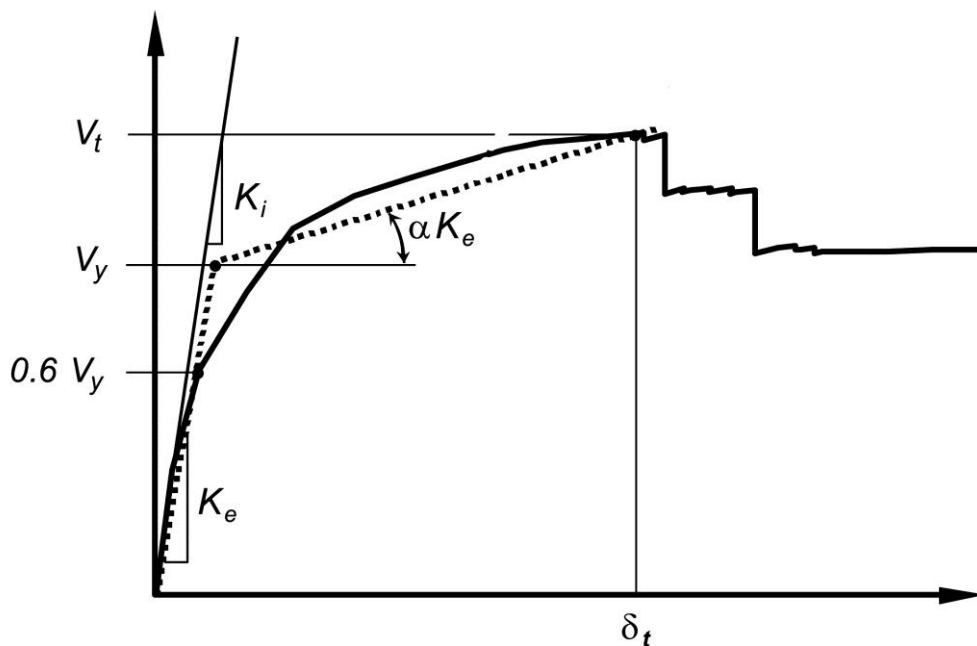


Figure 3.13 : Force-displacement curve with positive post-yield slope [2].

The effective fundamental period of a structure can be calculated from equation (3.28).

$$T_e = T_i \sqrt{\frac{K_i}{K_e}} \quad (3.28)$$

For buildings with rigid diaphragms at each floor level, the target displacement, δ_t , can be calculated by equation (3.29).

$$\delta_t = C_0 C_1 C_2 C_3 S_a \frac{T_e^2}{4\pi^2} g \quad (3.29)$$

C_0 is the modification factor to relate spectral displacement of an equivalent SDOF system to the roof displacement of the building. C_0 values are taken from Table 3.3 according to the load pattern and building type.

Table 3.3 : Values for Modification Factor C_0 [2].

Story No.	Shear Buildings		Other Buildings
	Triangular Load	Uniform Load	Any Load
1	1	1	1
2	1.2	1.15	1.2
3	1.2	1.2	1.3
5	1.3	1.2	1.4
10	1.3	1.2	1.5

C_1 is the modification factor that correlates the maximum inelastic displacements to linear elastic displacements. It is taken as 1 when T_e effective fundamental period is greater than or equal to T_s characteristic period of response spectrum.

C_2 represents the pinched hysteretic shape, stiffness degradation on maximum displacement. C_2 is taken from Table 3.4

Table 3.4 : Values for Modification Factor C_2 [2].

Performance Level	$T \leq 0.1$ second		$T \geq T_s$	
	Frame-1	Frame-2	Frame-1	Frame-2
I. Occupancy	1	1	1	1
Life Safety	1.3	1	1.1	1
Collapse Prevention	1.5	1	1.2	1

In Table 3.4 it is stated two types of frames. Frame-1 is the general name of structures, where the 30% of story shear forces are resisted by combination of frames, components or elements. The other type composes Frame-2. FEMA 356 proposed that C_2 should be taken as 1 for nonlinear procedures.

C_3 is a factor that takes care about the P- Δ effects. For buildings with positive post yield stiffness it can be taken as 1.0. For buildings with negative post yield stiffness, C_3 should be calculated with the given formulation in FEMA 356 document.

3.3.3 Improvements in FEMA 356 and ATC 40 Procedures, FEMA 440

Recent studies showed that, ATC 40 underestimate the maximum displacement for structures with hysteretic behaviour type *A* and *B*, whilst it overestimates for structures with hysteretic behaviour type *C*.

The overestimation increases as the strength decrease. It is assumed in ATC 40 that, the inelastic deformation for structures having behaviour type *B* will be larger than type *A*, while the nonlinear response history analyses show that the deformations are same or slightly larger for elastic perfectly plastic (EPP) model.

In addition, the current provisions of ATC 40 do not take care of the dynamic instability that can arise in systems with in-cycle strength degradation or P-delta effects.

The use of the equal displacement approximation to compute the coefficient C_1 for systems with periods longer than the characteristic periods leads to relatively good approximations of maximum inelastic deformations for systems with EPP behaviours for periods longer than about one second.

If the transition period is lengthened, the FEMA 356 equation to calculate C_1 does not adequately capture the changes in inelastic deformation demands for short-period structures [1].

There is not a clear division between the intent of coefficients C_2 and C_3 . C_2 is supposed to account for changes in lateral displacement whereas P- Δ effects are accounted by C_3 . In addition, FEMA 356 does not distinguish between cyclic strength degradation and in-cycle strength degradation.

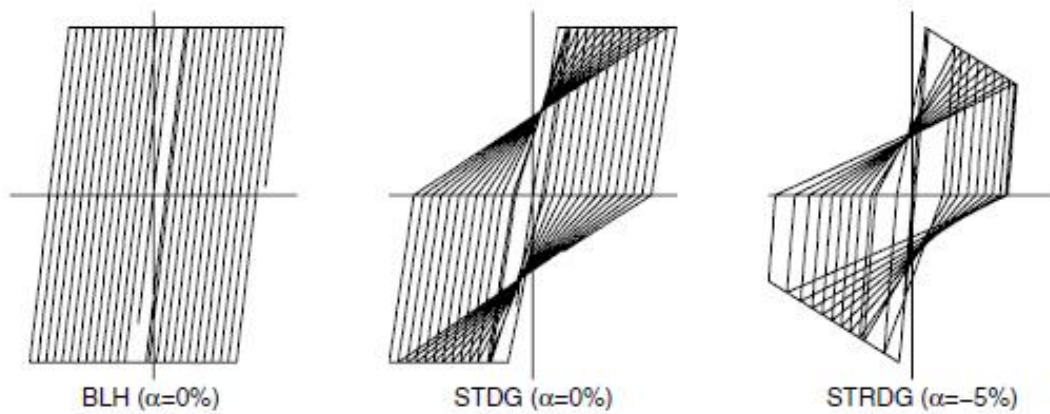


Figure 3.14 : Types of inelastic behavior considered in FEMA440 [1].

A variety of different inelastic hysteretic systems have been studied including *bilinear hysteretic (BLH)*, *stiffness-degrading (STDG)*, and *strength-degrading behaviours* in FEMA 440, as shown in Figure 3.14 [1]. The bilinear model (BLH) is the same as the elasto-plastic (EPP) model and the stiffness degrading model (STDG) is the same as the SD model, which are discussed in FEMA 356 [2] document. The strength-degrading model (STRDG) differs from the SSD model given in FEMA 356 [2]. A negative post-elastic stiffness ratio, α , is an indicative of in-cycle degradation.

3.3.4 N2 Procedure

Another nonlinear procedure used to determine the capacity is the *N2* method, which is proposed by Fajfar et al. in 2000 [56]. *N* denotes nonlinear analysis, whereas 2 is used to represent two mathematical models.

It can be said that, N2 is the modified version of the capacity spectrum method, where inelastic spectrum is used. Inelastic spectrum may be determined from the reduced elastic spectra by reduction factors. The lateral load pattern is related to the assumed displacement shape. This transforms the MDOF system to an equivalent SDOF system.

The steps of the procedure can be summarized as follows;

- a) A MDOF model and the nonlinear force deformation relationship are required.
- b) Seismic demand is defined in terms of an elastic acceleration spectrum (S_{ae}).

- c) Acceleration spectra are converted in to ADRS format for predefined damping values by using the equations (3.23-3.27). Figure 3.15 shows elastic spectrum in ADRS format.

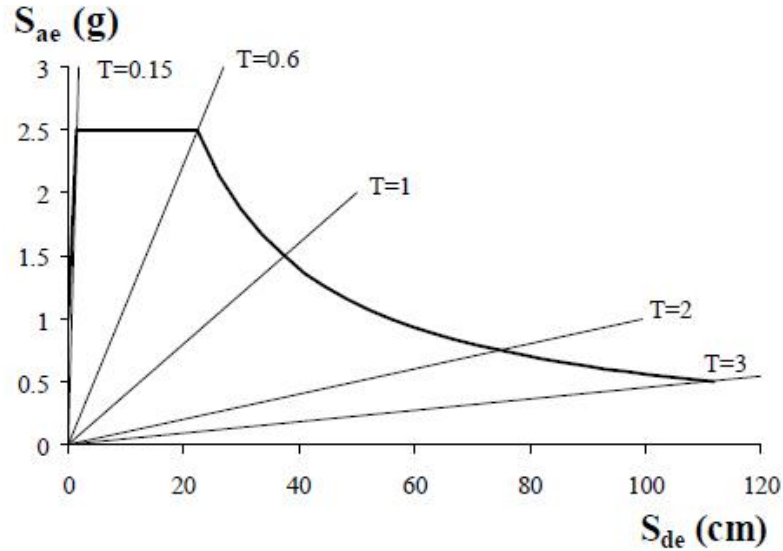


Figure 3.15 : Elastic spectrum in ADRS format [56].

- d) Inelastic spectrum should be obtained for the SDOF system by using the below (3.30) and (3.31) equations, where μ is the ductility factor defined as the ratio between the maximum displacement and the yield displacement, and R_μ is the reduction factor due to ductility.

$$S_a = \frac{S_{ae}}{R_\mu} \quad (3.30)$$

$$S_d = \frac{\mu}{R_\mu} S_{de} = \frac{\mu}{R_\mu} \frac{T^2}{4\pi^2} S_{ae} = \mu \frac{T^2}{4\pi^2} S_a \quad (3.31)$$

- e) R_μ should be determined using equation (3.32). T_C is the characteristic period of the ground motion.

$$R_\mu = \begin{cases} (\mu - 1) \frac{T}{T_C} + 1; & T < T_C \\ \mu; & T \geq T_C \end{cases} \quad (3.32)$$

- f) Applying the equations (3.30) and (3.32) on the elastic design spectrum showed in Figure in 3.15, the demand spectra for constant ductility factors in ADRS format can be obtained as shown in Figure 3.16.

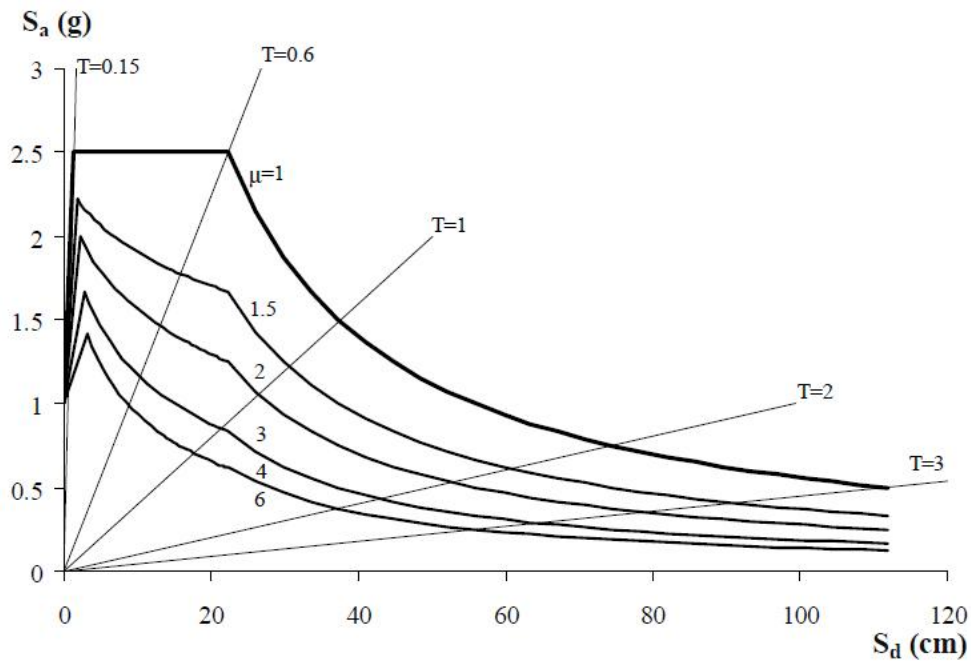


Figure 3.16 : Demand spectra for constant ductility factors in ADRS format [56].

g) Pushover analysis should be performed by subjecting the structure to a monotonically increasing pattern of lateral forces. At each yielding event, the structure loses its stiffness. Determination of the load pattern is the most crucial part of the procedure. It can be calculated by using the (3.33) equation, where M is the mass matrix. The distribution of lateral loads is denoted by Ψ which is related to the assumed modal shape Φ .

$$P = p\Psi = pM\Phi \quad (3.33)$$

h) MDOF system is transformed in to an equivalent SDOF system by proceeding the described procedures in ATC 40. Then the capacity curve of the SDOF system is plotted in terms of force-displacement.

i) Seismic demand of the SDOF system should be calculated. Figure 3.17 shows the elastic and inelastic demand spectra versus capacity. Here D_d^* is the design displacement value, D_y^* represents the yield displacement, S_{ay} is the yield acceleration, S_{ad} is the design acceleration.

j) SDOF system demand is converted to MDOF system, and MDOF system is subjected to a pushover analysis and the capacity curve is plotted.

For more detailed information Fajfar et al. [56] can be checked.

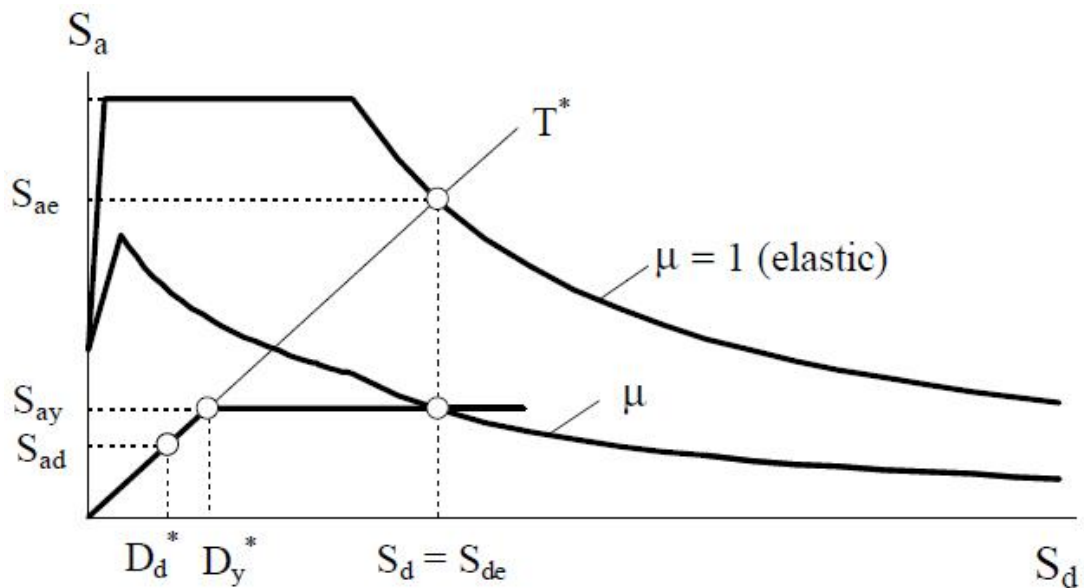


Figure 3.17 : Elastic and inelastic demand spectra versus capacity diagram [56].

3.3.5 Modal Pushover Analysis

For structures that vibrate primarily in the fundamental mode, the pushover analysis provides good estimates of inelastic demands. Also, story mechanisms, strength degradations etc. may be exposed during the analysis.

For structures, where the higher mode effects are significant, the estimated results of the pushover analysis may be inaccurate and misleading. It is now a known fact that, conventional pushover analysis may only catch the first local mechanism and may not consider the other weaknesses. Krawinkler et al. [54] stated in their work that, pushover analysis should be cooperated with elastic or plastic dynamic analysis, if higher modes are effective.

Both the force distribution and target displacement are based on the assumption that the response is controlled by the fundamental mode and that the mode shape remains unchanged after the structure yields. Researchers study for including the higher mode effects into pushover analysis. Literature review was given in Chapter-1. *Modal pushover procedure (MPA)* [18, 57] is one of those analysis methods, which is proposed by Chopra and Goel. MPA resembles linearly elastic structures and the procedure is mainly the same for *response spectrum analysis (RSA)*. It is then extended to inelastic structures. FEMA load pattern is used to assess the capacity of the structure by the proposers of the procedure [18, 57].

Chopra and Goel [57, 58] proposed modal pushover analysis in order to investigate the higher mode effects, where they suggest that, the response spectrum analysis for elastic structures can be reformulated by using modal pushover analysis (MPA). They showed that, the peak response of an elastic structure is equal to the values determined from the pushover analysis of the same structure by using the equation (3.34) for the lateral load distribution.

$$s_n^* = m\phi_n \quad (3.34)$$

Here, m is the mass matrix and ϕ_n is the n^{th} mode shape. Combining the peak modal responses by SRSS or CQC leads to the MPA procedure.

Steps of the procedure can be summarized as follows [57];

- a) First step is determining the peak response by the means of pushover analysis using the load pattern given in (3.34).
- b) Pushover curve is idealized as a bilinear force deformation relation for the inelastic SDOF.
- c) The peak deformation of the SDOF system is determined by the nonlinear response history analysis (RHA).
- d) Total demand is determined by combining the modal quantities by SRSS or CQC.

Figure 3.18 shows a sample load distribution for the modal pushover analysis procedure. SAC buildings are 9 story and 20 story steel buildings that are located in Los Angeles. More detailed information can be gathered in Chopra and Goel's work [57].

Chopra and Goel extended their work in 2004 as *modified modal pushover analysis* [6] with slight differences. The seismic demands associated higher modes are calculated assuming that the building remains elastic and P- Δ effects due to gravity loads have been included in pushover analysis for all modes; these were considered only for the first mode in the earlier version.

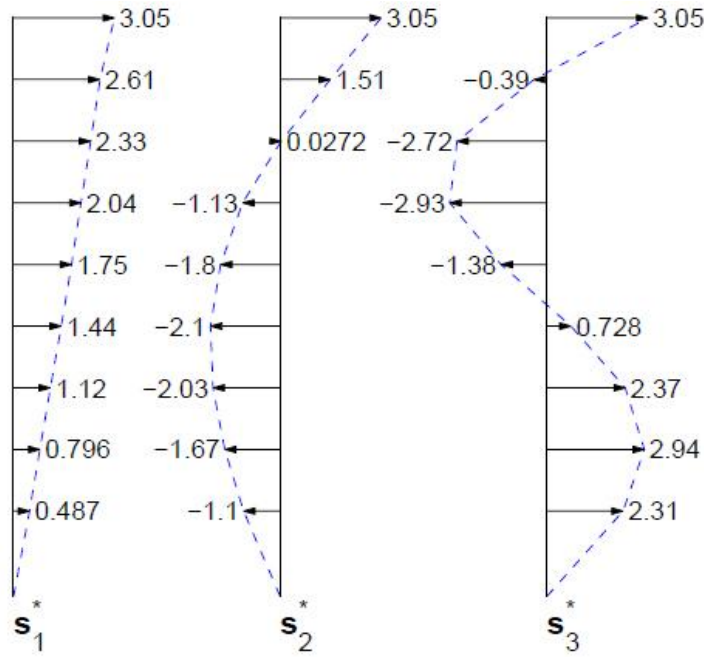


Figure 3.18 : Sample force distribution of SAC building for MPA procedure [57].

3.3.6 Energy Based Pushover Procedure

As a known fact, the roof displacement is used in pushover procedures to determine the capacity curve. It also establishes the seismic demands over the height of the structure at the estimated peak displacement.

Although the capacity curve could be based on the displacement at any floor, the researches show that the roof displacement emphasizes the overall response of the structure and provides better numerical accuracy, especially when higher modes are involved [59].

As a parameter, roof displacement is not an adequate parameter by itself. The displacement of the roof increases disproportionately as the lateral load increases. Montes et al. [59] showed that for systems with sharply defined yield points, displacements disproportionately increase over the height of the structure.

Sometimes, roof displacements increase or may even reverse, leading to capacity curves that display unusual behaviour. Montes et al [59] stated that the capacity curves of this situation indicate that, structure does not always absorb energy in a pushover analysis, but maybe a source of energy. This assumption is the result of the arbitrary choice to use the roof displacement as the index of the capacity curve.

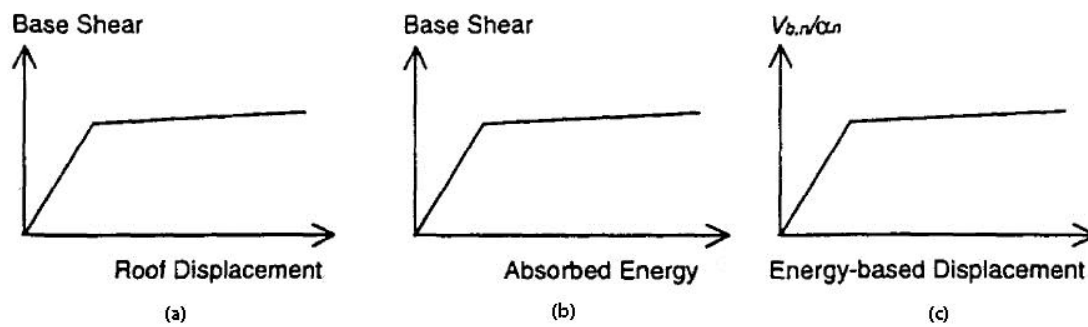


Figure 3.19 : Capacity curves of an equivalent SDOF system [59].

This is the main reason why roof displacement is not always convenient. An energy based procedure has been proposed by Montes et al [59] and Albenesi [34]. Both of the methods propose using the energy absorbed by the structure in each modal pushover analysis instead of roof displacement to determine the capacity curve of the equivalent SDOF system. The energy absorbed by the MDOF structure in the pushover analysis is used to derive an energy-based displacement that assembles the work done by the equivalent SDOF system [59].

Figure 3.19 shows three different types of pushover curves; in (a) conventional capacity curve is plotted base shear versus roof displacement, in (b) an alternative view of base shear versus absorbed energy or work done is given. From the data of (b) some can be able to determine the capacity curve of the equivalent SDOF system using conventional transformations of base shear with the energy based displacement as shown in (c).

For more detailed information [34, 59] can be investigated.

3.3.7 Direct Displacement Based Pushover Procedure

The above-mentioned force based procedures ends with displacement check to ensure that acceptable performance levels are achieved in the design or not. Priestly [60] stated that, force based procedures might sometimes lack determining the capacity. The deficiencies might be summarized as follows;

- a) The use of force-reduction factors for design makes the results suspicious.
- b) Generally, force-reduction factors are less than code indicative limits; this implies the need for iterative design.
- c) 3-D modal analysis should be compiled with the force based analogy.
- d) Torsional effects should be induced in the force based pushover analysis.

- e) Force based design requires the specification of initial stiffness of structural members.
- f) The assumption that the elastic characteristics of the building are the best indicator of inelastic performance, as implied by force-based design, is clearly of doubtful validity.

As a consequence of the above deficiencies, alternative design procedure has been developed by Priestly in 1992 [60], known as the *direct displacement based design*. It's a known fact that, force based design analogy bases on keeping the risk for a given structure below an acceptable threshold.

The main difference between the proposed method and the force based design is in the characterization of the stiffness. Force based procedures uses elastic properties at first yield, while displacement based design propose using the K_{eff} , *secant stiffness* at maximum displacement, as schematized in Figure 3.20.

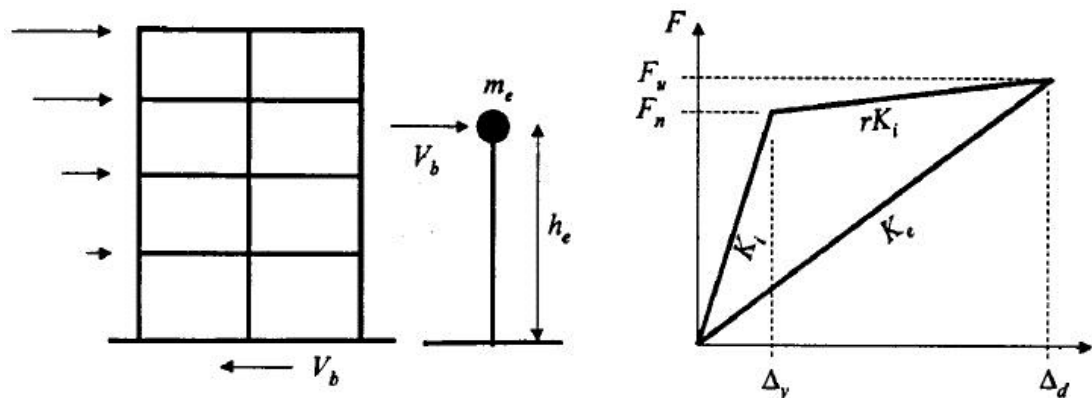


Figure 3.20 : Fundamentals of displacement based design [60].

With the determined design displacement Δ_d , the effective period T_e at maximum displacement response can be set up from a set of design displacement spectra, as shown in Figure 3.21.

The effective period of the SDOF system might be calculated from equation (3.35).

$$T_e = 2\pi \sqrt{\frac{M_e}{K_{eff}}} \tag{3.35}$$

Here, M_e is the effective mass and K_{eff} is the effective stiffness. The design base shear can be determined using (3.36).

$$V_B = K_{eff}\Delta_d \quad (3.36)$$

More information about displacement based design can be gathered from [60, 61, 62].

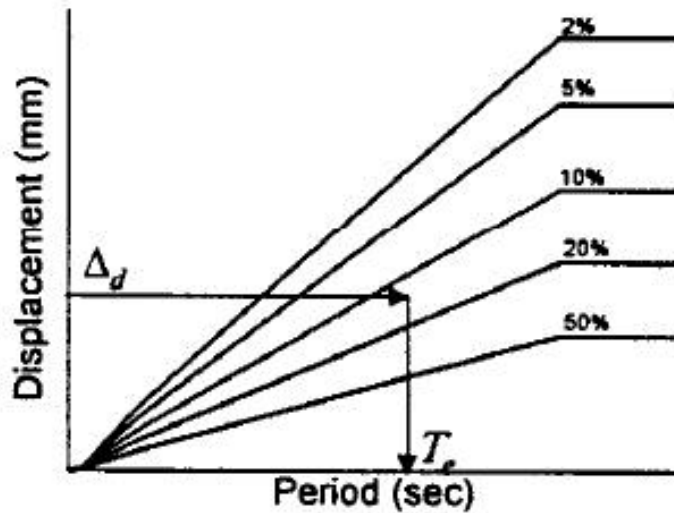


Figure 3.21 : Design displacement response spectra [60].

3.3.8 Issue of Torsion in Pushover Analysis

Originally, nonlinear static methods are limited to planar models. To extend the applicability of these methods to asymmetric structures, studies have been attempted in recent years. This requires a complete 3-D analysis of the structure. Researches Barros and Ayala [5], Aydınoğlu [8], Chopra and Goel [6], Fajfar [65] worked on including the torsional effects in pushover analysis.

De Stefano and Pintucchi [63] stated in their work that, in fact all of the real structures are almost irregular as regularity is an idealization. Most of the seismic codes classified irregularity in plan and in elevation, whilst it is a fact that structural irregularity is the combination of both types. Recent studies showed that, most of the structural damage during an earthquake excitation is due to plan irregularities, such as asymmetric distributed mass, stiffness and strength [63].

Most of the aforementioned studies were conducted using simple single-story asymmetric models. However, more studies that are realistic should be compiled. In the work of De Stefano and Pintucchi, they stated that in order to mitigate the torsional effects, passive control is a good alternative way. Base isolated systems, visco-elastic damped systems and friction dampers might be an appropriate example of these systems. In spite of extensive research efforts, the complexity of inelastic seismic response leads to lack of general and universally accepted conclusions [63]

Fajfar extended his N2 method [56] for including the irregularity effects. Based on the results of parametric studies Fajfar et al. [65] proposed to combine the results of pushover analysis with the results of elastic dynamic analysis for a 3D model. The basic idea is that the former results would lead the target displacement, whereas the dynamic results would resemble the torsional effects. In fact, the idea of combining the linear dynamic results with the pushover analysis was first proposed by Tso and Moghadam [64] in 1997. However, they determine the target displacements of substructures (e.g. walls, planar frames etc.) by the 3D elastic dynamic analysis of the whole structure; 2D pushover analyses are then followed. The on-going researches show that, the inelastic torsional response is nearly same as the elastic torsional response. It has been concluded that the torsional effects decrease with the increasing plastic deformations [65].

N2 method has been developed to include torsional effects with the following assumptions [65];

- a) The displacement results of the elastic dynamic analysis can be used for estimating the inelastic response.
- b) Any compatible torsional effects of elastic analysis may decrease or even disappear in the inelastic range.

Basic steps used to improve the N2 [56] procedure can be stated as follows;

- a) Pushover analyses are performed by using a 3D model. Loading is applied at the center of mass in horizontal direction for both the positive (+) and negative (-) sign. Target displacement is the larger value of the two, obtained for positive and negative sign.
- b) 3D model is subjected to a linear modal in two horizontal directions and the results are combined using the SRSS rule.

- c) A correction factor should be applied to the pushover results. It is defined as the ratio of the normalized roof displacements obtained by elastic modal analysis and pushover analysis. Normalized roof displacement can be calculated by dividing the roof displacement of an arbitrary location to center of mass. If this value is smaller than 1.0, then it should be taken as 1.0 [65].
- d) The results of the pushover analysis should be multiplied by the correction factors.

In the proposed procedure by Fajfar et al. [65], the displacement demand at the center of mass is determined by the conventional N2 method. The demand due to torsion is determined by elastic dynamic analysis.

Although single-story models represent the most extreme idealization of plan irregular buildings, in recent years multi-story building models have become increasingly popular due to overcome the deficiencies of resembling the real structure.

Chopra and Goel extend the modal pushover analysis [18] to multi modal pushover method [6] by applying torsional moments at each floor in addition to lateral forces. The mentioned methods were explained in Chapter 3.3.5.

Penelis and Kappos [66] consider the inelastic torsional response of buildings by considering 3D models. Response quantities were generalized by an equivalent SDOF system which is adopted to correspond both the translational and torsional modes.

It is stated in Jeong and Elnashai's report [32] that, when an excitation is given in one direction, it leads to asymmetry in both directions due to its coupled stiffness matrix. This is what generates the torsional responses which cannot be determined by static analysis. That is the main reason of determining the torsional effects by dynamic response analysis.

Figure 3.22 shows the difference between the maximum interstory drift ratios at the center of a story and at the flexible edge column that is subjected to the largest displacement. Interstory drift ratio might be defined as the ratio of interstory to story height.

Here; $975x-1$ represents the maximum interstory drift ratio of the first story when the Acc. 975 earthquake record is applied in the x direction. Similarly, $975y-3$ represents the maximum interstory drift ratio of the third story when the record is applied in the y direction. Acc. 975 represents the ground motion with return period of 975 years.

The significant difference between two interstory drifts, which is also the additional interstory drift (ID) of critical member, is due to the torsional response. Therefore, interstory drift at the center of a story can mislead the damage assessment. The effect of torsion should be accounted in the damage assessment of irregular structures [32].

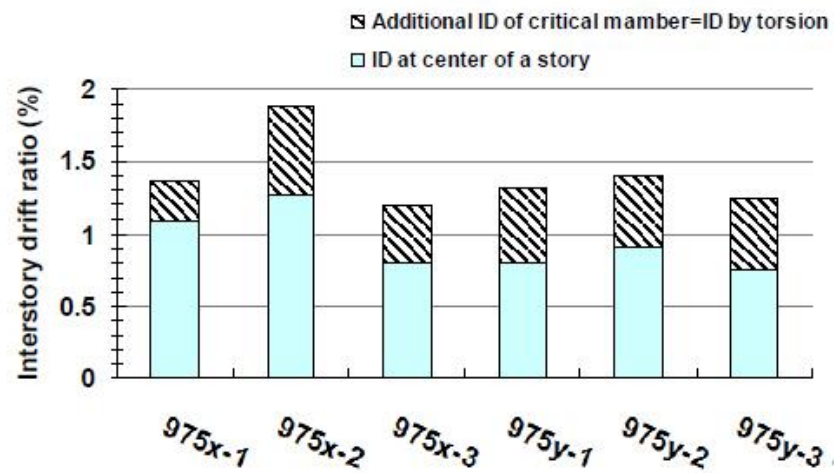


Figure 3.22 : Difference of interstory drifts [32].

When a floor is subjected to rotation, in addition to displacements in the x and y direction as shown in Figure 3.23, the displacements of a column C_i are given. Here; $C.R.$ resembles the center of rotation and can be any point on the plane as long as its Δ_x and Δ_y displacements and θ rotation are available [32].

If we assume that the origin and the C.R. intersect, then the point C_i would have an ordinate of x_i and y_i . If we named the deformed position as C'_i and the coordinates of the point with (x'_i, y'_i) ; the displaced coordinates can be calculated by using the equation (3.37).

$$\begin{Bmatrix} x'_i \\ y'_i \end{Bmatrix} = \begin{bmatrix} \cos \theta & -\sin \theta \\ \sin \theta & \cos \theta \end{bmatrix} \begin{Bmatrix} x_i \\ y_i \end{Bmatrix} + \begin{Bmatrix} \Delta_x \\ \Delta_y \end{Bmatrix} \quad (3.37)$$

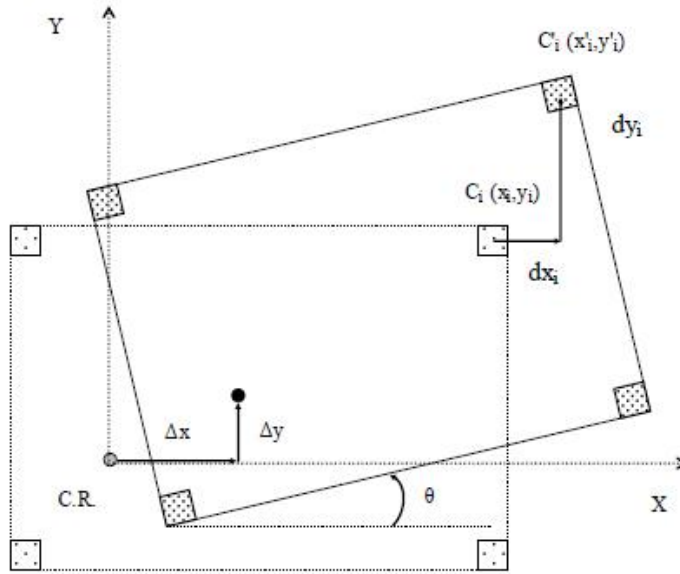


Figure 3.23 : Effect of torsion on member displacements [32].

By obtaining the displacements dx_i and dy_i and the angle of rotation of a column C_i , demand of the member is determined. This member is to be assessed considering shear, torsion and axial force.

FEMA 356 [2] defined two types of torsion, *actual torsion* and *accidental torsion*. Actual torsion is due to the eccentricity between centers of mass and stiffness, whilst accidental torsion is intended to cover the effects of the rotational component of the ground motion. Calculation of the actual torsional moment at a story is determined by multiplying the seismic story shear force by the eccentricity between the center of mass and the center of rigidity. FEMA 356 [2] explains that, the accidental torsion moment of a story can be calculated as the seismic story shear force multiplied by a distance equal to 5% of the horizontal dimension.

Also a methodology has been given in FEMA 356 [2] in order to consider the torsional effects;

- a) η , the displacement multiplier at each floor has to be calculated, as the ratio of the maximum displacement at any point to the average displacement.

$$\eta = \frac{\delta_{max}}{\delta_{avg}} \quad (3.38)$$

- b) Unless the accidental torsional moment is less than 25% of the actual torsional moment, accidental torsion should be considered.

- c) When the torsional moment exceeds 1.2 at any level then the accidental torsion should be amplified by a factor A_x defined in (3.39).

$$A_x = \left(\frac{\eta_x}{1.2}\right)^2 \leq 3.0 \quad (3.39)$$

- d) If the displacement modifier η , due to total torsional moment at any floor exceeds 1.50, 3-D model should be accounted.
- e) If a 2-D model is used, then the effects of horizontal torsion should be amplified by the maximum value of η for linear static and dynamic analysis, and for the nonlinear static procedure the target displacement should be amplified by the maximum value of η . Also for the nonlinear dynamic procedures, the amplitude of the ground acceleration should be amplified by η .
- f) The effects of accidental torsion should not be used to reduce force and deformation demands on elements.

3.3.9 Deficiencies of Conventional Pushover Analysis

Although pushover procedures have been developed in the last decade, there are still some points need to be improved. They reduce the computational effort and save time, but they still cannot represent the nonlinear behaviour perfectly. This is the bases why there is a necessity of advanced pushover procedures.

Elnashai et al. [4] stipulated the deficiencies of the conventional pushover procedures as follows;

1. Conventional pushover analyses investigate structural capacity and earthquake demand separately. However, recent studies show that because of the nonlinear load pattern, it is not adequate to separate the demand and capacity.
2. In the conventional pushover analysis, only the lateral load pattern and lateral deformations of the structure is investigated. The effect of energy over deformation is neglected. This misleads the results. Also, it neglects the changes of dynamic components such as kinetic and viscous damping energy.
3. The conventional pushover analysis procedure does not account for the higher mode effects as well as the changes in the modal properties during nonlinear yielding.

4. Torsional effects are induced after the analysis by combining the pushover results or by amplifying the results. This makes the analysis doubtful. As explained in 3.3.8, irregularity effects are very important especially for asymmetric structures.

Due to its easiness and time saving property, it is clear that conventional pushover analysis lacks of the dynamic quantities. That is the main reason why some developments such as the adaptive procedures are suggested by the researches.

3.4 Adaptive Pushover Methods

As explained in the previous chapters, determination of the lateral load pattern is the main issue for nonlinear pushover procedures. Mostly, the analysis procedures are named by the used load pattern in the analysis, e.g. conventional analysis uses conventional load patterns such as uniform, triangular or modal, whilst the adaptive procedures use adaptive load patterns. FEMA 356 [2], proposed the usage of at least two vertical distributions of lateral load pattern, where the first group is the modal load pattern and the other one is the uniform or the adaptive load pattern. Changes in the distribution of lateral inertial forces can be best investigated using adaptive load patterns which simultaneously change as the structure is displaced to larger amplitudes.

As explained in Chapter 1, lot of procedures are developed for adaptive load patterns in the literature. It is obvious that, using an adaptive load pattern will require more computational effort but the result will be more realistic and robust according to the conventional ones.

Elnashai [39] defined adaptive pushover as a method, where possible changes to the distribution of inertial forces can be taken into account during static analysis. Figure 3.24 shows the adaptive force distribution for a regular framed building.

The determined steps required to perform adaptive pushover analysis in seismic codes can be summarized as follows;

- a) The gravity loads are applied in a single step.
- b) With its current initial stiffness the structure has been subjected to an eigenvalue analysis and the modal properties are determined.
- c) Modal participation factor should be calculated using equation (3.13).

- d) Modal story forces at each floor level for the N modes should be determined by using equation (3.40). Here, M_i is the seismic mass of the i^{th} level, $F_{i,j}$ is the estimated force at the i^{th} level for the j^{th} mode, g is the acceleration force.

$$F_{i,j} = \Gamma_j M_i \Phi_{i,j} g \quad (3.40)$$

- e) Static pushover analysis is performed using the load pattern determined in step d given with equation (3.40).
- f) Each modal quantity for step k is combined using the SRSS rule to estimate the structural forces and displacements. These values are added to the previous $(k-1)^{th}$ step of the analysis.
- g) The aforementioned iterative procedure described in step f should be maintained until the specified target displacement is achieved.

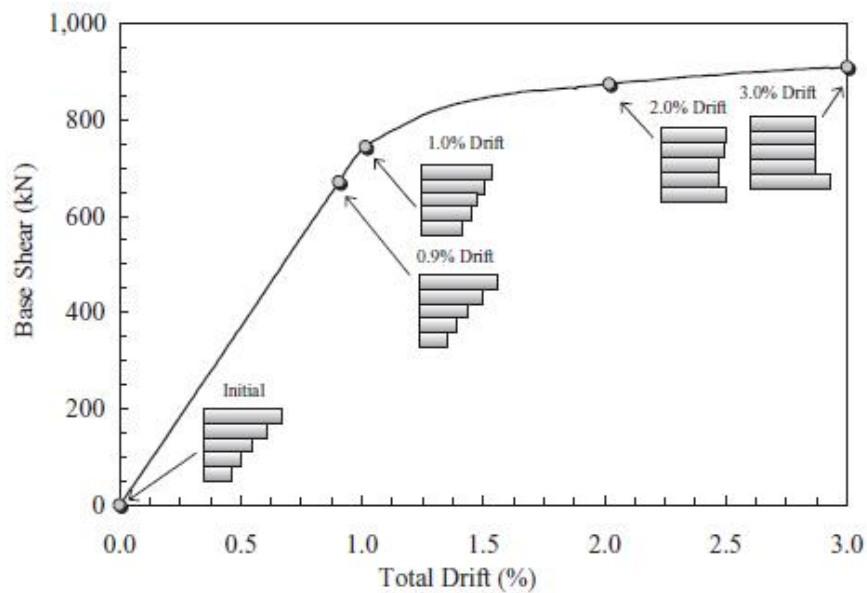


Figure 3.24 : Adaptive force distribution for a regular framed building [39].

Research to refine adaptive pushover methods is still an on-going dilemma for structures. Papanikolaou et al. [4] give comparisons between conventional and adaptive pushover curves for regular and irregular structural systems in their work. They compared their results with response history analyses. Figure 3.25 and Figure 3.26 shows the comparison of conventional and adaptive pushover curves with the response analysis for regular and irregular structures respectively [39].

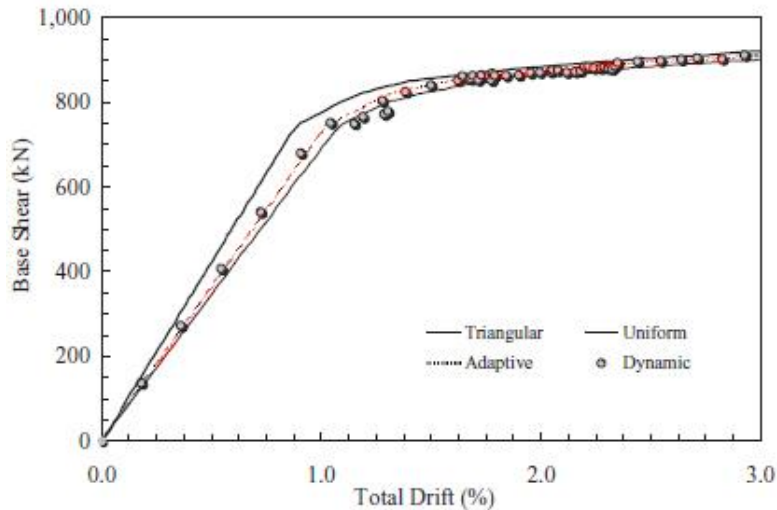


Figure 3.25 : Comparison for regular structures [39].

Papanikolaou et al. [4], performed the adaptive pushovers by utilizing the scaling of acceleration spectrum. They used the uniform and triangular load distributions for the conventional pushovers.

The most crucial point of their work is that; in the case of irregular systems, the conventional pushover analysis method can be classified as inadequate, whereas adaptive pushover procedure is in good agreement with the response analysis.

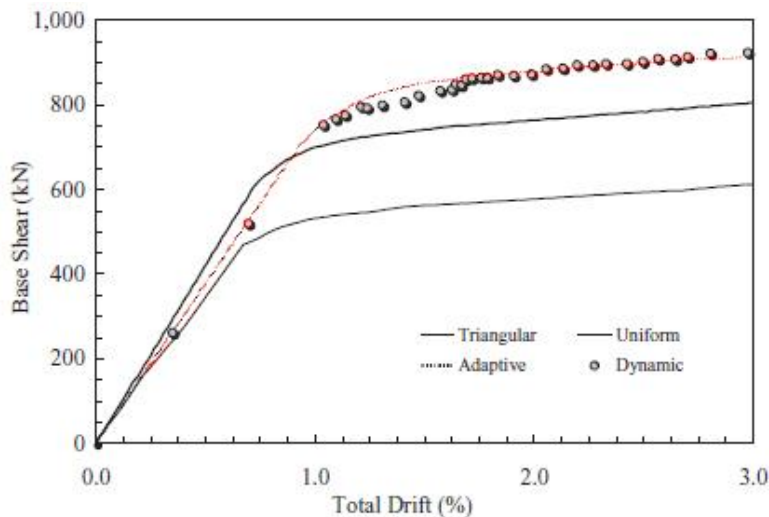


Figure 3.26 : Comparison for irregular structures [39].

Papanikolaou et al. [4] proposed an algorithm of fibre-based adaptive pushover procedure. The flowchart of the procedure is given in Figure 3.27. According to this approach, the lateral load pattern is continuously updated basing on the combination of the instantaneous modal shapes of the inelastic periods. Mode shapes are determined from the eigenvalue analysis using the K_T tangent stiffness matrix.

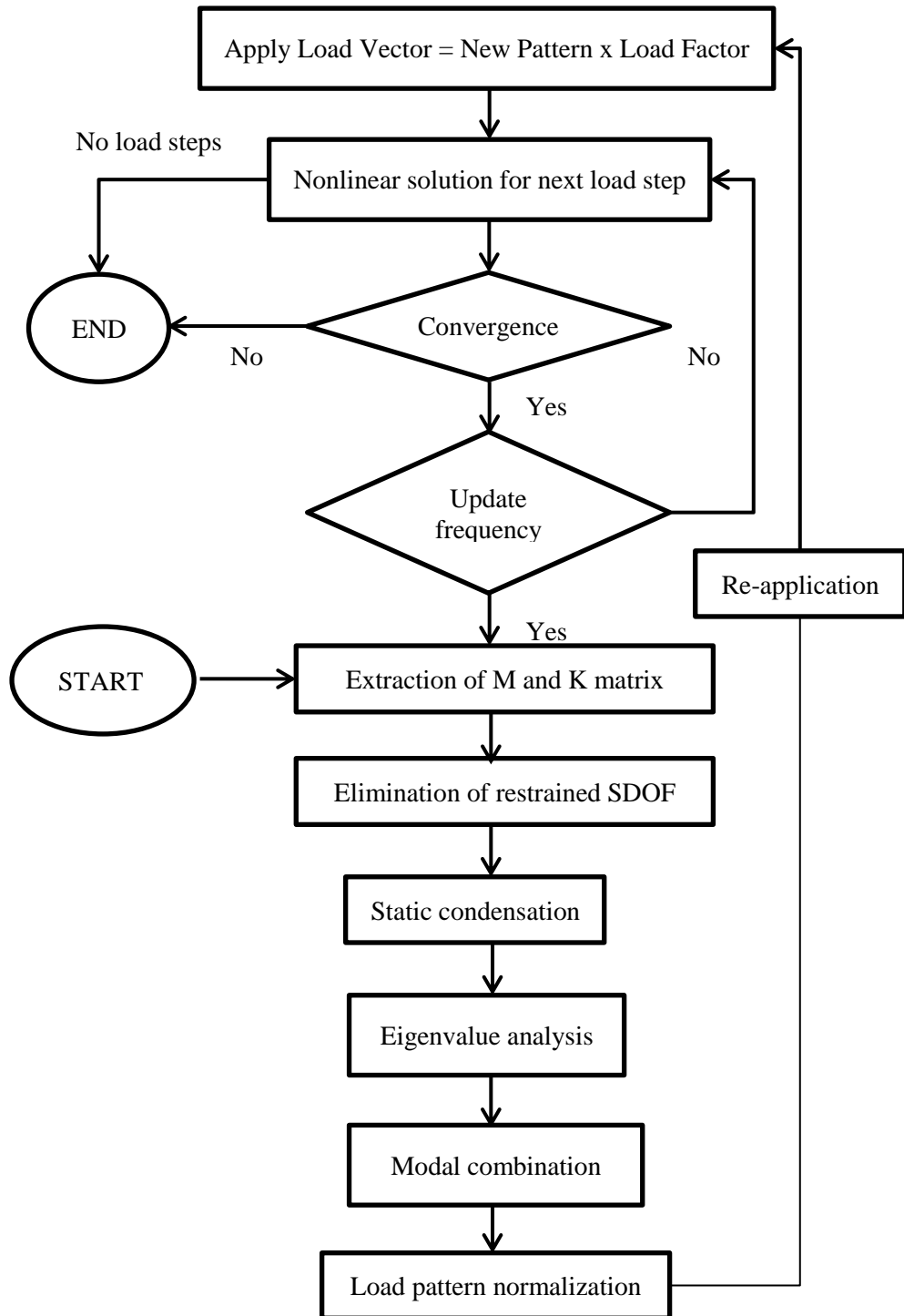


Figure 3.27 : Flowchart of the adaptive pushover procedure [4].

3.4.1 Fibre Modelling approach For Determining the Inelastic Response

There are two different strategies for modelling an inelastic response of the structures that are excited with an earthquake excitation; *concentrated plasticity* and the *distributed inelasticity*. The proposed lumped plasticity models can be grouped as, models including stiffness degradation in flexure and shear, having pinching effect

under load reversal and fixed end rotations at the beam-column joint [67]. It is now believed that, the *distributed inelasticity modelling* describes more accurately the structural characteristics.

The behaviour of the cross-section can be either formulated according to the classical plasticity theory, or derived by discretizing the cross section into fibres which is known as the *fibre modelling*. Fibre modelling assumes that the material inelasticity is spreaded through the member length and cross section. This phenomena gives chance to estimate the highly inelastic structural damage.

Stiffness based fibre modelling approach was first proposed by Izzuddin et al. [68] in 2001. They supposed obtaining the stress relationships of the elements through the integration of the nonlinear response of individual fibres. Fibres are where the section is divided into three main parts; confined concrete, unconfined concrete and steel sub section.

Figure 3.28 shows the discretization of a typical reinforced concrete (RC) cross section. The fibre model is schematized for a reinforced concrete section in Figure 3.29. Bending moment-curvature relationships are derived from the material behaviour of the fibre.

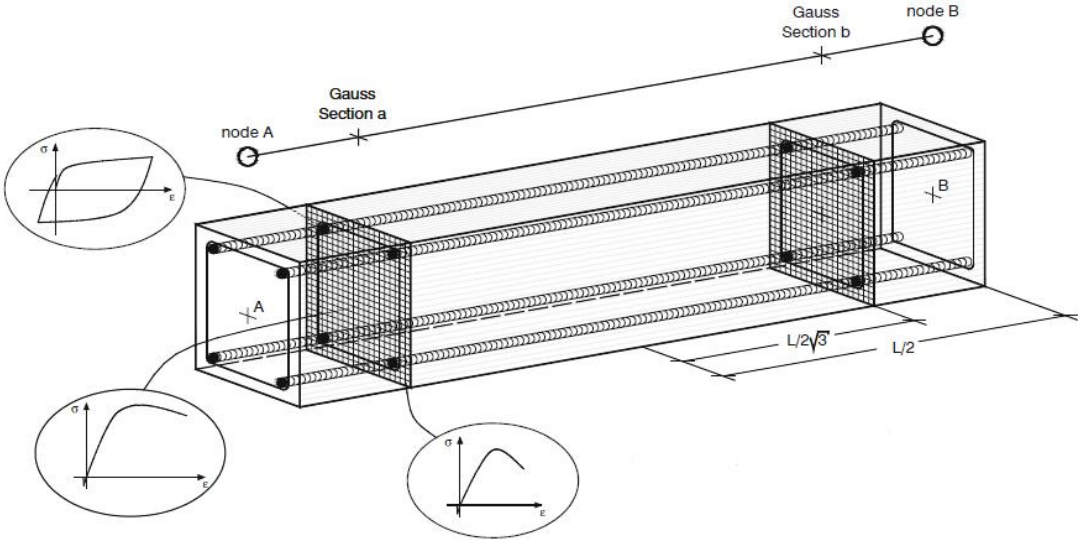


Figure 3.28 : Discretization of a typical reinforced concrete cross-section [67].

In lumped inelasticity models, the element response is represented by zero-length plastic hinges, referred as *point hinges* located at member ends. The point hinges are resembled by inelastic springs. The stiffness matrix of the member is computed from the stiffness of the single or multiple springs [39].

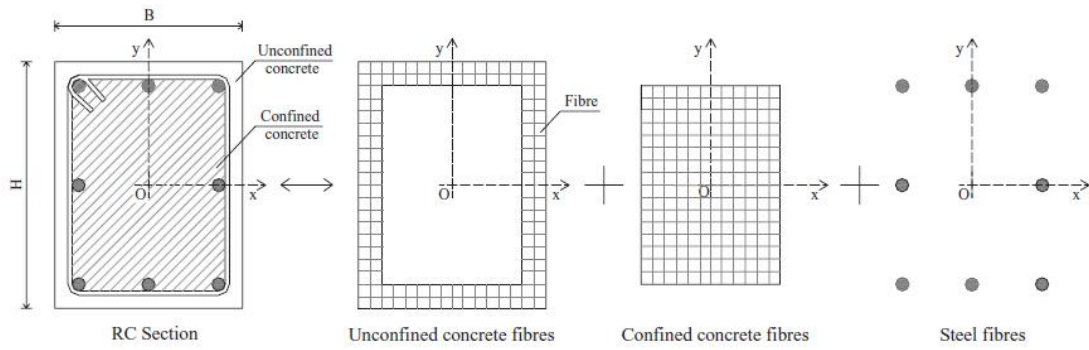


Figure 3.29 : Fibre model for a reinforced concrete section [39].

In Figure 3.30 a typical lumped model under bending moment effect has been showed.

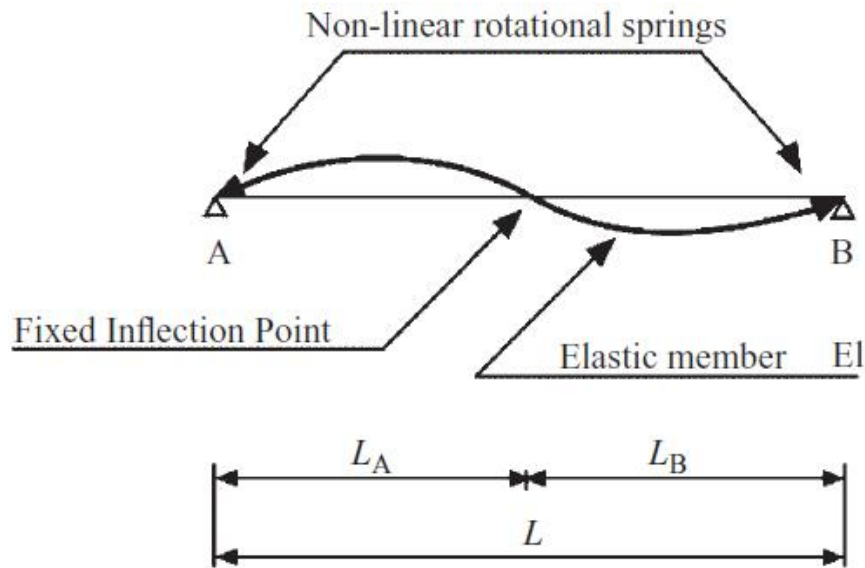


Figure 3.30 : Lumped plasticity model elements [39].

3.4.2 Adaptive Spectra Based Pushover Procedure

The main differences between traditional pushover analysis and the proposed adaptive method can be stated as;

- a) The proposed procedure implies a site specific spectrum to define the loading characteristics.
- b) The applied load pattern is continuously updated depending on the instantaneous dynamic properties of the structure.

The first proposed spectra based adaptive procedure was by Bracci et al [21]. They proposed using the results of the eigen value analysis directly to determine the

demand. However in Gupta and Kunnath [24] procedure, the demand is the basis for determining the incremental lateral forces.

The basic steps of the spectra based adaptive pushover procedure is stated below;

- a) A mathematical model is created.
- b) Using a section analyser (e.g. XTRACT, BIAx etc.) the section properties should be determined.
- c) The damped elastic response spectrum should be computed for the site-specific ground motion.
- d) An eigen value analysis should be performed and the modal participation factor should be calculated using (3.13).
- e) Using the elastic response spectrum, story forces for each story level should be implemented using the equation (3.41), where $F_{i,j}$ is the lateral story force at i^{th} level for j^{th} mode and $S_a(j)$ is the spectral acceleration corresponding to the j^{th} mode.

$$F_{i,j} = \Gamma_j M_i \Phi_{i,j} g S_a(j) \quad (3.41)$$

- f) Modal base shears (V_j) should be computed and they should be combined using SRSS to determine the building base shear (V) as given in (3.42) and (3.43) respectively.

$$V_j = \sum_{i=1}^N F_{i,j} \quad (3.42)$$

$$V = \sqrt{\sum_{i=1}^N V_j^2} \quad (3.43)$$

- g) The previously calculated story forces should be scaled using a scaling factor of S_n . Scaling of the forces is given in equation (3.44). Determination of the scaling factor is given equation (3.45) where N_s is the number of uniform steps (e.g. $N_s=100$).

$$\bar{V}_j = S_n V_j \quad (3.44)$$

$$S_n = \frac{V_B}{N_S V} \quad (3.45)$$

- h) Using the scaled incremental story forces determined in the previous step, a static pushover analysis should be performed.
- i) Displacements, story drifts, etc. should be computed by using the SRSS combination rule of the respective modal quantities. Those should be added to the previous step.
- j) If any member yields the stiffness matrix should be recalculated, and analysis should begin with step d.
- k) The process is repeated until, either the maximum base shear is reached or the global drift exceeds the specified limit.

3.4.3 Incremental Response Spectrum Analysis (IRSA)

It is a known fact that, the structural damage under an earthquake excitation is controlled by the inelastic deformations. As explained in 3.3.7, displacement based design gives more accurate results according to force based approaches. Although the majority of the seismic codes still use force based analogy, some started to propose the displacement based procedure, since it is more realistic to determine the capacity using the deformations.

Incremental Response Spectrum Analysis (IRSA) is a multi-mode pushover procedure, where the incremental response is assumed piecewise linear at each pushover step between the formation of two consecutive plastic hinges [69]. The modal scaling concept is applied at each step.

Figure 3.31 shows the scaling of modal displacements through monotonic scaling of response spectrum. Modal scale factor of the elastic response spectrum starts from zero until unity at each step. The equal displacement rule is applied to the elastic spectral displacements while calculating the target spectral displacements.

NEHRP Consultants Joint Venture; a Partnership of the Applied Technology Council and the Consortium of Universities for Research in Earthquake Engineering [48]; has reported in September 2010 that IRSA is a complex method to use in practice as well as the Displacement based adaptive pushover procedure though its accuracy [69, 70, 71].

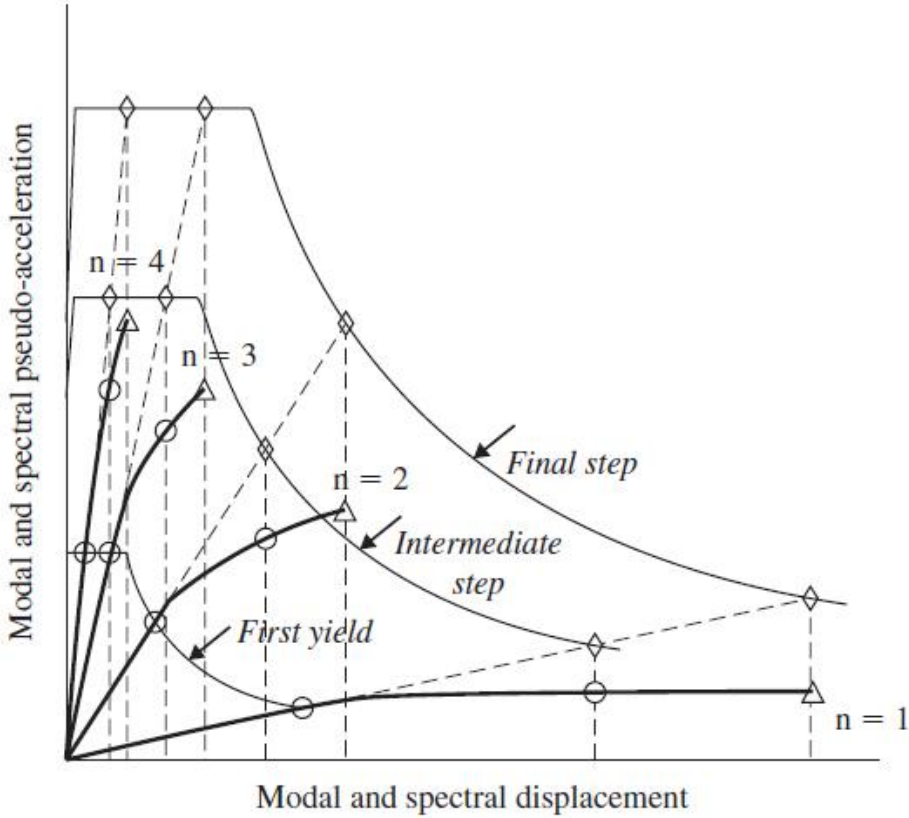


Figure 3.31 : Scaling of modal displacements through response spectrum [69].

3.4.4 Consecutive Pushover Procedure

The consecutive modal pushover (CMP) procedure has been proposed by Poursha et al. [72] in 2009. The procedure uses multi-stage and single-stage pushover analyses together. It considers up to three modes, applied consecutively in stages in a single pushover analysis after the application of gravity loads. The force distributions gathered from mode-shapes are obtained from an eigen value analysis of the linearly elastic structure.

The number of modes in the consecutive modal pushover analyses depends on the fundamental period of the building structure [72]. When the fundamental period of the structure is less than 2.2 s, then the multi-stage pushover analysis is carried out in two stages. For buildings with fundamental periods of 2.2 s or more, both two-and three-stage pushover analyses are used.

Poursha et al. [72] proposed to apply the first mode forces until a predefined displacement is reached. Then the load pattern is updated to use an incremental load pattern; using a second mode distribution, and then a third mode distribution. The maximum values of each pushover analysis are then determined.

In each stage of multi-stage analysis, the displacement increment of the roof is calculated as the product of a factor and the total target displacement of the roof. The steps of the CMP procedure are summarized below. Detailed information can be gathered from [72].

- a) Calculate the natural frequencies, modal shapes, and lateral load patterns using equation (3.34).
- b) δ_t , total target displacement should be determined using FEMA356 [2].
- c) Before the pushover analysis, gravity loads should be applied then following the below sub steps pushover analysis should be implemented.
 - The base shear, V_{bn} , versus roof displacement, u_{rn} , pushover curve using a single stage pushover analysis should be determined until the roof displacement equals to the target displacement, δ_t . An inverted triangular or first-mode lateral load pattern is used for mid-rise buildings and a uniform load pattern is used for high-rise buildings.
 - The second pushover analysis is a two-stage pushover analysis. In the first stage, lateral forces are proportional to the first mode, $s_1^* = m\phi_1$ until the roof displacement is $u_{r1} = \alpha_1\delta_t$, where α_1 is the first mode mass participation factor. The second stage is implemented with incremental lateral forces proportional to the second mode $s_2^* = m\phi_2$, until the roof displacement is $u_{r2} = (1 - \alpha_1)\delta_t$; where the initial condition of the second stage is the condition at the last increment of the first stage.

- For buildings with period $T_1 \geq 2.2s$, an additional third pushover (three-stage) analysis should be performed.
- d) The peak values of the response quantities, r_1 , r_2 , and r_3 , should be calculated from the multi staged pushover analyses.
- e) Envelope of the peak response values are determined ($r = \max\{r_1, r_2, r_3\}$).

3.4.5 Displacement Based Adaptive Pushover Procedure

Antoniou and Pinho [37] have proposed an innovative pushover concept in 2004 basing on the displacement values of the structural system. They named the procedure as displacement based adaptive pushover (DAP).

In the proposed procedure, predefined displacement vector is applied to the structure and the loading vector is updated at each analysis step. Detailed information can be gathered from [36, 37].

In their work, Antoniou and Pinho [37], they have concluded that, the shear distributions should be derived from the pushover analysis where the load pattern is the displacement vectors. This way the results would be more accurate.

The proposed method can be grouped in to main steps; determination of the nominal load vector and the inertia mass, computation of the load factor, determination of the normalized scaling vector and the update of loading displacement vector. According to Antoniou and Pinho [36], the first step is carried out only as an initial step of the analysis. The next three steps are repeated continuously at every equilibrium stage.

In the proposed method SRSS or CQC might be used to combine the modal results in a proper way. The main advantage of DAP is that the lateral deformations are directly determined through modal analysis that takes into consideration the stiffness of the structure at each step and the story shear forces are determined from the equilibrium at each analysis step [36]. This assumption overcomes the limitations of the force based pushover methods through the response prediction.

In their work, Antoniou and Pinho carried out a parametric study and they compare the results of displacement based adaptive pushover results with the dynamic time history results as well as the conventional pushover analysis. Figure 3.32 shows the comparison graph of the pushover methods. It was shown in their study, DAP provides improved predictions, throughout the entire deformation range of the dynamic response characteristics of different types of reinforced concrete frames [37].

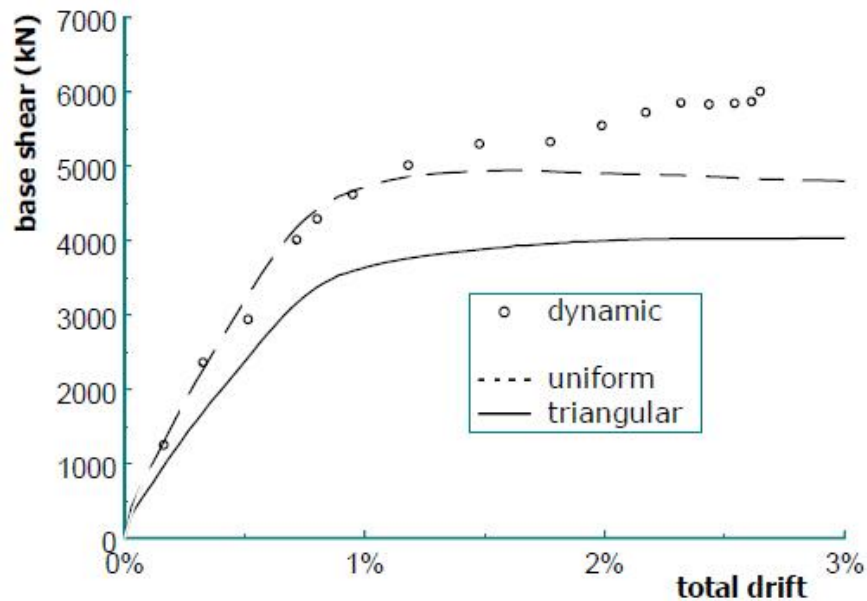


Figure 3.32 : Comparison of the DAP method with other pushover procedures [37].

Figure 3.33 shows the capacity curve of an experimented bridge deck. It is obvious how accurate is the displacement based adaptive pushover procedure among the other types. For this reason DAP procedure, should be assess as an alternative method to the conventional force based pushover analysis.

However, in their work Antoniou and Pinho [37] considered their method as simple as the other pushover procedures, NEHRP Consultants Joint Venture; a Partnership of the Applied Technology Council and the Consortium of Universities for Research in Earthquake Engineering [48]; in September 2010 has classified that Displacement based adaptive pushover procedure is a complex method to use in practice.

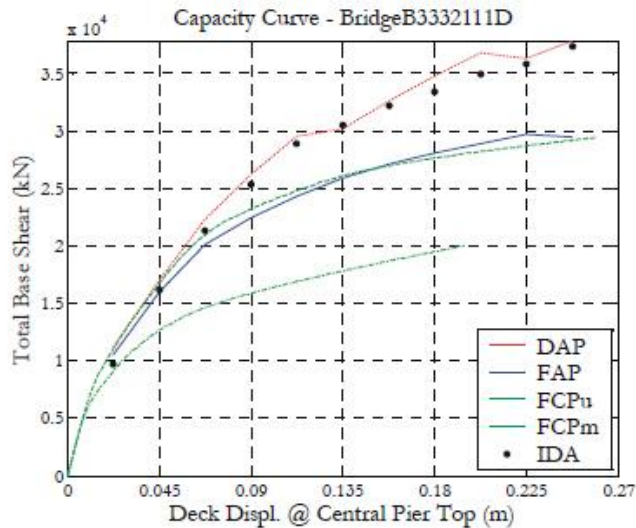


Figure 3.33 : Comparison of capacity curves for different pushover procedures [67].

3.4.6 Story Shear Based Adaptive Pushover Procedure

The story shear based adaptive pushover procedure (SSAP) has been proposed by Shakeri et al. [9] in 2010. In fact the used algorithm in the procedure is similar to Gupta and Kunnath [24] procedure with a difference in the assumed load pattern. The newly procedure considers the story shear effects instead of the base shears and uses this lateral load pattern during the analysis.

The procedure mainly consists of three parts [9];

- a) Firstly based on the modal story shear profile the load pattern is updated at each analysis step.
- b) Secondly, by using the previous load pattern, the mode shape is derived.
- c) The last step is converting the capacity curve of multi degree of freedom system (MDOF) to an equivalent single degree of freedom system (SDOF).

In the fibre based methodology which is first proposed by Elnashai et al. [4, 30, 31] later on developed by Antoniou and Pinho [36, 37] the modal story forces are obtained at each step according to the instantaneous stiffness matrix and the corresponding elastic spectral accelerations. Then the lateral load pattern is calculated by combining the story forces for each mode. Figure 3.34 shows the determination of the lateral load pattern for the proposed methodology.

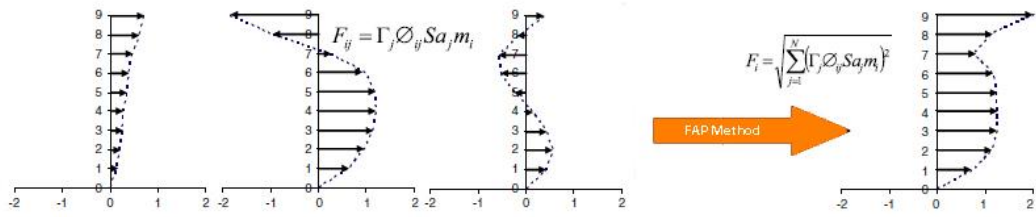


Figure 3.34 : Lateral load pattern for force based adaptive procedures [9].

The method is capable of considering the higher mode effects and the reversal of the modal quantities. It can also take care about the progressive changes in the modal properties, stiffness degradation and the frequency content of a design or particular response spectra.

The main reason for the newly proposed procedure is that, the SRSS rule used to combine the modal loads always leads to a positive value for all the story levels in the incremental load pattern as shown in Figure 3.35. In the figure, variation of the incremental applied load pattern is given for different steps. Figure 3.35.a resembles the Force based adaptive pushover procedures, whilst Figure 3.35.b resembles the story shear based adaptive pushover procedure. Antoniou and Pinho [35], Papanikolaou et al. [29, 30] have showed the deficiency of SRSS combination in their works. More information can be gathered using the references.

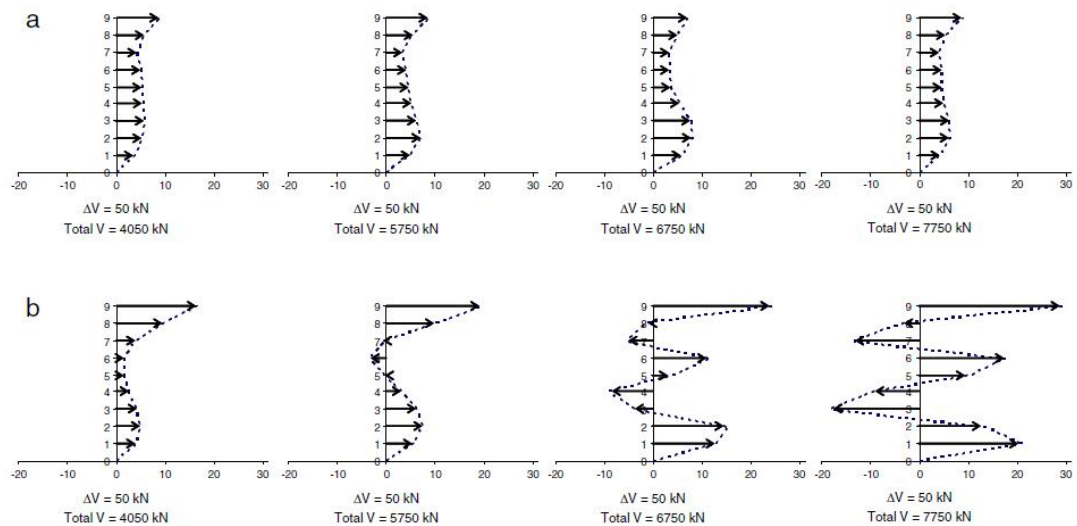


Figure 3.35 : Variation of the incremental applied load pattern at different steps [9].

At each analysis step, the story shears are calculated from the associated mode by using the equations (3.46) and (3.47).

$$F_{ij} = \Gamma_j \Phi_{ij} m_i S_a_i \quad (3.46)$$

$$SS_{ij} = \sum_{k=i}^n F_{kj} \quad (3.47)$$

Figure 3.36 shows the determination of the modal story forces by using (3.46) and calculating the story shear profile by (3.47).

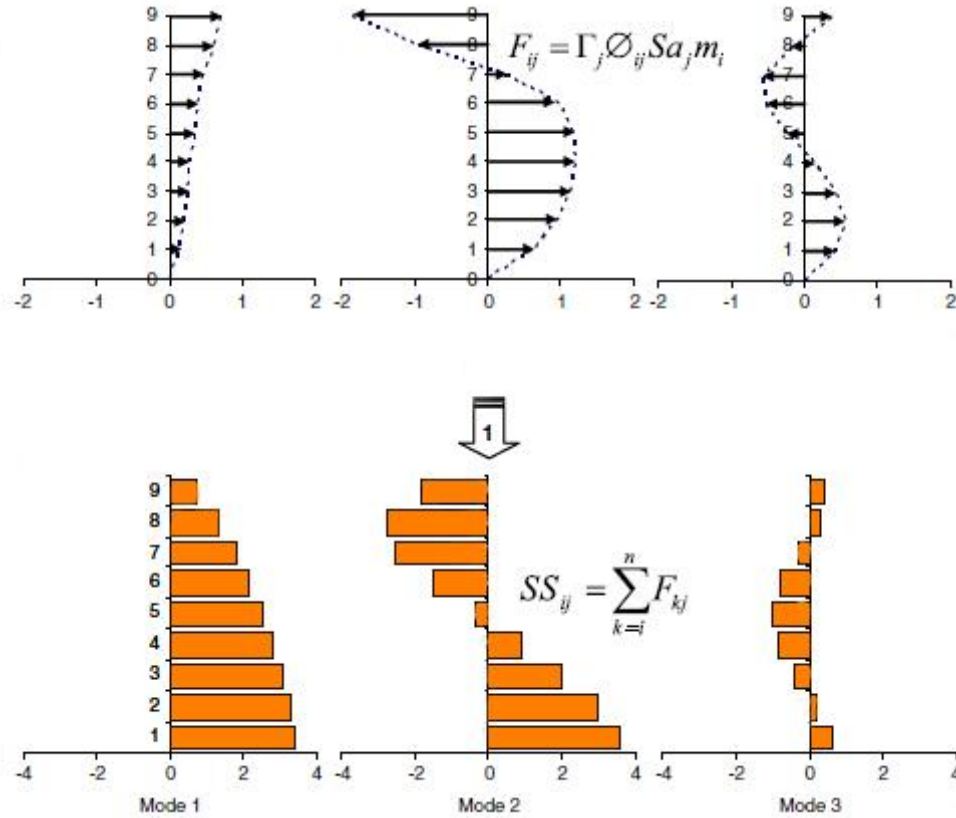


Figure 3.36 : Determination of modal story forces and story shear profiles [9].

$$SS_i = \sqrt{\sum_{j=1}^m SS_{ij}^2} \quad (3.48)$$

Ongoing step is the combination of the modal story shear profiles using equation (3.48) as shown in Figure 3.37. Here, i is the story number, j is the mode number, Φ_{ij} is the i^{th} component of the j^{th} mode shape, m_i is the mass of the i^{th} story, S_{aj} is the spectral acceleration corresponding to the j^{th} mode, Γ_j is the modal participation factor for the j^{th} mode, SS_{ij} is the story shear in level i associated with mode j , SS_i is the modal story shear in level i associated with all the considered modes.

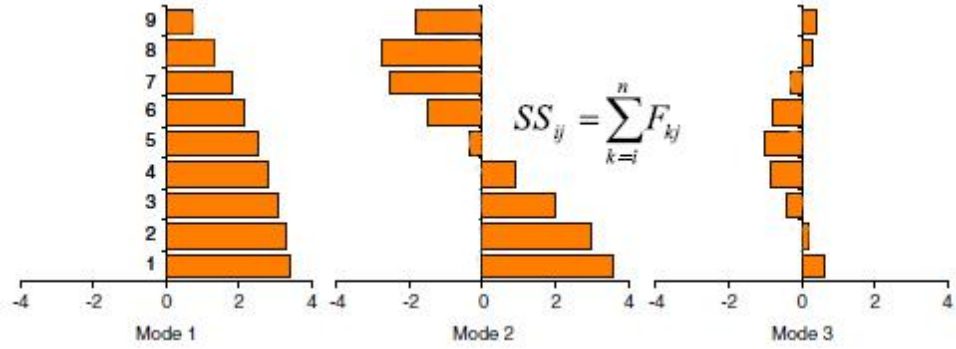


Figure 3.37 : Determination of the combined modal story shear profile [9].

The last step is the evaluation of the load pattern for the pushover analysis. The required story forces are calculated by subtracting the combined modal shear of consecutive stories using the equations (3.49) and (3.50).

$$F_i = SS_i - SS_{i+1} \quad i = 1, 2, \dots, (n - 1) \quad (3.49)$$

$$F_n = SS_n \quad i = n \quad (3.50)$$

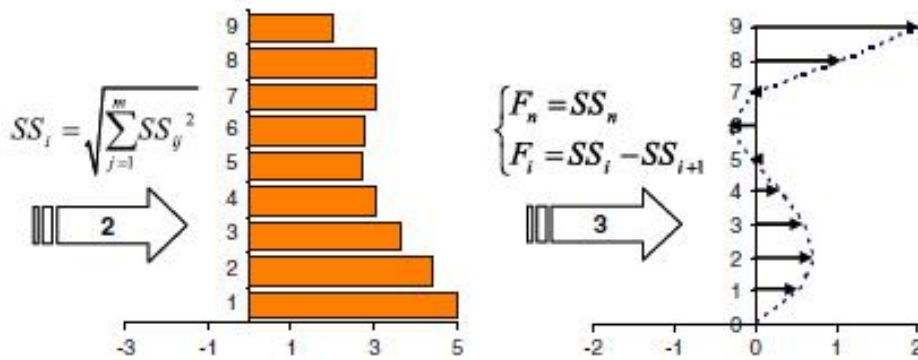


Figure 3.38 : Evaluation of the load pattern [9].

Figure 3.38 schematizes the evaluation of the load pattern for the pushover analysis.

The lateral load pattern is normalized with respect to its total value by;

$$\bar{F}_i = \frac{F_i}{\sum F_i} \quad (3.51)$$

$$\Delta F_i = \Delta V_b \times \bar{F}_i \quad (3.52)$$

Here; ΔV_b is the incremental base shear, ΔF_i is the i^{th} component of the incremental applied load at each step. The flowchart of the procedure has been given in Figure 3.39.

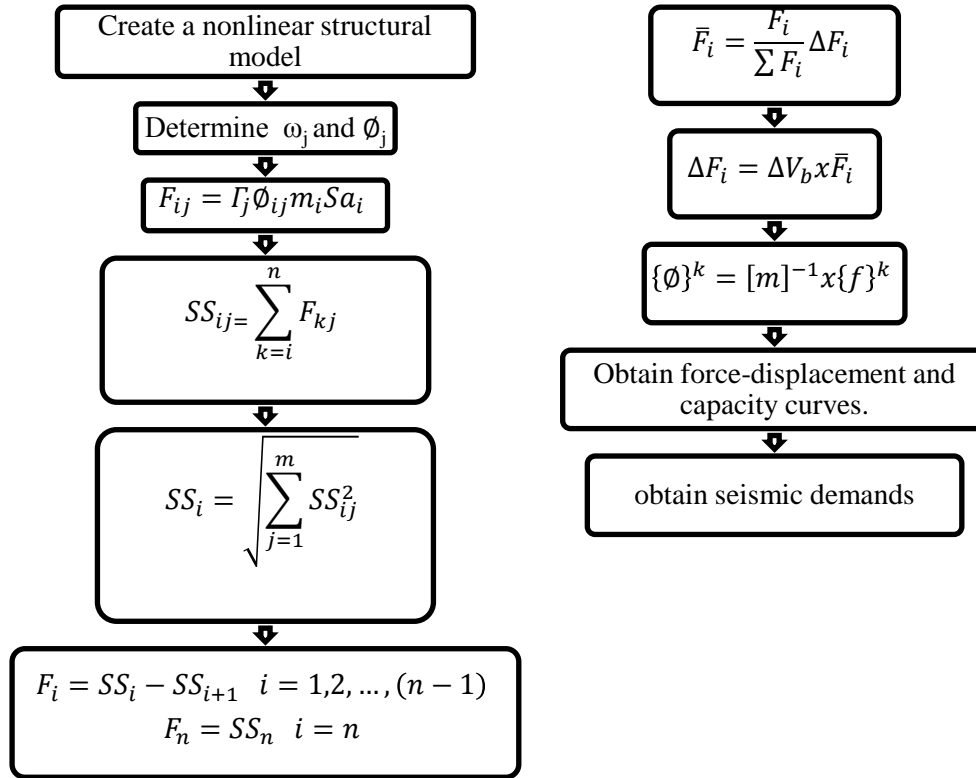


Figure 3.39 : Flowchart of the proposed procedure [9].

Shakeri et al. [9] tested their method on SAC-9 and SAC-20 buildings through a computer code incorporated Drain-2DX. The responses, resulted from the SSAP procedure, are compared with nonlinear time history analysis under six earthquake records. Figure 3.40 shows the drift comparisons of the different procedures under the selected earthquake excitations for SAC 20 building. Details of the work and the structural properties should be referred to Shakeri et al. [9].

As a conclusion, Shakeri et al. [9] stated that, the accuracy of the SSAP increases as the higher mode effects are significant as in the upper stories. The resulting inter-story drift profiles show that, the accuracy of the conventional nonlinear static procedure based on the first mode (M1) in the lower story levels is better where the effects of the higher modes are less; whilst the performance of the SSAP in the upper story levels is better than the other procedures. They proposed to use a combination of both the SSAP and M1 together for better accuracy [9].

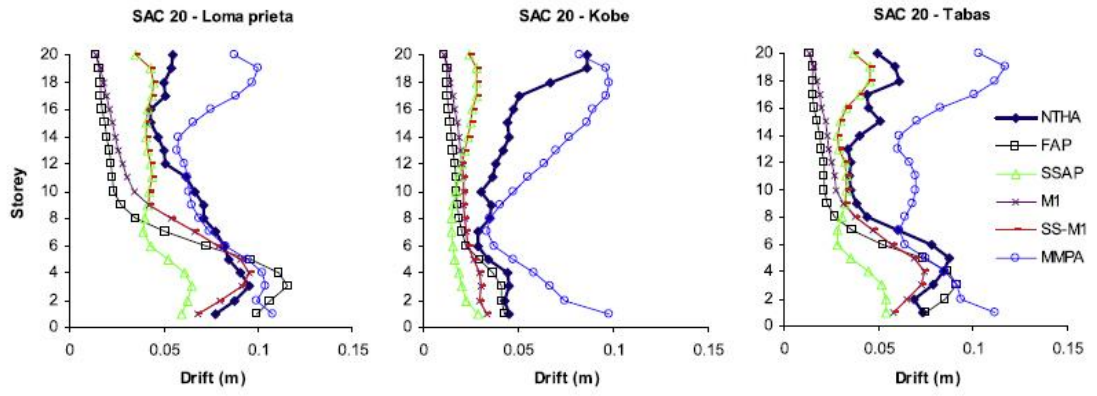


Figure 3.40 : Drift comparisons of SAC-20 for different earthquake excitations [9].

4. PERFORMANCE EVALUATION OF EXISTING IRREGULAR 3-D BUILDINGS

The aforementioned story shear based adaptive pushover procedure (SSAP) has been applied on an existing three-story irregular reinforced concrete building (RC). *Seismic Performance Assessment and Rehabilitation of Existing Buildings Project (SPEAR)* [11] has been investigated through a newly written computer code, NASAP. *Nonlinear adaptive structural analysis program* (NASAP) bases on 3-D modelling of the structural systems and is associated with a C++ procedure.

The theory of NASAP is based on OpenSees [73] modules. Those modules are used to develop a script for the previously defined story shear based adaptive procedure (SSAP) [9] algorithm, considering the torsional effects. OpenSeeS is an analysis software, which is developed by McKenna et al. [10, 73] in University of California, Berkeley, in 2006. It is supported by the National Science Foundation and Pacific Earthquake Engineering Research Center (PEER).

4.1 The Theory and Basis of OpenSees

Since OpenSees is an open-source code, the modelling is very flexible. It allows various combinations of different element and material formulations. A wide range of solution procedures to solve difficult nonlinear problems for static and dynamic loads are also included in the source codes. Another feature of OpenSees can be stated as that, it has a fully programmable scripting language for defining models, solution procedures, and post-processing that can provide simple problem solving capability [73].

OpenSees uses Tcl, a general purpose scripting language that has been extended with commands for OpenSees. Each of these commands is associated with a C++ procedure that is provided. The Tcl language provides useful programming tools.

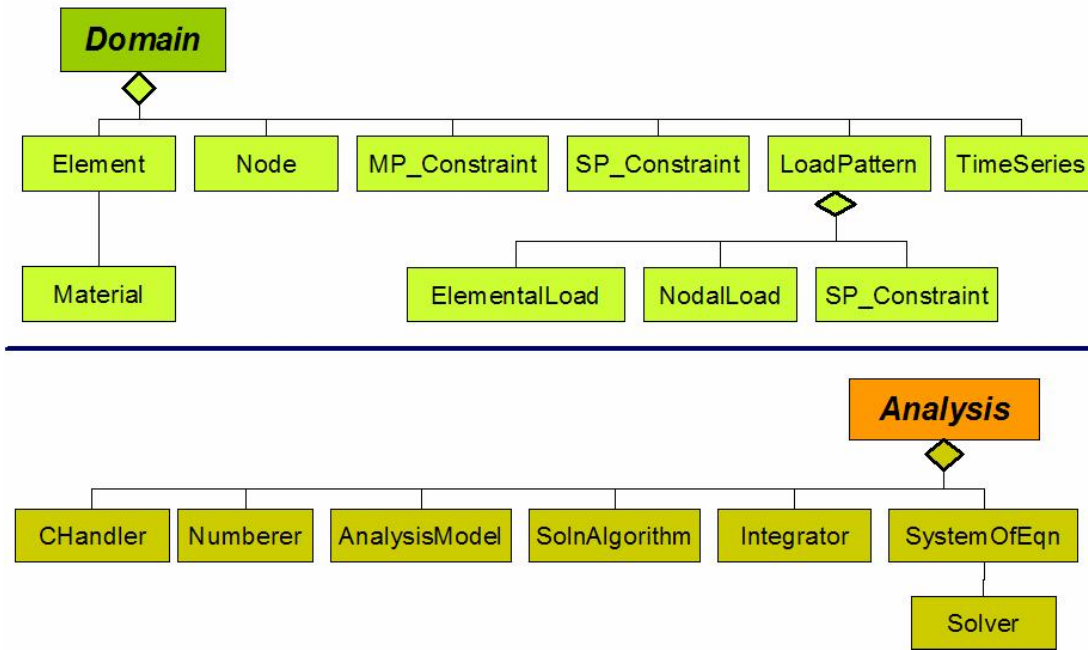


Figure 4.1 : Domain and Analysis objects of OpenSees [73].

The *domain* object is responsible for storing the objects created using the *Model Builder*. It provides the *analysis* and *recorder* objects access to them. The *recorder* object monitors user-defined parameters in the model during the analysis. The *analysis* objects are responsible for performing the analysis. In OpenSees each analysis object is composed of several component objects [73].

The *frame element* concept provides a three-dimensional modelling of beam-column representation, which able the designer to consider the torsional effects. There are two forced based element types. The first is the “*nonlinearBeamColumn*”, which considers the spread of plasticity along the element. The second type is “*beamWithHinges*” which considers concentrated plasticity over specified end hinge lengths. Deformations of the inelastic regions are concentrated at the hinge midpoints [73, 74, 75].

The “*algorithm Newton*” command is used to construct a solution algorithm which uses the Newton-Raphson method to advance to the next time step. Since the method converges rapidly to a solution, it is the most frequently used iteration procedure for the solution of nonlinear finite element equations [73].

4.2 Description of the Seismic Performance Assessment and Rehabilitation of Existing Buildings Project (SPEAR)

The SPEAR structure was designed by Fardis in 2002 [11]. It is a representative of an existing irregular three-story reinforced concrete (RC) building constructed in Greece, without code provisions for earthquake resistance. It has been designed using the design code criteria in Greece between 1954 and 1995, with the knowledge and materials of early 70's for only gravity loads.

Reinforced concrete structures, which were constructed in low or moderate seismicity regions traditionally designed for gravity loads only, without providing any seismic code restrictions. Those buildings are named as gravity load designed frames (GLD). Majority of the designs between 1930s-1970s are designed for GLD.

Structures which are designed for only gravity loads may be classified as poor detailed ones. They also lack of capacity. The following deficiencies can be stated as the typical features of GLD reinforced concrete frames [76, 77];

- a) Beams are stronger than the columns.
- b) Transverse reinforcement in columns for shear and confinement are minimal, especially in the plastic hinge zones.
- c) Little or no transverse reinforcement in beam column joint that results in a shear failure.
- d) Lap splices are located in potential plastic hinge zones above the floor slab levels.
- e) Plain reinforcing bars for longitudinal reinforcement are used.

Pseudo-dynamic testing of a full scale GLD building structure is performed at the European Laboratory for Structural Assessment (ELSA) at Ispra, within the EU project Seismic Performance Assessment and Rehabilitation (SPEAR). The structure is regular in elevation with a story height of 3 meters, whilst it is asymmetric in both longitudinal and transverse directions. The test model of SPEAR building is shown Figure 4.2.

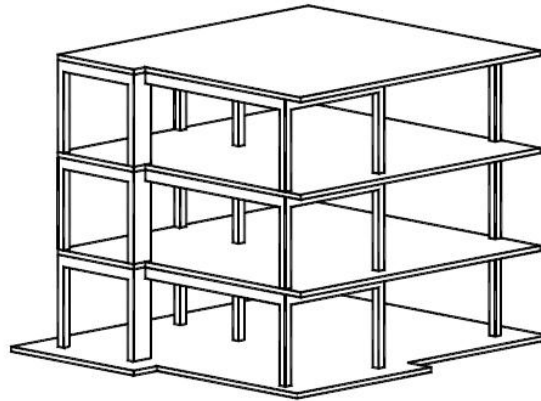


Figure 4.2 : Test model of SPEAR building in ELSA, Ispra [11].

The geometry and plan view of the SPEAR building is given in Figure 4.3. The story height is 3 m, with 2.5 m clear height of columns between the beams. The specified design strength of concrete is $f_c=25$ MPa, and the design yield strength of reinforcement is $f_y=320$ MPa. Design gravity loads on slabs are 0.5 kN/m^2 for dead loads and 2 kN/m^2 for live loads. Slab thickness is 150 mm and total beam depth is 500 mm. The slab is reinforced with 8 mm bars at 200 mm intervals.

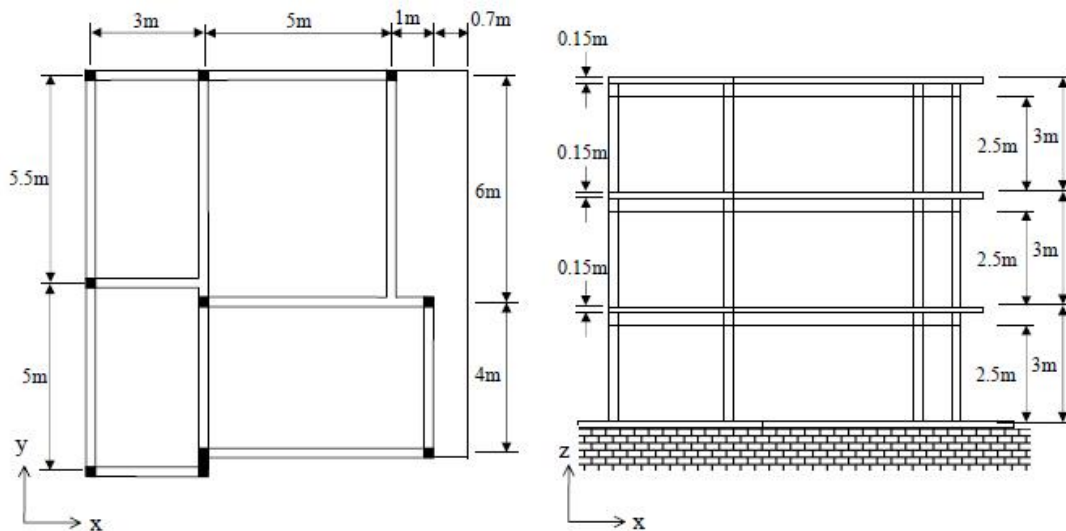


Figure 4.3 : Geometry of the test model [32].

Figure 4.4 shows the plan view of the structure. The sectional dimension of C6 column is 750×250 mm whereas all other columns are designed as 250×250 mm. Columns longitudinal reinforcement is composed of 12 mm plain bars. Column stirrups are 8 mm plain bars, closed with 90° hooks with 250 mm intervals.

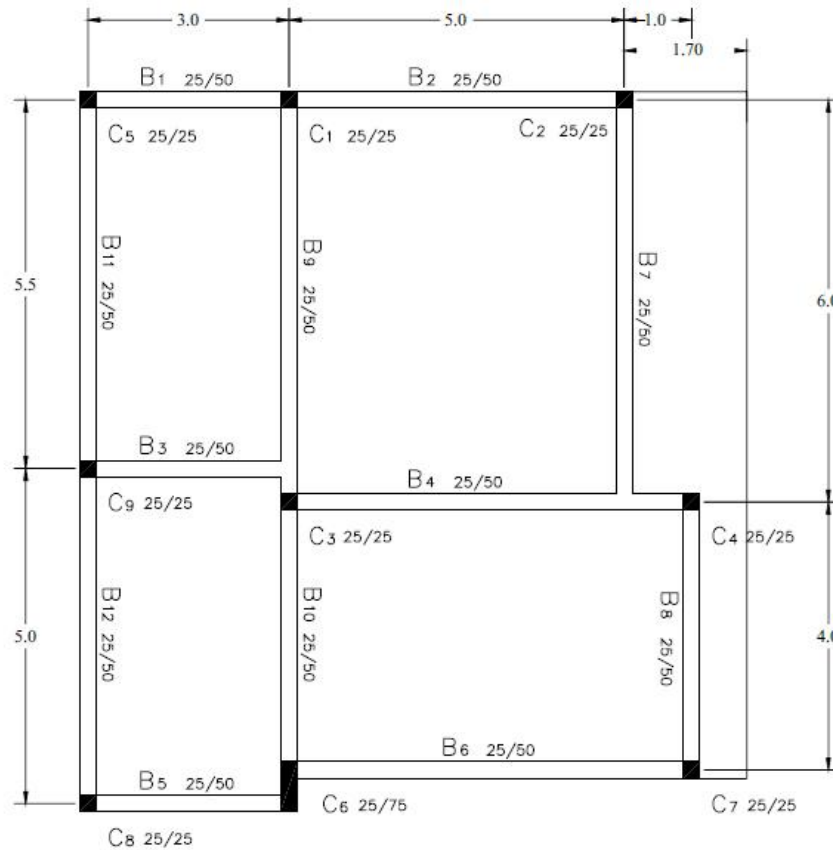


Figure 4.4 : Plan view of SPEAR building [77].

Beam longitudinal reinforcement is designed as two 12 mm bars at the top, anchored with 180° hooks at the end of the column. The bottom beam reinforcement consists of two 12 mm bars anchored at the end of the column with 180° hooks. Beam stirrups are 8 mm bars at 200 mm intervals, anchored with 90° hooks [77].

Beam and column cross sections are given in Figure 4.5 and Figure 4.6. Infill walls and stairs are omitted in the model. Strong and weak directions are referred to as y and x directions, respectively. More detailed of explanations of sections can be gathered from [11, 32, 33, 39, 76, 77, 78]. The foundation system is provided by strip footings; column longitudinal reinforcement is lap spliced over 400 mm at each floor level including the first one. Figure 4.7 shows the footings plan view [78].

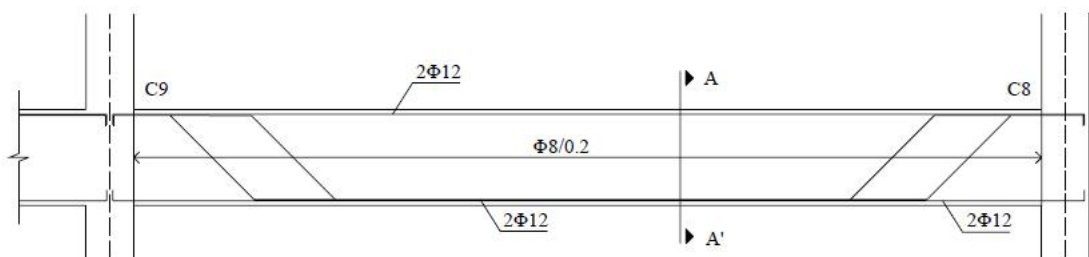


Figure 4.5 : Reinforcement layout for a typical beam (units are in mm) [32].

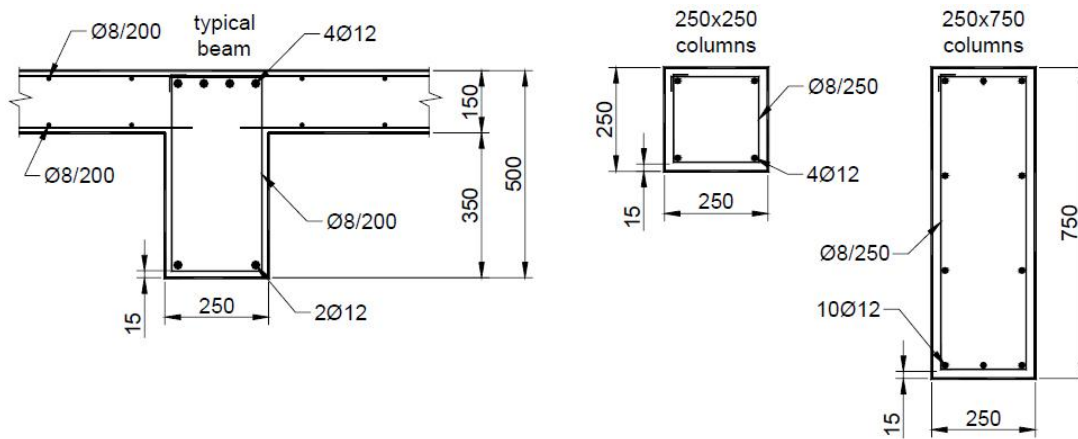


Figure 4.6 : Cross section properties of SPEAR (units are in mm) [77].

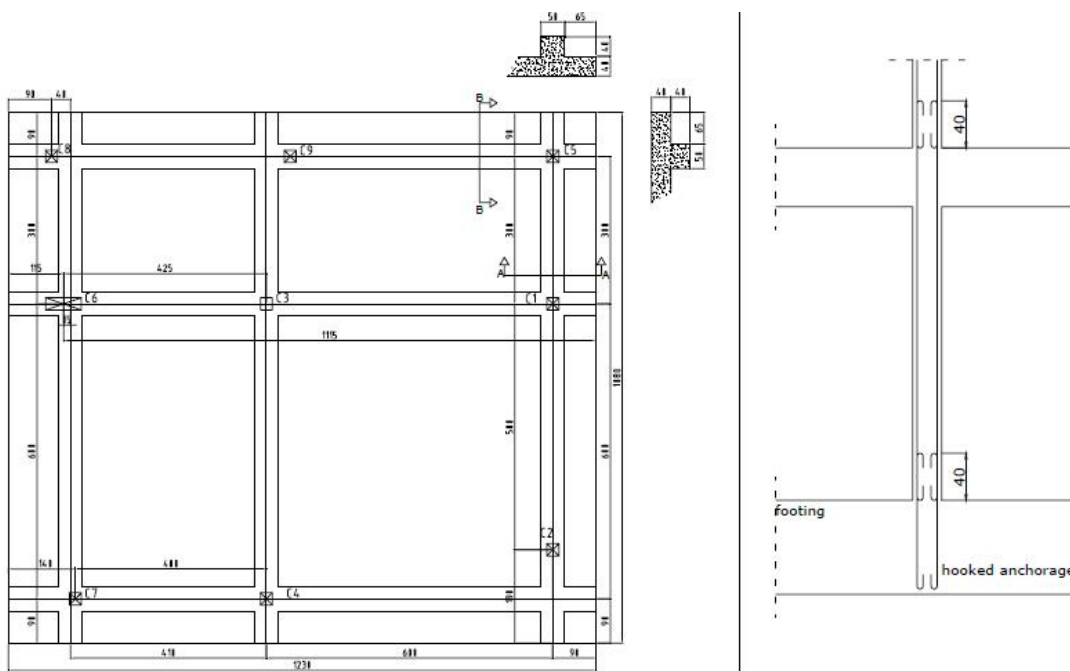


Figure 4.7 : Footings plan of SPEAR (units are in mm) [78].

4.2.1 Material and Mass Representation of the SPEAR structure

In the analytical model, cover concrete thickness is assumed to be 15 mm for all members. Slabs are omitted and their contribution to beam stiffness and strength is reflected by effective width of the T-section.

Cross sections of the building have been modelled using XTRACT [79]. As known Xtract is a cross sectional analysis program for structural components. It is capable of determining the inertial moment, moment curvature and interaction of structural components.

The stress-strain model for the confined and unconfined (cover) concrete is formulated by Mander procedure [80]. Values differ between zero and crushing strain. After the crushing strain is reached, the model assumes straight line strength degradation to the post crushing strength at the completion of spalling. For the confined model, when crushing strain is reached, the section is assumed to have failed and analysis will cease. The stress-strain model of the steel is parabolic strain hardening type behaviour. Figure 4.8 shows the XTRACT modelling of the materials.

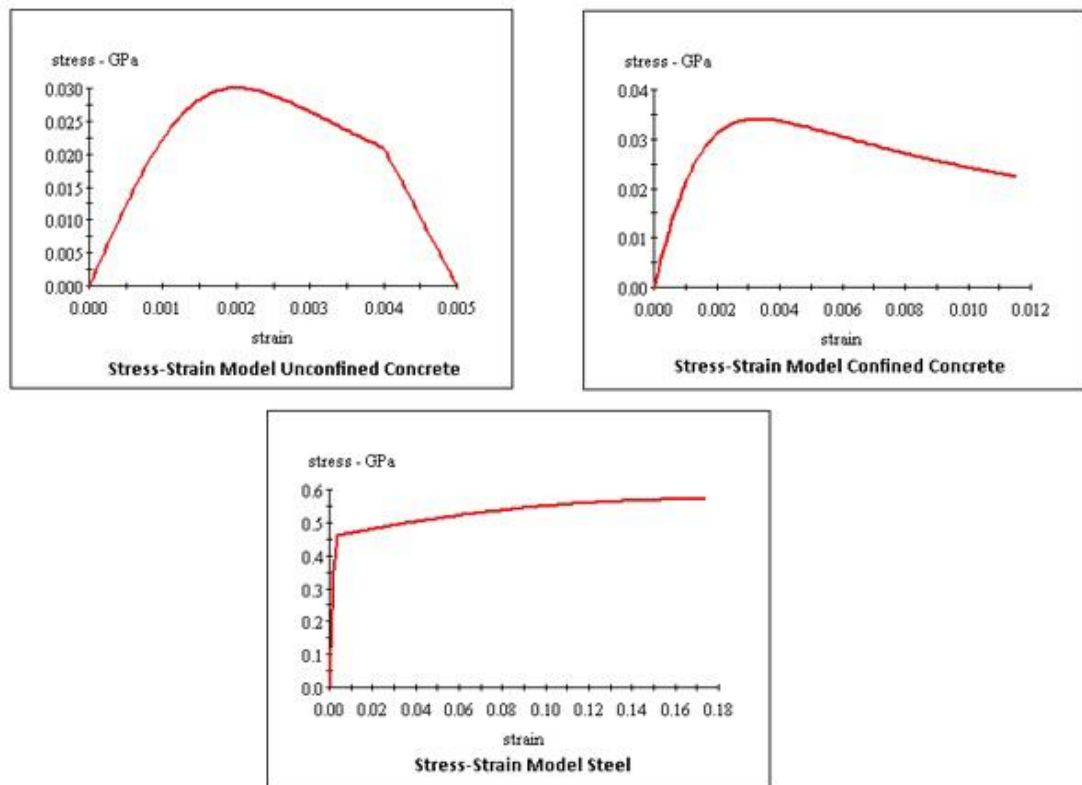


Figure 4.8 : XTRACT modeling of the materials (kN-mm).

Concrete compression strength is taken as $1.2 f_{ck}$, which is given in ACI 318, where f_{ck} represents the concrete characteristic compression strength. FeB32K from Italian market is used for the reinforcing steel which corresponds to 315 MPa of minimum yield strength, 360MPa of average yield strength, 450 MPa of ultimate strength and 206000 MPa of Young's modulus [32]. However, it is stated in Elnashai et al. [32] that the strength of the steel used in ELSA in Ispra does not satisfy these circumstances.

Test results of the steel used in ELSA has been taken in the modelling of SPEAR, which is given in [32] as, 458.7 MPa for the yield strength, 570.33 MPa for the ultimate strength, with a 0.0022 yield strain, 0.174 ultimate strain and 206000 MPa Young’s modulus for Ø12.

Gravity loads for the analytical model are calculated by summing parts of the design gravity loads on slabs and the self-weight of the structure itself. Elnashai et al. [32] proposed usage of total dead loads and 30% of live loads in their work. 0.5 kN/m² is assumed for slabs, and 2 kN/m² for live loads. As stated before, the concrete self-weight is taken as 25 kN/m³. The mass is calculated by dividing the gravity loads by the acceleration (9807 mm/sec²). Calculated gravity loads are distributed to beams and columns. Story masses and the modulus of inertia is given in Table 4.1. Gravity loads on slabs and self-weight of slabs are distributed to the nearest beams, as shown in Figure 4.9.

Table 4.1 : Center of Mass and Mass properties of SPEAR building.

	Centre of Mass (m)	Mass (KNs ² /m)	Modulus of Inertia [KNm ² /(m/s ²)]
FLOOR 1&2	X = 4.53 Y = 5.29	66.57	1249
ROOF	X = 4.57 Y = 5.33	64.43	1170

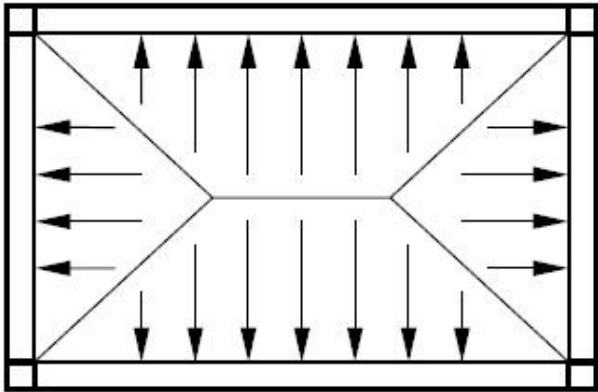


Figure 4.9 : Gravity load distribution [32].

4.2.2 Determination of Cross Sections

As explained in detail in Chapter 3, for inelastic analyses, two alternative models are available; Lumped (or concentrated) inelasticity models and the Spread (or distributed) inelasticity models. While modelling the SPEAR building concentrated model has been chosen.

In lumped inelasticity models, the element response is represented by zero-length plastic hinges which is called as the *hinges*. Concentrated inelasticity models may be utilized to describe complex hysteretic behaviour. Elnashai stated typical force displacement models for inelastic springs in Figure 4.10 [39].

Model type	Reference	Sketch
Bilinear with axial interaction	Takayanagi and Schnobrich (1979)	
Stiffness degrading	Clough and Johnston (1966)	
Stiffness degrading with strength deterioration	Saiidi and Sozen (1979)	
Takeda hysteretic model	Takeda <i>et al.</i> (1970)	
Ramberg–Osgood model	Park <i>et al.</i> (1987)	

Figure 4.10 : Common hysteresis for inelastic springs in lumped models [39].

For steel components, the *Ramberg-Osgood* model is generally the accurate. The main advantage of the lumped inelasticity models is their simplicity. In the modelling of SPEAR building, reinforcement steel is modelled as bilinear elasto-plastic model, whilst the concrete model is taken from Mander *et al.* [80].

The P-M interaction for column C6 is calculated with XTRACT and for both x and y direction is plotted in Figure 4.11. Figure 4.12 represents the P-M interaction of the other columns in x-direction since they are squared y-directional interaction is calculated to be very small. Figure 4.13 is where the M- ϕ relation for the beam element is shown. Rigid diaphragm action was considered at the floor levels.

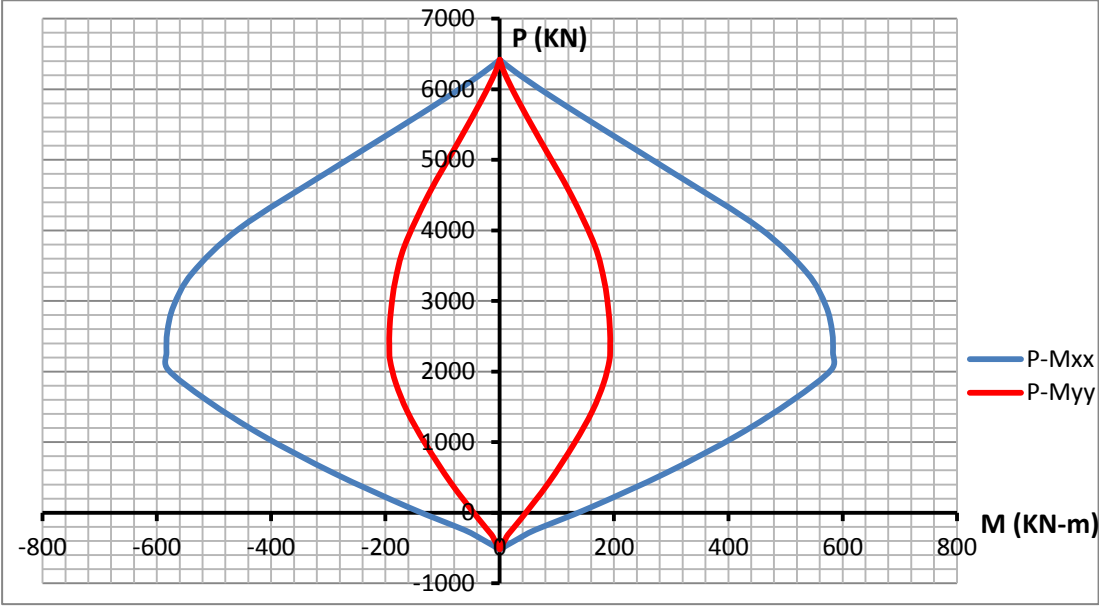


Figure 4.11 : P-M interaction for C6 column in both directions.

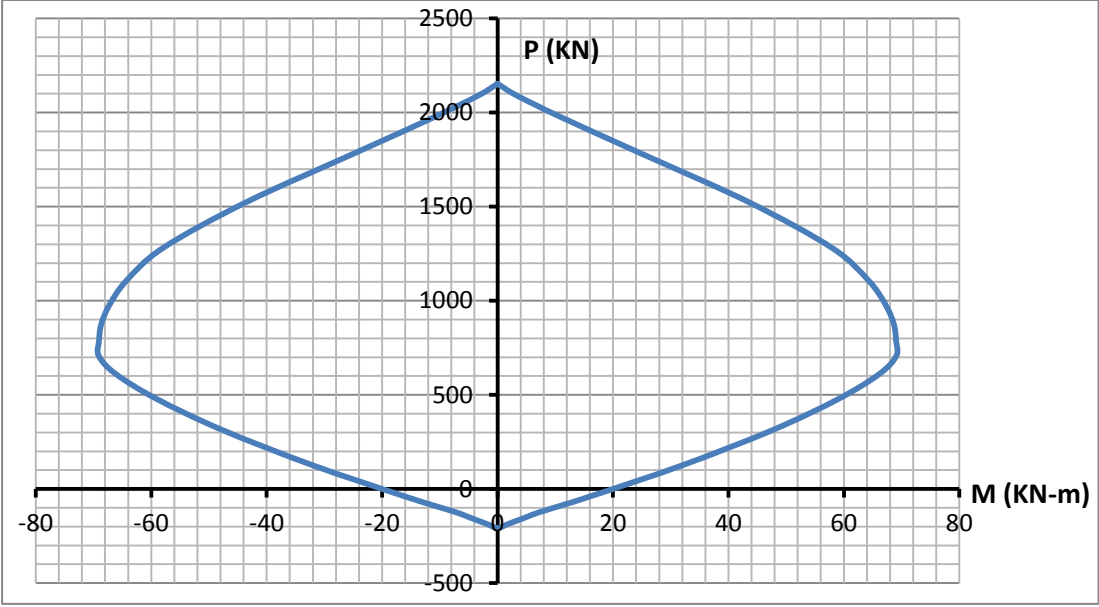


Figure 4.12 : P-M interaction for other columns in x direction.

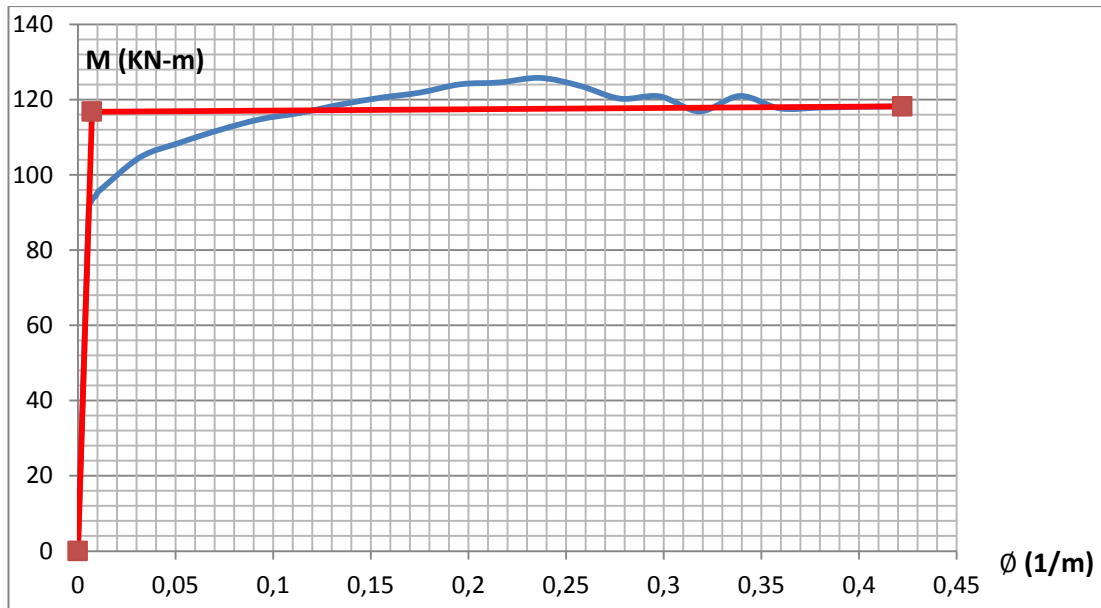


Figure 4.13 : M- ϕ relation for the beam elements.

4.2.3 Determination of the Irregularities Effect for SPEAR

Centre of stiffness and center of mass values are calculated according to EC8 [81] and plotted in Figure 4.14 at floor level. Torsional parameters of SPEAR building was calculated by Fajfar et al. [77]. Those values are given in Table 4.2. e_{0x} and e_{0y} are the eccentricities measured for the X and Y direction respectively. r_x and r_y are torsional radius and l_s is the radius of rotation of a floor in plan.

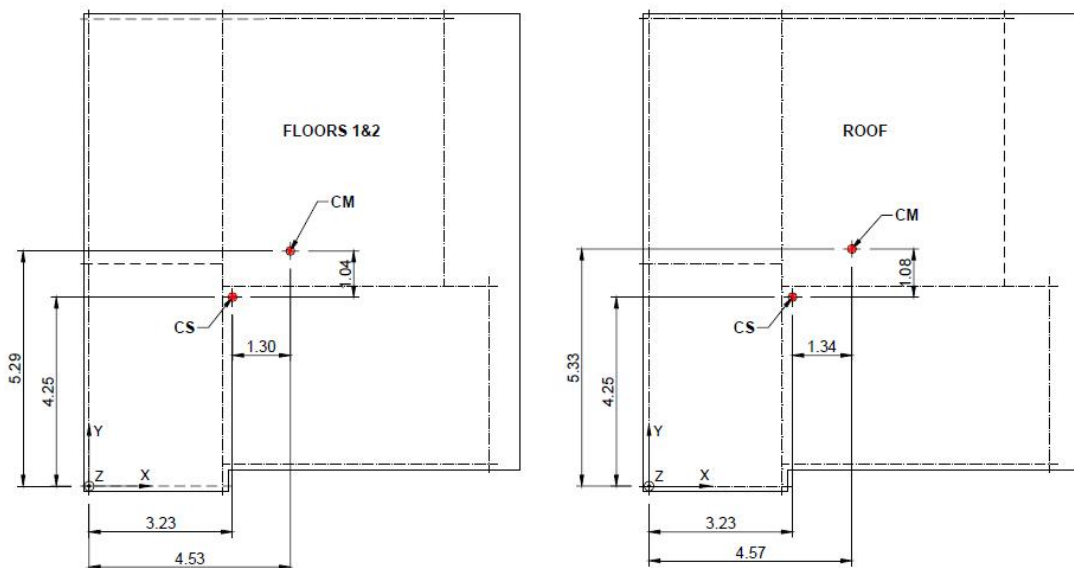


Figure 4.14 : Center of mass and center of stiffness of the SPEAR building [77].

Table 4.2: Torsional characteristics of the SPEAR building [77].

	e_{0x} (m)	e_{0y} (m)	r_x (m)	r_y (m)	l_s (m)	$0.3 r_x$	$0.3 r_y$
FLOOR 1&2	1.302	1.037	1.44	2.57	4.38	0.43	0.77
ROOF	1.338	1.081	1.44	2.57	4.32	0.43	0.77

According to EC8 [81] a structural system should satisfy the following (4.1) and (4.2) equations to be assumed as a regular one.

$$e_{0x} \leq 0.3r_x; e_{0y} \leq 0.3r_y \quad (4.1)$$

$$r_x \geq l_s; r_y \geq l_s \quad (4.2)$$

It is obvious that the SPEAR structure can be classified as irregular in plan according to EC8. Especially in y-direction torsional eccentricities are larger.

4.2.4 Determination of the Earthquake Record

The input signal consisted of seven semi-artificial series obtained by the modification of the North-South (NS) and West-East (WE) components of Herceg-Novti record of 1979 Montenegro earthquake. Those records are given in Table 4.3.

Each of the records consist of two orthogonal components, longitudinal and translational, of the horizontal acceleration. They are modified from the natural records to be compatible with the EC8 Type 1 design spectrum, soil Type C and 5% damping. The latter records were normalized to peak ground acceleration (PGA) of 1.0g on rock site, which means that PGA is 1.15g on soil type C.

The signal is scaled to 1g, by a scale factor of 0.869 for both directions. The scaled signals are shown in Figure 4.15. The artificial earthquake record data of Montenegro'79 for 1.15g are presented in Appendix A.1.

Table 4.3: List of semi artificial earthquakes [32].

No	Earthquakes	Stations	Components	PGA (g)
1	Montenegro 1979	Ulcinj	L,T	1.15
2	Montenegro 1979	Herceg Novi	L,T	1.15
3	Friuli 1976	Tolmezzo	L,T	1.15
4	Imperial Valley 1940	El Centro Array 9	L,T	1.15
5	Kalamata 1986	Prefecture	L,T	1.15
6	Loma Prieta 1989	Capitola	L,T	1.15
7	Imperial Valley 1979	Bonds Corner	L,T	1.15

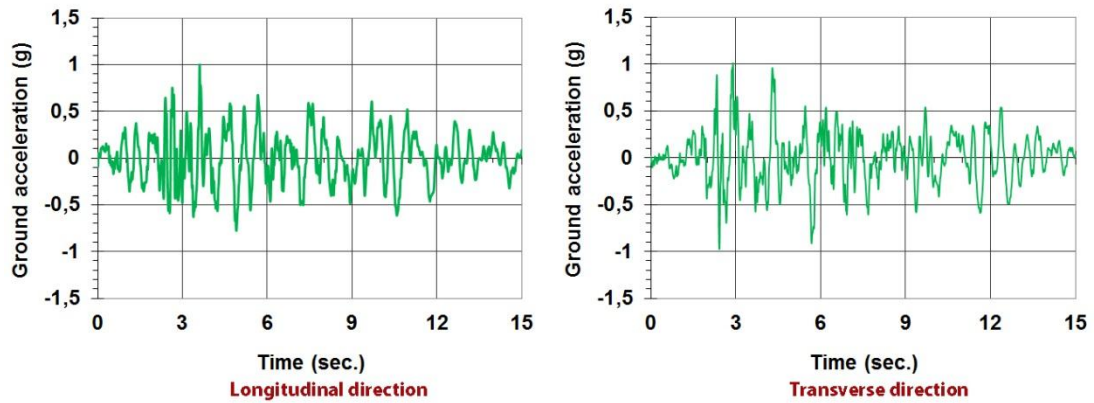


Figure 4.15 : Accelerograms for longitudinal and transverse directions.

The response spectrum, which is needed for adaptive pushover analysis, is determined by FFT analysis of the earthquake signal. Longitudinal and transverse response spectrums are fitted to EC8 and given in Figure 4.16.

The scaling of the records and the FFT analyses are conducted with Seismosignal, OASYS and PRISM computer codes. All of the products are capable of determining the elastic and inelastic response spectrum with a great accuracy. In the theoretic study that is conducted within the scope of this thesis, PRISM is chosen to be FFT converter. Figure 4.16 shows the response spectrum which is evaluated by PRISM.

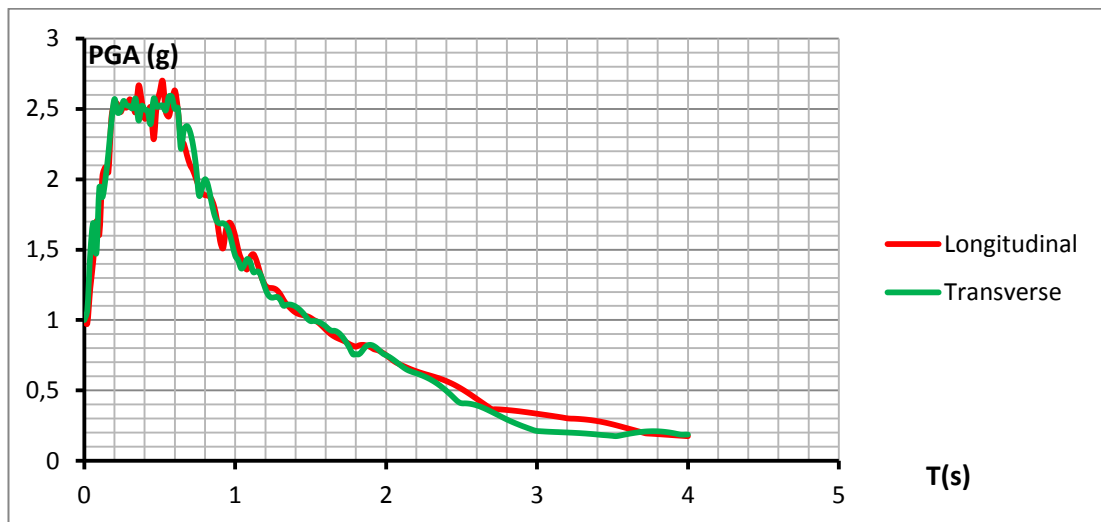


Figure 4.16 : Response spectrum of Montenegro'79 earthquake.

4.3 A Nonlinear Adaptive Structural Analysis Program (NASAP)

The 3-D software package used in the present work is called as “NASAP” coded by Özçıtak and Oyguç in 2010. This is a tool for finite element analysis of structural elements, meaning “Nonlinear Adaptive Structural Analysis Program”. It has friendly user menus.

The proposed adaptive pushover procedure by Shakeri et al. [9] has been developed for irregularity effects of existing reinforced concrete (RC) structures. Since NASAP is capable of proceeding 3-D analysis, it is able to investigate the higher mode effects and the reversal of the modes during the analysis. During each adaptive step, it updates the stiffness matrix by using the previous load pattern and instantaneously induces the torsional effects. New load pattern is applied to the next step of analysis.

Irregular SPEAR building has been analysed with NASAP, and the capacity of the structure is determined using the aforementioned adaptive pushover procedure. The drift profile of the structure is also plotted for comparison. PERFORM 3-D (CSI) [13] is chosen to test the accuracy of NASAP. Nonlinear time history analysis are evaluated with PERFORM 3-D (CSI). The drift profiles of the dynamic analysis are compared with the NASAP results. In addition to this, ELSA Lab results of the pseudo-dynamic tests of the SPEAR building, using a 0.2g scaled accelogram, have been compared with the adaptive pushover results of NASAP. It has been showed that the theoretic adaptive pushover curves are in good agreement with ELSA Lab results.

An option has been added to the coded program to implement a non-adaptive pushover analysis, whilst the load pattern is the same as defined previously. The main idea is to show that story shear based load pattern would give more accurate results than the conventional ones, since the modal quantities are not combined using SRSS. The non-adaptive and adaptive pushover results are also compared with the conventional pushover capacity curves in this study.

There is also an option in the program for the analyser, whether to choose SRSS or CQC while combining the modal story shear quantities. It has been showed by Chopra [6] that, CQC will give better estimates when the modal responses are closer.

The input menu order and the analysis step that NASAP follows can be summarized as follows;

1. The local axes are just as the same as SAP2000. There are 3 local axes x, y and z shown in Figure 4.17.

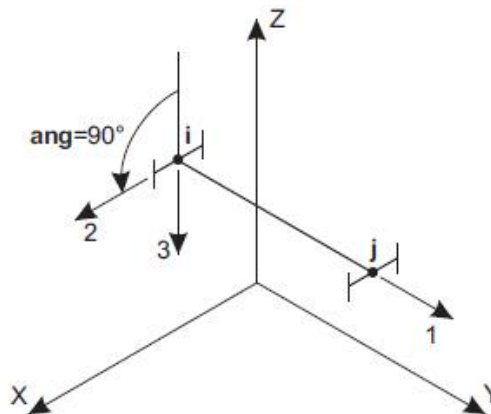


Figure 4.17 : Local Axes of NASAP.

2. The story levels and the material properties should be defined from the “Data” main menu. Figure 4.18 shows the submenus for story levels and material properties. Since the material type is not important for NASAP, 3 main criteria have to be defined by the user; the elasticity modulus, the Poisson’s ratio and the unit weight of the material.

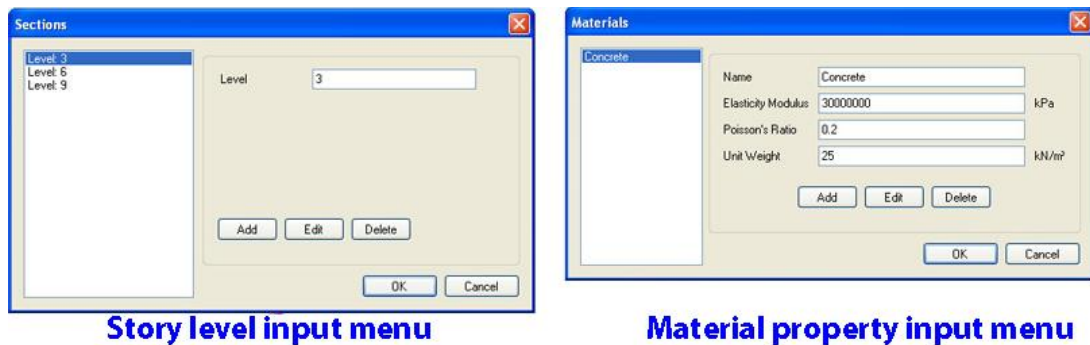


Figure 4.18 : Input menus for Story Levels and Material properties.

3. Next step is the definition of the section properties. Section menu uses the material submenu defined in (1). Figure 4.19 shows the section menu.
4. NASAP performs nonlinear spectra based pushover analysis by using the user defined materials and section properties. The material properties and the sectional properties should be determined before starting the analysis. It is not possible neither defining P-M interactions nor M- ϕ relations from NASAP define menu. However, by using another section solver program (e.g. Section Builder, Xtract etc.) those can be determined.

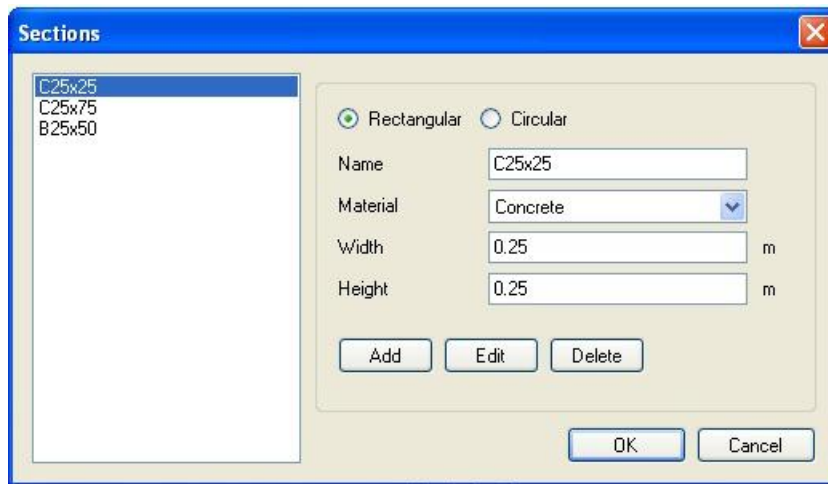


Figure 4.19 : Section input menu.

P-M interaction menu for column sections is divided into submenus such as;

- P_{min} is the maximum tension load value, which has a negative value. The negative sign is not written in the corresponding menu.
- P_{max} represents the maximum value of the compression load.
- P_b is the axial load at maximum moment.
- M_{30} resembles the point where the axial load is equal to zero, in other terms it can be called as M_{yy} .
- M_{3b} is the minimum moment value.
- $M_{20} = M_{30}$.
- $M_{2b} = M_{3b}$ if the section is symmetric.

Figure 4.20 shows the material input menu for P-M interaction for column sections. For the beam sections, yield moment value is the only parameter to be determined for the program. It is assumed to be stable till the hinge length. Concentrated plastic hinge procedure is followed by NASAP.

5. Under the Data menu, the last submenu is the Response Spectra. This is needed for the spectra based adaptive pushover analysis, since it uses elastic spectra. The elastic spectra of an earthquake excitation may be determined by the Fast Fourier Transform (FFT) analysis of the signal by using aforementioned computer programs (e.g. Oasys, Prism, seismosignal etc.).

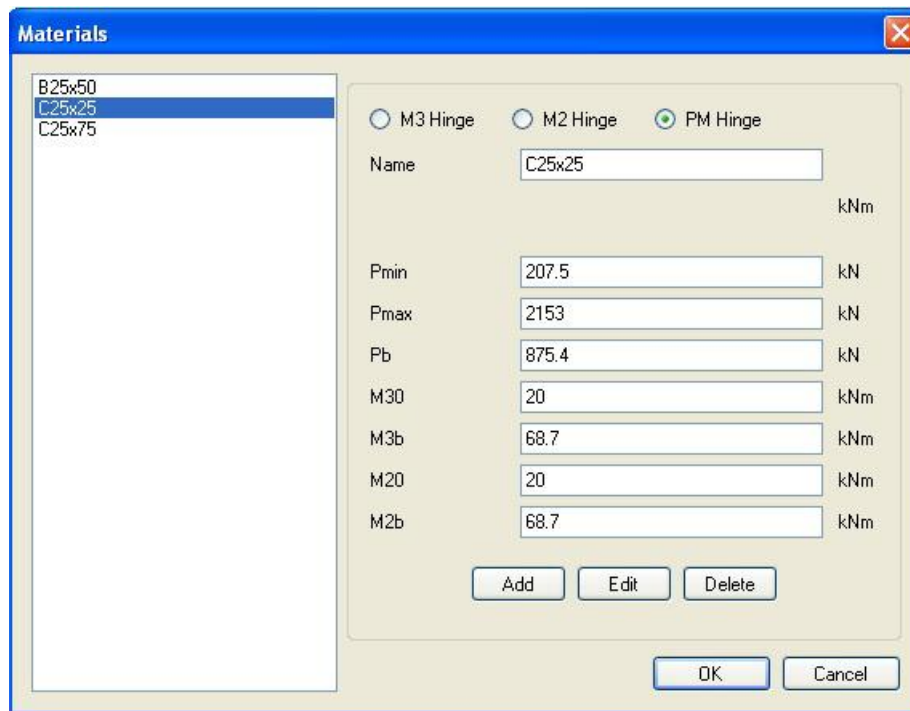


Figure 4.20 : Hinge input screen of NASAP.

6. From the “Draw” main menu user can draw any element that is needed for to define the structure. After determining the material and section properties, one can assign them to the developed building from the “Assign” menu. It gives ability to define joint mass, frame distributed loads, joint loads, hinges etc. to the selected element.
7. The next main menu is the “Analysis Case” menu. There are three analysis options by default, dead, modal and the pushover cases. It is user based to add or delete more analysis cases. Figure 4.21 shows the Analysis case menu.
8. The starting target displacement value might be calculated by using FEMA 440. Then after the analysis completed the exact value of the target displacement should be exchanged and the analysis should be repeated with the new value.
9. NASAP is not capable of including the second-order effects at least in this version of the program. Further studies should be implemented on this issue.

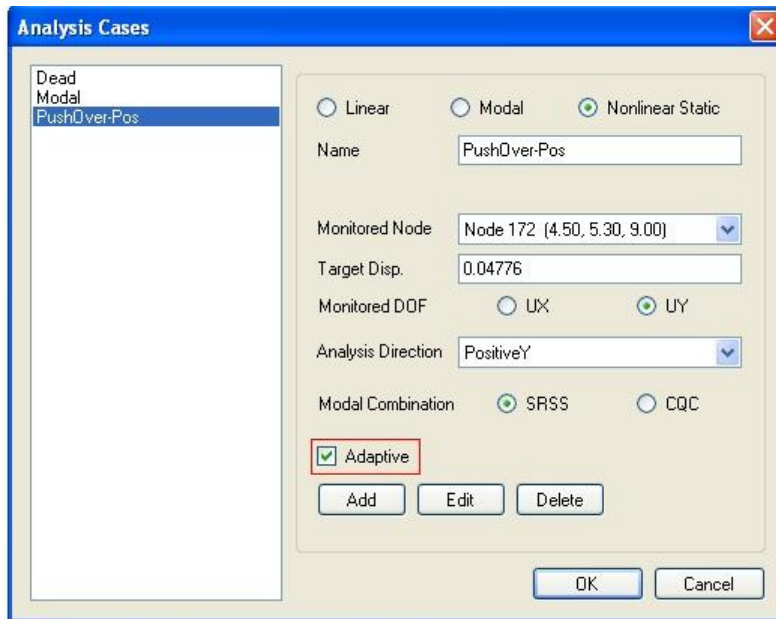


Figure 4.21 : Analysis case menu of NASAP.

Pushover procedure follows the steps of Shakeri et al. [9]. It uses the adaptive load pattern which is derived from the calculation of story shears as the explained procedure [9]. The procedure is developed to induce the torsional effects. As mentioned before, there is a non-adaptive option, which the box is by default checked. If a non-adaptive analysis is the aim, then the box should be emptied. Just to mention, the non-adaptive pushover procedure also follows the steps of the previously mentioned procedure [9]. Load pattern is derived from the modal story shear forces. Also, modal combination is may be either proceeded with SRSS or CQC.

The flowchart of NASAP, while implementing the analysis for the adaptive and non-adaptive cases has been given through Figure 4.22 and Figure 4.23 respectively.

As a known fact, the lateral deformability of structures is measured with the horizontal drift concept. Δ , story drifts are defined as the absolute displacement value of any floor relative to the base, while δ , the inter story drift is the relative lateral displacements between two consecutive floors [39]. Figure 4.24 shows the story drifts and the inter story drifts. Same assumptions are valid for NASAP.

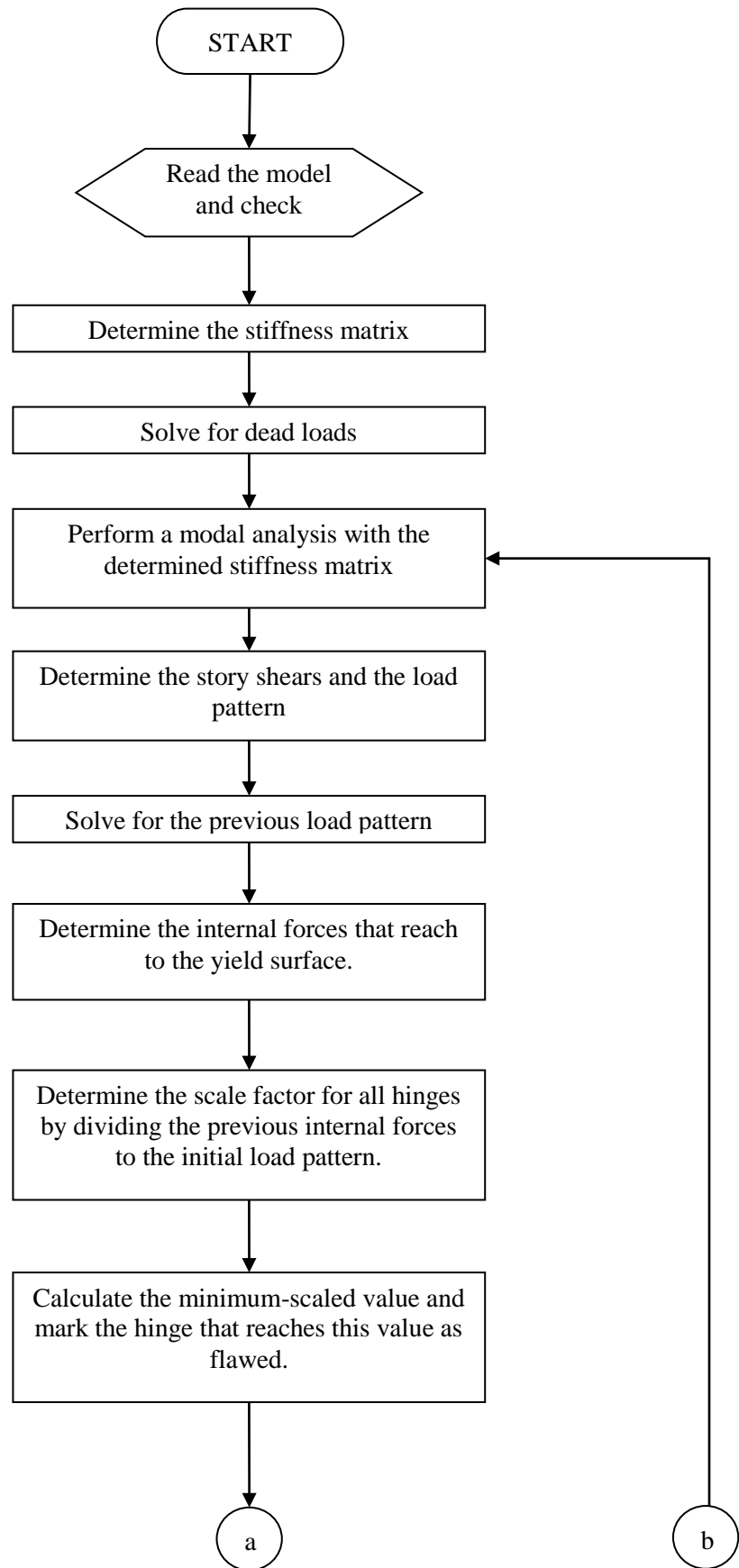


Figure 4.22 : Flowchart of NASAP for non-adaptive pushover procedure.

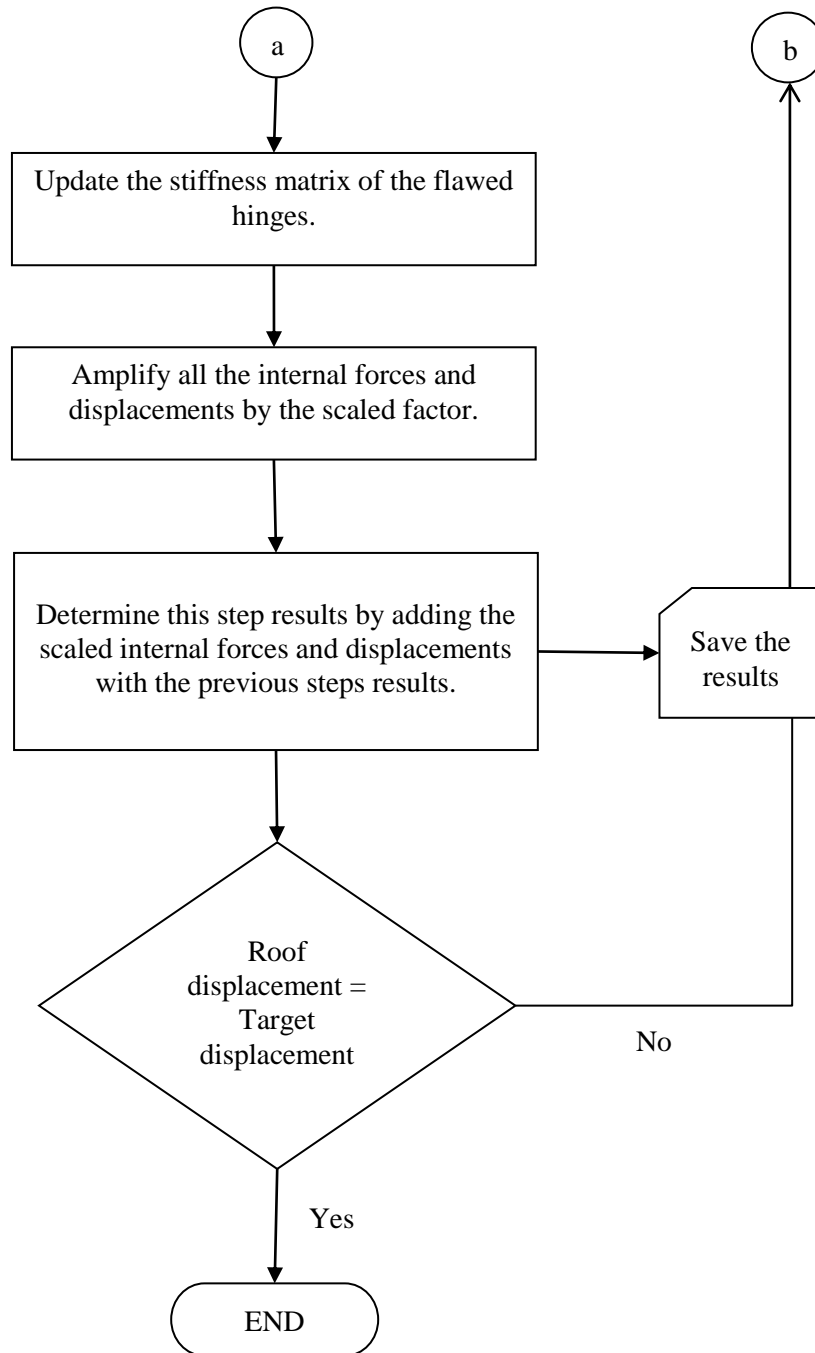


Figure 4.22 (continued) : Flowchart of NASAP for non-adaptive pushover.

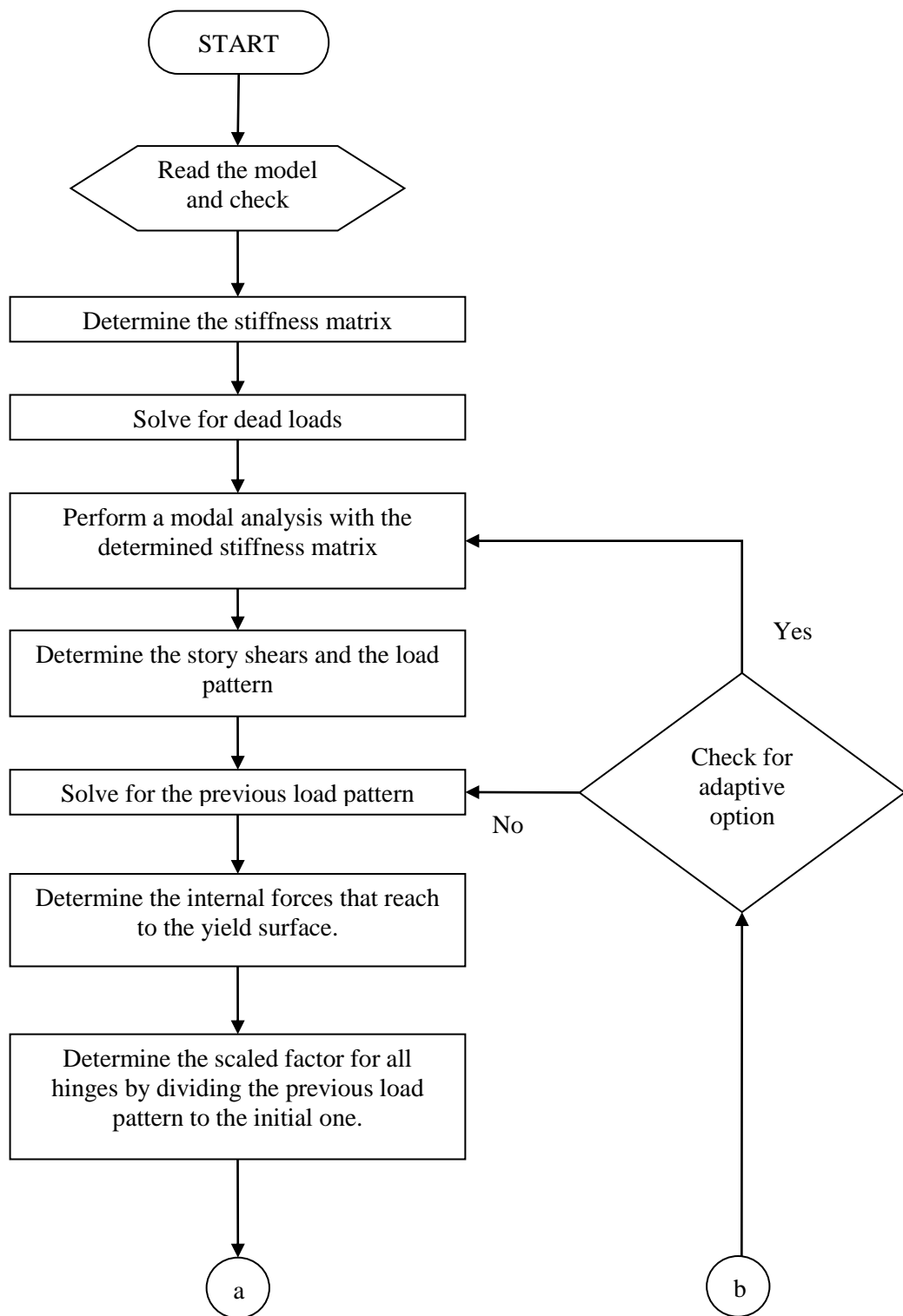


Figure 4.23 : Flowchart of NASAP for an adaptive pushover procedure.

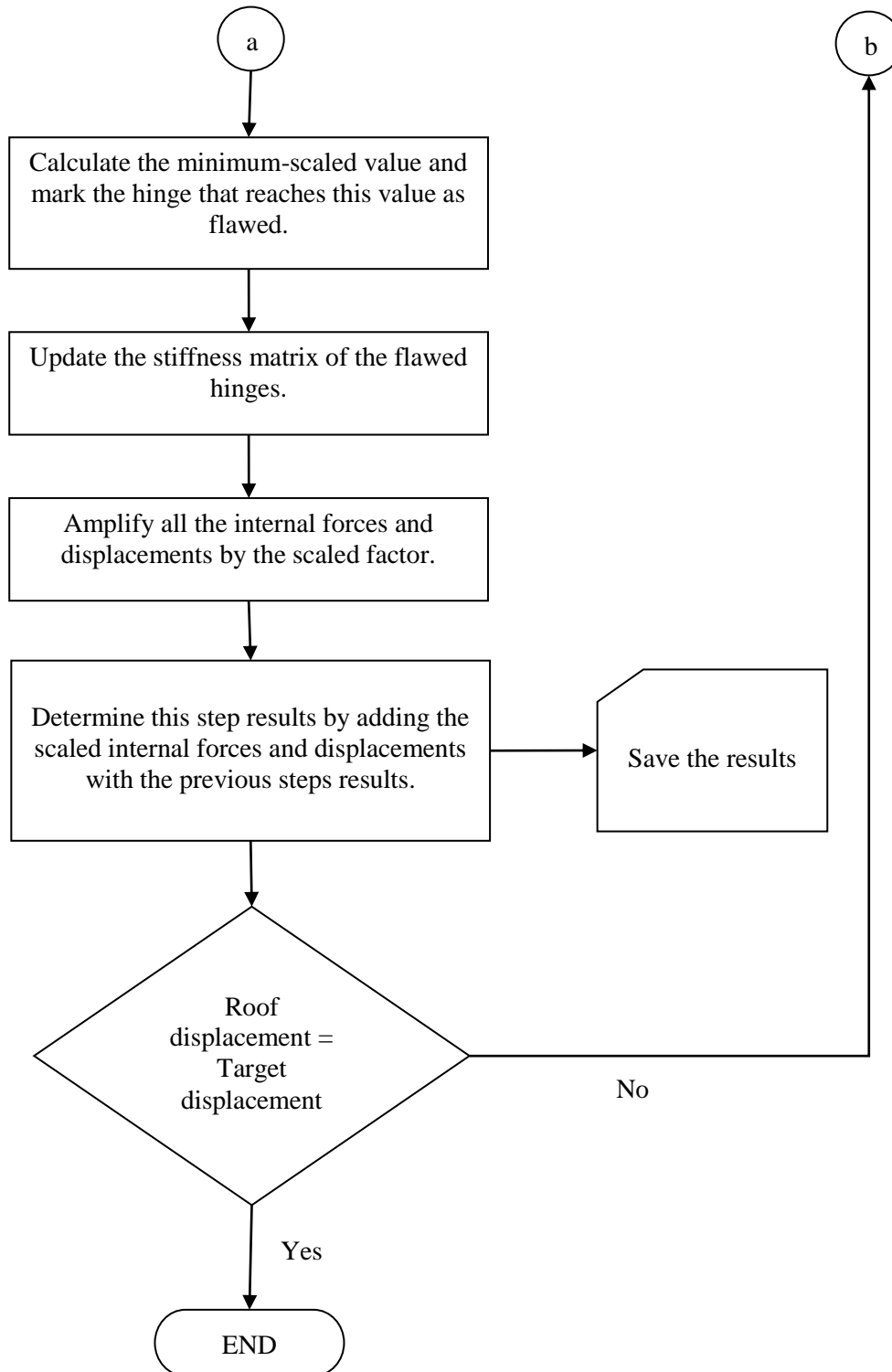


Figure 4.23 (continued) : Flowchart of NASAP for an adaptive pushover procedure.

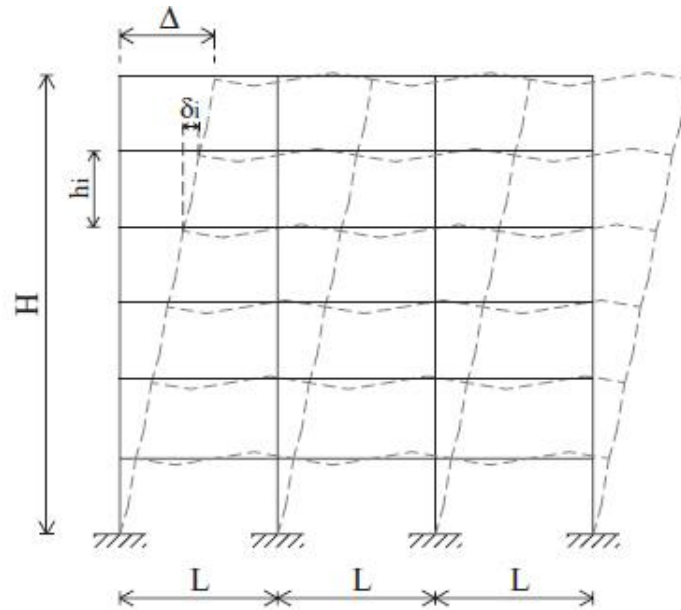


Figure 4.24 : Lateral drifts of multi-story building [39].

As stated while defining the steps of NASAP, geometric nonlinearity is neglected. There is three valid P- Δ theory in the literature; *small displacement theory*, P- Δ and the *large displacement theory*. All three assumes that the axial extension of the bar is infinity ($EA = \infty$). Figure 4.25 gives a representative of these theories.

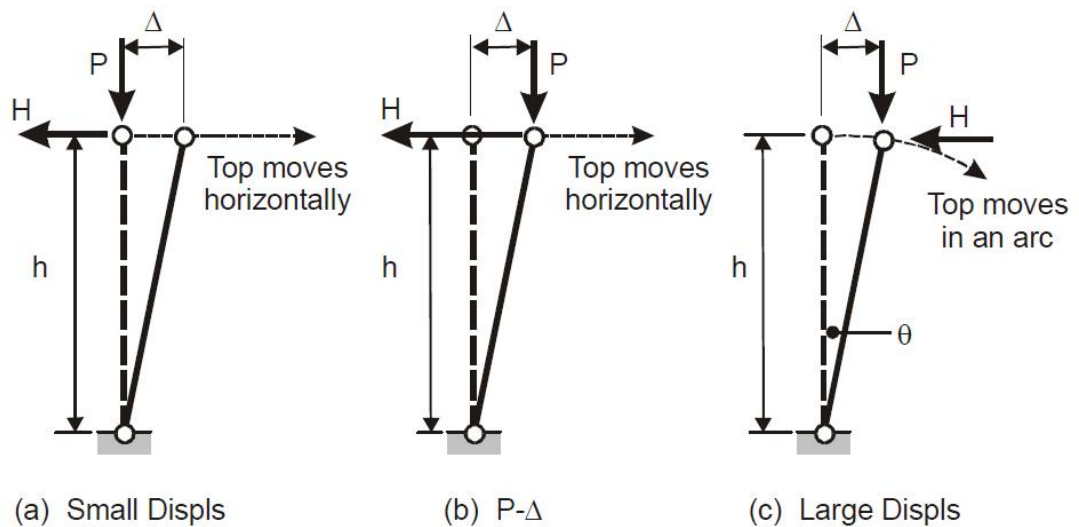


Figure 4.25 : Geometric Nonlinearities [13].

Small displacement theory assumes that the top of the bar moves horizontally but with a small displacement. This displacement is so small so that it can be neglected. The undeformed shape is valid for defining the equilibrium conditions since the lateral force $H=0$ for all values of Δ .

P-Δ theory is where the equilibrium conditions are valid through the deformed shape since the bar moves horizontally. Lateral force can be defined by dividing the $PΔ$ moment to the height of the element ($PΔ/h$).

In *large displacement theory*, the movement of the bar is assumed in an arc. It means two direction movements are valid in this theory; horizontal and vertical, but the extension is still assumed to be zero. The equilibrium conditions are gathered on the deformed shape. Lateral force is determined by dividing the $PΔ$ moment to the rotation angle of the bar ($PΔ/h \cos \theta$).

In fact it has been showed that [13] the $P-Δ$ theory and the large displacements theory give approximately the same results. For example for a large drift value of $Δ/h=0.05$, $P-Δ$ theory gives $H=0.05P$ and large displacements theory gives $H=0.05006P$, which is a negligible difference. This is why, for most structures, it is accurate enough to use just the $P-Δ$ theory.

$P-δ$ effect is called as the bending of the element in its length. Figure 4.26 shows an elastic cantilever column where both vertical and horizontal loads are applied to its free end.

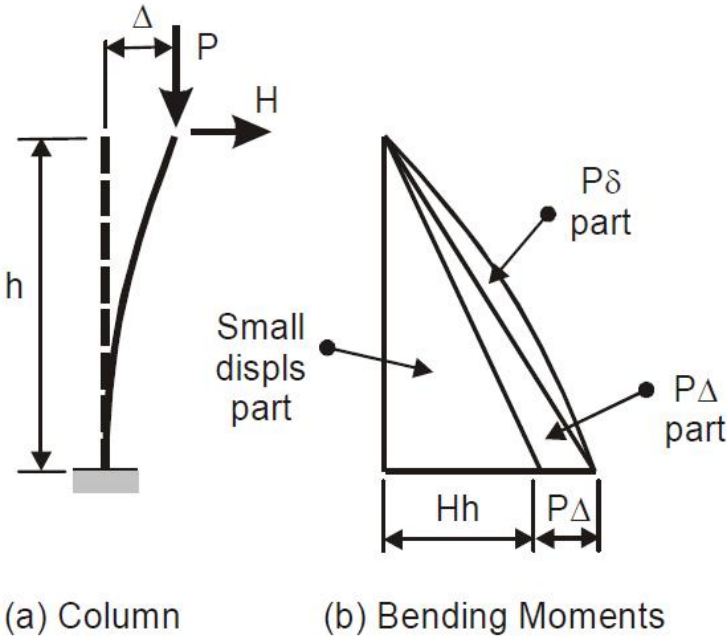


Figure 4.26 : $P-Δ$ and $P-δ$ effects for elastic cantilever column [13].

As shown in the figure, the bending moment is composed of three parts; *small displacements*, $P-\Delta$ and $P-\delta$ parts. Small displacement part resembles the moment from small displacement theory, which is equal to the multiplication of lateral load with the column height (Hh). $P-\Delta$ part, with a moment $P\Delta$, depends on the lateral displacement at the top of the column. $P-\delta$ part is the bending of the column within its length. $P-\delta$ part depends on the bending deformation of the column, whether it yields or remains elastic.

Figure 4.27 shows the same cantilever column after it yields and forms a plastic hinge at the base.

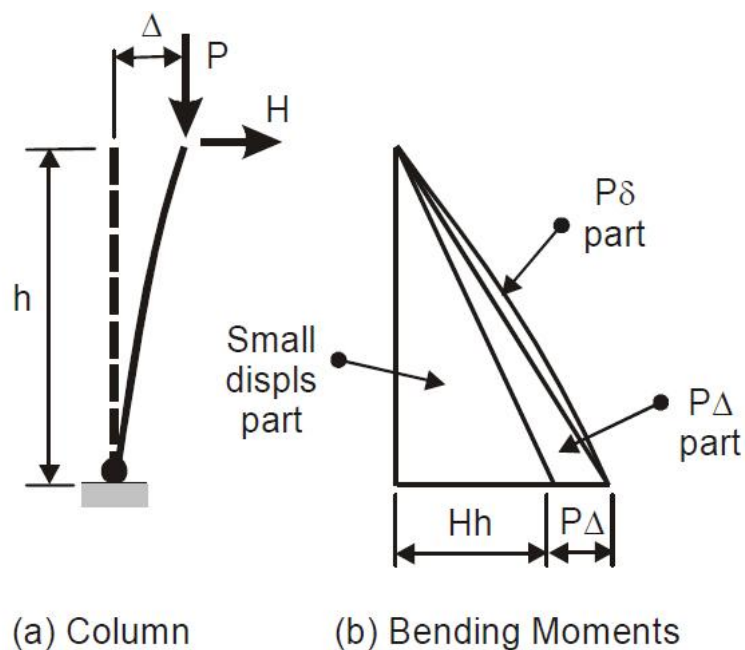


Figure 4.27 : $P-\delta$ effect when column yields [13].

The moment capacity of the plastic hinge (M) is not dependable on $P-\Delta$ effects. If small displacements theory is used, the plastic hinge forms when $M = Hh$, and the horizontal strength of the column will be $H = M/h$. If $P-\Delta$ effects are considered, then the hinge forms when $M = Hh + P\Delta$, and the predicted strength will be reduced by the $P\Delta$ moment; $H = (M - P\Delta)/h$. This is why the $P-\Delta$ effects reduce the strength of a column [13].

If a column forms plastic hinges at its ends, it is for sure that the P- δ moments will be significant. If a column is stiff enough, then its elastic bending deformations will usually be so small that P- δ effects are insignificant. If a column is flexible enough, it will again have a small elastic bending deformations. That is why; in most cases P- δ effects are ignored.

4.4 Adaptive Pushover Results and Comparison of SPEAR Building

Existing, 3-D irregular SPEAR building has been modelled using NASAP by following the above procedures. NASAP model of the SPEAR building is given in Figure 4.28. Time-History analysis are conducted with PERFORM 3-D (CSI). The results of the time history analysis are compared with the adaptive and non-adaptive pushover results of NASAP. As stated before, ELSA Lab results of the pseudo-dynamic tests of the SPEAR building, using a 0.2g scaled accelogram, have been compared with the adaptive pushover results of NASAP.

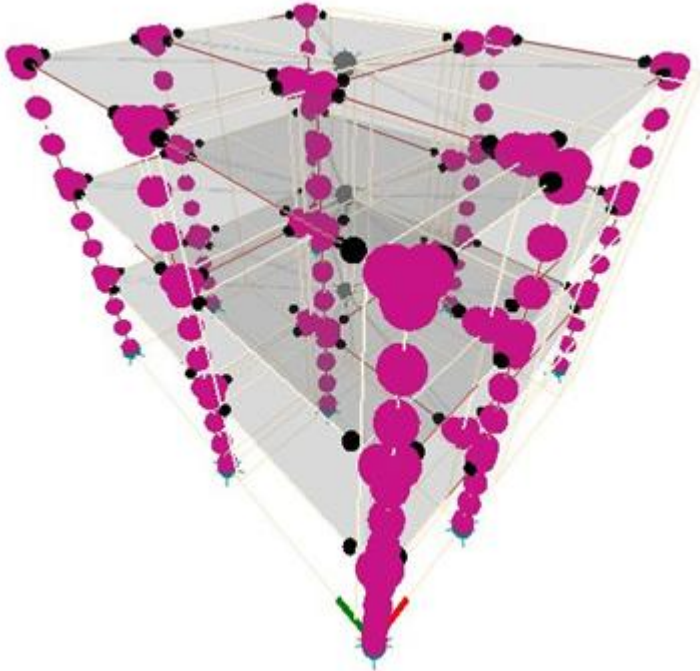


Figure 4.28 : 3-D SPEAR model of NASAP.

The determined mode shapes from the eigen value analysis are represented in Figure 4.39 and Figure 4.30. The calculated modal participation factors and the period values are given in Table 4.4 and Table 4.5 respectively.

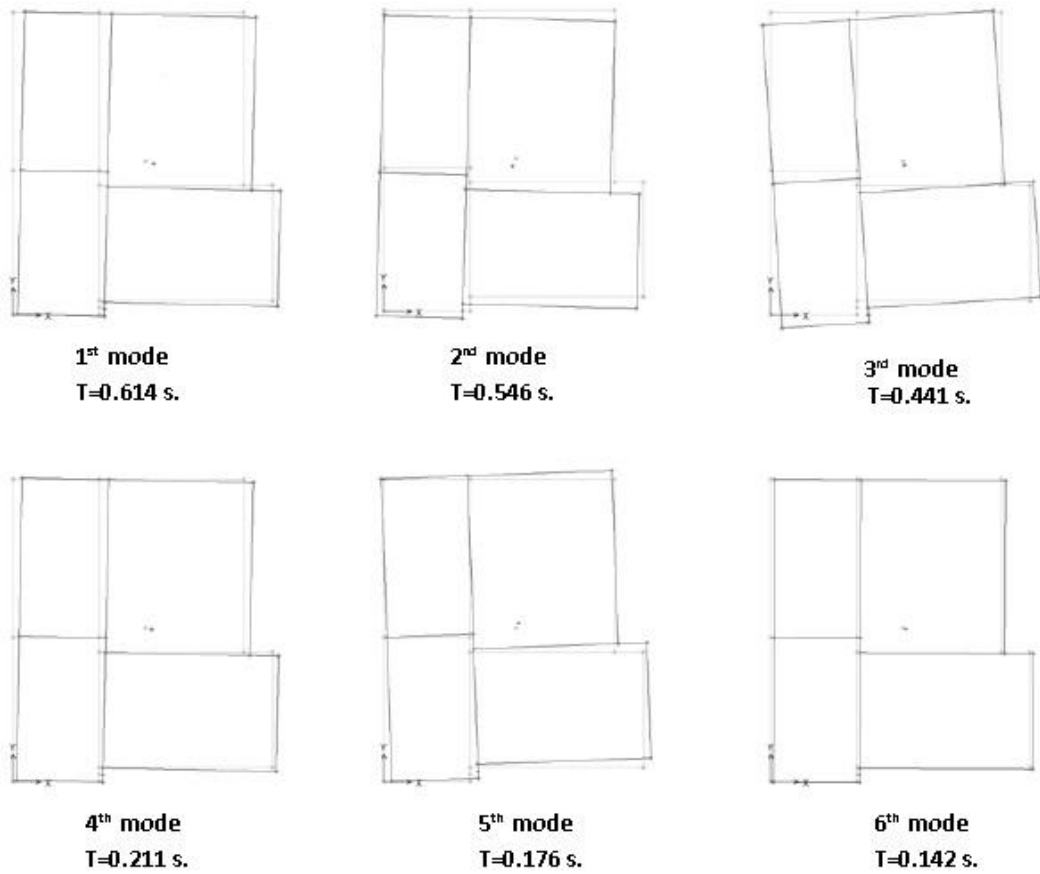


Figure 4.29 : Mode Shapes and periods of the 3-D Spear model.

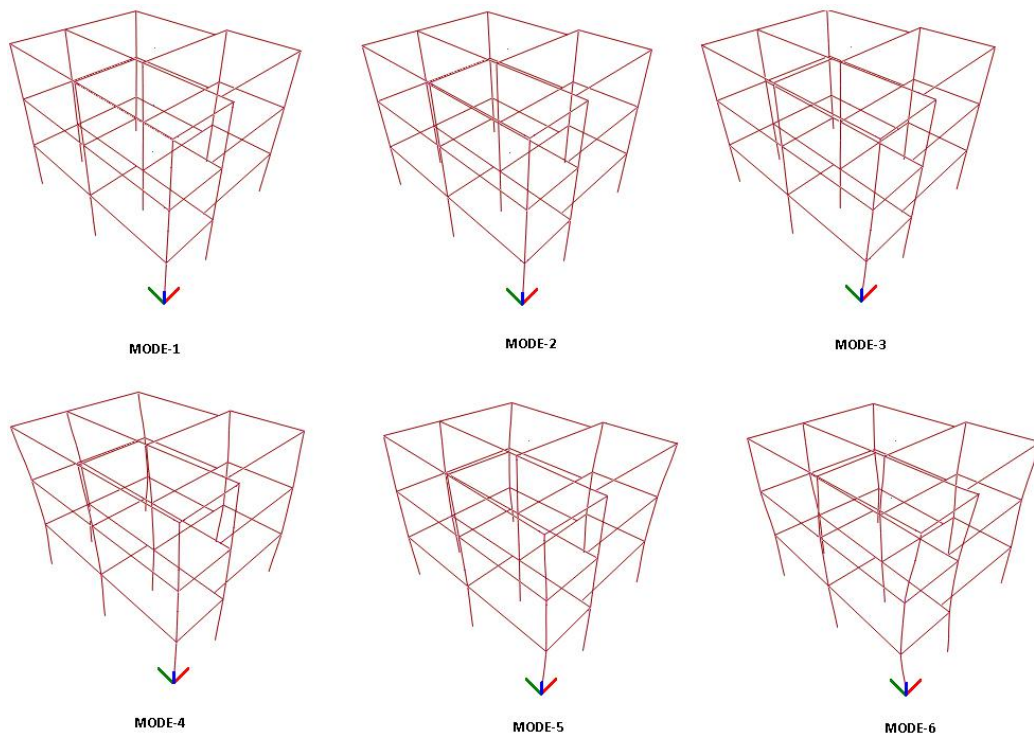


Figure 4.30 : Mode Shapes of the 3-D NASAP-Spear model.

Table 4.4: Modal participation factors calculated using NASAP.

Mode	X Direction	Y Direction	Around Z Direction
1	12.02	-3.14	-20.53
2	4.76	11.07	21.50
3	2.71	-5.56	52.46
4	3.83	-0.86	-6.38
5	1.55	3.53	10.36
6	-0.22	3.02	-14.94

After evaluating the modal quantities, adaptive and non-adaptive analysis are implemented for both longitudinal and transverse direction respectively.

Table 4.5: Period and Mass ratio values for both directions.

Mode	Period (s)	Long. M. Ratio	Trans. M. Ratio	Torsional M. Ratio
1	0.61	0.74	0.05	0.11
2	0.55	0.11	0.62	0.11
3	0.44	0.03	0.15	0.67
4	0.21	0.07	0.01	0.01
5	0.17	0.01	0.06	0.02
6	0.14	0	0.04	0.05

The calculated peak story shear profiles are given in Table 4.6. In the table “*Long*”, symbolizes the longitudinal and “*Tr*”, transverse direction.

Table 4.6: Peak story shear profiles.

		Story-1	Story-2	Story-3
Long. Adaptive	FX	132.32	104.54	62.72
	FY	152.04	124.42	75.40
Long. Non-adaptive	FX	173.46	139.16	84.77
	FY	173.16	144.48	88.78
Tr. adaptive	FX	168.44	133.11	80.28
	FY	168.68	137.34	83.63
Tr. non-adaptive	FX	213.62	171.37	104.39
	FY	213.24	177.92	109.33

The adaptive story shear profile results, for specified steps, are graphed in Figure 4.31 and Figure 4.32 for longitudinal and transverse directions respectively.

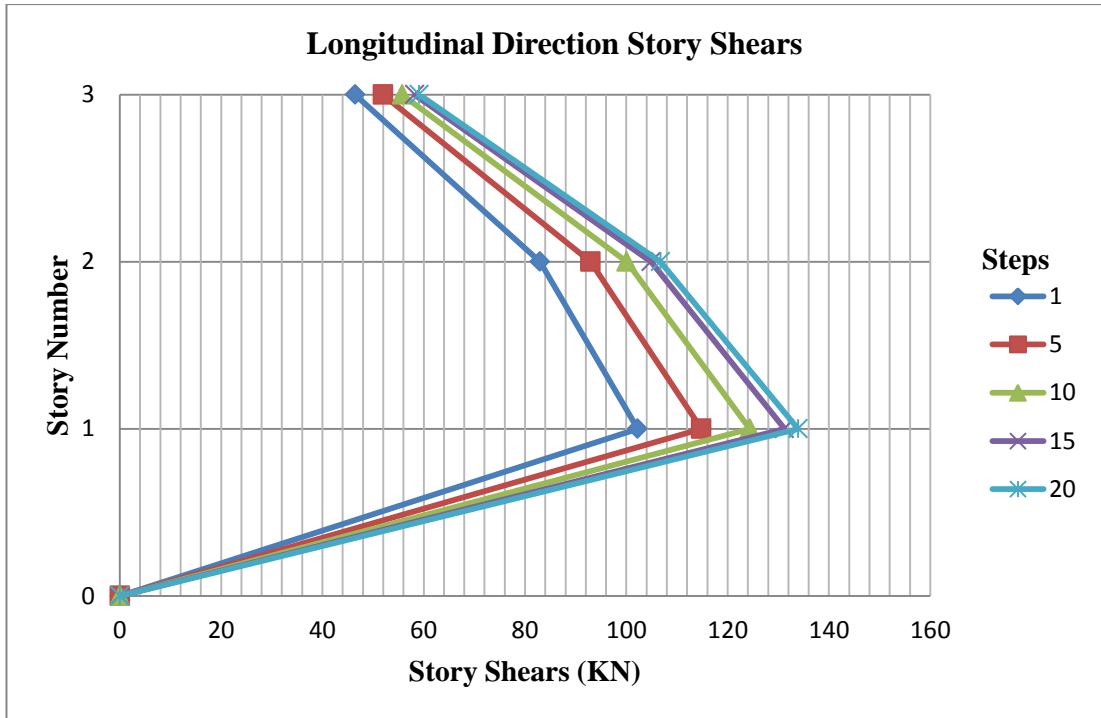


Figure 4.31 : Story shear profiles for longitudinal direction.

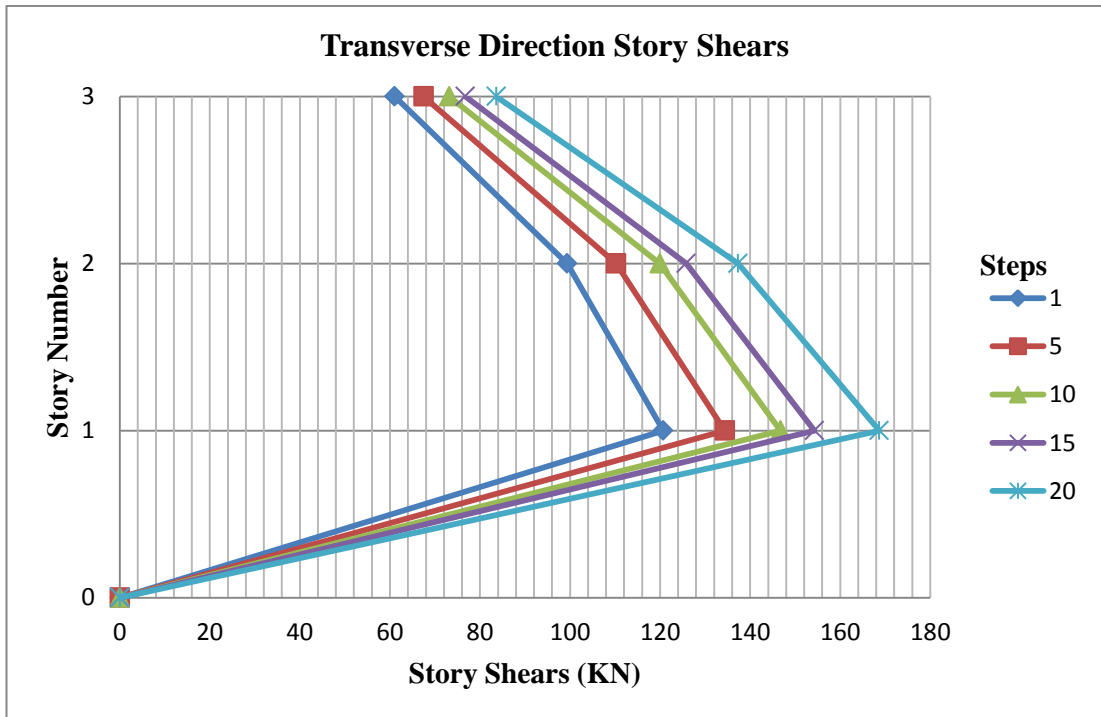


Figure 4.32 : Story shear profiles for transverse direction.

Time histories are conducted by using PERFORM 3-D (CSI). The time-history drift results are compared with the adaptive pushover of NASAP using the response spectra previously defined. The comparison graphs are given in Figure 4.33 and 4.34 respectively.

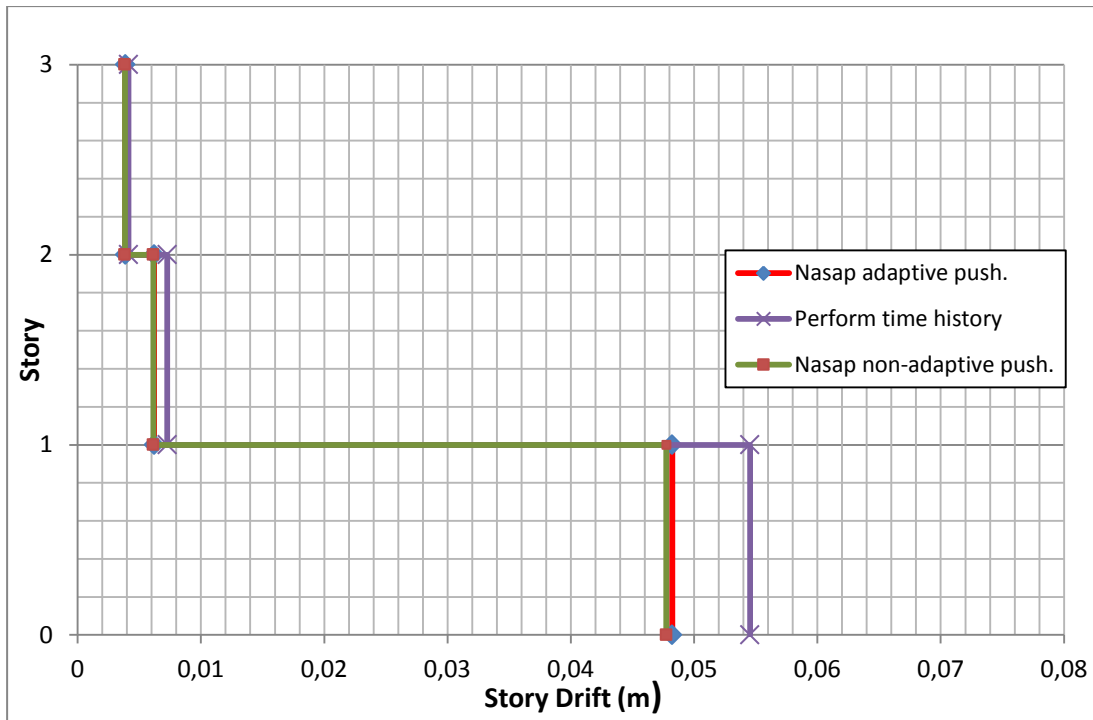


Figure 4.33 : Story drifts in longitudinal direction.

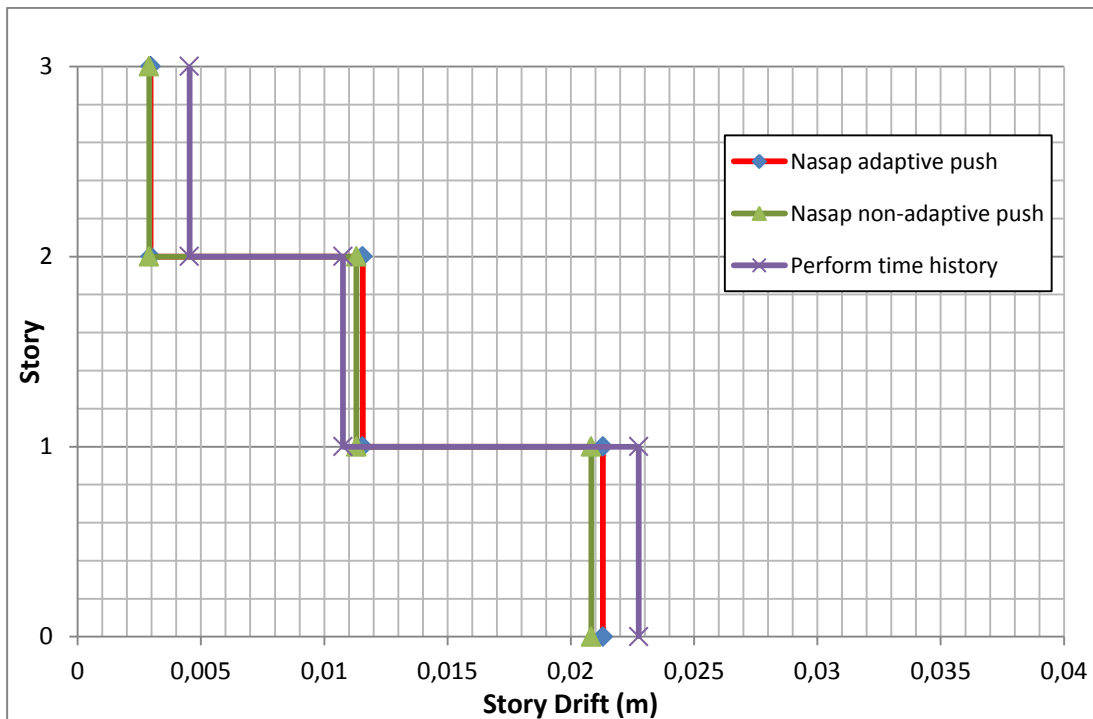


Figure 4.34 : Story drifts in transverse direction.

The target displacement values are calculated using FEMA [1, 2] as 0.042 m in the longitudinal direction and 0.047 m in the transverse direction. Figure 4.35 shows the comparison of one modal conventional pushover analysis and the story shear based pushover analysis for both directions.

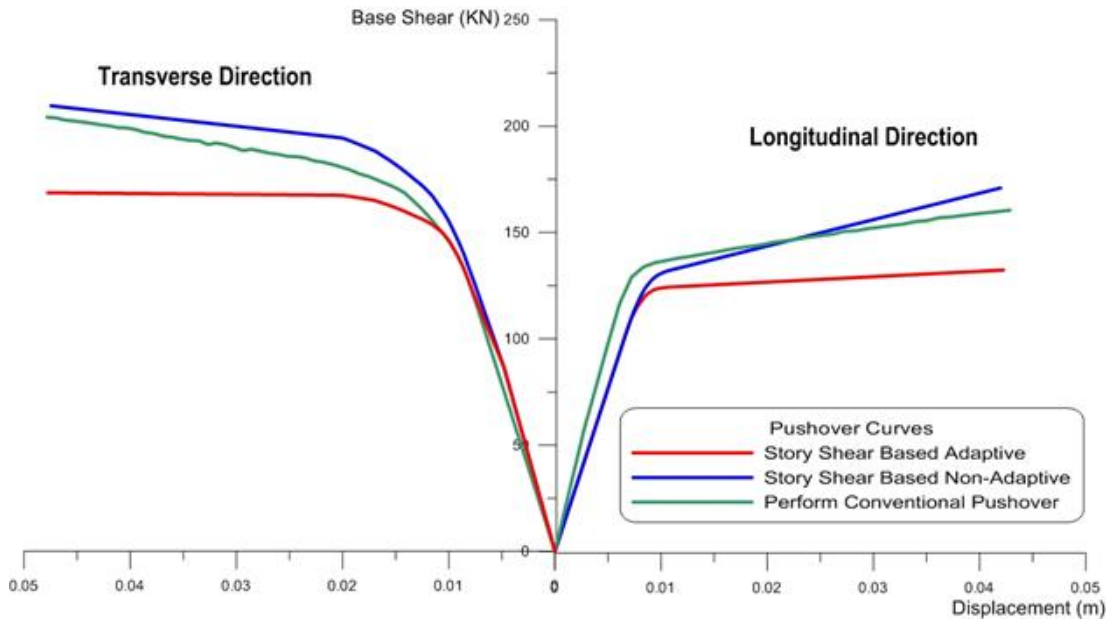


Figure 4.35 : Comparison of conventional and SSAP curves.

The plots for the calculated load patterns of the specified analysis steps are given in Figure 4.36 and 4.37, representing the longitudinal and transverse directions respectively. Although, the adaptive pushover analysis are designed to be performed in 40 steps; in the longitudinal direction after 20th step the applied load pattern started to decrease. The same decrease in the applied load pattern has been seen in the 10th step in transverse direction.

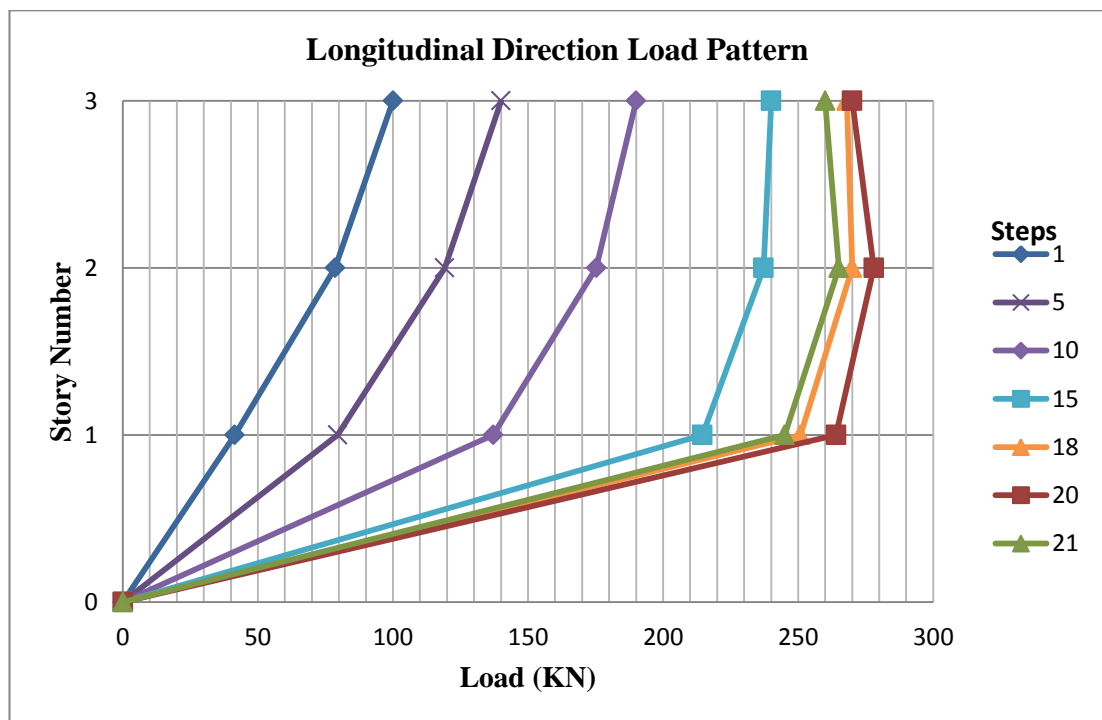


Figure 4.36 : Longitudinal direction load pattern.

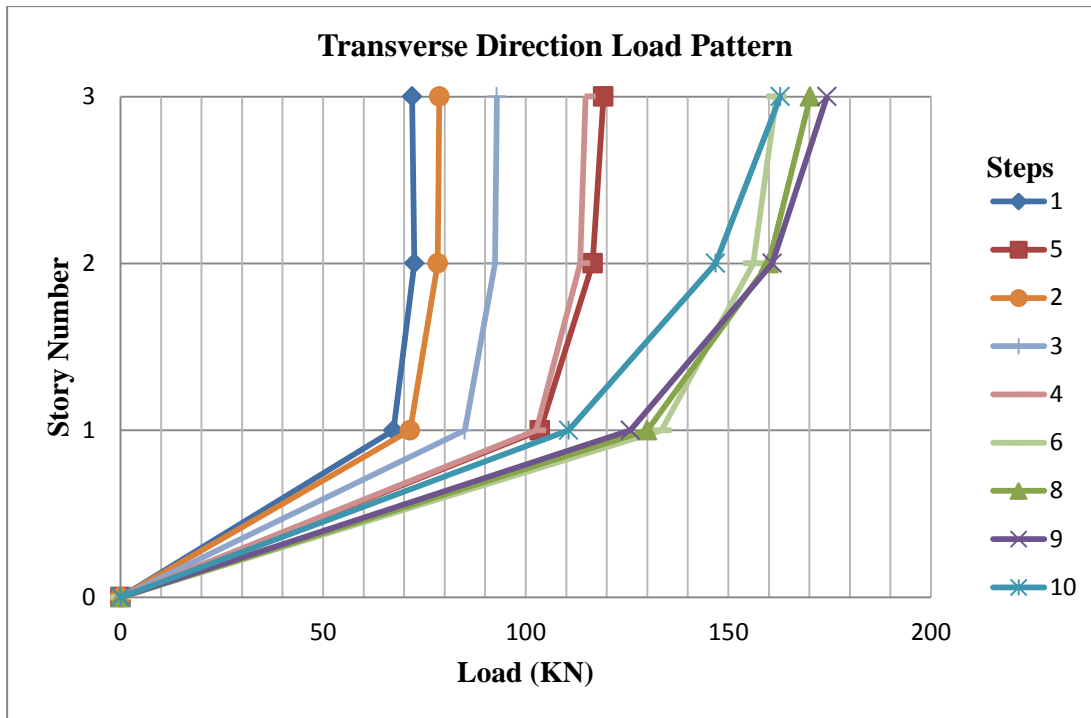


Figure 4.37 : Transverse direction load pattern.

As stated before, in the ELSA Lab, pseudo-dynamic tests of SPEAR building was implemented. In the tests, Montenegro earthquake record was scaled to 0.2g. Comparison of the pseudo-dynamic test results of each story level with the story shear-story drift results of NASAP are given through Figure 4.38-Figure 4.40. It can be seen from the graphs that the results of NASAP are in good agreement with the experimental results.

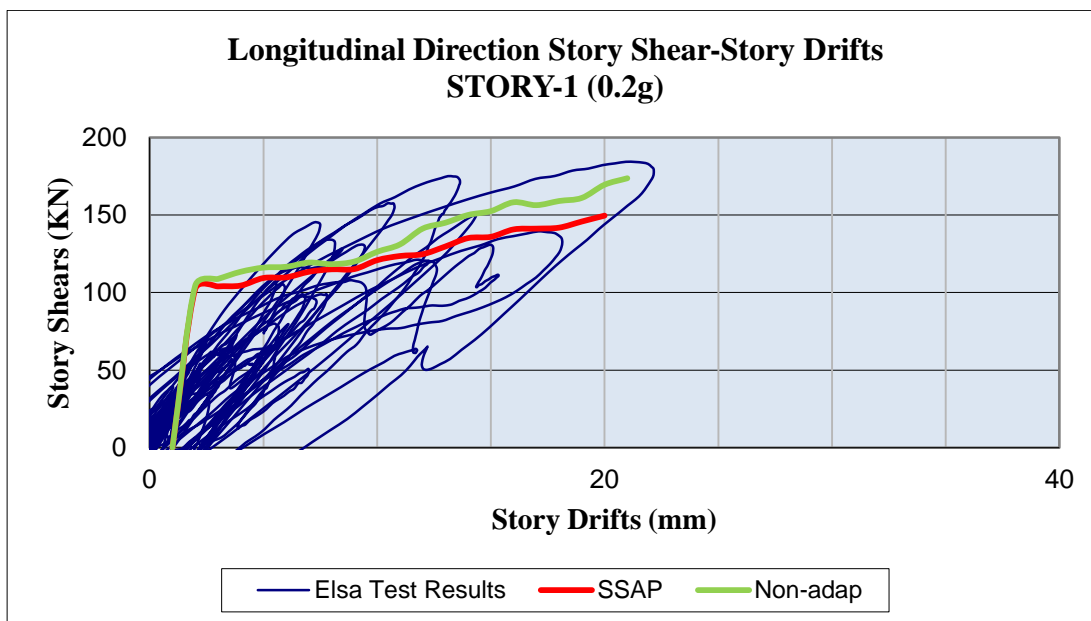


Figure 4.38 : Comparison of ELSA test results with pushover curves for Story-1.

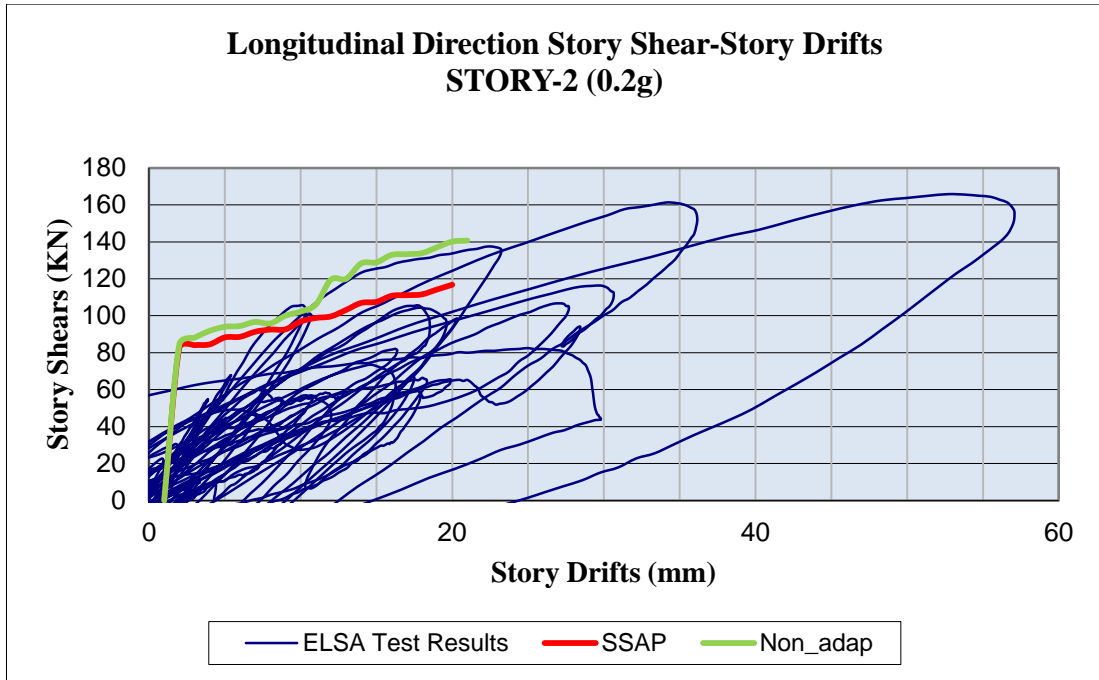


Figure 4.39 : Comparison of ELSA test results with pushover curves for Story-2.

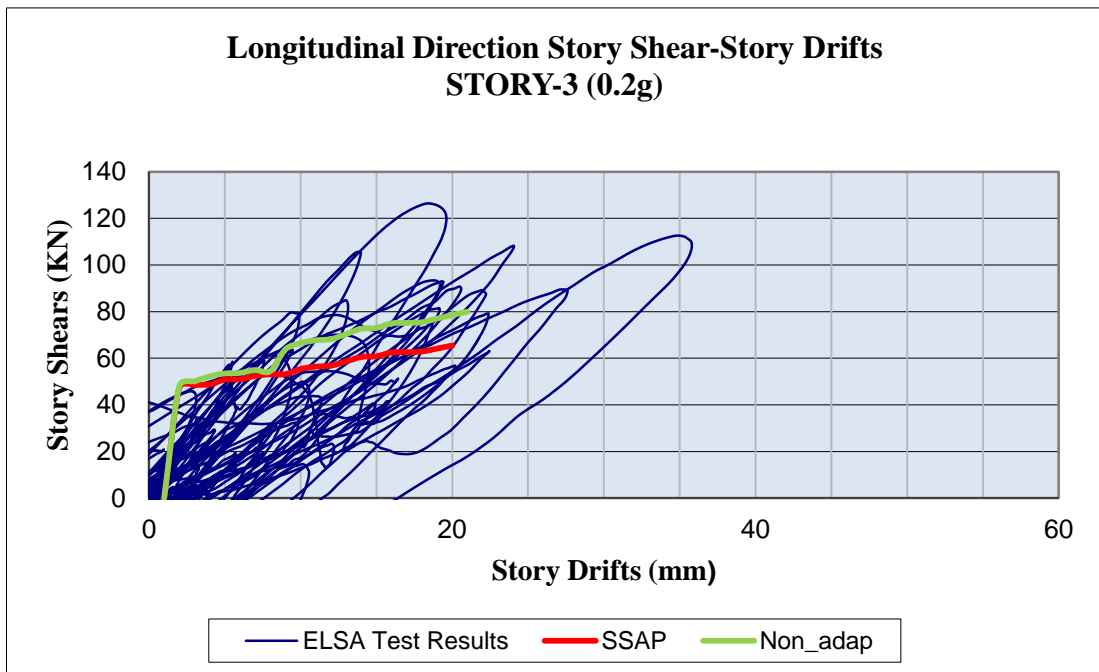


Figure 4.40 : Comparison of ELSA test results with pushover curves for Story-3.

The test result of the third story seems to be suspicious. If Figure 4.40 is investigated carefully, it can be concluded that the hysteretic curves are not acting properly in this level. While comparing the results, the deficiency of this story should be considered.

5. CONCLUSIONS AND RECOMMENDATIONS

The aforementioned story shear based adaptive pushover procedure has been adapted to a 3-D irregular building, SPEAR, without considering the P- Δ effects. The analysis results are given through Chapter 4 for both directions with adaptive and non-adaptive solutions. Seismic capacity was evaluated by inelastic dynamic analysis. Seven recorded bidirectional ground motions were scaled to match the EC8 spectra for soil type C.

The structure has torsional irregularities, with eccentricities higher in the transverse direction. Calculated base shear capacity is higher in the same direction due to the strong C6 (25x75cm) column. Displacement values are calculated to be higher in the weaker longitudinal direction.

Dynamic response history analyses were performed by Perform 3-D for assessment of peak displacement demand, amount of torsion etc. The corresponding time history results of drifts were compared with the adaptive pushover results of NASAP.

Pseudo-dynamic test results of SPEAR building are compared with the story shear-story drift results of NASAP. It is seen that, for adaptive and non-adaptive analysis, the results of NASAP are in good agreement with the experimental ones.

5.1 Application of The Work

Performance based design issue has become very important in the last decade. The main point of the performance based analyse techniques is to assess the capacity of the structure for an earthquake excitation and model the structure for the selected performance level criteria.

The majority of the building stocks in Turkey are irregular. Structural designer should include torsional effects in the design or while strengthening an existing building. The aforementioned procedure might be suitable to apply while assessing the capacity of the newly formed or existing irregular structures since it is a 3-D procedure. It takes care of the irregularity effects. This procedure would be a more accurate way of determining the capacity of an irregular building.

5.2 Conclusions

1. Adaptive procedures are more accurate than conventional ones while determining the capacity and the drift profiles of the structures. Recent studies have shown that adaptive results of the drift profiles are much closer to the time history results than the conventional ones. Figure 4.33 and 4.34 shows these phenomena. Since FEMA uses the horizontal displacement at the roof as the measure of building deformation, the drifts plotted here assemble the roof drift. Adaptive SSAP procedure is more accurate compared to non-adaptive ones. This should be added that; the accuracy of the SSAP in drift is increased when the higher modes are significant as in the upper stories. The accuracy of conventional nonlinear static procedures in the lower stories is better where the higher mode effects are less.
2. Uniform load pattern may only be applicable when higher mode effects are not significant. Ignoring the higher modes can result in highly inaccurate estimates of deformation demands. Force-based adaptive procedures use SRSS to combine the modal story effects. That makes it impossible to investigate the sign changes and reversal effects of higher modes during the analysis. Despite this fact, in a story shear based adaptive pushover analysis, the required story forces are calculated by subtracting the combined modal shear of consecutive stories. This is the main difference of SSAP from the other adaptive procedures. Also in SSAP, both the sign changes of the higher modes and the reversal effects can be taken into account while calculating story shear forces.
3. Previous studies showed that, conventional pushover analysis fail to estimate the dynamic drift profile. It is a known a fact that, conventional pushover analysis results cannot be relied on unless a time history analysis or an adaptive analysis conducted afterwards.

4. Since torsion is assessed by the fundamental mode shape under an earthquake excitation, most conventional pushover analysis programs are usually designed for two dimensionally neglecting torsional effects. It is a well-known fact that, conventional pushover analysis cannot predict torsional response accurately. That is why the dynamic response history analysis is a more appropriate analysis method to estimate the response of an asymmetric building. Additional displacements due to torsional behavior should be considered.
5. The previous studies indicated that the adaptive pushover in general does not provide major advantages over the conventional methodology due to the fact that, while combining the modal forces with SRSS or CQC, the sign changes are not included. That is why in this study, Story Shear Adaptive Pushover procedure is used. The procedure is also utilized for performance analysis of three dimensional frames with vertically and plan-wise irregular buildings. It is shown in Figure 4.35 that, the conventional pushover analysis overestimates the results by 20% approximately.
6. Comparison of the longitudinal direction pseudo-dynamic experimental results of irregular SPEAR building with the adaptive pushover results of NASAP showed that, the theoretic background of the developed program is robust and the implemented procedure gives good correlation with the test results. The transverse direction comparison of the pushover curves with the pseudo-dynamic test results of ELSA Lab, could not be achieved due to the lack of data absence in this direction.

5.3 Outlook

Through the aforementioned adaptive pushover analysis P-Delta effects are neglected. As mentioned in Chapter 4, P-Delta effects should be taken in to account especially for estimating the irregular building capacity. On-going study to include these effects in to the developed computer code has been mentioned.

Recent studies in earthquake engineering have shown the importance of soil-structure interaction. Neglecting the soil effects may cause misleading of the period values. If the calculated value for the structure is found to be equal to the ground period then a resonance is assumed to occur, whilst in real this may not be a valid situation. It misleads the structural engineer.

In this study, seven artificial earthquake records are used to form a modified real earthquake record. The number of the records that are used, and the number of the nonlinear time history analysis conducted should be increased in order to assess the drift limits more accurate way.

Further research in modelling the inelasticity is needed. It is now known that, fibre elements are more accurate in estimating the inelastic capacity then the concentrated hinge concept. A fibre model should be implemented.

REFERENCES

- [1] **FEMA 440**, 2005. Improvement of Nonlinear Static Seismic Analysis Procedures, *Federal Emergency Management Agency*, Washington, D.C.
- [2] **FEMA 356**, 2000. Prestandard and commentary for the seismic rehabilitation of buildings, *Federal Emergency Management Agency*, Washington, D.C.
- [3] **ATC 40**, 1996. Seismic Evaluation and Retrofit of Concrete Buildings, *Applied Technology Council*, Washington, D.C.
- [4] **Papanikolaou, V. K., and Elnashai, A. S.**, 2005: Evaluation of Conventional and Adaptive Pushover Analysis I: Methodology. *Journal of Earthquake Engineering*. Vol. **9**, no. 6, pp. 923-941.
- [5] **Barros, R. C., and Almeida, R.**, 2005: Pushover Analysis of Asymmetric Three Dimensional Building Frames. *Journal of Civil Engineering and Management*. Vol. **11**, no. 1, pp. 3-12.
- [6] **Goel, R. K., and Chopra, A. K.**, 2005: Role of Higher-“Mode” Pushover Analyses in Seismic Analysis of Buildings. *Earthquake Spectra*. Vol. **21**, no. 4, pp. 1027-1041.
- [7] **Vamvatsikos, D., and Cornell, C. A.**, 2002: Incremental dynamic analysis. *Earthquake Engineering and Structural Dynamics*. Vol. **31**, pp. 491-514.
- [8] **Aydinoğlu, N.**, 2003: An Incremental Response Spectrum Analysis Procedure Based on Inelastic Spectral Displacements for Multi-Mode Seismic Performance Evaluation. *Bulletin of Earthquake Engineering*. Vol. **1**, pp. 3-36.
- [9] **Shakeri, K., Shayanfar, M. A., and Kabeyasawa, T.**, 2010: A story shear-based adaptive pushover procedure for estimating seismic demands of buildings. *Engineering Structures*. Vol. **32**, no. 1, pp. 174-183.
- [10] **McKenna, F., Fenves, G. L., Filippou, F. C., & Mazzoni, S.** (2006). Open system for earthquake engineering simulation (OpenSees). *Pacific Earthquake Engineering Research Center, U.C. Berkeley*, from <http://opensees.berkeley.edu/OpenSees/home/about.php>.
- [11] **Fardis, M., Negro, P. A.**, 2005: Seismic Performance Assessment and Rehabilitation of Existing Buildings (SPEAR). Proceedings of the International Workshop, An event to honour the memory of Prof. Jean Donea, Institute for the Protection and Security of the Citizen European Laboratory for Structural Assessment (ELSA) I-21020 Ispra, Italy, 4-5 April.

- [12] **Boore, D. M., Sims, D. J., Kanamori, H., and Harding, S.,** 1981: The Montenegro, Yugoslavia, earthquake of April 15, 1979: Source orientation and strength. *Physics of the Earth and Planetary Interiors.*, Vol. **27**, pp. 133-142.
- [13] **Computers & Engineering,** (2004). Nonlinear Analysis and Performance Assessment for 3-D Structures, from <http://www.comp-engineering.com/products/PERFORM3D/Perform3D.html>.
- [14] **Freeman, S. A.,** 1998: The Capacity Spectrum Method as a Tool for Seismic Design, *Eleventh European Conference on Earthquake Engineering*, Paris, France, September 6-11.
- [15] **Paret, F. T., Sasaki, K. K., Eilbeck, D. H., Freeman, S. A.,** 1996: Approximate Inelastic Procedures to Identify Failure Mechanisms From Higher Mode Effects, *Eleventh World Conference on Earthquake Engineering*, Acapulco, Mexico, June 23-28.
- [16] **Sasaki, K. K., Freeman, S. A., and Paret, T. F.,** 1998: Multimode pushover procedure (MMP) – A method to identify the effects of higher modes in a pushover analysis. Proceedings of the U.S. National Conf. on Earthquake Engineering, Seattle. WA, 17–19 September (CD-ROM).
- [17] **Moghadam, A. S., and Tso, W. K.,** 2002: A pushover procedure for tall buildings. Proceedings of the 12th European Conference on Earthquake Engineering, Elsevier Science Ltd.
- [18] **Chopra, A. K., and Goel, R. K.,** 2002: A modal pushover analysis procedure for estimating seismic demands for buildings. *Earthquake Engineering and Structural Dynamics*. Vol. **31**, pp. 561-582.
- [19] **Chopra, A. K., Goel, R. K., and Chintanapakdee, C.,** 2004: Evaluation of a Modified MPA Procedure Assuming Higher Modes as Elastic to Estimate Seismic Demands. *Earthquake Spectra*. Vol. **20**, no. 3, pp. 757-778.
- [20] **Reinhorn, A. M.,** 1997: Seismic Design Methodologies for the Next Generation of Code. *Workshop on Inelastic Analysis Techniques in Seismic Evaluations*, Bled, Slovenia, June 24-27.
- [21] **Bracci, J. M., Kunnath, S. K., and Reinhorn, A. M.,** 1997: Seismic performance and retrofit evaluation for reinforced concrete structures. *ASCE Journal Structural Engineering*. Vol. **123**, no. 1, pp. 3-10.
- [22] **Satyarno, I., Carr, A. J., Restrepo, J.,** 1998: Refined pushover analysis for the assessment of older reinforced concrete buildings. In: Proceedings of NZSEE technology conference.
- [23] **Requena, M., and Ayala, A. G.,** 2000: Evaluation of a Simplified Method For The Determination of the Non Linear Seismic Response of RC Frames. Proceedings of the Twelfth World Conference on Earthquake Engineering. No. 2109, Auckland, New Zealand.
- [24] **Gupta, B., and Kunnath, S. K.,** 2000: Adaptive Spectra-Based Pushover Procedure for Seismic Evaluation of Structures. *Earthquake Spectra*. Vol. **16**, no. 2, pp. 367-391.

- [25] **Gupta, B., and Krawinkler, H.**, 1999: Seismic demands for performance evaluation of steel moment resisting frame structures (SAC Task 5.4.3). *Report No. 132*. John A. Blume Earthquake Engineering Center, Stanford University, Stanford, CA.
- [26] **Mwafy, A. M., and Elnashai, A. S.**, 2001: Static pushover versus dynamic collapse analysis of RC buildings. *Engineering Structures*. Vol. **23**, pp. 407-424.
- [27] **Elnashai, A. S.**, 2002: Do We Really Need Inelastic Dynamic Analysis?. *Journal of Earthquake Engineering*. Vol. **6**, no. 1, pp. 123-130.
- [28] **Borzi, B., Calvi, G. M., Elnashai, A. S., Faccioli, E. and Bommer, J. J.**, 2001: Inelastic spectra for displacement-based seismic design. *Soil Dynamics and Earthquake Engineering*. Vol. **21**, pp. 47-61.
- [29] **Papanikolaou, V. K., Elnashai, A. S., and Pareja, J. F.**, 2006: Evaluation of Conventional and Adaptive Pushover Analysis II: Comparative Results. *Journal of Earthquake Engineering*. Vol. **10**, no. 1, pp. 127-151.
- [30] **Jeong, S. H., and Elnashai, A. S.**, 2005: Analytical Assessment Of An Irregular RC Frame For Full-Scale 3d Pseudo-Dynamic Testing Part I: Analytical Model Verification. *Journal of Earthquake Engineering*. Vol. **9**, no. 1, pp. 95-128.
- [31] **Jeong, S. H., and Elnashai, A. S.**, 2005: Analytical Assessment Of An Irregular RC Frame For Full-Scale 3d Pseudo-Dynamic Testing Part II: Condition Assessment And Test Deployment. *Journal of Earthquake Engineering*. Vol. **9**, no. 2, pp. 265-284.
- [32] **Jeong, S. H., and Elnashai, A. S.**, 2004. Analytical Assessment of an Irregular RC Full Scale 3D Test Structure, *Mid-America Earthquake Center Technical Report, EEC-9701785*, Urbana, Illinois.
- [33] **Papanikolaou, V. K., Elnashai, A. S., and Pareja, J. F.**, 2005. Limits of Applicability of Conventional and Adaptive Pushover Analysis for Seismic Response Assessment, *Mid-America Earthquake Center Technical Report*, Urbana, Illinois.
- [34] **Albanesi, T., Biondi, S., and Petrangeli, M.**, 2002: Pushover Analysis: An Energy Based Approach. Proceedings of the 12th European Conference on Earthquake Engineering, Elsevier Science Ltd.
- [35] **Antoniou, S., and Pinho, R.**, 2004: Advantages And Limitations Of Adaptive And Non-Adaptive Force-Based Pushover Procedures. *Journal of Earthquake Engineering*. Vol. **8**, no. 4, pp. 497-522.
- [36] **Antoniou, S., and Pinho, R.**, 2004: Development And Verification Of A Displacement-Based Adaptive Pushover Procedure. *Journal of Earthquake Engineering*. Vol. **8**, no. 5, pp. 643-661.
- [37] **Antoniou, S., Pinho, R., and Pietra, D.**, 2006: A Displacement-Based Adaptive Pushover For Seismic Assessment Of Steel And Reinforced Concrete Buildings. Proceedings of the 8th U.S. Conference in Earthquake Engineering, San Francisco, U.S., April 17-21.

- [38] **Ferracuti, B., Pinho, R., Savoia, M., and Francia, R.**, 2009: Verification of displacement-based adaptive pushover through multi-ground motion incremental dynamic analyses. *Engineering Structures*. Vol. **31**, pp. 1789-1799.
- [39] **Elnashai, A. S., and Sarno, L. D.**, 2008. *Fundamentals Of Earthquake Engineering*, ISBN: **9780470024836**, A John Wiley & Sons, Ltd, Publication, United Kingdom.
- [40] **Naeim, F.**, 2001. *The Seismic Design Handbook*, ISBN: **0792373014**, Kluwer Academic Publication, United Kingdom.
- [41] **FEMA 274**, 1997. Nehr Commentry On The Guidelines For The Seismic Rehabilitation Of Buildings, *Federal Emergency Management Agency*, Washington, D.C.
- [42] **FEMA 445**, 2006. Next-Generation Performance-Based Seismic Design Guidelines Program Plan for New and Existing Buildings, *Federal Emergency Management Agency*, Washington, D.C.
- [43] **FEMA P440A**, 2009. Effects of Strength and Stiffness Degradation on Seismic Response, *Federal Emergency Management Agency*, Washington, D.C.
- [44] **Deierlein, G. G., Reinhorn, A. M., and Willford, M. R.**, 2009. Nonlinear Structural Analysis For Seismic Design, A Guide for Practicing Engineers, *NEHRP Seismic Design Technical Brief No. 4*, Applied Technology Council (ATC), California.
- [45] **Chen, W. F.**, 2000: Structural stability: from theory to practice. *Engineering Structures*. Vol. **22**, pp. 116-122.
- [46] **Yu-Rong, L., Tao, Q., and Bin-Nan, S.**, 2006: Elastic-plastic study on high building with SRC transferring story. *Journal of Zhejiang University SCIENCE A*. Vol. **7**, no. 3, pp. 407-414.
- [47] **Goel, R. K., and Chopra, A. K.**, 2005: Extension of Modal Pushover Analysis to Compute Member Forces. *Earthquake Spectra*. Vol. **21**, no. 1, pp. 125-139.
- [48] **NIST GCR 10-917-9**, 2010. Applicability of Nonlinear Multiple-Degree-of-Freedom Modeling for Design, *NEHRP Consultants Joint Venture*, Applied Technology Council (ATC), California.
- [49] **Clough, R. W., and Penzien, J.**, 1995. *Dynamics of Structures*, ISBN: **9780070113923**, Computers & Structures, Inc., Publication, Berkeley, U.S.A.
- [50] **Chopra, A. K.**, 1995. *Dynamics of Structures: Theory and Applications to Earthquake Engineering*, ISBN: **0138552142**, Prentice Hall Publication, New Jersey.
- [51] **Bozorgnia, Y., and Bertero, V. V.**, 2004. *From Engineering Seismology to Performance-Based Engineering*, ISBN: **9780203486245**, CRC Press LLC Publication.

- [52] **Gülkan, P., and Sözen, M. A.**, 1974: Inelastic Responses of Reinforced Concrete Structures to Earthquake Motions. *ACI Journal*. Vol. **71**, no. 12, pp. 604-610.
- [53] **Lopez-Menjivar, M. A., and Pinho, R.**, 2004. A review of existing pushover methods for 2-D reinforced concrete buildings, *An Individual Study Submitted in Partial Fulfillment of the Requirements for the PhD Degree*, Rose School, Pavia, Italy.
- [54] **Krawinkler, H., and Seneviratna, G. D. P. K.**, 1998: Pros and cons analysis of seismic evaluation. *Engineering Structures*. Vol. **20**, no. 4-6, pp. 452-464.
- [55] **FEMA 273**, 1997. Nehrp Guidelines For The Seismic Rehabilitation Of Buildings, *Federal Emergency Management Agency*, Washington, D.C.
- [56] **Fajfar, P.**, 2000: A Nonlinear Analysis Method for Performance Based Seismic Design. *Earthquake Spectra*. Vol. **16**, no. 3, pp. 573-592.
- [57] **Chopra, A. K., and Goel, R. K.**, 2001. A Modal Pushover Analysis Procedure to Estimate Seismic Demands for Buildings: Theory and Preliminary Evaluation, *Pacific Earthquake Engineering Research Center (PEER) Report, CMS-9812531*, University of California, Berkeley.
- [58] **Goel, R. K., and Chopra, A. K.**, 2004: Evaluation of Modal and FEMA Pushover Analyses: SAC Buildings. *Earthquake Spectra*. Vol. **20**, no. 1, pp. 225-254.
- [59] **Montez, E. H., Kwon, O. S., and Aschheim, M. A.**, 2004: An Energy-Based Formulation For First And Multiple-mode Nonlinear Static (Pushover) Analyses. *Journal of Earthquake Engineering*. Vol. **8**, no. 1, pp. 69-88.
- [60] **Priestley, M. J. N.**, 2000: Performance Based Seismic Design. Proceedings of the Twelfth World Conference on Earthquake Engineering. No. 2109, Auckland, New Zealand.
- [61] **Medhekar, M. S., and Kennedy, D. J. L.**, 2000: Displacement-based seismic design of buildings—theory. *Engineering Structures*. Vol. **22**, pp. 201-209.
- [62] **Priestley, M. J. N.**, 2003: *Myths and Fallacies in Earthquake Engineering, Revisited Engineering Structures*, ISBN: **88-7358-009-2**, IUSS Press Publication, Italy.
- [63] **Stefano, M. D., and Pintuchhi, B.**, 2008: A review of research on seismic behaviour of irregular building structures since 2002. *Bulletin of Engineering*. Vol. **6**, pp. 285-303.
- [64] **Tso, W. K., and Moghadam, A. S.**, 1998: Pushover procedure for seismic analysis of buildings. *Structural Engineering and Materials*. Vol. **1**, no. 3, pp. 337-344.
- [65] **Fajfar, P., Marusic, D., and Perus, I.**, 2005: Torsional Effects In The Pushover-Based Seismic Analysis Of Buildings. *Journal of Earthquake Engineering*. Vol. **9**, no. 6, pp. 831-854.

- [66] **Kappos, A. J., and Penelis, Gr. G.**, 2000: 3d Pushover Analysis: The Issue Of Torsion. Proceedings of the Twelfth World Conference on Earthquake Engineering. No. 2109, Auckland, New Zealand.
- [67] **Pecker, A.**, 2003: *Advanced Earthquake Engineering Analysis*, ISBN: 3211742131, SpringerWien Publication, NewYork.
- [68] **Izzuddin, B. A., and Smith, D. L.**, 2000: Efficient nonlinear analysis of elasto-plastic 3D R/C frames using adaptive techniques. *Computers and Structures*. Vol. 78, no. 4, pp. 549-573.
- [69] **Aydinoğlu, N., and Önem, G.**, 2008: Nonlinear performance assessment of bridges with Incremental Response Spectrum Analysis (IRSA) procedure. *Computational Structural Dynamics and Earthquake Engineering*. Ch.25, pp. 393-400.
- [70] **Aydinoğlu, N.**, 2007: A Response Spectrum-Based Nonlinear Assessment Tool For Practice: Incremental Response Spectrum Analysis (Irsa). *ISET Journal of Earthquake Technology*. Vol. 44, no. 1, pp. 169-192.
- [71] **Pinho, R., and Antoniou, S.**, 2005: A displacement-based adaptive pushover algorithm for assessment of vertically irregular frames. Proceedings of the Fourth European Workshop on the Seismic Behaviour of Irregular and Complex Structures, Thessaloniki, Greece.
- [72] **Pourscha, M., Khoshnoudian, F., and Moghadam, A. S.**, 2009: A consecutive modal pushover procedure for estimating the seismic demands of tall buildings. *Engineering Structures*. Vol. 31, pp. 591-599.
- [73] **McKenna, F., Fenves, G. L., Filippou, F. C., & Mazzoni, S.** (2006). OpenSees Command Language Manual.
- [74] **Zadeh, M. S., and Saïidi, M. S.**, 2007. Pre-test Analytical Studies of NEESR-SG 4-Span Bridge Model Using OpenSees, *Center of Civil Engineering Earthquake Research Report, CCEER-07-3*, Reno, Nevada.
- [75] **Meloa, J., Fernandes, C., Varuma, H., Rodrigues, H., Costa, A., Arêde, A.**, 2011: Numerical modelling of the cyclic behaviour of RC elements built with plain reinforcing bars. *Engineering Structures*. Vol. 33, pp. 273-286.
- [76] **Stratan, A., and Fajfar, P.**, 2002. Influence Of Modelling Assumptions And Analysis Procedure On The Seismic Evaluation Of Reinforced Concrete Gld Frames, *IKPIR Laboratory Technical Report*, Ljubljana.
- [77] **Stratan, A., and Fajfar, P.**, 2003. Seismic Assessment Of The Spear Test Structure, *IKPIR Laboratory Technical Report*, Ljubljana.
- [78] **Ludovico, M.D.**, 2006. Comparative Assessment Of Seismic Rehabilitation Techniques On The Full Scale Spear Structure, *PhD Thesis*, University Of Naples Federico II.
- [79] **Thao, Y.**, (2006). XTRACT, *Imbsen*, from <http://www.imbsen.com/xtract.htm>.
- [80] **Mander, J. B., Priestley, J. N., Park, R.**, 1988: Theoretical stress-strain model for confined concrete. *Journal of Structural Engineering*. Vol. 114, no. 8, pp. 1804-1826.

[81] **Eurocode 8**, 2004. Design of structures for earthquake resistance, *British Standards*, Washington, D.C.

APPENDICES

APPENDIX A.1 : 1.15g scaled artificial Montenegro Earthquake Record.

APPENDIX A.1

Table A.1 : 1.15g scaled artificial Montenegro Earthquake Record.

Longitudinal Direction		Transverse Direction	
Time	Acc (g)	Time	Acc (g)
0.01	-9.39E-02	0.01	1.50E-02
0.02	-1.03E-03	0.02	-3.18E-02
0.03	5.06E-02	0.03	-5.29E-02
0.04	2.16E-02	0.04	-5.81E-02
0.05	1.29E-02	0.05	-8.13E-02
0.06	3.38E-02	0.06	-1.04E-01
0.07	4.21E-02	0.07	-9.39E-02
0.08	2.23E-02	0.08	-5.61E-02
0.09	7.22E-03	0.09	-2.92E-02
0.1	3.19E-02	0.1	-3.63E-02
0.11	8.05E-02	0.11	-6.50E-02
0.12	1.05E-01	0.12	-8.24E-02
0.13	1.02E-01	0.13	-6.33E-02
0.14	9.91E-02	0.14	-1.71E-02
0.15	1.03E-01	0.15	1.43E-02
0.16	1.11E-01	0.16	4.11E-03
0.17	1.22E-01	0.17	-2.17E-02
0.18	1.26E-01	0.18	-2.37E-02
0.19	1.20E-01	0.19	-1.10E-02
0.2	1.09E-01	0.2	-2.23E-02
0.21	9.65E-02	0.21	-5.50E-02
0.22	8.27E-02	0.22	-6.55E-02
0.23	7.58E-02	0.23	-3.69E-02
0.24	8.11E-02	0.24	-7.02E-03
0.25	8.62E-02	0.25	-1.29E-02
0.26	7.69E-02	0.26	-3.53E-02
0.27	6.61E-02	0.27	-2.83E-02
0.28	8.42E-02	0.28	1.11E-02
0.29	1.29E-01	0.29	4.13E-02
0.3	1.55E-01	0.3	3.77E-02
0.31	1.35E-01	0.31	1.20E-02
0.32	1.00E-01	0.32	-1.24E-02
0.33	9.13E-02	0.33	-2.11E-02
0.34	1.06E-01	0.34	-8.61E-03
0.35	1.08E-01	0.35	8.96E-03
0.36	8.78E-02	0.36	8.17E-03
0.37	8.55E-02	0.37	-1.18E-02
0.38	1.15E-01	0.38	-2.15E-02
0.39	1.25E-01	0.39	-7.23E-03
0.4	6.46E-02	0.4	2.48E-03

Table A.1 (continued) : 1.15g scaled artificial Montenegro Earthquake Record.

Longitudinal Direction		Transverse Direction	
Time	Acc (g)	Time	Acc (g)
0.41	-2.36E-02	0.41	-1.41E-02
0.42	-4.85E-02	0.42	-2.63E-02
0.43	-1.29E-03	0.43	-1.07E-03
0.44	2.55E-02	0.44	3.39E-02
0.45	-1.99E-02	0.45	3.30E-02
0.46	-7.37E-02	0.46	-5.19E-04
0.47	-6.67E-02	0.47	-2.15E-02
0.48	-3.23E-02	0.48	-7.60E-03
0.49	-4.18E-02	0.49	2.03E-02
0.5	-8.70E-02	0.5	2.58E-02
0.51	-9.91E-02	0.51	5.63E-03
0.52	-6.10E-02	0.52	-6.89E-03
0.53	-3.49E-02	0.53	1.53E-02
0.54	-7.21E-02	0.54	5.77E-02
0.55	-1.41E-01	0.55	9.04E-02
0.56	-1.70E-01	0.56	1.01E-01
0.57	-1.37E-01	0.57	1.05E-01
0.58	-8.96E-02	0.58	1.17E-01
0.59	-8.96E-02	0.59	1.29E-01
0.6	-1.17E-01	0.6	1.20E-01
0.61	-1.10E-01	0.61	8.23E-02
0.62	-4.97E-02	0.62	3.78E-02
0.63	2.63E-03	0.63	9.91E-03
0.64	4.51E-03	0.64	-1.54E-02
0.65	-1.69E-02	0.65	-6.14E-02
0.66	-1.27E-02	0.66	-1.10E-01
0.67	2.40E-02	0.67	-1.17E-01
0.68	6.29E-02	0.68	-8.96E-02
0.69	6.72E-02	0.69	-8.09E-02
0.7	1.75E-02	0.7	-1.03E-01
0.71	-6.37E-02	0.71	-1.10E-01
0.72	-1.19E-01	0.72	-8.87E-02
0.73	-1.18E-01	0.73	-6.92E-02
0.74	-9.57E-02	0.74	-7.23E-02
0.75	-1.03E-01	0.75	-8.87E-02
0.76	-1.32E-01	0.76	-1.16E-01
0.77	-1.46E-01	0.77	-1.51E-01
0.78	-1.40E-01	0.78	-1.79E-01
0.79	-1.32E-01	0.79	-1.90E-01
0.8	-1.12E-01	0.8	-2.03E-01
0.81	-5.43E-02	0.81	-2.23E-01
0.82	2.63E-02	0.82	-2.25E-01
0.83	9.22E-02	0.83	-2.12E-01

Table A.1 (continued) : 1.15g scaled artificial Montenegro Earthquake Record.

Longitudinal Direction		Transverse Direction	
Time	Acc (g)	Time	Acc (g)
0.84	1.28E-01	0.84	-2.10E-01
0.85	1.50E-01	0.85	-2.09E-01
0.86	1.70E-01	0.86	-1.83E-01
0.87	1.90E-01	0.87	-1.53E-01
0.88	2.14E-01	0.88	-1.40E-01
0.89	2.44E-01	0.89	-1.20E-01
0.9	2.69E-01	0.9	-8.62E-02
0.91	2.66E-01	0.91	-9.57E-02
0.92	2.37E-01	0.92	-1.59E-01
0.93	2.11E-01	0.93	-2.01E-01
0.94	2.13E-01	0.94	-1.77E-01
0.95	2.49E-01	0.95	-1.53E-01
0.96	2.98E-01	0.96	-1.74E-01
0.97	3.27E-01	0.97	-1.83E-01
0.98	3.12E-01	0.98	-1.33E-01
0.99	2.62E-01	0.99	-8.87E-02
1	1.97E-01	1	-8.96E-02
1.01	1.37E-01	1.01	-7.73E-02
1.02	9.13E-02	1.02	-5.90E-03
1.03	6.23E-02	1.03	4.96E-02
1.04	3.90E-02	1.04	2.19E-02
1.05	-1.47E-04	1.05	-3.87E-02
1.06	-6.63E-02	1.06	-5.01E-02
1.07	-1.41E-01	1.07	-2.64E-02
1.08	-1.95E-01	1.08	-2.53E-02
1.09	-2.25E-01	1.09	-4.67E-02
1.1	-2.54E-01	1.1	-4.90E-02
1.11	-2.97E-01	1.11	-3.13E-02
1.12	-3.45E-01	1.12	-2.83E-02
1.13	-3.57E-01	1.13	-4.10E-02
1.14	-3.13E-01	1.14	-3.63E-02
1.15	-2.53E-01	1.15	-2.23E-02
1.16	-2.37E-01	1.16	-4.04E-02
1.17	-2.59E-01	1.17	-8.13E-02
1.18	-2.55E-01	1.18	-9.04E-02
1.19	-1.98E-01	1.19	-6.54E-02
1.2	-1.51E-01	1.2	-5.42E-02
1.21	-1.74E-01	1.21	-7.16E-02
1.22	-2.26E-01	1.22	-7.90E-02
1.23	-2.30E-01	1.23	-5.59E-02
1.24	-1.85E-01	1.24	-2.65E-02
1.25	-1.51E-01	1.25	-2.67E-03
1.26	-1.42E-01	1.26	3.26E-02

Table A.1 (continued) : 1.15g scaled artificial Montenegro Earthquake Record.

Longitudinal Direction		Transverse Direction	
Time	Acc (g)	Time	Acc (g)
1.27	-1.10E-01	1.27	7.92E-02
1.28	-3.43E-02	1.28	1.17E-01
1.29	6.45E-02	1.29	1.53E-01
1.3	1.57E-01	1.3	1.90E-01
1.31	2.32E-01	1.31	1.99E-01
1.32	2.81E-01	1.32	1.68E-01
1.33	3.04E-01	1.33	1.38E-01
1.34	3.26E-01	1.34	1.43E-01
1.35	3.57E-01	1.35	1.67E-01
1.36	3.72E-01	1.36	1.87E-01
1.37	3.41E-01	1.37	1.99E-01
1.38	2.92E-01	1.38	1.90E-01
1.39	2.69E-01	1.39	1.49E-01
1.4	2.59E-01	1.4	1.13E-01
1.41	2.19E-01	1.41	1.17E-01
1.42	1.55E-01	1.42	1.17E-01
1.43	1.20E-01	1.43	7.14E-02
1.44	1.23E-01	1.44	2.70E-02
1.45	1.23E-01	1.45	6.83E-02
1.46	1.02E-01	1.46	1.63E-01
1.47	8.37E-02	1.47	2.23E-01
1.48	6.99E-02	1.48	2.38E-01
1.49	3.24E-02	1.49	2.62E-01
1.5	-2.59E-02	1.5	2.90E-01
1.51	-6.57E-02	1.51	2.83E-01
1.52	-8.23E-02	1.52	2.58E-01
1.53	-1.11E-01	1.53	2.55E-01
1.54	-1.67E-01	1.54	2.64E-01
1.55	-2.21E-01	1.55	2.59E-01
1.56	-2.68E-01	1.56	2.49E-01
1.57	-3.11E-01	1.57	2.22E-01
1.58	-3.25E-01	1.58	1.47E-01
1.59	-2.95E-01	1.59	3.46E-02
1.6	-2.70E-01	1.6	-4.63E-02
1.61	-2.96E-01	1.61	-7.18E-02
1.62	-3.43E-01	1.62	-7.63E-02
1.63	-3.57E-01	1.63	-8.02E-02
1.64	-3.40E-01	1.64	-5.50E-02
1.65	-3.19E-01	1.65	-1.21E-02
1.66	-2.98E-01	1.66	8.35E-03
1.67	-2.74E-01	1.67	-5.70E-03
1.68	-2.59E-01	1.68	-3.21E-02
1.69	-2.61E-01	1.69	-6.52E-02

Table A.1 (continued) : 1.15g scaled artificial Montenegro Earthquake Record.

Longitudinal Direction		Transverse Direction	
Time	Acc (g)	Time	Acc (g)
1.7	-2.62E-01	1.7	-7.44E-02
1.71	-2.62E-01	1.71	-2.37E-02
1.72	-2.58E-01	1.72	5.70E-02
1.73	-2.18E-01	1.73	8.96E-02
1.74	-1.39E-01	1.74	6.16E-02
1.75	-8.87E-02	1.75	3.51E-02
1.76	-1.05E-01	1.76	3.63E-02
1.77	-1.26E-01	1.77	3.36E-02
1.78	-7.45E-02	1.78	2.20E-02
1.79	3.79E-02	1.79	6.31E-02
1.8	1.55E-01	1.8	1.76E-01
1.81	2.38E-01	1.81	2.90E-01
1.82	2.70E-01	1.82	3.36E-01
1.83	2.41E-01	1.83	3.10E-01
1.84	1.95E-01	1.84	2.64E-01
1.85	1.83E-01	1.85	2.43E-01
1.86	2.09E-01	1.86	2.52E-01
1.87	2.25E-01	1.87	2.51E-01
1.88	2.25E-01	1.88	1.89E-01
1.89	2.34E-01	1.89	7.93E-02
1.9	2.46E-01	1.9	-7.52E-03
1.91	2.37E-01	1.91	2.96E-03
1.92	2.18E-01	1.92	1.00E-01
1.93	2.01E-01	1.93	2.06E-01
1.94	1.73E-01	1.94	2.06E-01
1.95	1.60E-01	1.95	6.63E-02
1.96	1.97E-01	1.96	-1.57E-01
1.97	2.50E-01	1.97	-3.50E-01
1.98	2.47E-01	1.98	-4.37E-01
1.99	2.02E-01	1.99	-4.08E-01
2	1.97E-01	2	-3.32E-01
2.01	2.45E-01	2.01	-2.97E-01
2.02	2.58E-01	2.02	-3.13E-01
2.03	1.89E-01	2.03	-3.19E-01
2.04	1.12E-01	2.04	-2.92E-01
2.05	9.04E-02	2.05	-2.77E-01
2.06	9.13E-02	2.06	-2.85E-01
2.07	7.21E-02	2.07	-2.65E-01
2.08	5.69E-02	2.08	-2.11E-01
2.09	8.96E-02	2.09	-2.01E-01
2.1	1.65E-01	2.1	-2.61E-01
2.11	2.22E-01	2.11	-3.18E-01
2.12	2.06E-01	2.12	-3.20E-01

Table A.1 (continued) : 1.15g scaled artificial Montenegro Earthquake Record.

Longitudinal Direction		Transverse Direction	
Time	Acc (g)	Time	Acc (g)
2.13	1.06E-01	2.13	-3.04E-01
2.14	-3.16E-02	2.14	-3.01E-01
2.15	-1.23E-01	2.15	-2.73E-01
2.16	-1.37E-01	2.16	-2.09E-01
2.17	-1.54E-01	2.17	-1.56E-01
2.18	-2.46E-01	2.18	-1.43E-01
2.19	-3.47E-01	2.19	-1.37E-01
2.2	-3.34E-01	2.2	-1.04E-01
2.21	-2.08E-01	2.21	-5.27E-02
2.22	-1.00E-01	2.22	8.52E-03
2.23	-7.73E-02	2.23	9.39E-02
2.24	-7.88E-02	2.24	2.30E-01
2.25	-4.86E-02	2.25	4.06E-01
2.26	-2.18E-02	2.26	5.20E-01
2.27	-3.41E-02	2.27	4.66E-01
2.28	-6.90E-02	2.28	3.07E-01
2.29	-1.17E-01	2.29	2.50E-01
2.3	-1.87E-01	2.3	3.83E-01
2.31	-2.65E-01	2.31	5.81E-01
2.32	-3.37E-01	2.32	7.28E-01
2.33	-4.12E-01	2.33	8.36E-01
2.34	-4.33E-01	2.34	8.78E-01
2.35	-2.92E-01	2.35	7.23E-01
2.36	-2.09E-03	2.36	3.89E-01
2.37	2.90E-01	2.37	9.13E-02
2.38	4.87E-01	2.38	-4.77E-02
2.39	6.07E-01	2.39	-1.68E-01
2.4	6.45E-01	2.4	-4.38E-01
2.41	5.68E-01	2.41	-7.91E-01
2.42	4.63E-01	2.42	-9.74E-01
2.43	4.63E-01	2.43	-9.74E-01
2.44	4.77E-01	2.44	-7.69E-01
2.45	2.90E-01	2.45	-4.75E-01
2.46	-3.86E-02	2.46	-3.07E-01
2.47	-2.63E-01	2.47	-2.62E-01
2.48	-3.55E-01	2.48	-1.83E-01
2.49	-4.64E-01	2.49	-4.80E-04
2.5	-5.63E-01	2.5	1.37E-01
2.51	-5.16E-01	2.51	1.30E-01
2.52	-3.96E-01	2.52	1.12E-01
2.53	-3.98E-01	2.53	2.03E-01
2.54	-5.20E-01	2.54	2.54E-01
2.55	-5.90E-01	2.55	6.42E-02

Table A.1 (continued) : 1.15g scaled artificial Montenegro Earthquake Record.

Longitudinal Direction		Transverse Direction	
Time	Acc (g)	Time	Acc (g)
2.56	-5.54E-01	2.56	-2.73E-01
2.57	-4.38E-01	2.57	-4.85E-01
2.58	-1.70E-01	2.58	-4.64E-01
2.59	2.39E-01	2.59	-3.66E-01
2.6	5.19E-01	2.6	-3.43E-01
2.61	5.01E-01	2.61	-4.07E-01
2.62	4.35E-01	2.62	-4.61E-01
2.63	5.61E-01	2.63	-4.65E-01
2.64	7.50E-01	2.64	-4.72E-01
2.65	7.37E-01	2.65	-5.46E-01
2.66	5.65E-01	2.66	-6.48E-01
2.67	4.50E-01	2.67	-6.97E-01
2.68	5.04E-01	2.68	-6.58E-01
2.69	6.27E-01	2.69	-5.51E-01
2.7	6.72E-01	2.7	-4.09E-01
2.71	4.91E-01	2.71	-2.84E-01
2.72	7.39E-02	2.72	-2.15E-01
2.73	-3.24E-01	2.73	-2.12E-01
2.74	-4.33E-01	2.74	-2.40E-01
2.75	-3.63E-01	2.75	-2.42E-01
2.76	-3.76E-01	2.76	-1.84E-01
2.77	-4.17E-01	2.77	-1.10E-01
2.78	-2.47E-01	2.78	-8.06E-02
2.79	3.75E-02	2.79	-7.94E-02
2.8	9.57E-02	2.8	1.38E-02
2.81	-1.34E-01	2.81	2.69E-01
2.82	-3.63E-01	2.82	5.50E-01
2.83	-4.37E-01	2.83	6.69E-01
2.84	-4.43E-01	2.84	6.30E-01
2.85	-4.54E-01	2.85	6.68E-01
2.86	-4.38E-01	2.86	9.30E-01
2.87	-4.14E-01	2.87	9.22E-01
2.88	-3.98E-01	2.88	9.48E-01
2.89	-3.44E-01	2.89	9.65E-01
2.9	-2.33E-01	2.9	9.30E-01
2.91	-1.08E-01	2.91	1.00E+00
2.92	2.34E-02	2.92	7.15E-01
2.93	1.81E-01	2.93	4.48E-01
2.94	2.93E-01	2.94	3.28E-01
2.95	2.76E-01	2.95	3.02E-01
2.96	1.47E-01	2.96	3.98E-01
2.97	-2.60E-02	2.97	5.58E-01
2.98	-2.47E-01	2.98	6.02E-01

Table A.1 (continued) : 1.15g scaled artificial Montenegro Earthquake Record.

Longitudinal Direction		Transverse Direction	
Time	Acc (g)	Time	Acc (g)
2.99	-4.51E-01	2.99	4.63E-01
3	-4.79E-01	3	2.81E-01
3.01	-3.03E-01	3.01	2.42E-01
3.02	-1.21E-01	3.02	3.63E-01
3.03	-5.08E-02	3.03	5.16E-01
3.04	-1.97E-02	3.04	6.10E-01
3.05	-1.26E-02	3.05	6.51E-01
3.06	-1.03E-01	3.06	6.34E-01
3.07	-2.18E-01	3.07	5.43E-01
3.08	-1.95E-01	3.08	4.28E-01
3.09	-6.55E-02	3.09	3.32E-01
3.1	8.78E-03	3.1	2.10E-01
3.11	2.86E-02	3.11	2.10E-02
3.12	1.32E-01	3.12	-1.91E-01
3.13	3.21E-01	3.13	-3.36E-01
3.14	4.62E-01	3.14	-4.12E-01
3.15	4.98E-01	3.15	-4.55E-01
3.16	4.69E-01	3.16	-4.53E-01
3.17	3.95E-01	3.17	-3.83E-01
3.18	2.90E-01	3.18	-3.17E-01
3.19	2.01E-01	3.19	-3.22E-01
3.2	1.39E-01	3.2	-3.30E-01
3.21	6.85E-02	3.21	-2.70E-01
3.22	-1.51E-02	3.22	-1.72E-01
3.23	-8.55E-02	3.23	-8.78E-02
3.24	-1.37E-01	3.24	7.40E-03
3.25	-1.42E-01	3.25	1.06E-01
3.26	-3.37E-02	3.26	1.23E-01
3.27	1.74E-01	3.27	3.38E-02
3.28	3.38E-01	3.28	-4.98E-02
3.29	3.72E-01	3.29	-4.55E-02
3.3	3.43E-01	3.3	-1.67E-02
3.31	2.92E-01	3.31	-3.09E-02
3.32	1.36E-01	3.32	-5.28E-02
3.33	-1.30E-01	3.33	-7.47E-02
3.34	-3.19E-01	3.34	-1.62E-01
3.35	-3.23E-01	3.35	-2.84E-01
3.36	-2.94E-01	3.36	-3.10E-01
3.37	-4.02E-01	3.37	-2.03E-01
3.38	-5.73E-01	3.38	-6.49E-02
3.39	-6.30E-01	3.39	3.21E-02
3.4	-5.78E-01	3.4	9.65E-02
3.41	-5.54E-01	3.41	1.26E-01

Table A.1 (continued) : 1.15g scaled artificial Montenegro Earthquake Record.

Longitudinal Direction		Transverse Direction	
Time	Acc (g)	Time	Acc (g)
3.42	-5.68E-01	3.42	1.10E-01
3.43	-5.33E-01	3.43	1.08E-01
3.44	-4.69E-01	3.44	1.78E-01
3.45	-4.75E-01	3.45	2.69E-01
3.46	-5.26E-01	3.46	3.11E-01
3.47	-5.14E-01	3.47	3.55E-01
3.48	-4.29E-01	3.48	4.43E-01
3.49	-3.69E-01	3.49	4.67E-01
3.5	-3.50E-01	3.5	3.42E-01
3.51	-2.91E-01	3.51	1.90E-01
3.52	-1.79E-01	3.52	1.93E-01
3.53	-7.58E-02	3.53	2.91E-01
3.54	5.04E-02	3.54	2.97E-01
3.55	2.22E-01	3.55	2.05E-01
3.56	3.22E-01	3.56	1.93E-01
3.57	3.07E-01	3.57	3.02E-01
3.58	3.59E-01	3.58	3.88E-01
3.59	5.35E-01	3.59	3.42E-01
3.6	7.78E-01	3.6	2.29E-01
3.61	1.00E+00	3.61	1.32E-01
3.62	8.34E-01	3.62	5.94E-02
3.63	7.72E-01	3.63	-1.09E-02
3.64	7.79E-01	3.64	-5.24E-02
3.65	7.60E-01	3.65	-7.77E-02
3.66	7.12E-01	3.66	-1.45E-01
3.67	5.59E-01	3.67	-2.81E-01
3.68	3.27E-01	3.68	-4.27E-01
3.69	1.11E-01	3.69	-5.34E-01
3.7	-3.77E-02	3.7	-5.77E-01
3.71	-1.29E-01	3.71	-5.34E-01
3.72	-1.92E-01	3.72	-3.89E-01
3.73	-2.61E-01	3.73	-2.30E-01
3.74	-3.00E-01	3.74	-2.05E-01
3.75	-2.78E-01	3.75	-3.42E-01
3.76	-2.20E-01	3.76	-4.77E-01
3.77	-1.50E-01	3.77	-4.68E-01
3.78	-5.83E-02	3.78	-3.86E-01
3.79	3.90E-02	3.79	-3.58E-01
3.8	1.13E-01	3.8	-3.70E-01
3.81	1.67E-01	3.81	-3.23E-01
3.82	2.21E-01	3.82	-2.44E-01
3.83	2.57E-01	3.83	-2.30E-01
3.84	2.25E-01	3.84	-2.68E-01

Table A.1 (continued) : 1.15g scaled artificial Montenegro Earthquake Record.

Longitudinal Direction		Transverse Direction	
Time	Acc (g)	Time	Acc (g)
3.85	1.20E-01	3.85	-2.57E-01
3.86	3.30E-02	3.86	-1.87E-01
3.87	3.78E-02	3.87	-1.55E-01
3.88	1.13E-01	3.88	-1.80E-01
3.89	1.83E-01	3.89	-2.00E-01
3.9	2.12E-01	3.9	-1.93E-01
3.91	2.16E-01	3.91	-2.00E-01
3.92	2.40E-01	3.92	-2.21E-01
3.93	2.86E-01	3.93	-2.23E-01
3.94	3.18E-01	3.94	-2.25E-01
3.95	3.13E-01	3.95	-2.61E-01
3.96	2.82E-01	3.96	-2.90E-01
3.97	2.32E-01	3.97	-2.43E-01
3.98	1.67E-01	3.98	-1.36E-01
3.99	9.57E-02	3.99	-4.74E-02
4	2.70E-02	4	-1.87E-02
4.01	-5.88E-02	4.01	-2.82E-02
4.02	-1.88E-01	4.02	-4.25E-02
4.03	-3.25E-01	4.03	-6.71E-02
4.04	-3.74E-01	4.04	-1.30E-01
4.05	-2.87E-01	4.05	-2.43E-01
4.06	-1.51E-01	4.06	-3.70E-01
4.07	-1.05E-01	4.07	-4.49E-01
4.08	-1.87E-01	4.08	-4.72E-01
4.09	-2.89E-01	4.09	-4.97E-01
4.1	-2.97E-01	4.1	-5.47E-01
4.11	-2.44E-01	4.11	-5.61E-01
4.12	-2.54E-01	4.12	-5.13E-01
4.13	-3.53E-01	4.13	-4.72E-01
4.14	-4.41E-01	4.14	-4.89E-01
4.15	-4.57E-01	4.15	-4.88E-01
4.16	-4.56E-01	4.16	-3.85E-01
4.17	-4.95E-01	4.17	-2.22E-01
4.18	-5.39E-01	4.18	-1.06E-01
4.19	-5.40E-01	4.19	-6.30E-02
4.2	-5.05E-01	4.2	-3.57E-02
4.21	-4.75E-01	4.21	5.86E-03
4.22	-4.76E-01	4.22	4.96E-02
4.23	-5.22E-01	4.23	1.32E-01
4.24	-5.67E-01	4.24	2.92E-01
4.25	-5.35E-01	4.25	4.84E-01
4.26	-4.23E-01	4.26	6.23E-01
4.27	-3.28E-01	4.27	7.20E-01

Table A.1 (continued) : 1.15g scaled artificial Montenegro Earthquake Record.

Longitudinal Direction		Transverse Direction	
Time	Acc (g)	Time	Acc (g)
4.28	-2.94E-01	4.28	8.28E-01
4.29	-2.49E-01	4.29	9.30E-01
4.3	-1.43E-01	4.3	9.57E-01
4.31	-5.49E-02	4.31	9.13E-01
4.32	-5.21E-02	4.32	8.78E-01
4.33	-8.32E-02	4.33	8.55E-01
4.34	-6.64E-02	4.34	7.79E-01
4.35	-2.57E-02	4.35	7.00E-01
4.36	-2.18E-02	4.36	7.28E-01
4.37	-5.12E-02	4.37	8.27E-01
4.38	-5.38E-02	4.38	8.35E-01
4.39	-2.80E-03	4.39	6.81E-01
4.4	7.23E-02	4.4	4.58E-01
4.41	1.36E-01	4.41	2.73E-01
4.42	1.97E-01	4.42	1.68E-01
4.43	2.89E-01	4.43	1.44E-01
4.44	3.90E-01	4.44	1.72E-01
4.45	4.43E-01	4.45	1.81E-01
4.46	4.37E-01	4.46	1.58E-01
4.47	4.17E-01	4.47	1.50E-01
4.48	3.91E-01	4.48	1.51E-01
4.49	3.27E-01	4.49	8.22E-02
4.5	2.43E-01	4.5	-5.96E-02
4.51	2.12E-01	4.51	-1.80E-01
4.52	2.41E-01	4.52	-2.51E-01
4.53	2.47E-01	4.53	-3.30E-01
4.54	2.03E-01	4.54	-4.23E-01
4.55	1.85E-01	4.55	-4.79E-01
4.56	2.36E-01	4.56	-4.98E-01
4.57	2.85E-01	4.57	-5.02E-01
4.58	2.85E-01	4.58	-4.75E-01
4.59	2.85E-01	4.59	-4.25E-01
4.6	3.26E-01	4.6	-3.90E-01
4.61	3.66E-01	4.61	-3.43E-01
4.62	3.55E-01	4.62	-2.10E-01
4.63	3.12E-01	4.63	-1.50E-02
4.64	2.98E-01	4.64	1.16E-01
4.65	3.40E-01	4.65	1.53E-01
4.66	4.24E-01	4.66	1.59E-01
4.67	5.21E-01	4.67	1.53E-01
4.68	5.84E-01	4.68	1.28E-01
4.69	5.78E-01	4.69	1.28E-01
4.7	5.46E-01	4.7	1.54E-01

Table A.1 (continued) : 1.15g scaled artificial Montenegro Earthquake Record.

Longitudinal Direction		Transverse Direction	
Time	Acc (g)	Time	Acc (g)
4.71	5.48E-01	4.71	1.04E-01
4.72	5.55E-01	4.72	-3.21E-02
4.73	4.79E-01	4.73	-1.20E-01
4.74	3.28E-01	4.74	-8.78E-02
4.75	2.07E-01	4.75	-4.30E-02
4.76	1.78E-01	4.76	-6.97E-02
4.77	1.76E-01	4.77	-1.06E-01
4.78	1.17E-01	4.78	-9.65E-02
4.79	-4.30E-03	4.79	-8.12E-02
4.8	-1.32E-01	4.8	-1.10E-01
4.81	-2.11E-01	4.81	-1.49E-01
4.82	-2.37E-01	4.82	-1.57E-01
4.83	-2.76E-01	4.83	-1.38E-01
4.84	-3.98E-01	4.84	-1.30E-01
4.85	-5.70E-01	4.85	-1.56E-01
4.86	-6.70E-01	4.86	-1.78E-01
4.87	-6.60E-01	4.87	-1.07E-01
4.88	-6.39E-01	4.88	5.76E-02
4.89	-6.89E-01	4.89	1.71E-01
4.9	-7.60E-01	4.9	1.50E-01
4.91	-7.77E-01	4.91	7.67E-02
4.92	-7.43E-01	4.92	4.03E-02
4.93	-6.88E-01	4.93	-1.69E-02
4.94	-6.19E-01	4.94	-1.38E-01
4.95	-5.58E-01	4.95	-2.57E-01
4.96	-5.31E-01	4.96	-2.96E-01
4.97	-5.05E-01	4.97	-2.77E-01
4.98	-4.33E-01	4.98	-2.33E-01
4.99	-3.40E-01	4.99	-1.88E-01
5	-2.80E-01	5	-1.85E-01
5.01	-2.41E-01	5.01	-2.24E-01
5.02	-1.71E-01	5.02	-2.04E-01
5.03	-9.22E-02	5.03	-8.50E-02
5.04	-7.37E-02	5.04	3.87E-03
5.05	-1.10E-01	5.05	-3.63E-02
5.06	-1.34E-01	5.06	-9.83E-02
5.07	-1.11E-01	5.07	-4.96E-02
5.08	-6.70E-02	5.08	4.35E-02
5.09	-1.23E-03	5.09	6.43E-02
5.1	8.30E-02	5.1	4.63E-02
5.11	1.43E-01	5.11	7.66E-02
5.12	1.48E-01	5.12	1.21E-01
5.13	1.51E-01	5.13	8.96E-02

Table A.1 (continued) : 1.15g scaled artificial Montenegro Earthquake Record.

Longitudinal Direction		Transverse Direction	
Time	Acc (g)	Time	Acc (g)
5.14	2.23E-01	5.14	-1.52E-02
5.15	3.50E-01	5.15	-1.19E-01
5.16	4.63E-01	5.16	-1.66E-01
5.17	5.25E-01	5.17	-1.47E-01
5.18	5.50E-01	5.18	-9.74E-02
5.19	5.54E-01	5.19	-7.78E-02
5.2	5.34E-01	5.2	-1.10E-01
5.21	4.90E-01	5.21	-1.43E-01
5.22	4.35E-01	5.22	-1.26E-01
5.23	3.66E-01	5.23	-7.64E-02
5.24	2.67E-01	5.24	-3.33E-02
5.25	1.48E-01	5.25	1.03E-02
5.26	4.67E-02	5.26	6.96E-02
5.27	-4.10E-03	5.27	1.25E-01
5.28	-1.01E-02	5.28	1.48E-01
5.29	-8.63E-03	5.29	1.29E-01
5.3	-2.50E-02	5.3	7.98E-02
5.31	-4.57E-02	5.31	4.08E-02
5.32	-5.29E-02	5.32	5.63E-02
5.33	-6.16E-02	5.33	1.04E-01
5.34	-9.39E-02	5.34	1.06E-01
5.35	-1.43E-01	5.35	5.93E-02
5.36	-1.97E-01	5.36	7.62E-02
5.37	-2.71E-01	5.37	2.10E-01
5.38	-3.78E-01	5.38	3.40E-01
5.39	-4.88E-01	5.39	3.40E-01
5.4	-5.51E-01	5.4	2.54E-01
5.41	-5.58E-01	5.41	2.10E-01
5.42	-5.30E-01	5.42	2.52E-01
5.43	-4.77E-01	5.43	3.41E-01
5.44	-4.10E-01	5.44	4.47E-01
5.45	-3.63E-01	5.45	5.37E-01
5.46	-3.37E-01	5.46	5.50E-01
5.47	-2.92E-01	5.47	4.83E-01
5.48	-2.02E-01	5.48	4.09E-01
5.49	-9.65E-02	5.49	3.65E-01
5.5	-2.89E-02	5.5	3.03E-01
5.51	-8.51E-03	5.51	2.13E-01
5.52	-1.03E-02	5.52	1.51E-01
5.53	-4.94E-03	5.53	1.30E-01
5.54	3.50E-02	5.54	6.94E-02
5.55	1.07E-01	5.55	-5.43E-02
5.56	1.68E-01	5.56	-1.66E-01

Table A.1 (continued) : 1.15g scaled artificial Montenegro Earthquake Record.

Longitudinal Direction		Transverse Direction	
Time	Acc (g)	Time	Acc (g)
5.57	1.97E-01	5.57	-2.14E-01
5.58	2.31E-01	5.58	-2.40E-01
5.59	2.89E-01	5.59	-2.74E-01
5.6	3.40E-01	5.6	-2.89E-01
5.63	3.79E-01	5.63	-3.80E-01
5.64	4.54E-01	5.64	-4.63E-01
5.65	5.55E-01	5.65	-5.56E-01
5.66	6.40E-01	5.66	-6.89E-01
5.67	6.74E-01	5.67	-8.38E-01
5.68	6.53E-01	5.68	-9.13E-01
5.69	6.12E-01	5.69	-8.96E-01
5.7	5.81E-01	5.7	-8.35E-01
5.71	5.50E-01	5.71	-8.08E-01
5.72	5.06E-01	5.72	-8.01E-01
5.73	4.57E-01	5.73	-7.78E-01
5.74	3.83E-01	5.74	-7.45E-01
5.75	2.55E-01	5.75	-7.34E-01
5.76	9.65E-02	5.76	-7.55E-01
5.77	-9.30E-03	5.77	-7.58E-01
5.78	-1.23E-02	5.78	-6.67E-01
5.79	4.91E-02	5.79	-4.67E-01
5.8	9.65E-02	5.8	-2.60E-01
5.81	9.39E-02	5.81	-1.65E-01
5.82	6.84E-02	5.82	-1.75E-01
5.83	7.00E-02	5.83	-1.75E-01
5.84	1.11E-01	5.84	-1.32E-01
5.85	1.64E-01	5.85	-1.25E-01
5.86	2.09E-01	5.86	-1.70E-01
5.87	2.51E-01	5.87	-1.50E-01
5.88	2.68E-01	5.88	3.22E-03
5.89	2.06E-01	5.89	1.84E-01
5.9	7.10E-02	5.9	2.57E-01
5.91	-3.58E-02	5.91	2.16E-01
5.92	-5.63E-02	5.92	1.67E-01
5.93	-6.27E-02	5.93	1.66E-01
5.94	-1.40E-01	5.94	2.01E-01
5.95	-2.44E-01	5.95	2.53E-01
5.96	-2.75E-01	5.96	3.17E-01
5.97	-2.23E-01	5.97	3.68E-01
5.98	-1.68E-01	5.98	3.77E-01
5.99	-1.55E-01	5.99	3.50E-01
6	-1.70E-01	6	3.04E-01
6.01	-1.70E-01	6.01	2.31E-01

Table A.1 (continued) : 1.15g scaled artificial Montenegro Earthquake Record.

Longitudinal Direction		Transverse Direction	
Time	Acc (g)	Time	Acc (g)
6.02	-1.32E-01	6.02	1.52E-01
6.03	-8.29E-02	6.03	1.26E-01
6.04	-9.22E-02	6.04	1.89E-01
6.05	-1.86E-01	6.05	2.81E-01
6.06	-2.99E-01	6.06	3.37E-01
6.07	-3.62E-01	6.07	3.64E-01
6.08	-3.83E-01	6.08	4.02E-01
6.09	-4.07E-01	6.09	4.02E-01
6.1	-4.44E-01	6.1	2.95E-01
6.11	-4.66E-01	6.11	1.14E-01
6.12	-4.43E-01	6.12	-3.33E-02
6.13	-3.45E-01	6.13	-8.78E-02
6.14	-1.77E-01	6.14	-4.78E-02
6.15	-1.96E-03	6.15	9.04E-02
6.16	9.83E-02	6.16	2.88E-01
6.17	1.03E-01	6.17	4.51E-01
6.18	3.47E-02	6.18	5.20E-01
6.19	-8.78E-02	6.19	5.36E-01
6.2	-2.07E-01	6.2	5.26E-01
6.21	-2.29E-01	6.21	4.56E-01
6.22	-1.43E-01	6.22	3.10E-01
6.23	-6.51E-02	6.23	1.69E-01
6.24	-6.37E-02	6.24	9.22E-02
6.25	-7.79E-02	6.25	6.62E-02
6.26	-3.17E-02	6.26	7.49E-02
6.27	4.65E-02	6.27	1.50E-01
6.28	1.11E-01	6.28	2.57E-01
6.29	1.70E-01	6.29	2.88E-01
6.3	2.27E-01	6.3	1.98E-01
6.31	2.43E-01	6.31	7.90E-02
6.32	2.30E-01	6.32	6.41E-03
6.33	2.42E-01	6.33	-1.17E-02
6.34	2.81E-01	6.34	-4.60E-03
6.35	2.72E-01	6.35	-7.84E-03
6.36	1.88E-01	6.36	-7.01E-02
6.37	1.02E-01	6.37	-1.82E-01
6.38	7.78E-02	6.38	-2.66E-01
6.39	9.30E-02	6.39	-2.82E-01
6.4	1.00E-01	6.4	-2.60E-01
6.41	8.87E-02	6.41	-2.16E-01
6.42	5.70E-02	6.42	-1.38E-01
6.43	5.66E-03	6.43	-8.54E-02
6.44	-2.22E-02	6.44	-1.47E-01

Table A.1 (continued) : 1.15g scaled artificial Montenegro Earthquake Record.

Longitudinal Direction		Transverse Direction	
Time	Acc (g)	Time	Acc (g)
6.45	2.50E-02	6.45	-2.78E-01
6.46	1.23E-01	6.46	-3.37E-01
6.47	1.87E-01	6.47	-2.72E-01
6.48	1.61E-01	6.48	-1.50E-01
6.49	7.90E-02	6.49	-2.66E-03
6.5	-1.63E-02	6.5	1.68E-01
6.51	-1.36E-01	6.51	3.03E-01
6.52	-2.70E-01	6.52	3.62E-01
6.53	-3.46E-01	6.53	3.99E-01
6.54	-3.26E-01	6.54	4.60E-01
6.55	-2.94E-01	6.55	4.87E-01
6.56	-3.21E-01	6.56	4.61E-01
6.57	-3.57E-01	6.57	4.58E-01
6.58	-3.23E-01	6.58	4.89E-01
6.59	-2.51E-01	6.59	4.57E-01
6.6	-2.12E-01	6.6	3.66E-01
6.61	-1.82E-01	6.61	3.29E-01
6.62	-8.57E-02	6.62	3.30E-01
6.63	5.09E-02	6.63	2.43E-01
6.64	1.35E-01	6.64	9.48E-02
6.65	1.43E-01	6.65	6.90E-02
6.66	1.36E-01	6.66	1.83E-01
6.67	1.57E-01	6.67	2.54E-01
6.68	1.93E-01	6.68	1.93E-01
6.69	2.23E-01	6.69	1.29E-01
6.7	2.36E-01	6.7	1.58E-01
6.71	2.30E-01	6.71	2.24E-01
6.72	2.04E-01	6.72	2.37E-01
6.73	1.77E-01	6.73	2.03E-01
6.74	1.64E-01	6.74	1.89E-01
6.75	1.77E-01	6.75	2.44E-01
6.76	1.95E-01	6.76	3.39E-01
6.77	1.96E-01	6.77	3.54E-01
6.78	1.77E-01	6.78	2.04E-01
6.79	1.74E-01	6.79	-2.87E-02
6.8	1.94E-01	6.8	-2.01E-01
6.81	1.83E-01	6.81	-2.94E-01
6.82	1.13E-01	6.82	-3.86E-01
6.83	6.10E-02	6.83	-4.73E-01
6.84	1.02E-01	6.84	-4.75E-01
6.85	1.59E-01	6.85	-3.78E-01
6.86	1.03E-01	6.86	-2.85E-01
6.87	-3.80E-02	6.87	-2.85E-01

Table A.1 (continued) : 1.15g scaled artificial Montenegro Earthquake Record.

Longitudinal Direction		Transverse Direction	
Time	Acc (g)	Time	Acc (g)
6.88	-1.16E-01	6.88	-3.83E-01
6.89	-8.78E-02	6.89	-4.98E-01
6.9	-6.57E-02	6.9	-5.61E-01
6.91	-9.91E-02	6.91	-5.71E-01
6.92	-8.87E-02	6.92	-5.90E-01
6.93	2.45E-02	6.93	-6.07E-01
6.94	1.17E-01	6.94	-5.28E-01
6.95	6.82E-02	6.95	-3.30E-01
6.96	-4.53E-02	6.96	-1.47E-01
6.97	-7.19E-02	6.97	-7.70E-02
6.98	3.72E-04	6.98	-5.11E-02
6.99	6.19E-02	6.99	4.45E-02
7	4.54E-02	7	1.83E-01
7.01	7.58E-03	7.01	2.70E-01
7.02	2.32E-02	7.02	2.94E-01
7.03	7.43E-02	7.03	3.13E-01
7.04	9.13E-02	7.04	3.21E-01
7.05	5.57E-02	7.05	2.46E-01
7.06	3.83E-03	7.06	7.87E-02
7.07	-3.92E-02	7.07	-7.97E-02
7.08	-7.47E-02	7.08	-1.17E-01
7.09	-1.00E-01	7.09	-3.44E-02
7.1	-1.01E-01	7.1	7.71E-02
7.11	-8.50E-02	7.11	1.83E-01
7.12	-8.87E-02	7.12	3.02E-01
7.13	-1.33E-01	7.13	3.89E-01
7.14	-2.12E-01	7.14	3.47E-01
7.15	-3.23E-01	7.15	1.87E-01
7.16	-4.40E-01	7.16	2.60E-02
7.17	-4.99E-01	7.17	-7.28E-02
7.18	-4.83E-01	7.18	-1.70E-01
7.19	-4.62E-01	7.19	-2.93E-01
7.2	-4.81E-01	7.2	-3.71E-01
7.21	-4.97E-01	7.21	-3.50E-01
7.22	-4.77E-01	7.22	-2.79E-01
7.23	-4.61E-01	7.23	-2.05E-01
7.24	-4.70E-01	7.24	-1.23E-01
7.25	-4.69E-01	7.25	-1.97E-02
7.26	-4.57E-01	7.26	9.22E-02
7.27	-4.77E-01	7.27	2.03E-01
7.28	-5.03E-01	7.28	2.91E-01
7.29	-4.37E-01	7.29	3.28E-01
7.3	-2.93E-01	7.3	2.93E-01

Table A.1 (continued) : 1.15g scaled artificial Montenegro Earthquake Record.

Longitudinal Direction		Transverse Direction	
Time	Acc (g)	Time	Acc (g)
7.31	-2.04E-01	7.31	2.17E-01
7.32	-2.10E-01	7.32	1.45E-01
7.33	-2.08E-01	7.33	1.16E-01
7.34	-1.46E-01	7.34	1.43E-01
7.35	-8.30E-02	7.35	2.13E-01
7.36	-6.29E-02	7.36	2.76E-01
7.37	-6.32E-02	7.37	3.03E-01
7.38	-5.16E-02	7.38	3.07E-01
7.39	-7.85E-03	7.39	3.05E-01
7.4	8.46E-02	7.4	2.85E-01
7.41	2.04E-01	7.41	2.38E-01
7.42	3.02E-01	7.42	1.78E-01
7.43	3.71E-01	7.43	1.35E-01
7.44	4.61E-01	7.44	1.27E-01
7.45	5.60E-01	7.45	1.62E-01
7.46	5.90E-01	7.46	2.13E-01
7.47	5.60E-01	7.47	2.43E-01
7.48	5.52E-01	7.48	2.20E-01
7.49	5.63E-01	7.49	1.49E-01
7.5	5.14E-01	7.5	5.10E-02
7.51	4.37E-01	7.51	-2.85E-02
7.52	4.39E-01	7.52	-4.89E-02
7.53	4.97E-01	7.53	-2.42E-02
7.54	4.83E-01	7.54	-2.46E-02
7.55	3.89E-01	7.55	-9.04E-02
7.56	3.50E-01	7.56	-1.74E-01
7.57	4.23E-01	7.57	-2.16E-01
7.58	5.04E-01	7.58	-2.30E-01
7.59	5.31E-01	7.59	-2.69E-01
7.6	5.52E-01	7.6	-3.29E-01
7.61	5.82E-01	7.61	-3.84E-01
7.62	5.62E-01	7.62	-4.36E-01
7.63	4.89E-01	7.63	-4.92E-01
7.64	4.23E-01	7.64	-5.28E-01
7.65	3.80E-01	7.65	-5.26E-01
7.66	3.13E-01	7.66	-5.23E-01
7.67	2.23E-01	7.67	-5.61E-01
7.68	1.65E-01	7.68	-6.08E-01
7.69	1.49E-01	7.69	-5.90E-01
7.7	1.16E-01	7.7	-4.96E-01
7.71	4.18E-02	7.71	-3.87E-01

Table A.1 (continued) : 1.15g scaled artificial Montenegro Earthquake Record.

Longitudinal Direction		Transverse Direction	
Time	Acc (g)	Time	Acc (g)
7.72	-4.48E-02	7.72	-3.10E-01
7.73	-1.17E-01	7.73	-2.38E-01
7.74	-1.60E-01	7.74	-1.43E-01
7.75	-1.47E-01	7.75	-6.54E-02
7.76	-8.06E-02	7.76	-6.47E-02
7.77	-2.14E-02	7.77	-1.39E-01
7.78	-3.18E-02	7.78	-2.12E-01
7.79	-1.04E-01	7.79	-2.19E-01
7.8	-1.71E-01	7.8	-1.65E-01
7.81	-1.77E-01	7.81	-1.04E-01
7.82	-1.26E-01	7.82	-7.15E-02
7.83	-7.77E-02	7.83	-6.52E-02
7.84	-1.03E-01	7.84	-6.71E-02
7.85	-1.97E-01	7.85	-6.74E-02
7.86	-2.68E-01	7.86	-5.83E-02
7.87	-2.41E-01	7.87	-2.98E-02
7.88	-1.52E-01	7.88	8.78E-03
7.89	-7.58E-02	7.89	1.70E-02
7.9	-1.48E-02	7.9	-1.78E-02
7.91	7.72E-02	7.91	-3.64E-02
7.92	1.99E-01	7.92	8.78E-03
7.93	2.90E-01	7.93	6.00E-02
7.94	3.09E-01	7.94	2.72E-02
7.95	2.72E-01	7.95	-6.27E-02
7.96	2.38E-01	7.96	-1.10E-01
7.97	2.60E-01	7.97	-1.00E-01
7.98	3.50E-01	7.98	-1.13E-01
7.99	4.38E-01	7.99	-1.73E-01
8	4.34E-01	8	-2.16E-01
8.01	3.32E-01	8.01	-2.05E-01
8.02	2.27E-01	8.02	-2.09E-01
8.03	1.90E-01	8.03	-2.71E-01
8.04	1.91E-01	8.04	-3.38E-01
8.05	1.74E-01	8.05	-3.22E-01
8.06	1.49E-01	8.06	-2.16E-01
8.07	1.60E-01	8.07	-9.65E-02
8.08	1.94E-01	8.08	-3.98E-02
8.09	1.91E-01	8.09	-4.83E-02
8.1	1.37E-01	8.1	-7.33E-02
8.11	9.04E-02	8.11	-9.22E-02
8.12	9.30E-02	8.12	-1.18E-01
8.13	1.14E-01	8.13	-1.27E-01
8.14	1.10E-01	8.14	-6.97E-02

Table A.1 (continued) : 1.15g scaled artificial Montenegro Earthquake Record.

Longitudinal Direction		Transverse Direction	
Time	Acc (g)	Time	Acc (g)
8.15	7.17E-02	8.15	3.37E-02
8.16	1.01E-02	8.16	8.78E-02
8.17	-6.87E-02	8.17	6.48E-02
8.18	-1.54E-01	8.18	5.50E-02
8.19	-2.22E-01	8.19	1.29E-01
8.2	-2.57E-01	8.2	2.25E-01
8.21	-2.80E-01	8.21	2.55E-01
8.22	-3.10E-01	8.22	2.19E-01
8.23	-3.39E-01	8.23	1.70E-01
8.24	-3.63E-01	8.24	1.33E-01
8.25	-3.85E-01	8.25	1.04E-01
8.26	-4.03E-01	8.26	8.03E-02
8.27	-3.93E-01	8.27	6.07E-02
8.28	-3.52E-01	8.28	6.10E-02
8.29	-3.12E-01	8.29	8.96E-02
8.3	-2.85E-01	8.3	1.09E-01
8.31	-2.55E-01	8.31	6.08E-02
8.32	-2.30E-01	8.32	-2.25E-02
8.33	-2.57E-01	8.33	-3.27E-02
8.34	-3.38E-01	8.34	7.28E-02
8.35	-3.99E-01	8.35	2.01E-01
8.36	-3.67E-01	8.36	2.49E-01
8.37	-2.87E-01	8.37	2.17E-01
8.38	-2.52E-01	8.38	1.61E-01
8.39	-2.73E-01	8.39	1.10E-01
8.4	-2.69E-01	8.4	7.48E-02
8.41	-2.03E-01	8.41	7.60E-02
8.42	-1.36E-01	8.42	1.04E-01
8.43	-1.26E-01	8.43	1.35E-01
8.44	-1.50E-01	8.44	1.60E-01
8.45	-1.24E-01	8.45	1.83E-01
8.46	-2.19E-02	8.46	1.80E-01
8.47	1.09E-01	8.47	1.37E-01
8.48	2.00E-01	8.48	1.04E-01
8.49	2.29E-01	8.49	1.34E-01
8.5	2.14E-01	8.5	2.07E-01
8.51	1.93E-01	8.51	2.62E-01
8.52	1.89E-01	8.52	2.77E-01
8.53	1.96E-01	8.53	2.77E-01
8.54	1.90E-01	8.54	2.80E-01
8.55	1.60E-01	8.55	2.76E-01
8.56	1.23E-01	8.56	2.52E-01
8.57	1.01E-01	8.57	1.87E-01

Table A.1 (continued) : 1.15g scaled artificial Montenegro Earthquake Record.

Longitudinal Direction		Transverse Direction	
Time	Acc (g)	Time	Acc (g)
8.58	8.78E-02	8.58	7.57E-02
8.59	6.38E-02	8.59	-4.50E-02
8.6	3.30E-02	8.6	-1.15E-01
8.61	1.83E-02	8.61	-1.36E-01
8.62	2.11E-02	8.62	-1.50E-01
8.63	1.93E-02	8.63	-1.54E-01
8.64	4.91E-03	8.64	-9.13E-02
8.65	-1.03E-02	8.65	2.53E-02
8.66	-1.69E-02	8.66	1.03E-01
8.67	-2.11E-02	8.67	9.65E-02
8.68	-2.65E-02	8.68	7.11E-02
8.69	-3.18E-02	8.69	9.83E-02
8.7	-3.25E-02	8.7	1.54E-01
8.71	-3.25E-02	8.71	1.83E-01
8.72	-4.23E-02	8.72	1.87E-01
8.73	-8.69E-02	8.73	2.10E-01
8.74	-1.69E-01	8.74	2.63E-01
8.75	-2.43E-01	8.75	3.17E-01
8.76	-2.41E-01	8.76	3.35E-01
8.77	-1.66E-01	8.77	2.90E-01
8.78	-9.74E-02	8.78	2.05E-01
8.79	-9.65E-02	8.79	1.42E-01
8.8	-1.29E-01	8.8	1.37E-01
8.81	-1.26E-01	8.81	1.57E-01
8.82	-8.70E-02	8.82	1.46E-01
8.83	-7.45E-02	8.83	1.25E-01
8.84	-1.16E-01	8.84	1.24E-01
8.85	-1.66E-01	8.85	1.06E-01
8.86	-1.79E-01	8.86	1.41E-02
8.87	-1.75E-01	8.87	-1.03E-01
8.88	-1.97E-01	8.88	-1.37E-01
8.89	-2.48E-01	8.89	-6.59E-02
8.9	-2.94E-01	8.9	1.93E-02
8.91	-3.41E-01	8.91	5.29E-02
8.92	-4.12E-01	8.92	6.24E-02
8.93	-4.81E-01	8.93	9.04E-02
8.94	-4.84E-01	8.94	1.23E-01
8.95	-4.22E-01	8.95	1.11E-01
8.96	-3.57E-01	8.96	4.57E-02
8.97	-3.35E-01	8.97	-2.43E-02
8.98	-3.23E-01	8.98	-4.02E-02
8.99	-2.87E-01	8.99	-9.04E-03
9	-2.27E-01	9	6.02E-03

Table A.1 (continued) : 1.15g scaled artificial Montenegro Earthquake Record.

Longitudinal Direction		Transverse Direction	
Time	Acc (g)	Time	Acc (g)
9.01	-1.64E-01	9.01	-2.91E-02
9.02	-1.21E-01	9.02	-7.54E-02
9.03	-1.18E-01	9.03	-9.74E-02
9.04	-1.51E-01	9.04	-1.23E-01
9.05	-1.77E-01	9.05	-1.83E-01
9.06	-1.75E-01	9.06	-2.32E-01
9.07	-1.74E-01	9.07	-2.08E-01
9.08	-2.08E-01	9.08	-1.23E-01
9.09	-2.55E-01	9.09	-4.19E-02
9.1	-2.75E-01	9.1	2.98E-03
9.11	-2.65E-01	9.11	2.75E-02
9.12	-2.50E-01	9.12	6.37E-02
9.13	-2.30E-01	9.13	1.26E-01
9.14	-1.95E-01	9.14	1.93E-01
9.15	-1.49E-01	9.15	2.27E-01
9.16	-1.10E-01	9.16	2.16E-01
9.17	-8.70E-02	9.17	1.92E-01
9.18	-7.23E-02	9.18	1.80E-01
9.19	-4.07E-02	9.19	1.68E-01
9.2	1.51E-02	9.2	1.49E-01
9.21	7.05E-02	9.21	1.35E-01
9.22	9.22E-02	9.22	1.21E-01
9.23	7.59E-02	9.23	9.65E-02
9.24	4.77E-02	9.24	7.71E-02
9.25	3.03E-02	9.25	8.55E-02
9.26	2.57E-02	9.26	9.65E-02
9.27	2.74E-02	9.27	7.32E-02
9.28	2.99E-02	9.28	2.39E-02
9.29	2.78E-02	9.29	-2.92E-02
9.3	2.31E-02	9.3	-9.91E-02
9.31	2.31E-02	9.31	-2.00E-01
9.32	3.01E-02	9.32	-3.06E-01
9.33	4.46E-02	9.33	-3.86E-01
9.34	6.99E-02	9.34	-4.50E-01
9.35	9.65E-02	9.35	-5.14E-01
9.36	1.03E-01	9.36	-5.63E-01
9.37	8.70E-02	9.37	-5.83E-01
9.38	6.88E-02	9.38	-5.83E-01
9.39	4.71E-02	9.39	-5.65E-01
9.4	-4.44E-03	9.4	-5.27E-01
9.41	-9.04E-02	9.41	-4.67E-01
9.42	-1.86E-01	9.42	-3.94E-01
9.43	-2.72E-01	9.43	-3.17E-01

Table A.1 (continued) : 1.15g scaled artificial Montenegro Earthquake Record.

Longitudinal Direction		Transverse Direction	
Time	Acc (g)	Time	Acc (g)
9.44	-3.50E-01	9.44	-2.53E-01
9.45	-4.03E-01	9.45	-2.00E-01
9.46	-4.01E-01	9.46	-1.16E-01
9.47	-3.56E-01	9.47	2.52E-02
9.48	-3.06E-01	9.48	1.63E-01
9.49	-2.58E-01	9.49	2.24E-01
9.5	-1.90E-01	9.5	2.25E-01
9.51	-1.06E-01	9.51	2.27E-01
9.52	-3.83E-02	9.52	2.22E-01
9.53	-6.93E-03	9.53	1.63E-01
9.54	-8.17E-03	9.54	6.43E-02
9.55	-3.44E-02	9.55	7.00E-04
9.56	-6.91E-02	9.56	-1.76E-02
9.57	-7.41E-02	9.57	-3.81E-02
9.58	-3.15E-02	9.58	-7.51E-02
9.59	2.65E-02	9.59	-8.64E-02
9.6	6.56E-02	9.6	-5.22E-02
9.61	9.04E-02	9.61	5.21E-04
9.62	1.24E-01	9.62	5.23E-02
9.63	1.73E-01	9.63	1.12E-01
9.64	2.36E-01	9.64	1.84E-01
9.65	3.16E-01	9.65	2.56E-01
9.66	4.01E-01	9.66	3.22E-01
9.67	4.73E-01	9.67	3.91E-01
9.68	5.28E-01	9.68	4.65E-01
9.69	5.77E-01	9.69	5.20E-01
9.7	6.06E-01	9.7	5.37E-01
9.71	5.81E-01	9.71	5.23E-01
9.72	4.98E-01	9.72	4.83E-01
9.73	3.94E-01	9.73	4.10E-01
9.74	3.08E-01	9.74	3.08E-01
9.75	2.60E-01	9.75	1.96E-01
9.76	2.44E-01	9.76	7.97E-02
9.77	2.38E-01	9.77	-4.08E-02
9.78	2.14E-01	9.78	-1.45E-01
9.79	1.66E-01	9.79	-2.00E-01
9.8	1.14E-01	9.8	-2.04E-01
9.81	6.48E-02	9.81	-1.90E-01
9.82	2.18E-02	9.82	-1.61E-01
9.83	4.71E-03	9.83	-9.48E-02
9.84	3.13E-02	9.84	-1.25E-02
9.85	6.96E-02	9.85	4.15E-02
9.86	8.54E-02	9.86	7.50E-02

Table A.1 (continued) : 1.15g scaled artificial Montenegro Earthquake Record.

Longitudinal Direction		Transverse Direction	
Time	Acc (g)	Time	Acc (g)
9.87	9.74E-02	9.87	1.31E-01
9.88	1.56E-01	9.88	2.02E-01
9.89	2.46E-01	9.89	2.28E-01
9.9	3.15E-01	9.9	1.91E-01
9.91	3.31E-01	9.91	1.25E-01
9.92	3.23E-01	9.92	4.92E-02
9.93	3.22E-01	9.93	-4.53E-02
9.94	3.37E-01	9.94	-1.43E-01
9.95	3.63E-01	9.95	-2.11E-01
9.96	3.81E-01	9.96	-2.54E-01
9.97	3.69E-01	9.97	-2.93E-01
9.98	3.43E-01	9.98	-3.16E-01
9.99	3.50E-01	9.99	-2.97E-01
10	3.90E-01	10	-2.64E-01
10.01	4.08E-01	10.01	-2.51E-01
10.02	3.90E-01	10.02	-2.48E-01
10.03	3.74E-01	10.03	-2.22E-01
10.04	3.70E-01	10.04	-1.89E-01
10.05	3.35E-01	10.05	-1.89E-01
10.06	2.64E-01	10.06	-2.23E-01
10.07	2.03E-01	10.07	-2.53E-01
10.08	1.60E-01	10.08	-2.59E-01
10.09	8.55E-02	10.09	-2.59E-01
10.1	-2.78E-02	10.1	-2.70E-01
10.11	-1.29E-01	10.11	-2.82E-01
10.12	-1.94E-01	10.12	-2.87E-01
10.13	-2.63E-01	10.13	-2.90E-01
10.14	-3.50E-01	10.14	-3.00E-01
10.15	-4.03E-01	10.15	-3.25E-01
10.16	-3.97E-01	10.16	-3.63E-01
10.17	-3.88E-01	10.17	-4.02E-01
10.18	-4.06E-01	10.18	-4.17E-01
10.19	-4.16E-01	10.19	-3.92E-01
10.2	-3.77E-01	10.2	-3.37E-01
10.21	-3.19E-01	10.21	-2.75E-01
10.22	-2.82E-01	10.22	-2.34E-01
10.23	-2.69E-01	10.23	-2.14E-01
10.24	-2.45E-01	10.24	-1.96E-01
10.25	-1.91E-01	10.25	-1.63E-01
10.26	-1.07E-01	10.26	-1.20E-01
10.27	-8.87E-03	10.27	-7.62E-02
10.28	7.63E-02	10.28	-3.39E-02
10.29	1.32E-01	10.29	7.63E-03

Table A.1 (continued) : 1.15g scaled artificial Montenegro Earthquake Record.

Longitudinal Direction		Transverse Direction	
Time	Acc (g)	Time	Acc (g)
10.3	1.75E-01	10.3	3.74E-02
10.31	2.27E-01	10.31	3.57E-02
10.32	2.83E-01	10.32	1.13E-03
10.33	3.24E-01	10.33	-3.92E-02
10.34	3.62E-01	10.34	-5.85E-02
10.35	4.08E-01	10.35	-6.38E-02
10.36	4.48E-01	10.36	-7.37E-02
10.37	4.51E-01	10.37	-8.66E-02
10.38	4.22E-01	10.38	-8.30E-02
10.39	3.93E-01	10.39	-6.84E-02
10.4	3.75E-01	10.4	-6.26E-02
10.41	3.44E-01	10.41	-6.24E-02
10.42	2.83E-01	10.42	-3.66E-02
10.43	2.05E-01	10.43	2.22E-02
10.44	1.36E-01	10.44	7.57E-02
10.45	8.17E-02	10.45	9.48E-02
10.46	2.39E-02	10.46	1.02E-01
10.47	-5.73E-02	10.47	1.32E-01
10.48	-1.44E-01	10.48	1.66E-01
10.49	-2.08E-01	10.49	1.69E-01
10.5	-2.54E-01	10.5	1.50E-01
10.51	-3.23E-01	10.51	1.50E-01
10.52	-4.22E-01	10.52	1.64E-01
10.53	-5.00E-01	10.53	1.56E-01
10.54	-5.21E-01	10.54	1.30E-01
10.55	-5.17E-01	10.55	1.35E-01
10.56	-5.37E-01	10.56	1.83E-01
10.57	-5.79E-01	10.57	2.39E-01
10.58	-6.10E-01	10.58	2.71E-01
10.59	-6.15E-01	10.59	2.92E-01
10.6	-6.04E-01	10.6	3.17E-01
10.61	-5.89E-01	10.61	3.37E-01
10.62	-5.75E-01	10.62	3.44E-01
10.63	-5.63E-01	10.63	3.36E-01
10.64	-5.37E-01	10.64	3.06E-01
10.65	-4.86E-01	10.65	2.73E-01
10.66	-4.37E-01	10.66	2.63E-01
10.67	-4.24E-01	10.67	2.79E-01
10.68	-4.35E-01	10.68	2.83E-01
10.69	-4.13E-01	10.69	2.60E-01
10.7	-3.38E-01	10.7	2.37E-01
10.71	-2.58E-01	10.71	2.37E-01
10.72	-2.20E-01	10.72	2.43E-01

Table A.1 (continued) : 1.15g scaled artificial Montenegro Earthquake Record.

Longitudinal Direction		Transverse Direction	
Time	Acc (g)	Time	Acc (g)
10.73	-2.19E-01	10.73	2.34E-01
10.74	-2.11E-01	10.74	2.29E-01
10.75	-1.67E-01	10.75	2.38E-01
10.76	-8.96E-02	10.76	2.55E-01
10.77	-8.20E-03	10.77	2.69E-01
10.78	4.72E-02	10.78	2.79E-01
10.79	6.55E-02	10.79	2.65E-01
10.8	6.10E-02	10.8	2.09E-01
10.81	6.57E-02	10.81	1.41E-01
10.82	1.05E-01	10.82	1.16E-01
10.83	1.76E-01	10.83	1.29E-01
10.84	2.42E-01	10.84	1.32E-01
10.85	2.82E-01	10.85	1.22E-01
10.86	2.97E-01	10.86	1.48E-01
10.87	3.07E-01	10.87	2.15E-01
10.88	3.17E-01	10.88	2.57E-01
10.89	3.31E-01	10.89	2.35E-01
10.9	3.50E-01	10.9	1.76E-01
10.91	3.64E-01	10.91	1.22E-01
10.92	3.73E-01	10.92	8.18E-02
10.93	3.92E-01	10.93	6.08E-02
10.94	4.42E-01	10.94	7.43E-02
10.95	5.02E-01	10.95	1.10E-01
10.96	5.20E-01	10.96	1.32E-01
10.97	4.70E-01	10.97	1.38E-01
10.98	3.83E-01	10.98	1.60E-01
10.99	3.09E-01	10.99	2.00E-01
11	2.60E-01	11	2.30E-01
11.01	2.13E-01	11.01	2.37E-01
11.02	1.45E-01	11.02	2.30E-01
11.03	6.19E-02	11.03	2.17E-01
11.04	-8.17E-03	11.04	1.88E-01
11.05	-4.17E-02	11.05	1.43E-01
11.06	-5.00E-02	11.06	1.00E-01
11.07	-4.77E-02	11.07	6.36E-02
11.08	-2.70E-02	11.08	3.79E-02
11.09	2.51E-02	11.09	2.51E-02
11.1	8.87E-02	11.1	1.37E-02
11.11	1.37E-01	11.11	-1.28E-02
11.12	1.75E-01	11.12	-4.50E-02
11.13	2.15E-01	11.13	-5.91E-02
11.14	2.44E-01	11.14	-6.16E-02
11.15	2.45E-01	11.15	-7.71E-02

Table A.1 (continued) : 1.15g scaled artificial Montenegro Earthquake Record.

Longitudinal Direction		Transverse Direction	
Time	Acc (g)	Time	Acc (g)
11.16	2.42E-01	11.16	-9.83E-02
11.17	2.63E-01	11.17	-9.39E-02
11.18	2.83E-01	11.18	-6.76E-02
11.19	2.63E-01	11.19	-5.96E-02
11.2	2.22E-01	11.2	-8.03E-02
11.21	2.06E-01	11.21	-9.83E-02
11.22	2.16E-01	11.22	-1.01E-01
11.23	2.19E-01	11.23	-1.18E-01
11.24	2.21E-01	11.24	-1.70E-01
11.25	2.44E-01	11.25	-2.34E-01
11.26	2.78E-01	11.26	-2.73E-01
11.27	2.85E-01	11.27	-2.80E-01
11.28	2.60E-01	11.28	-2.61E-01
11.29	2.29E-01	11.29	-2.16E-01
11.3	2.04E-01	11.3	-1.43E-01
11.31	1.77E-01	11.31	-5.40E-02
11.32	1.46E-01	11.32	3.00E-02
11.33	1.23E-01	11.33	9.48E-02
11.34	1.19E-01	11.34	1.49E-01
11.35	1.25E-01	11.35	2.10E-01
11.36	1.23E-01	11.36	2.78E-01
11.37	1.04E-01	11.37	3.28E-01
11.38	8.60E-02	11.38	3.42E-01
11.39	7.90E-02	11.39	3.32E-01
11.4	7.01E-02	11.4	3.17E-01
11.41	4.78E-02	11.41	3.03E-01
11.42	2.89E-02	11.42	2.86E-01
11.43	3.30E-02	11.43	2.62E-01
11.44	4.59E-02	11.44	2.20E-01
11.45	4.36E-02	11.45	1.49E-01
11.46	3.69E-02	11.46	4.55E-02
11.47	4.92E-02	11.47	-6.74E-02
11.48	6.77E-02	11.48	-1.59E-01
11.49	6.44E-02	11.49	-2.13E-01
11.5	4.39E-02	11.5	-2.38E-01
11.51	2.99E-02	11.51	-2.63E-01
11.52	1.82E-02	11.52	-3.14E-01
11.53	-1.22E-02	11.53	-3.79E-01
11.54	-5.71E-02	11.54	-4.28E-01
11.55	-8.29E-02	11.55	-4.49E-01
11.56	-7.29E-02	11.56	-4.69E-01
11.57	-4.22E-02	11.57	-5.03E-01
11.58	-1.78E-02	11.58	-5.34E-01

Table A.1 (continued) : 1.15g scaled artificial Montenegro Earthquake Record.

Longitudinal Direction		Transverse Direction	
Time	Acc (g)	Time	Acc (g)
11.59	-1.34E-02	11.59	-5.37E-01
11.6	-2.24E-02	11.6	-5.30E-01
11.61	-2.85E-02	11.61	-5.42E-01
11.62	-2.69E-02	11.62	-5.70E-01
11.63	-3.03E-02	11.63	-5.90E-01
11.64	-4.97E-02	11.64	-5.90E-01
11.65	-8.05E-02	11.65	-5.88E-01
11.66	-1.13E-01	11.66	-5.80E-01
11.67	-1.48E-01	11.67	-5.53E-01
11.68	-1.90E-01	11.68	-5.10E-01
11.69	-2.43E-01	11.69	-4.64E-01
11.7	-3.04E-01	11.7	-4.23E-01
11.71	-3.63E-01	11.71	-3.83E-01
11.72	-4.03E-01	11.72	-3.40E-01
11.73	-4.21E-01	11.73	-2.90E-01
11.74	-4.34E-01	11.74	-2.12E-01
11.75	-4.53E-01	11.75	-1.03E-01
11.76	-4.64E-01	11.76	1.61E-02
11.77	-4.50E-01	11.77	1.26E-01
11.78	-4.23E-01	11.78	2.30E-01
11.79	-4.09E-01	11.79	3.16E-01
11.8	-4.06E-01	11.8	3.61E-01
11.81	-4.03E-01	11.81	3.74E-01
11.82	-3.98E-01	11.82	3.78E-01
11.83	-3.95E-01	11.83	3.73E-01
11.84	-3.87E-01	11.84	3.46E-01
11.85	-3.78E-01	11.85	3.17E-01
11.86	-3.75E-01	11.86	3.14E-01
11.87	-3.74E-01	11.87	3.28E-01
11.88	-3.66E-01	11.88	3.29E-01
11.89	-3.52E-01	11.89	3.27E-01
11.9	-3.31E-01	11.9	3.36E-01
11.91	-2.88E-01	11.91	3.27E-01
11.92	-2.13E-01	11.92	2.84E-01
11.93	-1.33E-01	11.93	2.53E-01
11.94	-6.97E-02	11.94	2.76E-01
11.95	-1.55E-02	11.95	3.23E-01
11.96	4.49E-02	11.96	3.43E-01
11.97	1.00E-01	11.97	3.30E-01
11.98	1.31E-01	11.98	3.03E-01
11.99	1.42E-01	11.99	2.54E-01
12	1.35E-01	12	1.85E-01
12.01	1.03E-01	12.01	1.31E-01

Table A.1 (continued) : 1.15g scaled artificial Montenegro Earthquake Record.

Longitudinal Direction		Transverse Direction	
Time	Acc (g)	Time	Acc (g)
12.02	5.69E-02	12.02	1.10E-01
12.03	2.64E-02	12.03	8.78E-02
12.04	1.91E-02	12.04	3.98E-02
12.05	1.50E-02	12.05	-1.43E-02
12.06	1.96E-03	12.06	-6.19E-02
12.07	-6.97E-03	12.07	-1.19E-01
12.08	-2.50E-03	12.08	-1.78E-01
12.09	6.67E-03	12.09	-2.04E-01
12.1	5.01E-03	12.1	-1.90E-01
12.11	-1.24E-02	12.11	-1.72E-01
12.12	-3.83E-02	12.12	-1.72E-01
12.13	-5.71E-02	12.13	-1.69E-01
12.14	-5.58E-02	12.14	-1.50E-01
12.15	-4.56E-02	12.15	-1.39E-01
12.16	-5.43E-02	12.16	-1.51E-01
12.17	-9.57E-02	12.17	-1.71E-01
12.18	-1.54E-01	12.18	-1.75E-01
12.19	-2.01E-01	12.19	-1.64E-01
12.2	-2.17E-01	12.2	-1.56E-01
12.21	-2.02E-01	12.21	-1.51E-01
12.22	-1.77E-01	12.22	-1.43E-01
12.23	-1.56E-01	12.23	-1.24E-01
12.24	-1.42E-01	12.24	-9.57E-02
12.25	-1.17E-01	12.25	-5.37E-02
12.26	-7.43E-02	12.26	-1.85E-03
12.27	-1.88E-02	12.27	4.84E-02
12.28	3.33E-02	12.28	9.04E-02
12.29	7.38E-02	12.29	1.36E-01
12.3	1.00E-01	12.3	1.97E-01
12.31	1.14E-01	12.31	2.71E-01
12.32	1.18E-01	12.32	3.43E-01
12.33	1.09E-01	12.33	4.06E-01
12.34	8.12E-02	12.34	4.64E-01
12.35	4.27E-02	12.35	5.12E-01
12.36	7.85E-03	12.36	5.35E-01
12.37	-2.23E-02	12.37	5.32E-01
12.38	-6.17E-02	12.38	5.30E-01
12.39	-1.10E-01	12.39	5.35E-01
12.4	-1.46E-01	12.4	5.22E-01
12.41	-1.46E-01	12.41	4.67E-01
12.42	-1.22E-01	12.42	3.75E-01
12.43	-9.65E-02	12.43	2.77E-01
12.44	-7.96E-02	12.44	1.97E-01

Table A.1 (continued) : 1.15g scaled artificial Montenegro Earthquake Record.

Longitudinal Direction		Transverse Direction	
Time	Acc (g)	Time	Acc (g)
12.45	-6.64E-02	12.45	1.36E-01
12.46	-5.03E-02	12.46	9.30E-02
12.47	-2.78E-02	12.47	6.57E-02
12.48	-7.37E-03	12.48	4.11E-02
12.49	-8.78E-03	12.49	5.73E-03
12.5	-4.02E-02	12.5	-4.17E-02
12.51	-7.33E-02	12.51	-9.13E-02
12.52	-7.35E-02	12.52	-1.39E-01
12.53	-4.38E-02	12.53	-1.88E-01
12.54	-1.63E-02	12.54	-2.37E-01
12.55	6.15E-03	12.55	-2.75E-01
12.56	4.83E-02	12.56	-3.05E-01
12.57	1.16E-01	12.57	-3.43E-01
12.58	1.79E-01	12.58	-3.93E-01
12.59	2.26E-01	12.59	-4.39E-01
12.6	2.70E-01	12.6	-4.67E-01
12.61	3.21E-01	12.61	-4.83E-01
12.62	3.65E-01	12.62	-4.93E-01
12.63	3.88E-01	12.63	-4.93E-01
12.64	3.94E-01	12.64	-4.87E-01
12.65	3.90E-01	12.65	-4.88E-01
12.66	3.80E-01	12.66	-4.95E-01
12.67	3.67E-01	12.67	-4.83E-01
12.68	3.62E-01	12.68	-4.52E-01
12.69	3.61E-01	12.69	-4.28E-01
12.7	3.50E-01	12.7	-4.26E-01
12.71	3.26E-01	12.71	-4.23E-01
12.72	3.03E-01	12.72	-3.94E-01
12.73	2.93E-01	12.73	-3.49E-01
12.74	2.81E-01	12.74	-3.16E-01
12.75	2.42E-01	12.75	-2.89E-01
12.76	1.83E-01	12.76	-2.40E-01
12.77	1.29E-01	12.77	-1.70E-01
12.78	9.22E-02	12.78	-1.08E-01
12.79	5.75E-02	12.79	-6.87E-02
12.8	7.85E-03	12.8	-3.37E-02
12.81	-4.91E-02	12.81	1.40E-02
12.82	-1.00E-01	12.82	6.30E-02
12.83	-1.42E-01	12.83	9.74E-02
12.84	-1.79E-01	12.84	1.20E-01
12.85	-2.08E-01	12.85	1.38E-01
12.86	-2.24E-01	12.86	1.48E-01
12.87	-2.38E-01	12.87	1.41E-01

Table A.1 (continued) : 1.15g scaled artificial Montenegro Earthquake Record.

Longitudinal Direction		Transverse Direction	
Time	Acc (g)	Time	Acc (g)
12.88	-2.55E-01	12.88	1.18E-01
12.89	-2.66E-01	12.89	8.87E-02
12.9	-2.64E-01	12.9	5.71E-02
12.91	-2.49E-01	12.91	3.34E-02
12.92	-2.23E-01	12.92	2.20E-02
12.93	-1.84E-01	12.93	1.44E-02
12.94	-1.40E-01	12.94	-7.12E-04
12.95	-9.91E-02	12.95	-2.67E-02
12.96	-7.02E-02	12.96	-6.03E-02
12.97	-5.14E-02	12.97	-1.02E-01
12.98	-3.72E-02	12.98	-1.47E-01
12.99	-2.71E-02	12.99	-1.92E-01
13	-2.29E-02	13	-2.36E-01
13.01	-2.50E-02	13.01	-2.74E-01
13.02	-3.28E-02	13.02	-2.95E-01
13.03	-4.43E-02	13.03	-2.97E-01
13.04	-5.45E-02	13.04	-2.98E-01
13.05	-5.94E-02	13.05	-3.08E-01
13.06	-5.66E-02	13.06	-3.09E-01
13.07	-4.22E-02	13.07	-2.86E-01
13.08	-1.29E-02	13.08	-2.56E-01
13.09	2.99E-02	13.09	-2.24E-01
13.1	7.98E-02	13.1	-1.83E-01
13.11	1.31E-01	13.11	-1.25E-01
13.12	1.81E-01	13.12	-7.76E-02
13.13	2.25E-01	13.13	-5.59E-02
13.14	2.63E-01	13.14	-4.23E-02
13.15	2.91E-01	13.15	-1.78E-02
13.16	3.03E-01	13.16	2.53E-03
13.17	2.91E-01	13.17	-8.03E-04
13.18	2.63E-01	13.18	-1.19E-02
13.19	2.40E-01	13.19	-2.47E-03
13.2	2.23E-01	13.2	2.94E-02
13.21	2.01E-01	13.21	6.11E-02
13.22	1.69E-01	13.22	8.14E-02
13.23	1.41E-01	13.23	1.00E-01
13.24	1.23E-01	13.24	1.28E-01
13.25	1.08E-01	13.25	1.60E-01
13.26	7.97E-02	13.26	1.88E-01
13.27	3.96E-02	13.27	2.08E-01
13.28	-5.63E-03	13.28	2.25E-01
13.29	-5.20E-02	13.29	2.39E-01
13.3	-9.04E-02	13.3	2.43E-01

Table A.1 (continued) : 1.15g scaled artificial Montenegro Earthquake Record.

Longitudinal Direction		Transverse Direction	
Time	Acc (g)	Time	Acc (g)
13.31	-1.10E-01	13.31	2.31E-01
13.32	-1.21E-01	13.32	2.10E-01
13.33	-1.44E-01	13.33	1.90E-01
13.34	-1.83E-01	13.34	1.70E-01
13.35	-2.20E-01	13.35	1.42E-01
13.36	-2.35E-01	13.36	1.08E-01
13.37	-2.32E-01	13.37	8.43E-02
13.38	-2.31E-01	13.38	7.78E-02
13.39	-2.32E-01	13.39	7.05E-02
13.4	-2.23E-01	13.4	3.74E-02
13.41	-2.01E-01	13.41	-2.23E-02
13.42	-1.74E-01	13.42	-8.49E-02
13.43	-1.46E-01	13.43	-1.28E-01
13.44	-1.13E-01	13.44	-1.54E-01
13.45	-7.19E-02	13.45	-1.79E-01
13.46	-3.53E-02	13.46	-2.02E-01
13.47	-1.83E-02	13.47	-1.97E-01
13.48	-1.66E-02	13.48	-1.60E-01
13.49	-1.38E-02	13.49	-1.30E-01
13.5	-5.42E-03	13.5	-1.42E-01
13.51	-4.22E-04	13.51	-1.71E-01
13.52	-1.98E-03	13.52	-1.65E-01
13.53	-5.25E-03	13.53	-1.14E-01
13.54	-8.68E-03	13.54	-5.45E-02
13.55	-1.46E-02	13.55	-5.51E-03
13.56	-1.88E-02	13.56	4.95E-02
13.57	-1.80E-02	13.57	1.16E-01
13.58	-1.97E-02	13.58	1.67E-01
13.59	-2.57E-02	13.59	1.97E-01
13.6	-1.91E-02	13.6	2.21E-01
13.61	8.62E-03	13.61	2.45E-01
13.62	4.02E-02	13.62	2.60E-01
13.63	6.20E-02	13.63	2.73E-01
13.64	8.59E-02	13.64	2.99E-01
13.65	1.15E-01	13.65	3.30E-01
13.66	1.27E-01	13.66	3.34E-01
13.67	1.12E-01	13.67	3.10E-01
13.68	9.39E-02	13.68	2.85E-01
13.69	8.32E-02	13.69	2.66E-01
13.7	5.77E-02	13.7	2.37E-01
13.71	1.31E-02	13.71	2.02E-01
13.72	-1.36E-02	13.72	1.86E-01
13.73	-6.57E-03	13.73	1.97E-01

Table A.1 (continued) : 1.15g scaled artificial Montenegro Earthquake Record.

Longitudinal Direction		Transverse Direction	
Time	Acc (g)	Time	Acc (g)
13.74	-5.37E-04	13.74	2.19E-01
13.75	-1.89E-02	13.75	2.32E-01
13.76	-3.55E-02	13.76	2.25E-01
13.77	-2.03E-02	13.77	1.90E-01
13.78	1.85E-02	13.78	1.32E-01
13.79	5.77E-02	13.79	7.81E-02
13.8	8.63E-02	13.8	4.45E-02
13.81	9.83E-02	13.81	1.79E-02
13.82	9.39E-02	13.82	-1.91E-02
13.83	9.48E-02	13.83	-6.01E-02
13.84	1.13E-01	13.84	-9.13E-02
13.85	1.23E-01	13.85	-1.16E-01
13.86	1.02E-01	13.86	-1.42E-01
13.87	5.66E-02	13.87	-1.57E-01
13.88	2.23E-02	13.88	-1.50E-01
13.89	1.23E-02	13.89	-1.31E-01
13.9	2.17E-02	13.9	-1.27E-01
13.91	4.17E-02	13.91	-1.41E-01
13.92	6.15E-02	13.92	-1.47E-01
13.93	7.40E-02	13.93	-1.28E-01
13.94	8.78E-02	13.94	-9.74E-02
13.95	1.20E-01	13.95	-7.75E-02
13.96	1.69E-01	13.96	-6.43E-02
13.97	2.15E-01	13.97	-4.07E-02
13.98	2.48E-01	13.98	-1.11E-02
13.99	2.71E-01	13.99	6.03E-03
14	2.77E-01	14	1.45E-02
14.01	2.55E-01	14.01	3.76E-02
14.02	2.15E-01	14.02	7.66E-02
14.03	1.80E-01	14.03	1.04E-01
14.04	1.58E-01	14.04	1.05E-01
14.05	1.46E-01	14.05	9.39E-02
14.06	1.38E-01	14.06	8.78E-02
14.07	1.30E-01	14.07	8.70E-02
14.08	1.10E-01	14.08	8.58E-02
14.09	8.43E-02	14.09	8.23E-02
14.1	7.25E-02	14.1	8.00E-02
14.11	8.50E-02	14.11	7.99E-02
14.12	9.91E-02	14.12	7.69E-02
14.13	9.30E-02	14.13	6.22E-02
14.14	7.55E-02	14.14	3.65E-02
14.15	6.39E-02	14.15	1.91E-02
14.16	5.33E-02	14.16	3.03E-02

Table A.1 (continued) : 1.15g scaled artificial Montenegro Earthquake Record.

Longitudinal Direction		Transverse Direction	
Time	Acc (g)	Time	Acc (g)
14.17	3.11E-02	14.17	6.38E-02
14.18	4.61E-03	14.18	9.48E-02
14.19	-1.42E-02	14.19	1.13E-01
14.2	-2.94E-02	14.2	1.30E-01
14.21	-4.81E-02	14.21	1.48E-01
14.22	-6.38E-02	14.22	1.53E-01
14.23	-6.96E-02	14.23	1.39E-01
14.24	-7.20E-02	14.24	1.19E-01
14.25	-7.56E-02	14.25	1.02E-01
14.26	-7.03E-02	14.26	9.13E-02
14.27	-4.77E-02	14.27	9.22E-02
14.28	-1.58E-02	14.28	1.01E-01
14.29	1.57E-02	14.29	1.01E-01
14.3	4.80E-02	14.3	8.30E-02
14.31	8.06E-02	14.31	6.06E-02
14.32	1.07E-01	14.32	5.49E-02
14.33	1.26E-01	14.33	6.04E-02
14.34	1.44E-01	14.34	5.74E-02
14.35	1.62E-01	14.35	4.89E-02
14.36	1.68E-01	14.36	5.70E-02
14.37	1.59E-01	14.37	8.78E-02
14.38	1.35E-01	14.38	1.23E-01
14.39	9.65E-02	14.39	1.46E-01
14.4	5.61E-02	14.4	1.58E-01
14.41	2.20E-02	14.41	1.69E-01
14.42	-9.74E-03	14.42	1.77E-01
14.43	-4.89E-02	14.43	1.81E-01
14.44	-8.67E-02	14.44	1.70E-01
14.45	-1.03E-01	14.45	1.43E-01
14.46	-9.65E-02	14.46	1.14E-01
14.47	-9.48E-02	14.47	9.13E-02
14.48	-1.09E-01	14.48	7.01E-02
14.49	-1.27E-01	14.49	3.90E-02
14.5	-1.43E-01	14.5	1.80E-03
14.51	-1.65E-01	14.51	-2.70E-02
14.52	-1.98E-01	14.52	-4.54E-02
14.53	-2.31E-01	14.53	-6.48E-02
14.54	-2.59E-01	14.54	-9.30E-02
14.55	-2.86E-01	14.55	-1.25E-01
14.56	-3.13E-01	14.56	-1.52E-01
14.57	-3.25E-01	14.57	-1.72E-01
14.58	-3.13E-01	14.58	-1.85E-01
14.59	-2.87E-01	14.59	-1.91E-01

Table A.1 (continued) : 1.15g scaled artificial Montenegro Earthquake Record.

Longitudinal Direction		Transverse Direction	
Time	Acc (g)	Time	Acc (g)
14.6	-2.58E-01	14.6	-1.87E-01
14.61	-2.28E-01	14.61	-1.72E-01
14.62	-1.95E-01	14.62	-1.51E-01
14.63	-1.63E-01	14.63	-1.30E-01
14.64	-1.39E-01	14.64	-1.10E-01
14.65	-1.30E-01	14.65	-9.57E-02
14.66	-1.36E-01	14.66	-8.87E-02
14.67	-1.44E-01	14.67	-9.13E-02
14.68	-1.34E-01	14.68	-9.57E-02
14.69	-1.10E-01	14.69	-8.87E-02
14.7	-1.02E-01	14.7	-6.23E-02
14.71	-1.28E-01	14.71	-2.32E-02
14.72	-1.62E-01	14.72	1.57E-02
14.73	-1.67E-01	14.73	4.36E-02
14.74	-1.46E-01	14.74	5.96E-02
14.75	-1.34E-01	14.75	7.25E-02
14.76	-1.41E-01	14.76	8.57E-02
14.77	-1.43E-01	14.77	9.13E-02
14.78	-1.21E-01	14.78	8.58E-02
14.79	-8.30E-02	14.79	8.39E-02
14.8	-4.93E-02	14.8	9.65E-02
14.81	-2.79E-02	14.81	1.09E-01
14.82	-1.20E-02	14.82	9.57E-02
14.83	4.13E-03	14.83	6.83E-02
14.84	2.19E-02	14.84	6.15E-02
14.85	3.93E-02	14.85	8.03E-02
14.86	4.86E-02	14.86	9.74E-02
14.87	4.00E-02	14.87	1.02E-01
14.88	1.90E-02	14.88	1.05E-01
14.89	4.26E-03	14.89	1.07E-01
14.9	9.30E-03	14.9	8.96E-02
14.91	2.50E-02	14.91	5.67E-02
14.92	2.87E-02	14.92	3.35E-02
14.93	1.62E-02	14.93	2.96E-02
14.94	6.61E-03	14.94	2.46E-02
14.95	6.34E-03	14.95	9.57E-03
14.96	8.62E-03	14.96	-3.16E-03
14.97	1.88E-02	14.97	-4.02E-03
14.98	3.69E-02	14.98	7.35E-03
14.99	5.45E-02	14.99	2.49E-02
15	8.30E-02	15	1.43E-02

CURRICULUM VITAE

Candidate's full name: Reşat Atalay OYGUÇ

Place and date of birth: İstanbul, 1978

**Universities and
Colleges attended:**

2003-2011 Philosophy of Doctorate (Earthquake Engineering) Istanbul Technical University, Istanbul, Turkey.

2001-2003 Master of Science (Structure), Yıldız Technical University, Istanbul, Turkey

1996–2000 Bachelor of Science (Civil Engineering), Yıldız Technical University, Istanbul, Turkey

1993-1996 Eyüboğlu Science Highschool, Istanbul, Turkey

Publications:

Boduroglu, H., Oyguc, R. A., 2010: Performance assessment of irregular buildings using an adaptive pushover method. *International Workshop - Seismic Risk Management in Urban Areas- A Turkish-Iranian-American Workshop*, December 14-16, 2010 Istanbul, Turkey.

